Activation of G protein-coupled receptors : the role of extracellular loops in adenosine receptors

Peeters, M.C.

ACTIVATION OF G PROTEIN-COUPLED RECEPTORS

THE ROLE OF EXTRACELLULAR LOOPS IN ADENOSINE RECEPTOR ACTIVATION

ACTIVATION OF G PROTEIN-COUPLED RECEPTORS

THE ROLE OF EXTRACELLULAR LOOPS IN ADENOSINE RECEPTOR ACTIVATION

Proefschrift

ter verkrijging van

de graad van Doctor aan de Universiteit Leiden,

op gezag van Rector Magnificus prof. mr. P.F. van der Heijden,

volgens besluit van het College voor Promoties

te verdedigen op donderdag 17 november 2011

klokke 15.00 uur

door

Miriam Cornelia Peeters

geboren te Hoevelaken

in 1982

PROMOTIECOMMISSIE

Promotor:	Prof. Dr. A.P. IJzerman
Overige leden:	Prof. Dr. T.J.C. van Berkel
	Prof. Dr. J. Brouwer
	Prof. Dr. G. Vriend
	Prof. Dr. M. Danhof

The research described in this thesis was performed at the Division of Medicinal Chemistry of the Leiden/Amsterdam Center for Drug Research, Leiden University (Leiden, The Netherlands). The research was part of the TI-Pharma initiative “The GPCR forum for established targets” (project number D1-105).

This thesis was printed by Wöhrmann Print Service (Zutphen, The Netherlands).

To see the sakura
In flower for the first time
Is to experience a new sensation

Percival Lowell
The soul of the Far East (1888)

Cherry Blossoms
I view knowing there must be
Something more

Tayojo (1775-1865)

CONTENTS

CHAPTER 1

GENERAL INTRODUCTION

G PROTEIN-COUPLED RECEPTORS (GPCRS)

G protein-coupled receptors (GPCRs) form one of the largest protein families known. In humans, already over 800 members have been identified. When we take into account all the different variants, for example differences in mRNA splicing, this number is even considerably larger. GPCRs are involved in crucial signal transduction pathways, including vital processes such as reproduction and immunological responses [1]. Many drugs that are currently on the market (~ 40%) are directed against members of this immense superfamily for the treatment of a wide variety of diseases. Unfortunately, we still do not know exactly what happens between the event of drug binding and the intracellular response that eventually results in the drug's effect on the body. Increasing our knowledge of GPCRs would greatly aid in the design of new drugs with increased selectivity, thereby potentially decreasing the occurrence of side-effects. For this reason, research groups all over the world are intensively studying these receptors, and initiatives are formed to fast improve our knowledge. All of these efforts are paying off; in 2010 alone over 12,000 research papers discussing GPCRs were published (keywords: GPCR, G protein-coupled receptor, 7TM receptor, seven transmembrane receptor; www.pubmed.com). We even have access to a handful of high resolution crystal structures now that give us a good view of what these receptors actually look like [2,3,4] (see also Chapter 2 of this thesis).

The GPCR superfamily consists of five main classes, of which class A (or rhodopsin-like) GPCRs by far form the largest subfamily [5]. They all have a similar structure, with an extracellular N-terminus, seven transmembrane helices connected by three extracellular and three intracellular loops (IL1-3), and an intracellular C-terminus. However, when looking more closely at the crystal structures, we do notice many differences between class A family members. Especially the lesser conserved regions of the receptor, and in particular the extracellular loops, can adopt many different structural poses (see Chapter 2).

ADENOSINE RECEPTORS

The adenosine receptors (ARs) form a small subfamily within the class A GPCRs. Four subtypes of adenosine receptors are known (A_1R, $A_{2A}R$, $A_{2B}R$, and A_3R), all of which are ubiquitously expressed in the human body [6]. The endogenous ligand for this subfamily is adenosine, a nucleoside composed of an adenine ring attached to a ribose moiety via a β-N_9-glycosidic bond (**Figure 1**). Extracellular adenosine originates from the breakdown of ATP by 5'-ectonucleotidases and is then quickly metabolized by adenosine kinase to form AMP or by adenosine deaminase to form inosine. Under normal conditions, extracellular adenosine concentrations are in the nM-μM range. In response to metabolic stress and cell damage, e.g. in conditions of ischaemia, hypoxia, inflammation and trauma, adenosine accumulates in the extracellular space [7]. This stress signal subsequently leads to the activation of adenosine receptors, generating a range of tissue responses mainly focused on organ protection [8].

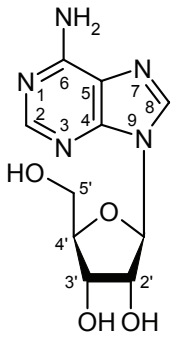

Figure 1. Chemical structure of adenosine

Although all four subtypes respond to adenosine, they do so at different adenosine concentrations and they are coupled to different intracellular signaling pathways. The A_1R and the A_3R subtypes mainly signal through G_i proteins mediating the inhibition of adenylyl cyclase, which leads to decreased levels of cAMP in the cell. The $A_{2A}R$ and $A_{2B}R$ cause an increase in intracellular cAMP levels by coupling mainly to G_s proteins resulting in the activation of adenylyl cyclase [9].

In this thesis, two subtypes of adenosine receptors are the main focus of our studies: the A_1R and the $A_{2B}R$. The A_1R is considered to be the high affinity receptor of the subfamily. The $A_{2B}R$ has the lowest affinity for the endogenous ligand adenosine. Only when adenosine levels increase to high micromolar concentrations in response to metabolic stress, the $A_{2B}R$ can be activated [7]. This only occurs in pathological conditions and subsequently leads to the activation of the immune system (**Figure 2**). For this reason, the adenosine A_{2B} receptor ($A_{2B}R$) is an interesting drug target and it has been implicated in asthma [10], chronic obstructive pulmonary disease (COPD) [11], and other inflammatory diseases [8]. Ligands for the A_1R are also of great interest for the pharmaceutical industry and a number of A_1R agonists and

antagonists have reached the clinical phase, and are or were under investigation for the treatment of peripheral nerve injury, hypertriglyceridemia in diabetes, heart failure, and kidney dysfunction [12]. Also, its high expression in the central nervous system (CNS) and the neuroprotective effects of activation has implicated the A_1R as a promising drug target in neurological disorders such as in Huntington's and Alzheimer disease [9,13,14]. This receptor has been studied in more detail compared to the $A_{2B}R$, and many more selective ligands have been identified, including allosteric ligands. Allosteric modulators are compounds that are able to bind the receptor at a site distinct from the orthosteric site where the endogenous ligand binds. These allosteric binding sites are thought to be less conserved than the endogenous binding site and can therefore provide more selectivity for a single receptor subtype.

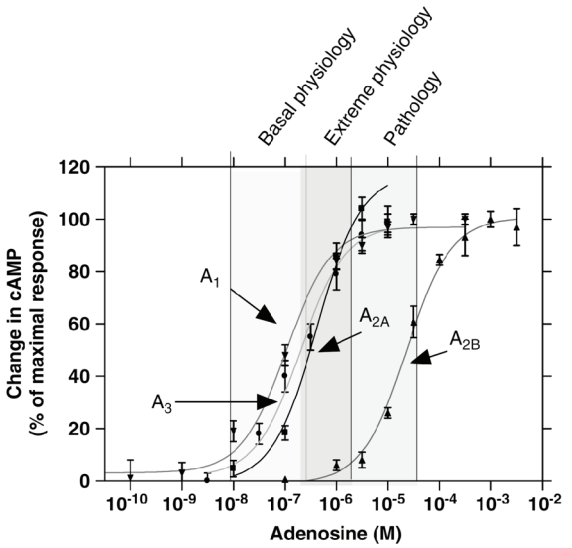

Figure 2. Activation profiles of the different adenosine receptor subtypes. The adenosine A_{2B} receptor is only activated when adenosine levels reach pathological concentrations. Figure was originally published in *Fredholm, B.B., Cell Death Differ 14 (2007).*

ADENOSINE RECEPTOR STRUCTURE

In 2008, the crystal structure of the adenosine A_{2A} receptor was published (**Figure 3**) [15]. At that point, it was only the third human GPCR of which the structure was elucidated. Just one year previously, the structures of the human β_1- and β_2-adrenergic receptors were published [16,17,18]. Even though the $A_{2A}R$ was greatly modified to enable the crystallization process, the structure was a great contribution to the adenosine receptor research field. Now we were able to explain mutational and pharmacological data in a more relevant three-dimensional fashion. In the beginning of 2011 another high resolution $A_{2A}R$ crystal structure was elucidated: the receptor in an active conformation with the agonist UK-432097 bound to it, followed quickly by two other active structures bound to NECA and adenosine, respectively [19,20].

With these structures another big leap was taken. By comparing the inactive and active structures, we can learn to understand the transitions the receptor goes through during the activation process better. However, there are some considerations that need to be taken into account: (1) the receptors were heavily modified to increase stability, with the T4-lysosyme fused to the third intracellular loop and a deleted C-terminal tail (ZM241385 and UK-432097 structures [15,19]) or with several thermo-stabilizing mutations (NECA and adenosine structures [20]) (2) the active structures provide single views of possibly multiple active conformations, providing a limited view on the activation mechanism, and (3) crystal packing may have had an effect on the structure, especially on the intra- and extracellular regions of the receptor. Nonetheless, all four structures provide the framework for a better understanding of adenosine receptor activation. These should be supplemented with combined mutagenesis and functional studies for appreciating the dynamics of this activation process, and that is exactly what we aimed for in this thesis.

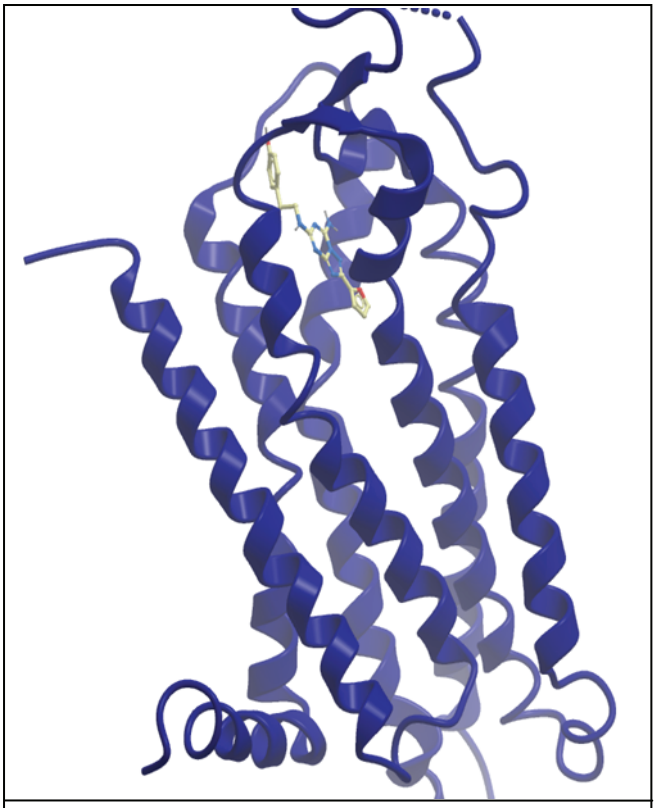

Figure 3. Crystal structure of the human adenosine A_{2A} receptor (in blue ribbon) bound to the antagonist ZM241385 (in ball & stick representation).

MUTAGENESIS

Mutagenesis is a powerful tool when examining GPCR function and activation. By changing single residues or even entire receptor domains followed by functional pharmacological studies, we can greatly improve our insight in how activation occurs upon ligand binding, but also which regions are specifically involved. Especially since the structural information is relatively limited in GPCRs, we still greatly depend on mutagenic data.

Mutagenic techniques range from approaches purely based on rational, such as site-directed mutagenesis where a single residue in the protein is targeted and changed to a specific alternative residue, to highly unbiased approaches like random mutagenesis where mutations are left to occur by chance [1].

Site-directed mutagenesis is the most used technique, the rationale for which mainly originates from computational analyses and/or structure-activity-relationship studies of receptor ligands indicating an important role of the residue in the protein [21,22].

A variation to this technique that is slightly less specific is site-saturation mutagenesis in which a single residue is changed into every other (naturally) occurring amino acid (see Chapter 3) [23]. This method provides insight into the structure-function-relationship of the residue of interest and the role of its side chain in binding and activation. Another approach is scanning analysis; this technique is mostly chosen when there are indications of the importance of a protein region, but not which exact amino acid would be involved (see Chapter 6). In this approach consecutive residues are replaced by one type of amino acid, for example alanine or cysteine. Alanine is often chosen as the replacing amino acid due to its small size and lack of reactive functional groups. It also has no or minor influence on the protein backbone, contrary to the more flexible glycine [24]. The advantage of cysteine replacements is that these residues are highly reactive and can form disulfide bridges with other cysteines. This property can be used to examine ligand-dependant conformational changes without the need to purify the protein in a disulfide-cross linking approach [25]. Another application can be in a cysteine-accessibility study using a cysteine-reactive biotin probe. Here, the ability of biotinylated mutant receptors to react with a steptavidin-HRP-conjugated antibody is used to examine differences in accessibility of the residue, providing insight in the conformational state of the receptor [26]. A less detailed, but just as informative method is the creation of chimeric receptors. Domains of one receptor are swapped with the corresponding domains of another (often related) receptor to investigate effects of selectivity, signaling or to identify the ligand binding site [27].

The most unbiased approach in mutagenic studies is random mutagenesis, where mutations are randomly introduced in the gene encoding (parts of) the receptor (see Chapters 3, 4, and 5). This can be achieved by UV irradiation, chemical methods like alkylation and deamination, or by error prone PCR. The first two approaches can be very successful, but it is difficult to control the frequency in which the mutations are

introduced. The third technique is based on manipulating the PCR reaction by changing the ratio between Mg^{2+} and Mn^{2+} ions, compromising the fidelity of the DNA polymerase. Furthermore, an excess of one of the nucleotides is added to force errors to occur. By choosing the conditions carefully, the frequency in which the mutations are introduced can be fine-tuned. Both low frequency random mutagenesis and saturation random mutagenesis have been applied in studying GPCR function [28,29]. This method was first described in 1995 [30] and since then has been optimized to use larger fragments in this technique and even commercial kits that are able to aid in the introduction of random mutations in whole gene sequences have become available [31]. In coupling a screening assay to a random mutagenesis approach, residues that show a phenotype of interest when mutated can be easily identified. In this way, information about how the receptor is activated or inactivated can be obtained as well as the role specific residues play in this process. One convenient screening platform is the *S. cerevisiae* model that when modified can function as a reporter system with growth as an easy read-out [32].

CONSTITUTIVE ACTIVITY

Constitutive activity, or basal activity, is the basal level of signaling a receptor displays without a ligand present. In a simple scheme an equilibrium exists between an inactive (R) and active conformation (R*) [33]. The fraction of R* in the total receptor population as well as the energy needed to transition between the two states determines the level of constitutive activity. This activation state is essential in maintaining physiological function and many pathogenic mutations have been reported that disturb the equilibrium causing an increase in activation (Constitutively Active Mutants or CAMs) or a decrease in basal activity (Constitutively Inactive Mutants or CIMs) [34,35,36]. These mutations have not only increased our knowledge on the pathophysiology in which GPCRs play a role, but also advanced our insight in the structure-function relationship of GPCRs.

The α_{1B}-adrenergic receptor (α_{1B}AR) was the first GPCR in which point mutations were shown to trigger receptor activation [23]. A conservative substitution (A293L) in the cytosolic extension of TM6 of the α_{1B}AR resulted in its constitutive activity. In the absence of an agonist, cells expressing the mutated receptor exhibited higher basal

levels of inositol phosphates compared to cells expressing the wild type α_{1B}AR. Since then, an impressive number of CAMs have been identified located in practically every domain of the receptors [37] (www.gpcr.org/7tm).This indicates that activation of a GPCR can be triggered by manipulations of the receptor structure in many different regions whose function cannot be obviously linked to agonist binding or G protein interaction [34]. Identifying specific regions and/or residues that can shift the equilibrium between the active and inactive conformation when mutated can be a strong tool in elucidating triggers involved in the activation mechanism. Several screening methods have been applied in search for these mutations [29,31,38].

S. CEREVISIAE AS A MODEL SYSTEM

GPCRs are among the oldest devices devoted to signal transduction and can be found in all eukaryotes. They are present in large numbers in vertebrates but are also expressed in plants, yeast, and protozoa [39,40].

In *S. cerevisiae*, three endogenous GPCRs have been identified: the Ste2 and Ste3 receptors and the Grp1 receptor [41]. Gpr1 is a glucose and sucrose sensing receptor that couples to the G protein Gpa2 leading to increased levels of intracellular cAMP. The subsequent events lead to a large remodeling of the yeast metabolism that results in an increase in yeast growth rate (**Figure 4A**) [42,43].

S. cerevisiae can stably exist as either haploid or diploid. The haploid cell types MAT**a** and MATα are to mate to form a diploid cell. Both cell types express mating specific proteins such as the **a**-factor pheromone and the α-factor receptor (Ste2) in MAT**a**-cells, and the α-factor and the **a**-factor receptor (Ste3) in MATα-cells [41,44]. Activation of the Ste2 or Ste3 receptor results in the activation of the MAP kinase pathway through the G protein Gpa1 following activation of nuclear proteins that control transcription, cell polarity, and progression through the cell cycle (**Figure 4B**) [44]. *S. cerevisiae* is an attractive expression system to study GPCRs and until now, more than 50 GPCRs have been functionally expressed in various yeast strains. Besides the presence of a full functional GPCR signaling machinery and mammalian-like post-translational modification, yeast is relatively easy to genetically manipulate, has a well characterized physiology and is inexpensive [44,45].

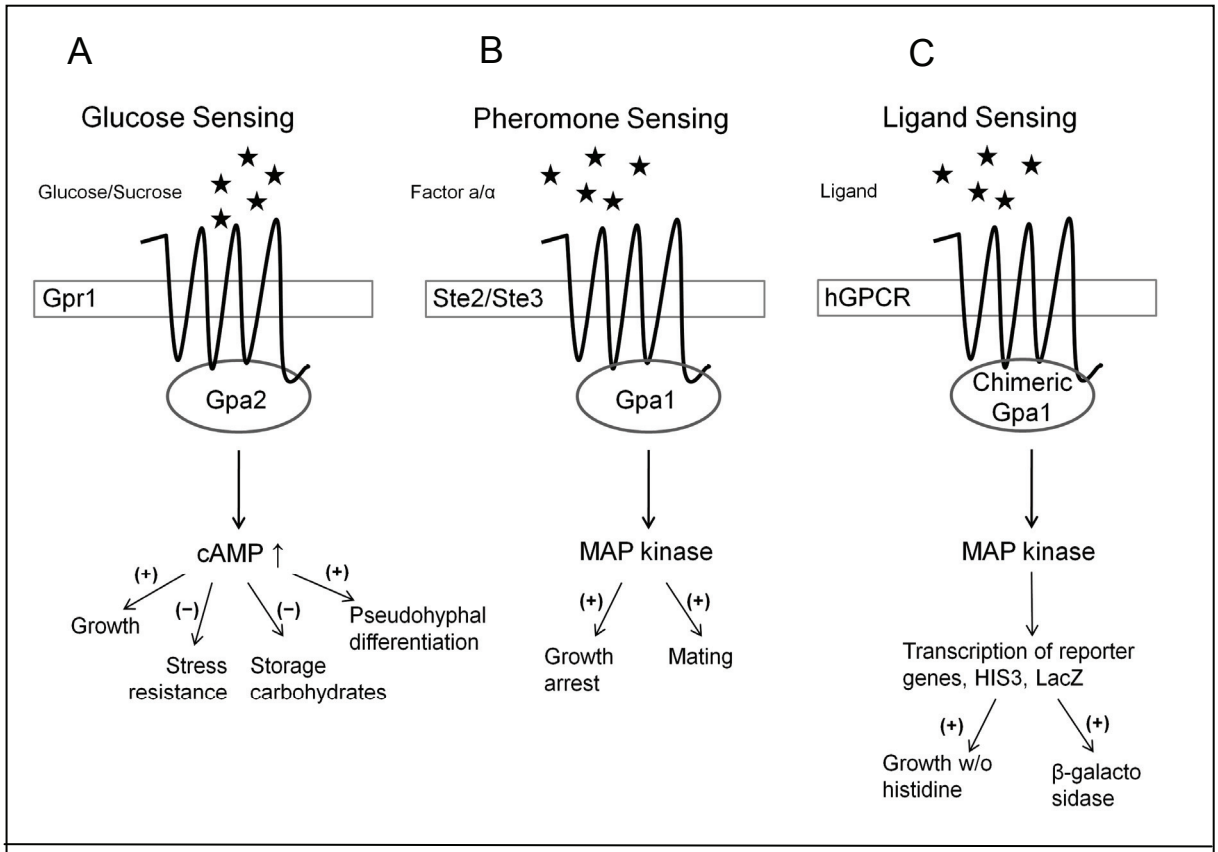

Figure 4. Schematic overview of GPCR signaling in *S. cerevisiae*. (*A*) Signaling pathway of the glucose sensing GPCR Gpr1. (*B*) Signaling pathway of the Mating GPCRs Ste2 and Ste3. (*C*) Signaling pathway in the engineered yeast strain MMY24 expressing a human GPCR.

The general approach is the conversion of a *S. cerevisiae* strain to function as a reporter gene assay [1,44,46]. For this purpose, the pheromone signaling pathway through the Gpa1 G protein is high jacked (**Figure 4**). In order for a human GPCR to take control of the signaling pathway, the endogenous G protein Gpa1 had to be "humanized". This has been accomplished by exchanging the C-terminal end of the yeast Gα protein by the mammalian Gα protein sequence, resulting in a chimeric G protein that is now able to couple to human GPCRs as well as activate the yeast pheromone pathway [32,47]. Activation of the expressed receptor activates the MAP kinase pathway in the same way as the pheromone response and subsequently induces the *FUS1* promoter that leads to the transcription of reporter genes. Several reporter genes can be used for the activation read-out. For instance, the *FUS1-HIS3* reporter gene provides yeast cells the ability to grow on histidine deficient medium upon activation [32]. Similarly, the *FUS1-Hph* reporter gene allows yeast cells containing an activated receptor to grow on hygromycin-containing medium [48]. A reverse growth method is the use of the reporter gene *FUS1-Can1*. Here, an active receptor results in the expression of the Can1 channel that can transport the toxin

canavanine and leads to cell death. This system has been specifically designed to screen for and investigate inactivating mutations in GPCRs [49]. A different non-growth approach is the *FUS1-LacZ* reporter gene that increases the production of the enzyme β-galactosidase when the GPCR is activated. This provides a colorimetric read-out by using chlorophenolred-β-D-galactosidase (CPRG) or *o*-nitrophenyl-β-D-galactopyranoside (ONPG) as substrates for the enzyme. Contrary to the growth read-outs, this method only requires a short response time [32,44].

The yeast strain used in this thesis for the screening approaches as well as the pharmacological studies of the $A_{2B}R$ and A_1R is the MMY24 *S. cerevisiae* strain created by Andrew Brown and Simon Dowell at GlaxoSmithKline [32]. This strain was derived from the MMY11 strain described by Olesnicky and coworkers [47]. The MMY24 yeast strain contains a chimeric Gpa1 G protein of which the last 5 amino acids are from a mammalian $G\alpha_i$ protein. This modification allows both $A_{2B}R$ and A_1R to couple to the yeast pheromone pathway and activate transcription of the reporter genes HIS3 and LacZ that were also incorporated into the genome.

AIM AND OUTLINE OF THIS THESIS

The aim of the work presented in this thesis was to gain insight in the activation mechanism of class A GPCRs, more specifically of the adenosine receptors, and how the extracellular loops are involved in this process. This research was part of the project “GPCR forum for established targets” of Top Institute Pharma (D1-105). This Dutch public-private partnership strives to join forces of industry and academia to speed up the drug research process. At the start of this research project, little was known about the role of the highly variable extracellular loops in receptor activation. The general perception was that one overall activation mechanism should exist among class A GPCRs and that mainly the ligand binding site and the (intracellular) region that couples to the G protein were involved in determining how intracellular signaling pathways are activated. This view changed dramatically over the last years, due to mutagenesis studies and to the elucidation of several high resolution crystal structures of class A GPCRs mentioned before that all show different structural conformations of the extracellular loops.

In **Chapter 2**, we demonstrate the importance of the extracellular loops in receptor activation in a review of the current literature on this subject in which we made use of the structures available at that time.

In the investigation of the activation mechanism of the $A_{2B}R$ and the A_1R, we made use of a wide variety of mutagenesis techniques, combined with screening and pharmacological validation in the expression system *S. cerevisiae*. This approach has proven to be highly successful as we were able to identify several regions and specific residues in the $A_{2B}R$ and the A_1R that are essential for normal receptor function. The results presented in this thesis will greatly help increasing the knowledge on how adenosine receptors are being activated through ligand binding as well as how they maintain their basal or constitutive activation state.

In **Chapter 3**, we reveal an essential role for the first extracellular loop in the adenosine A_{2B} receptor. In particular, two residues, a phenylalanine and an aspartic acid at positions 71 and 74 respectively, proved to be vital in maintaining the tertiary structure of the extracellular domain that is crucial for receptor activation and constitutive activity.

In **Chapter 4**, we describe a random mutagenesis screen in which we selected constitutively active mutant receptors in a fragment of the $A_{2B}R$ involving the transmembrane domains 4 and 5 and the second extracellular loop. Three specific clusters were identified that presumably are responsible for silencing the receptor in its basal state.

In **Chapter 5**, we introduce a new screening method using our MMY24 yeast strain. This screening method makes it possible to select constitutively inactive mutant receptors (CIMs). Applying this method to the adenosine A_{2B} receptor revealed many residues involved in maintaining the equilibrium that exists between the inactive and active conformation.

Chapter 6 discusses another subtype of adenosine receptors, the adenosine A_1 receptor. A mutagenic alanine scanning study on the second and third extracellular loop of this receptor showed a particularly important role for EL2 in receptor activation and even allosteric modulation. This role is opposite to the role seen in the $A_{2B}R$, acting more as a positive rather than a negative regulator of activation.

Chapter 7 will bring the discussions together, comparing the activating and inactivating regions identified in Chapter 4 and 5 and its structural implications as well as reflecting on the clearly different roles of EL2 in receptor activation within the

adenosine receptor subfamily. Also, future perspectives that emerge from the results of this thesis will be presented.

REFERENCES

[1] Beukers, M., IJzerman, A., *Trends Pharmacol Sci.* (2005) 26:533-539.
[2] Hanson, M.A., Stevens, R.C., *Structure* (2009) 17:8-14.
[3] Lane, J.R., Jaakola, V.P., Ijzerman, A.P., *Adv Pharmacol* (2011) 61:1-40.
[4] Deupi, X., Standfuss, J., *Curr Opin Struct Biol* (2011) doi:10.1016/j.sbi.2011.06.002
[5] Fredriksson, R., Lagerstrom, M.C., Lundin, L.G., Schioth, H.B., *Mol Pharmacol* (2003) 63:1256-1272.
[6] Fredholm, B.B., Arslan, G., Halldner, L., Kull, B., Schulte, G., Wasserman, W., *Naunyn Schmiedebergs Arch Pharmacol* (2000) 362:364-374.
[7] Fredholm, B.B., *Cell Death Differ* (2007) 14:1315-1323.
[8] Hasko, G., Linden, J., Cronstein, B., Pacher, P., *Nat Rev Drug Discov* (2008) 7:759-770.
[9] Fredholm, B.B., IJzerman, A.P., Jacobson, K.A., Klotz, K.N., Linden, J., *Pharmacol Rev* (2001) 53:527-552.
[10] Wilson, C.N., *Br J Pharmacol* (2008) 155:475-486.
[11] Spicuzza, L., Di Maria, G., Polosa, R., *Eur J Pharmacol* (2006) 533:77-88.
[12] Fredholm, B.B., IJzerman, A.P., Jacobson, K.A., Linden, J., Muller, C.E., *Pharmacol Rev* (2011) 63:1-34.
[13] Ribeiro, J.A., Sebastiao, A.M., de Mendonca, A., *Prog Neurobiol* (2002) 68:377-392.
[14] Blum, D., Hourez, R., Galas, M.C., Popoli, P., Schiffmann, S.N., *Lancet Neurol* (2003) 2:366-374.
[15] Jaakola, V.P., Griffith, M.T., Hanson, M.A., Cherezov, V., Chien, E.Y., Lane, J.R., IJzerman, A.P., Stevens, R.C., *Science* (2008) 322:1211-1217.
[16] Cherezov, V., et al., *Science* (2007) 318:1258-1265.
[17] Rasmussen, S.G., et al., *Nature* (2007) 450:383-387.
[18] Warne, T., Serrano-Vega, M.J., Baker, J.G., Moukhametzianov, R., Edwards, P.C., Henderson, R., Leslie, A.G., Tate, C.G., Schertler, G.F., *Nature* (2008) 454:486-491.
[19] Xu, F., Wu, H., Katritch, V., Han, G.W., Jacobson, K.A., Gao, Z.G., Cherezov, V., Stevens, R.C., *Science* (2011) 332(6027):322-327.
[20] Lebon, G., Warne, T., Edwards, P.C., Bennett, K., Langmead, C.J., Leslie, A.G., Tate, C.G., *Nature* (2011) 474:521-525.
[21] Martinelli, A., Tuccinardi, T., *Med Res Rev* (2008) 28:247-277.
[22] Heilker, R., Wolff, M., Tautermann, C.S., Bieler, M., *Drug Discov Today* (2009) 14:231-240.
[23] Cotecchia, S., Exum, S., Caron, M.G., Lefkowitz, R.J., *Proc Natl Acad Sci U S A* (1990) 87:2896-2900.
[24] Ahn, K.H., Bertalovitz, A.C., Mierke, D.F., Kendall, D.A., *Mol Pharmacol* (2009) 76:833-842.
[25] Li, J.H., Hamdan, F.F., Kim, S.K., Jacobson, K.A., Zhang, X., Han, S.J., Wess, J., *Biochemistry* (2008) 47:2776-2788.
[26] Unal, H., Jagannathan, R., Bhat, M.B., Karnik, S.S., *J Biol Chem* (2010) 285:16341-16350.
[27] Olah, M.E., *J Biol Chem* (1997) 272:337-344.
[28] Klco, J., Nikiforovich, G., Baranski, T., *J Biol Chem.* (2006) 281:12010-12019.
[29] Scarselli, M., Li, B., Kim, S., Wess, J., *J Biol Chem.* (2007) 282:7385-7396.
[30] Fromant, M., Blanquet, S., Plateau, P., *Anal Biochem* (1995) 224:347-353.
[31] Beukers, M., van Oppenraaij, J., van der Hoorn, P., Blad, C., den Dulk, H., Brouwer, J., IJzerman, A., *Mol Pharmacol.* (2004) 65:702-710.
[32] Brown, A., et al., *Yeast* (2000) 16:11-22.
[33] Leff, P., *Trends Pharmacol Sci* (1995) 16:89-97.
[34] Cotecchia, S., Fanelli, F., Costa, T., *Assay Drug Dev Technol.* (2003) 1:311-316.
[35] Tao, Y.X., *Pharmacol Ther* (2006) 111:949-973.
[36] Kleinau, G., Jaeschke, H., Mueller, S., Worth, C.L., Paschke, R., Krause, G., *Cell Mol Life Sci* (2008) 65:3664-3676.
[37] Parnot, C., Miserey-Lenkei, S., Bardin, S., Corvol, P., Clauser, E., *Trends Endocrinol Metab.* (2002) 13:336-343.

[38] Klco, J., Wiegand, C., Narzinski, K., Baranski, T., *Nat Struct Mol Biol.* (2005) 12:320-326.
[39] Inoue, Y., Ikeda, M., Shimizu, T., *Comput Biol Chem* (2004) 28:39-49.
[40] Bockaert, J., Pin, J.P., *Embo J* (1999) 18:1723-1729.
[41] Versele, M., Lemaire, K., Thevelein, J.M., *EMBO Rep* (2001) 2:574-579.
[42] Gancedo, J.M., *FEMS Microbiol Rev* (2008) 32:673-704.
[43] Lemaire, K., Van de Velde, S., Van Dijck, P., Thevelein, J.M., *Mol Cell* (2004) 16:293-299.
[44] Minic, J., Sautel, M., Salesse, R., Pajot-Augy, E., *Curr Med Chem* (2005) 12:961-969.
[45] Ladds, G., Goddard, A., Davey, J., *Trends Biotechnol* (2005) 23:367-373.
[46] Dowell, S.J., Brown, A.J., *Receptors Channels* (2002) 8:343-352.
[47] Olesnicky, N.S., Brown, A.J., Dowell, S.J., Casselton, L.A., *Embo J* (1999) 18:2756-2763.
[48] Pajot-Augy, E., Crowe, M., Levasseur, G., Salesse, R., Connerton, I., *J Recept Signal Transduct Res* (2003) 23:155-171.
[49] Li, B., Scarselli, M., Knudsen, C., Kim, S., Jacobson, K., McMillin, S., Wess, J., *Nat Methods.* (2007) 4:169-174.

CHAPTER 2

IMPORTANCE OF THE EXTRACELLULAR LOOPS IN G PROTEIN-COUPLED RECEPTORS FOR LIGAND RECOGNITION AND RECEPTOR ACTIVATION

This chapter was based upon:

M.C. Peeters, G.J.P. van Westen, Q. Li, A.P. IJzerman. Trends in Pharmacological Sciences **2011**, 32(1):35-42.

ABSTRACT

G protein-coupled receptors (GPCRs) are the major drug target of today's medicines. Therefore, much research is and has been devoted to the elucidation of the function and three-dimensional structure of this large family of membrane proteins, which includes multiple conserved transmembrane domains connected by intra- and extracellular loops. In the last few years the less conserved extracellular loops are becoming of increasing interest, particularly after the publication of several GPCR crystal structures that clearly show the extracellular loops are involved in ligand binding. This review will summarize the recent progress made in the clarification of the ligand binding and activation mechanism of class A GPCRs and the role of the extracellular loops in this process.

INTRODUCTION

G protein-coupled receptors (GPCRs) form a large family of transmembrane proteins that convey an extracellular signal as exerted by a hormone or neurotransmitter to an intracellular response through G proteins. They all have a similar structure, with an extracellular N-terminus, 7 transmembrane helices connected by three extracellular (EL1-3) and three intracellular loops (IL1-3), and an intracellular C-terminus. The GPCR super-family consists of five main classes, of which the class A (or rhodopsin-like) GPCRs form by far the largest subfamily [1]. Next to the N- and C-terminus, the extracellular loops of GPCRs are the most variable structural elements of the receptor, differing greatly in both length and sequence. Even within subfamilies, the extracellular loops often show low sequence homology, if any at all. Also, the early data on receptor architecture stemming from bacterio rhodopsin and bovine rhodopsin provided limited and incomplete information regarding these more flexible GPCR domains. This data paucity and ambiguity meant that structural studies of receptor function and activation (through e.g. mutagenesis) focused on the more conserved and better characterized regions of the receptor such as the transmembrane domains [2]. As a consequence, the average ‘textbook model’ states that mainly two domains are determinants for receptor activation, i.e. the region where the ligand binds and the domain that interacts with the G protein. In this view, the extracellular loops are mainly regarded as peptide linkers to hold the functionally important transmembrane helices together and keep these stably positioned in the cell membrane. However, over the last decade, it has become clear that the extracellular loops fulfill important functional roles in receptor activation and in ligand binding. For example, quite a number of somatic mutations in the loops have been linked to disease [3,4,5]. Therefore, the purpose of this review is to provide evidence that these neglected receptor domains are vital for proper receptor recognition and function.

EXTRACELLULAR LOOPS AS SEEN IN THE CRYSTAL STRUCTURES

GPCR crystallization is extremely challenging. There are at least two reasons for that: GPCRs are unstable outside the cell membrane and they are known to adopt many conformational states. The relatively unstructured loops add to the conformational diversity. This combination of fragility and flexibility is a major hurdle in obtaining good-quality crystals. Nevertheless, we now have access to a handful of GPCR structures [6]. From these structures it is apparent that the extracellular regions can indeed adopt very different structural forms (**Figures 1 and 2**); in particular the unique topologies of the second extracellular loop (EL2) are striking. In rhodopsin, EL2 dives deep into the ligand binding cavity, completely shielding the binding site from solvent access [7]. Within the loop itself, a β-hairpin is present, which together with the N-terminus, forms a four-stranded β-sheet with additional interactions between EL3 and EL1 [8]. In both the β_1- and the β_2-adrenergic receptors, EL2 shows a more open conformation, contains a small α-helix and is given extra rigidity by an intra-loop disulfide bridge [9,10]. The adenosine A_{2A} receptor shows a third structural feature, where EL2 forms an anti-parallel β-sheet with the first extracellular loop and is mainly constrained by the formation of three disulfide bridges with EL1. This anti-parallel β-sheet also causes EL1 to bend more towards EL2 than is seen in the other structures (**Figures 1 and 2**). EL2 has not been completely resolved in the adenosine A_{2A} receptor structure, emphasizing the great flexibility EL2 has, despite the restricting structural features. In addition, a non-conserved disulfide bridge is found within EL3 [11]. Very recently the crystal structure of another GPCR, the chemokine receptor CXCR4, was elucidated by Stevens and coworkers [12]. The authors managed to obtain two separate structures of this chemokine receptor subtype; one with a peptide antagonist bound, the other with a small molecule antagonist. The extracellular region of these structures adapts another, more open, conformation (**Figure 2**). EL2 contains an anti-parallel β-sheet within the loop that can be extended with another strand in the peptide when it is bound to the receptor. The conserved disulfide bridge connects the anti-parallel β-sheet in EL2 with the top of TM3. An additional disulfide bridge can be found between EL3 and the N-terminus. It is here, between the N-terminus and EL2, that the peptide ligand is bound. The small molecule ligand occupies the same binding pocket as the peptide ligand, filling only the deeper part of the binding site. The

presence of the additional disulfide bridge and the extended helix of TM6 make EL3 to be differently positioned compared to the other three structures (**Figure 1**).

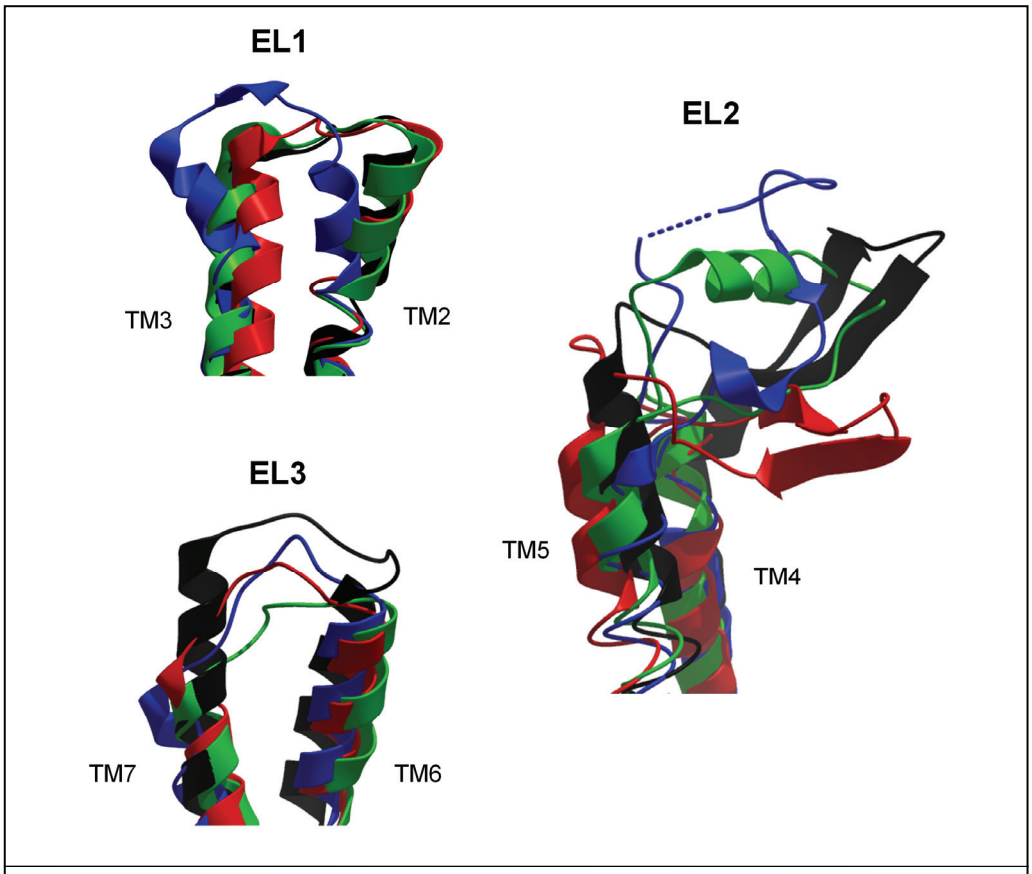

Figure 1. Overlay of extracellular loops of the crystal structures of the β2-adrenergic receptor (green) (PDB: 2RH1), the adenosine A_{2A} receptor (blue) (PDB: 3EML),CXCR4 (black) (PDB: 3ODU), and bovine rhodopsin (red) (PDB: 1U19). The transmembrane helices were superimposed by the backbone of the upper 17 amino acids in each helix while leaving the extracellular loops free during superposition. The superposition was created with Molsoft ICM version 3.6-1 h. The resulting figure shows the different orientation and structure of the loops between the four receptors.

Most GPCRs are expected to have disulfide bridges at their extracellular surfaces, possibly rigidifying the extracellular domains and providing structure to the receptor. It is interesting to note that in the A_{2A} receptor structure all available cysteines in the three extracellular loops are indeed involved in bridge formation. The most conserved disulfide bridge, between the third transmembrane domain and the second extracellular loop, is present in almost all class A GPCRs [7]. The formation of extra disulfide bridges may be an important general mechanism for regulating the activity of GPCRs [13]. Mutagenesis studies of extracellular cysteines have shown that these non-conserved residues are not always essential for receptor structure or binding; however, they might be important in other aspects, e.g. the kinetics of ligand binding

[13,14]. Worth and coworkers have recently listed all structural features present in the crystal structures in the transmembrane domains and the loops [15].

THE FIRST EXTRACELLULAR LOOP PROVIDES STRUCTURE TO THE EXTRACELLULAR COMPLEX

The first extracellular loop of class A GPCRs is usually very small, consisting of only a few amino acids. As in all three loops, its amino acid sequence is highly variable among family members. However, the length of the first extracellular loop is highly conserved (**Figure 3**), with over 70% of class A GPCRs having 52 amino acids separating the two most conserved residues in helices 2 and 3 (2.50 and 3.50) according to Ballesteros and Weinstein notation [16]. Similar analyses on other GPCR families showed that the EL1 of class C GPCRs is also highly conserved in length, with only one amino acid difference between the longest and smallest loop. Interestingly, among class B GPCRs, the first extracellular loop is highly divergent. It is even more variable in length than the second extracellular loop, which is the most divergent loop in class A GPCRs.

Even though EL1 is quite small and not directly involved in the binding of small ligands, several reports mention that the loop influences the shape of the binding pocket [17,18,19,20,21]. Together with other extracellular regions, the loop can provide rigidity and structure essential in receptor activation. Härterich et al. described an aromatic π-stacking region in the neurotensin 1 receptor that provides rigidity to the loop, keeping TM2 and TM3 together. Disturbance of the π-π interactions between aromatic residues within EL1 interfered with receptor activation and strongly reduced ligand binding [18]. A recent mutagenesis study of the neuropeptide S receptor showed that polar residues within the loop seem especially to influence receptor conformation [17]. This had been observed previously in the CCR2 receptor, where an asparagine and a glutamic acid residue were found to be essential for high affinity binding [22]. Charged residues in the loop were suggested to be important in vasopressin receptor activation; in particular, the positive charge of an arginine residue appeared required for stabilizing the active conformation of the receptor [23]. Very recently, two residues in EL1 of the M_4 muscarinic acetylcholine receptor, an isoleucine and a lysine, were identified as important for the signaling efficacy of the allosteric agonist LY2033298. This indicates that EL1 might also

influence signaling originating from a site distinct from the orthosteric binding site [24].

In contrast to most class A GPCRs, the binding site of receptors that bind large protein ligands is most likely found predominantly at the extracellular surface of the receptor. The large N-terminal part of glycoprotein hormone receptors may form the main contact for binding the hormones, as suggested from the crystal structure of the N-terminal domain of the follicle stimulating hormone receptor (FSHR) with its ligand [25]. In another study, the authors concluded that the extracellular loops in the thyroid stimulating hormone receptor (TSHR) work closely together in activation, as shown in the combined action of constitutively active mutants (CAMs) in these regions of the receptor. The strongest influence on the combined signaling activity was provided by EL1 [26]. The first extracellular loop might also contact (peptide) ligands directly. An indication for this was recently shown by a photo-affinity labeling study of the angiotensin II type 1 receptor (AT_1R). For this research, the authors labeled each consecutive residue of the endogenous ligand AngII with a photo-reactive label that can form a covalent complex with the site of interaction at the receptor. They found that the N-terminal part of AngII simultaneously interacts with several regions of the AT_1R, including the N-terminal domain and EL1 [21].

WXFG and DXXCR motifs in EL1

Two conserved structural motifs, WXFG and DXXCR, were identified within the first extracellular loop. The WXFG motif was first described by Klco et al. [19] and is present in 80% of class A GPCRs, including rhodopsin and the β-adrenergic receptors. Interestingly, the adenosine A_{2A} receptor is one of the few receptors that does not contain the WXFG motif. Several studies have shown that mutations in the WXFG motif disrupt receptor activation but not ligand binding [17,19,23]. Klco et al. [19] propose that the WXFG motif may be important in translating the ligand-binding signal directly to movements within the TM bundle. In addition, the motif might play a role in regulating the percentage of receptors that are in the high affinity ligand binding state. In the angiotensin II receptor, the WXFG motif has been postulated to form a type II β-turn that is involved in angiotensin II binding [27]. The second motif, DXXCR, is located in the carboxyl-terminal part of EL1 at the interface with TM3 and is highly conserved among peptidergic GPCRs. This region is probably engaged in

the formation of the classical disulfide bond with EL2 and has been shown to be involved in signal transduction and receptor activation in the V_{1A} vasopressin receptor [23,28]. In marked contrast, GPCRs that bind aminergic ligands, favour a negative charge (D or E) in the last position of the motif [23].

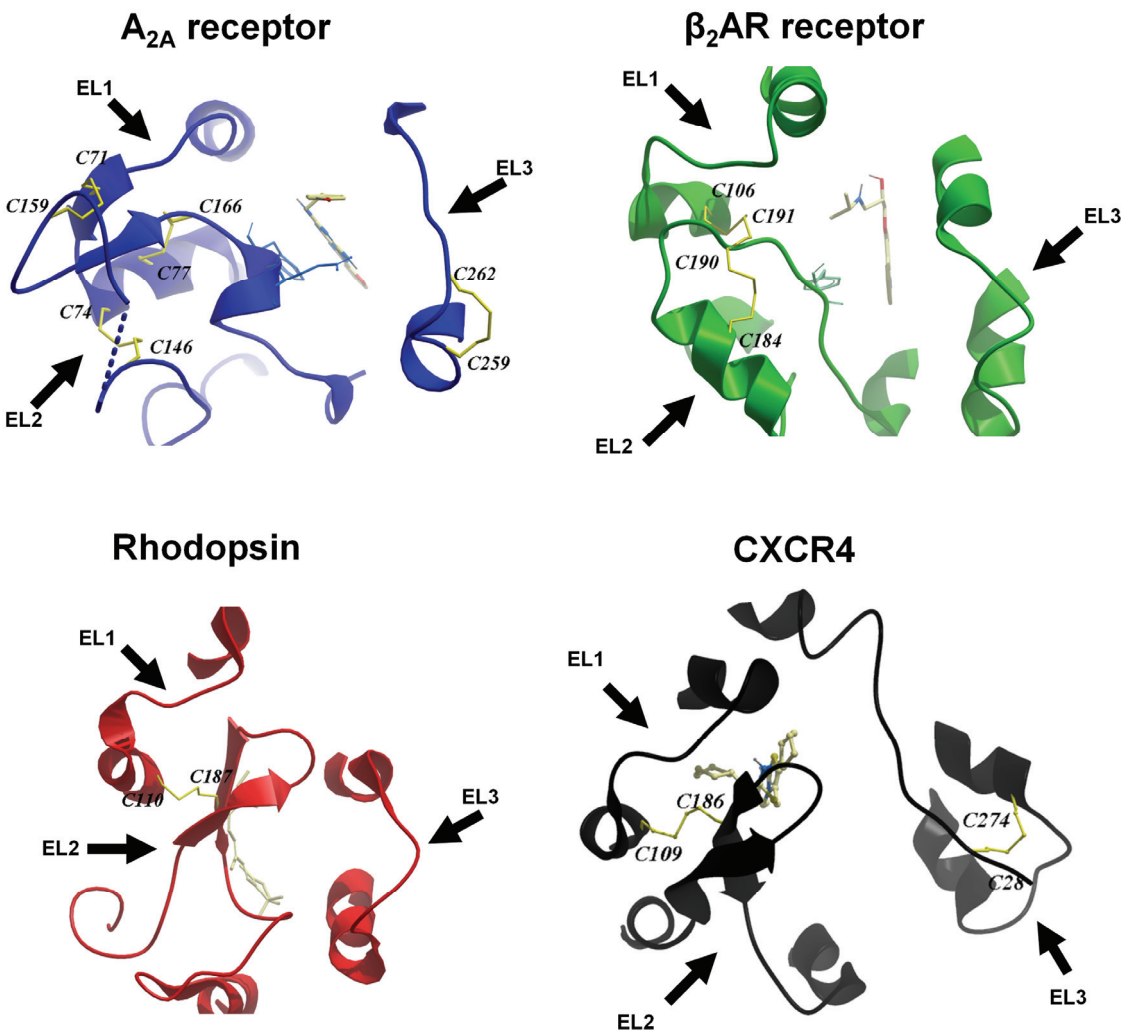

Figure 2. Top view of the crystal structures of the adenosine A_{2A} receptor (blue) (PDB: 3EML), the β2-adrenergic receptor (green) (PDB: 2RH1), CXCR4 (black) (PDB:3ODU), and bovine rhodopsin (red) (PDB: 1U19). The crystal structures are positioned so that all three extracellular loops are in view with their structural features (ribbons), the disulfide bridges (yellow), and the ligand bound in the ligand binding pocket. The conserved cysteine bridge between EL2 and TM3 is seen in all four structures: in the A_{2A} receptor betwee Cys77 and Cys166; in the β2-adrenergic receptor between Cys106 and Cys191; in CXCR4 between Cys 109 and Cys186; and in rhodopsin between Cys110 and Cys187. The figure was created with Molsoft ICM version 3.6-1 h.

AN ALL-ENCOMPASSING ROLE FOR THE SECOND EXTRACELLULAR LOOP (EL2)

The second extracellular loop in class A GPCRs is the largest and most divergent of the three. Both in length and in sequence, it can differ greatly even within subfamilies (**Figure 3**). In class B and C GPCRs, this difference in length is much less pronounced. These families are much smaller than class A GPCRs, especially family C only consists of 23 human receptors. The receptors in class B and C GPCRs all have large N-termini that mainly determine ligand selectivity between receptors. In class A GPCRs, EL2 might be associated with ligand selectivity, which would explain their large variety. Contrary to the concept that 'more conserved means more important', the second extracellular loop has been reported to be essential in normal receptor behaviour. EL2 is often the site for glycosylation; over 32% of class A GPCRs possess at least one consensus N-glycosylation site in the second extracellular loop [29]. Glycosylated or not, EL2 is thought to play a role in receptor structure, signaling, and ligand recognition, as well as ligand binding, both orthosteric and allosteric. Constraining the loop seems to be essential for receptor activation among all class A GPCRs, because disturbance of the conserved disulfide bridge between EL2 and TM3 largely diminishes receptor function [30].

EL2 as a "gatekeeper"

Despite the presence of a restricting disulfide bridge, the second extracellular loop needs a certain amount of conformational flexibility for efficient receptor activation [31,32,33]. In the M_2 muscarinic acetylcholine receptor, constraining EL2 loop flexibility by introducing extra disulfide bridges between the loop and TM7 had a profound inhibitory effect on intracellular signaling [31]. Forcing the EL2 of the receptor into a "locked" state impeded the binding of orthosteric ligands and, interestingly, had a great influence on the binding kinetics in both reducing association and dissociation rates [31,34]. The loop might adopt different conformations during the activation mechanism, starting with an open conformation to enable the entry of the ligand. After the ligand has moved into the binding site within the transmembrane helices, EL2 closes over the ligand and is further stabilized by engaging in additional interactions [31,35]. The stability and orientation of the EL2 lid is dependent on the extreme ends of the loop, though glycosylation sites within

the loop may also determine its positioning [29]. The proposed change from an open to a closed conformation was recently corroborated by cysteine scanning studies on the angiotensin II type I receptor. Cysteines introduced in two segments of EL2 were accessible by the cysteine-reactive biotin probe from the extracellular environment in the empty receptor, indicating the open conformation. These segments, positioned on either side of the conserved cysteine, were inaccessible when an agonist or antagonist was bound to the receptor. The residues that were inaccessible in the open conformation might regulate low basal activity of the ligand-free receptor [34]. Sum et al. suggested the presence of ionic locks at the extracellular surface, similar to the one seen at the cytoplasmic region of the crystal structure of rhodopsin [7,36]. These locks between EL2 and TM5 and between EL2 and TM7, would keep the receptor in its basal inactive state and cause constitutive activity when disturbed [36]. Klco et al. performed saturation mutagenesis of the complement factor 5a receptor (C5aR) that revealed many constitutively active mutant receptors. These results led to the conclusion that EL2 is a negative regulator of the receptor that keeps the receptor in a silent state prior to agonist-induced activation [33,37]. Also, alanine-scanning mutagenesis of the M_1 muscarinic acetylcholine receptor revealed that the access of ligands to the binding site was increased by mutation of EL2 residues [38]. Contrary to these findings, several other EL2 mutagenesis studies did not yield constitutively active mutants. However, also in these studies, specific residues that were shown to be important in stabilizing the active conformation of the receptor were identified [32,39].

The recent advances in nuclear magnetic resonance (NMR) technology enable us to look more closely at protein dynamics and structure and will help us greatly in unraveling conformational changes during receptor activation. So far, no whole GPCR structure has been resolved by NMR. However, parts of the receptor, including the extracellular regions, have been elucidated which provided similar results to what is seen in the crystal structures [40]. In crystallography the receptor structures are highly constrained due to crystal packing. This is not so much the case in NMR spectroscopy, rendering it possible to gain insight in receptor dynamics and activation. Solid state NMR studies revealed that EL2 of rhodopsin might form a reversible gate that opens during the activation process. Upon activation, a coupling between movements of EL2 and TM5 has been observed, as well as a rearrangement in the hydrogen-bonding networks connecting EL2 with the

extracellular ends of TM4, TM5, and TM6 [41]. Even more recently, Bokoch et al. used NMR spectroscopy to investigate ligand-specific conformational changes around a salt bridge in the β_2-adrenergic receptor that links EL2 with EL3. They were able to detect a relative motion between EL3-TM7 and EL2 upon ligand binding and to distinguish three different conformations of the extracellular surface: a ligand-free/antagonist, an inverse agonist, and an agonist conformation [42].

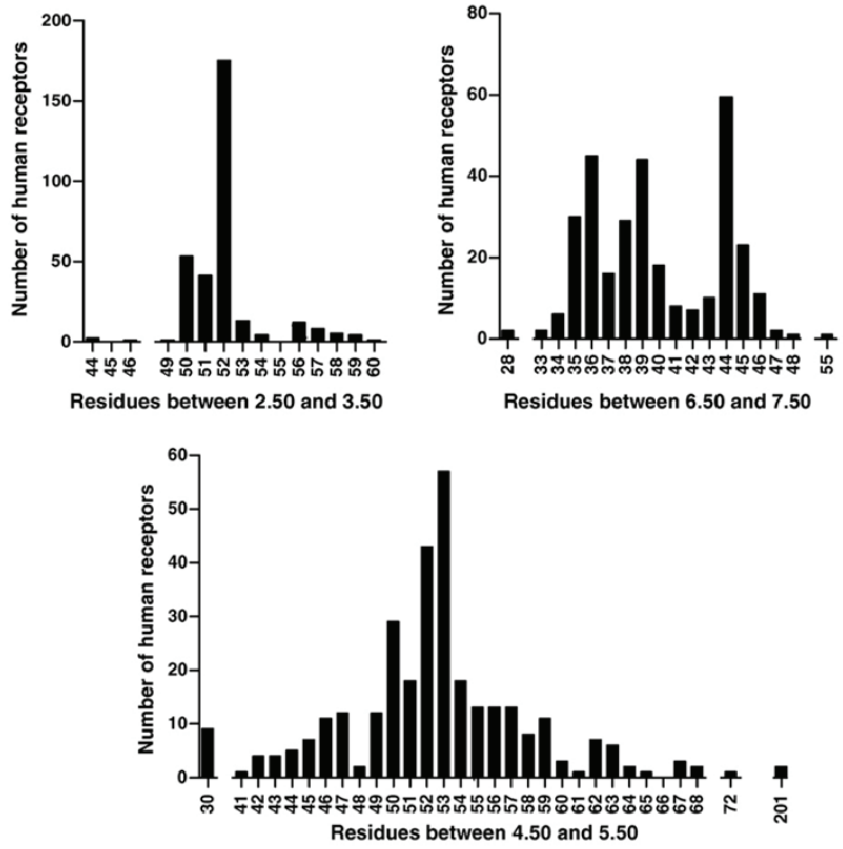

Figure 3. Distribution of the length of the extracellular loops among Class A GPCRs. The distance between the conserved Ballesteros and Weinstein marks in the transmembrane domains that are connected by the extracellular loops were taken as a measure for the distribution of the length of the loops. The distance between positions 2.50 and 3.50 was calculated for EL1, between 4.50 and 5.50 for EL2, and between 6.50 and 7.50 for EL3. The graph represents all human Class A GPCRs present in the GPCRDB (http://www.gpcr.org/7tm/), with on the x-axes the distance between the conserved marks. The average number of amino acids between the marks is 52 ± 2 (EL1), 53 ± 13 (EL2), and 40 ± 4 (EL3).

EL2 in ligand recognition and binding

The second extracellular loop can contribute to the specificity of ligand binding by directly forming part of the ligand binding cavity. This had been shown in studies on ligand selectivity in aminergic and other small molecule binding GPCRs [30,31,32,37,43]. Direct interactions of EL2 with the bound ligand are observed in the crystal structures, in which the EL2s interact directly with the ligand by a phenylalanine in the centre of the loop [7,9,10,11]. In the structure of the adenosine A_{2A} receptor, a glutamic acid residue in EL2 also contributes to the ligand binding pocket (**Figure 2**) [11]. The newest crystal structure of CXCR4 is an exception. The ELs shape the binding pocket with electrostatic and hydrophobic interactions, but no direct contact is made with the small ligand. The peptide ligand does form hydrogen bond connections with the EL2 backbone residues Asp187 and Tyr190. Also, the peptide forms a β-strand that extends the β-sheet present in EL2 [12]. The agonist binding pocket is most likely different from the antagonist binding domain, but considerable overlap should exist between the different cavities with EL2 as a participant. Consistent with this suggestion, mutagenesis studies of the prostacyclin receptor showed distinct but also overlapping residues in EL2 that are important for agonist and antagonist recognition [44]. EL2 was identified in the gonadotropin releasing hormone (GnRH) receptor, the cannabinoid 1 receptor and the adenosine receptors as a determinant in recognizing a ligand as an agonist, antagonist, or inverse agonist. In particular, the C-terminal part of the loop appears to influence the signaling ability of a ligand [20,45,46,47].

EL2 might also be an important determinant in subtype selectivity of ligands. The bound antagonist in the crystal structure of the adenosine A_{2A} receptor, ZM241385, is clearly protruding out of the transmembrane regions into the extracellular domain with a long side chain (**Figure 4**). Structure-activity relationship (SAR) studies performed in our laboratory revealed that smaller substituents at this part of the ligand greatly reduced the A_{2A} receptor selectivity [48]. The conformation EL2 can adopt to accommodate these large side chains might be receptor-specific and can be used in the design of subtype-selective ligands.

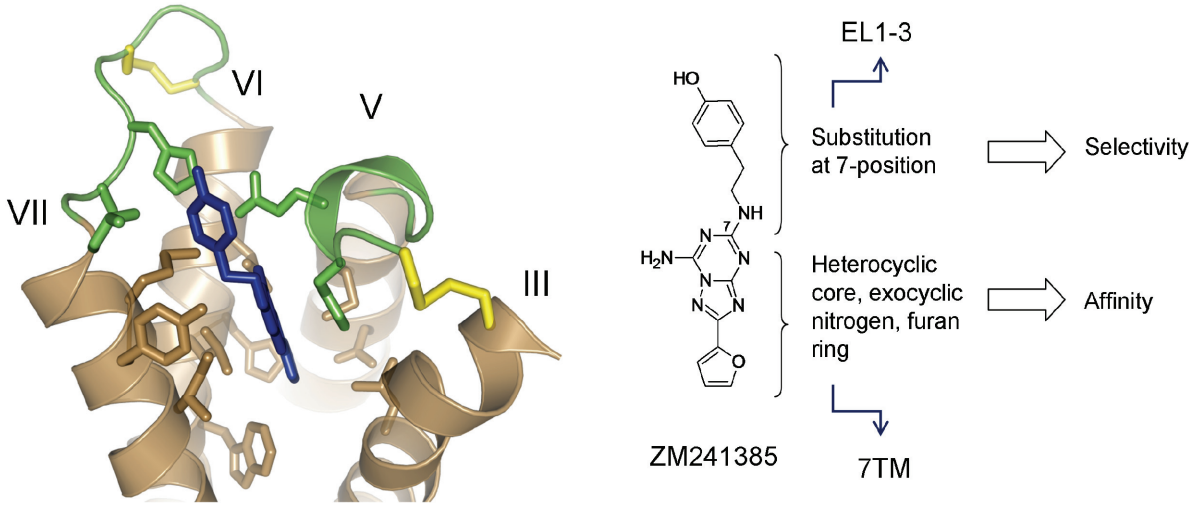

Figure 4. The binding pose of ZM241385 in the adenosine A_{2A} receptor crystal structure. Tan: TM domains, green: EL domains, yellow: disulfide bridges, blue: ZM241385. For clarity only helices III, V, VI and VII are shown, as they make up most of the binding site. The 4-hydroxyphenylethylamine side chain of ZM241385 interacts with the extracellular loops and is largely responsible for receptor subtype selectivity, whereas the rest of the ligand molecule is located within the TM domains of the receptor.

EL2 in allosteric modulation

GPCRs are subject to allosteric modulation [35], suggesting the presence of ligand binding sites other than the orthosteric site. These alternative binding sites are able to bind non-endogenous molecules in a specific manner and can influence the binding and function of an orthosteric ligand (e.g., a neurotransmitter or hormone). Allosteric binding sites may be found in non-conserved receptor regions that originated by chance during evolution. Therefore, it is entirely feasible that such binding pockets may be found at the extracellular surface of the receptor. The muscarinic acetylcholine receptors (mAChR) have been studied most in the search for binding sites of allosteric modulators in GPCRs. Several residues in EL2 have been shown to contribute to the allosteric binding of prototypical mAChR modulators, in particular the EDGE motif centrally located in the loop of the M_2 mAChR [31,49]. Also, a phenylalanine in EL2 of the M_4 mAChR has been shown to interact with the allosteric agonist LY2033298, whereas it did not influence binding of orthosteric agonists [24]. In a recent study on the adenosine A_1 receptor, bivalent ligands were used that connect an orthosteric ligand with an allosteric modulator to probe the location of the allosteric site relative to the orthosteric site. The authors speculated that the allosteric binding site of the adenosine A_1 receptor is located within the

boundaries of the second extracellular loop [50]. The ability of many modulators to slow down orthosteric ligand dissociation has been explained by a “capping” mechanism of the EL2 lid, stabilizing its closure [30,31,51].

THE THIRD EXTRACELLULAR LOOP (EL3) INFLUENCES LIGAND BINDING AND ACTIVATION

The third extracellular loop (EL3) is perhaps the least investigated of the three loops. Like EL1, it is small in all class A GPCRs (**Figure 3**). This is also the case in class B and class C GPCRs. Nonetheless, the third extracellular loop has been proposed to be important in GPCR signaling [19,26,52]. Claus et al. identified the presence of a hydrophobic cluster of amino acid residues within EL3 of the thyrotropin receptor that strongly influences signal transduction and G protein activation [53]. This confirmed the earlier described presence of such a hydrophobic cluster in EL3 of the δ-opioid receptor, in which it was suggested to form a hairpin-like structure essential in the early steps of receptor activation [39]. Claus et al. also showed evidence supporting an interaction between EL2 and EL3 in the form of a hydrogen bond that is necessary for proper folding and signaling of the receptor [53]. An interaction between aromatic residues in EL2 and EL3 has recently been proposed to play a key role for allosteric/orthosteric binding and activation cooperativity in the muscarinic M_2 acetylcholine receptor [49,51]. One particular residue in EL3 of the human M_4 mAChR, D432, appears to be involved in the functional cooperativity between the allosteric modulator and the endogenous agonist [24]. EL3 has been shown to form interactions with other extracellular regions as well; in rhodopsin, EL3 is connected to the N-terminal domain through hydrogen bonds with the oligosaccharide chain on N2 [7]. In the angiotensin II receptor, a cysteine bridge seems to link the two domains together. Such interactions must be receptor-specific as the presence of cysteine residues and glycosylation patterns vary considerably [52].

For the neurotensin 1 receptor, the urotensin receptor and the CC chemokine 2 receptor (CCR2), EL3 has been suggested to be part of the ligand binding site that is supposed to form a tunnel between EL3, TM6 and TM7 [18,20,54,55]. The crystal structure of the chemokine receptor CXCR4 indeed shows that EL3, together with the N-terminus, shapes the entrance to the ligand-binding pocket [12]. In the structure of

the adenosine A_{2A} receptor, a histidine in EL3 and a leucine at the interface between EL3 and TM7 are in close proximity to the bound ligand ZM241385 [11].
These results clearly imply an important role of the third extracellular loop in GPCR function. It has yet to be determined whether EL3 individually is essential in ligand binding and receptor activation, or whether it is a vital and integral part of the extracellular domain.

ANTIBODIES AGAINST THE EXTRACELLULAR LOOPS

Many commercially available monoclonal antibodies for GPCRs are raised against epitopes located at the extracellular surface of the receptor, most often EL2. However, these antibodies frequently are receptor conformation-dependent and have met with limited success, for example in immuno-histochemistry [56]. Owing to subtle changes in receptor conformation, segments of the loop become more or less accessible. If the flexible EL2 moves to interact with the ligand, then the necessary epitopes for antibody recognition are potentially shielded [34,56,57]. The changes in receptor conformation may also explain how auto-antibodies against human GPCRs are involved in auto-immune diseases, such as preeclampsia and malignant hypertension [34,56,58]. These endogenous antibodies functionally interfere with the target, showing an agonist-like effect and thus also contribute to changes in receptor conformation. Several reports have also described monoclonal antibodies directed against EL2 of the M_2AChR and the β_2-adrenergic receptor with functional effects, acting as agonists or inverse agonists [59,60,61].

CONCLUSION: A CLOSE COLLABORATION AMONG THE EXTRACELLULAR LOOPS

All three extracellular loops are relevant for the activation mechanism of class A GPCRs. EL1 probably provides structure to the extracellular region of the ligand binding site and enables movement of the transmembrane helices upon ligand binding. EL2 seems to play the most important role in activation, because it is involved in direct ligand binding, ligand recognition and ligand entry. It might also host allosteric binding sites. EL3 seems essential for proper folding and signaling of

the receptor, might be a binding site itself, and may also contribute to allosteric binding sites. However, the strength of the extracellular loops lies in their collaboration. Proper receptor activation appears to be greatly dependent on a complex network of interactions at the extracellular region that recognizes and transmits the initial activation signals. The extracellular region should be looked at as a whole, in which the extracellular loops together provide structure and cooperative signal triggering that is required for full receptor activation [26].

Although all loops play an important role in the activation mechanism of GPCRs, details of their mode of action may differ among the family members. The great divergence of the loops and their flexibility provide each receptor with its own structural interactions and conformations to reach selectivity and specificity in binding their ligands and subsequent signaling.

In conclusion, the complex intra- and intermolecular interactions that develop and wane over time at the extracellular region of class A GPCRs, are vital for receptor activation as well as ligand binding.

ACKNOWLEDGEMENTS

The authors are grateful for the financial support by the Dutch Top Institute Pharma (project D1-105). They are very thankful to Prof. Stevens from the Department of Molecular Biology at The Scripps Research Institute (USA) for providing us with the coordinates of the CXCR4 crystal structure ahead of publication. They thank Bas Vroling and the GPCRDB (http://www.gpcr.org/7tm/) for help with the bioinformatics and Veli-Pekka Jaakola for providing Figure 4.

REFERENCES

[1] Fredriksson, R., Lagerstrom, M.C., Lundin, L.G., Schioth, H.B., *Mol Pharmacol* (2003) 63:1256-1272.
[2] Costanzi, S., Siegel, J., Tikhonova, I.G., Jacobson, K.A., *Curr Pharm Des* (2009) 15:3994-4002.
[3] Schoneberg, T., Schulz, A., Biebermann, H., Hermsdorf, T., Rompler, H., Sangkuhl, K., *Pharmacol Ther* (2004) 104:173-206.
[4] Tao, Y.X., *Pharmacol Ther* (2006) 111:949-973.
[5] Insel, P.A., Tang, C.M., Hahntow, I., Michel, M.C., *Biochim Biophys Acta* (2007) 1768:994-1005.
[6] Jaakola, V.P., IJzerman, A.P., *Curr Opin Struct Biol* (2010) 20:1-14.

[7] Palczewski, K., et al., *Science* (2000) 289:739-745.
[8] Hanson, M.A., Stevens, R.C., *Structure* (2009) 17:8-14.
[9] Rosenbaum, D.M., et al., *Science* (2007) 318:1266-1273.
[10] Warne, T., Serrano-Vega, M.J., Baker, J.G., Moukhametzianov, R., Edwards, P.C., Henderson, R., Leslie, A.G., Tate, C.G., Schertler, G.F., *Nature* (2008) 454:486-491.
[11] Jaakola, V.P., Griffith, M.T., Hanson, M.A., Cherezov, V., Chien, E.Y., Lane, J.R., IJzerman, A.P., Stevens, R.C., *Science* (2008) 322:1211-1217.
[12] Wu, B., et al., *Science* (2010) 330:1066-1071.
[13] Storjohann, L., Holst, B., Schwartz, T.W., *Biochemistry* (2008) 47:9198-9207.
[14] Scholl, D.J., Wells, J.N., *Biochem Pharmacol* (2000) 60:1647-1654.
[15] Worth, C.L., Kleinau, G., Krause, G., *PLoS One* (2009) 4(9):e7011.
[16] Ballesteros, J.A., Weinstein, H., *Methods Neurosci* (1995) 25:366–428.
[17] Clark, S.D., Tran, H.T., Zeng, J., Reinscheid, R.K., *Peptides* (2010) 31:130-138.
[18] Härterich, S., Koschatzky, S., Einsiedel, J., Gmeiner, P., *Bioorg Med Chem* (2008) 16:9359-9368.
[19] Klco, J., Nikiforovich, G., Baranski, T., *J Biol Chem.* (2006) 281:12010-12019.
[20] Nygaard, R., Frimurer, T.M., Holst, B., Rosenkilde, M.M., Schwartz, T.W., *Trends Pharmacol Sci* (2009) 30:249-259.
[21] Fillion, D., Lemieux, G., Basambombo, L.L., Lavigne, P., Guillemette, G., Leduc, R., Escher, E., *J Med Chem* (2010) 53:2063-2075.
[22] Han, K.H., Green, S.R., Tangirala, R.K., Tanaka, S., Quehenberger, O., *J Biol Chem* (1999) 274:32055-32062.
[23] Hawtin, S., Simms, J., Conner, M., Lawson, Z., Parslow, R., Trim, J., Sheppard, A., Wheatley, M., *J Biol Chem.* (2006) 281:38478-38488.
[24] Nawaratne, V., Leach, K., Felder, C.C., Sexton, P.M., Christopoulos, A., *J Biol Chem* (2010) 285:19012-19021.
[25] Fan, Q.R., Hendrickson, W.A., *Nature* (2005) 433:269-277.
[26] Kleinau, G., Jaeschke, H., Mueller, S., Raaka, B.M., Neumann, S., Paschke, R., Krause, G., *Faseb J* (2008) 22:2798-2808.
[27] Nicastro, G., Peri, F., Franzoni, L., de Chiara, C., Sartor, G., Spisni, A., *J Pept Sci* (2003) 9:229-243.
[28] Wheatley, M., et al., *Biochem Soc Trans* (2007) 35:717-720.
[29] Conner, M., Hawtin, S.R., Simms, J., Wootten, D.L., Lawson, Z., Conner, A.C., Parslow, R.A., Wheatley, M., *J Biol Chem* (2007) 282:17405-17412.
[30] Shi, L., Javitch, J.A., *Annu Rev Pharmacol Toxicol* (2002) 42:437-467.
[31] Avlani, V.A., Gregory, K.J., Morton, C.J., Parker, M.W., Sexton, P.M., Christopoulos, A., *J Biol Chem* (2007) 282:25677-25686.
[32] Scarselli, M., Li, B., Kim, S., Wess, J., *J Biol Chem.* (2007) 282:7385-7396.
[33] Massotte, D., Kieffer, B.L., *Nat Struct Mol Biol* (2005) 12:287-288.
[34] Unal, H., Jagannathan, R., Bhat, M.B., Karnik, S.S., *J Biol Chem* (2010) 285:16341-16350.
[35] May, L.T., Leach, K., Sexton, P.M., Christopoulos, A., *Annu Rev Pharmacol Toxicol* (2007) 47:1-51.
[36] Sum, C.S., Tikhonova, I.G., Costanzi, S., Gershengorn, M.C., *J Biol Chem* (2009) 284:3529-3536.
[37] Klco, J., Wiegand, C., Narzinski, K., Baranski, T., *Nat Struct Mol Biol.* (2005) 12:320-326.
[38] Goodwin, J.A., Hulme, E.C., Langmead, C.J., Tehan, B.G., *Mol Pharmacol* (2007) 72:1484-1496.
[39] Decaillot, F., Befort, K., Filliol, D., Yue, S., Walker, P., Kieffer, B., *Nat Struct Biol.* (2003) 10:629-636.
[40] Tikhonova, I.G., Costanzi, S., *Curr Pharm Des* (2009) 15:4003-4016.
[41] Ahuja, S., et al., *Nat Struct Mol Biol* (2009) 16:168-175.
[42] Bokoch, M.P., et al., *Nature* (2010) 463:108-112.
[43] Shi, L., Javitch, J., *Proc Natl Acad Sci* (2004) 101:440-445.
[44] Ni, F., So, S.P., Cervantes, V., Ruan, K.H., *Febs J* (2007) 275:128-137.
[45] Ott, T.R., Troskie, B.E., Roeske, R.W., Illing, N., Flanagan, C.A., Millar, R.P., *Mol Endocrinol* (2002) 16:1079-1088.
[46] Ahn, K.H., Bertalovitz, A.C., Mierke, D.F., Kendall, D.A., *Mol Pharmacol* (2009) 76:833-842.
[47] Olah, M.E., Jacobson, K.A., Stiles, G.L., *J Biol Chem* (1994) 269:24692-24698.
[48] de Zwart, M., Vollinga, R.C., Beukers, M.W., Sleegers, D.F., Kunzel, J.K.V.D., de Groote, M., IJzerman, A.P., *Drug Development Research* (1999) 48:95-103.
[49] Jager, D., et al., *J Biol Chem* (2007) 282:34968-34976.
[50] Narlawar, R., Lane, J.R., Doddareddy, M., Lin, J., Brussee, J., IJzerman, A.P., *J Med Chem* (2010) 53:3028-3037.

[51] Gregory, K.J., Hall, N.E., Tobin, A.B., Sexton, P.M., Christopoulos, A., *J Biol Chem* (2010) 285:7459-7474.
[52] Lawson, Z., Wheatley, M., *Biochem Soc Trans* (2004) 32:1048-1050.
[53] Claus, M., Jaeschke, H., Kleinau, G., Neumann, S., Krause, G., Paschke, R., *Endocrinology* (2005) 146:5197-5203.
[54] Izhak, L., Wildbaum, G., Zohar, Y., Anunu, R., Klapper, L., Elkeles, A., Seagal, J., Yefenof, E., Ayalon-Soffer, M., Karin, N., *J Immunol* (2009) 183:732-739.
[55] Boivin, S., Segalas-Milazzo, I., Guilhaudis, L., Oulyadi, H., Fournier, A., Davoust, D., *Peptides* (2008) 29:700-710.
[56] Paes, C., Ingalls, J., Kampani, K., Sulli, C., Kakkar, E., Murray, M., Kotelnikov, V., Greene, T.A., Rucker, J.B., Doranz, B.J., *J Am Chem Soc* (2009) 131:6952-6954.
[57] de Ligt, R.A., Kourounakis, A.P., A.P., I., *Br J Pharmacol* (2000) 130:1-12.
[58] Mobini, R., Magnusson, Y., Wallukat, G., Viguier, M., Hjalmarson, A., Hoebeke, J., *J Autoimmun* (1999) 13:179-186.
[59] Peter, J.C., Eftekhari, P., Billiald, P., Wallukat, G., Hoebeke, J., *J Biol Chem* (2003) 278:36740-36747.
[60] Peter, J.C., Wallukat, G., Tugler, J., Maurice, D., Roegel, J.C., Briand, J.P., Hoebeke, J., *J Biol Chem* (2004) 279:55697-55706.
[61] Elies, R., Fu, L.X., Eftekhari, P., Wallukat, G., Schulze, W., Granier, C., Hjalmarson, A., Hoebeke, J., *Eur J Biochem* (1998) 251:659-666.

CHAPTER 3

GPCR STRUCTURE AND ACTIVATION: AN ESSENTIAL ROLE FOR THE FIRST EXTRACELLULAR LOOP IN ACTIVATING THE ADENOSINE A_{2B} RECEPTOR

This chapter was based upon:

M.C. Peeters, D. Guo, G.J.P van Westen, L.E. Wisse, M.W. Beukers, A.P. IJzerman. FASEB journal **2011**, 25(2):632-43

ABSTRACT

The highly variable extracellular loops in G protein-coupled receptors (GPCRs) have been implicated in receptor activation, the mechanism of which is poorly understood. In a random mutagenesis screen on the human adenosine A_{2B} receptor ($A_{2B}R$) using the MMY24 *Saccharomyces cerevisiae* strain as a read-out system, we found that two residues in the first extracellular loop, a phenylalanine and an aspartic acid at positions 71 and 74, respectively, are involved in receptor activation. We subsequently performed further site-directed and site-saturation mutagenesis. These experiments revealed that the introduction of mutations at either of the identified positions results in a wide variety of receptor activation profiles, with changes in agonist potency, constitutive activity, and intrinsic activity. Radioligand binding studies showed that the changes in activation were not due to changes in receptor expression. We interpret these data in the light of the recently revealed structure of the adenosine $A_{2A}R$, the closest homologue of the $A_{2B}R$. The two residues are suggested to be vital in maintaining the tertiary structure of a β-sheet in the extracellular domain of the $A_{2B}R$. We hypothesize that deterioration of structure in the extracellular domains of GPCRs compromises overall receptor structure with profound consequences for receptor activation and constitutive activity.

INTRODUCTION

Recently, considerable progress has been made in understanding the structure of G protein-coupled receptors (GPCRs) and their mechanisms of activation. The highly variable extracellular region of GPCRs is increasingly recognized as an important determinant in receptor activation, next to the intracellular and transmembrane domains [1,2,3,4,5]. However, for many GPCRs it is still poorly understood how the N-terminus and extracellular loops are able to influence receptor activation. The extracellular domains have been reported as managers of activation, either by keeping the receptor in a silent state or by stabilizing the active conformation of the receptor [3,6,7]. Several recent reports have shown that all extracellular regions together, including the hinge region, are required for full TSH receptor activation with the first extracellular loop (EL1) as a key player [8,9,10].

In this study, we have investigated the first extracellular loop in the adenosine A_{2B} receptor (A_{2B}R), a typical class A GPCR. Four subtypes of adenosine receptors are known (A_1R, A_{2A}R, A_{2B}R, and A_3R), all of which are ubiquitously expressed in the human body [11]. Although all four subtypes respond to the same endogenous ligand adenosine, they target different intracellular signaling pathways. The A_1R and the A_3R subtypes mainly signal through G_i proteins mediating the inhibition of adenylyl cyclase, which leads to decreased levels of cAMP in the cell. The A_{2A}R and A_{2B}R cause an increase in intracellular cAMP levels by coupling mainly to G_s proteins resulting in the activation of adenylyl cyclase [12]. Of the adenosine subfamily, the A_{2B}R subtype has been investigated least. However, the adenosine A_{2B} receptor is an interesting drug target as it has been implicated in asthma [13], chronic obstructive pulmonary disease (COPD) [14], and other inflammatory diseases [15].

Here, we report a useful and fast approach to elucidate receptor activation mechanisms using successive mutagenesis experiments. We started with an unbiased random mutagenesis screen for increased activity in a robust yeast system. The *S. cerevisiae* strain used to evaluate receptor activation has been genetically modified to serve as a reporter system with growth as an output parameter. This yeast system is an ideal background to monitor activation of a single GPCR, since its only endogenous GPCR has been removed from the system while still maintaining the complete GPCR signaling machinery [16]. Several previous reports have proved this eukaryotic system to be predictive of the mammalian situation [17,18].

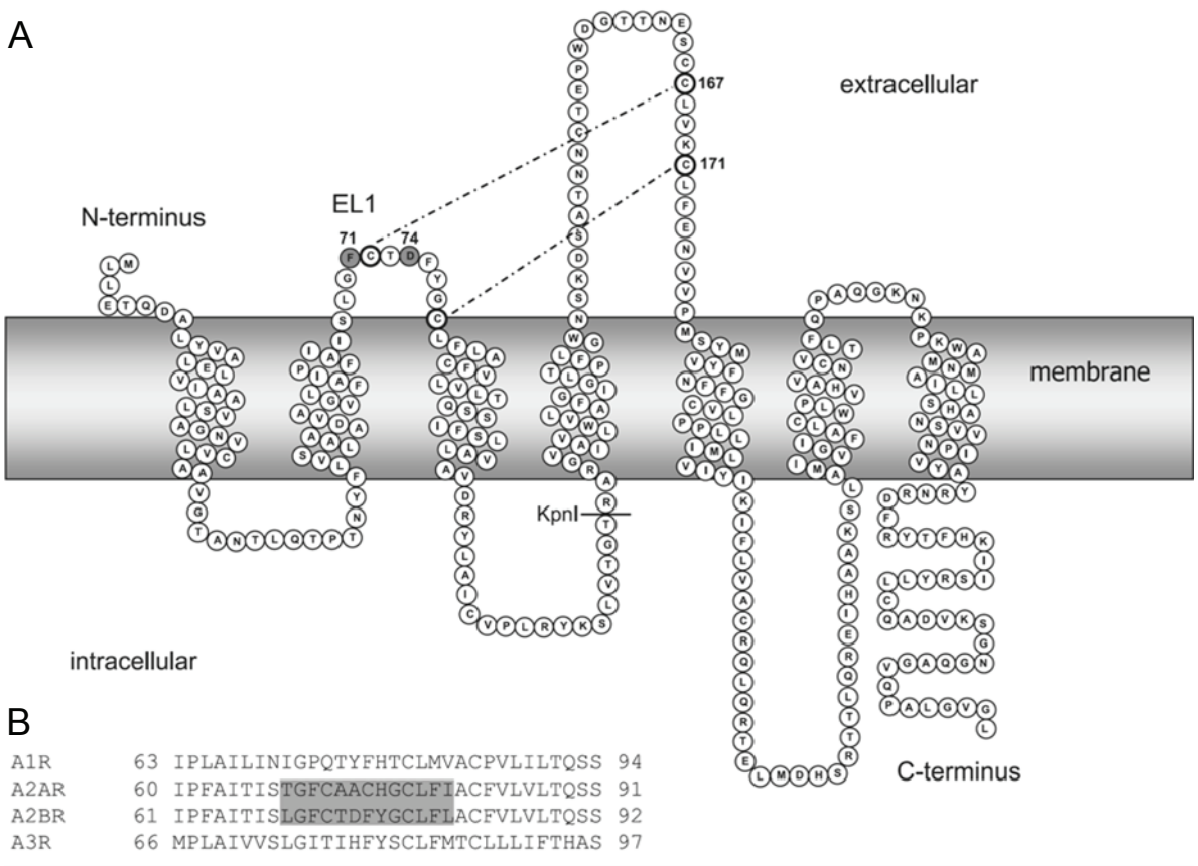

Figure 1. (*A*) Snake plot of the adenosine A_{2B}R. Residues F71 and D74 in the first extracellular loop of the A_{2B}R are shaded. Dotted lines indicate disulfide bridges. The disulfide bridge conserved in many class A GPCRs links C78 and C171. The nonconserved second disulfide bridge between EL1 and EL2, based on the crystal structure of the adenosine A_{2A}R (PDB: 3EML), links C72 and C167. In the second intracellular loop, the restriction site *Kpn*I that was used to obtain the fragment for random mutagenesis is indicated. (*B*) Multiple sequence alignment of the 4 adenosine receptor subtypes. Shading indicates the sequence of EL1 that was substituted in the creation of the chimeric A_{2A}R-A_{2B}R model in Figure 8.

From a random mutagenesis screen Beukers et al. [18] previously identified mutations located in the transmembrane domains and the intracellular regions of the A_{2B}R that caused high receptor constitutive activity. In the present study we investigated a mutant receptor with two mutated residues in the first extracellular loop, consisting of a phenylalanine and an aspartic acid that are involved in receptor activation (**Figure 1**). These residues were not predicted to be important for adenosine receptor activation by any rational approach. The two positions were further characterized by site-directed mutagenesis and subsequent site-saturation mutagenesis, further emphasizing the involvement of positions 71 and 74 in receptor structure and activation. The importance of maintaining receptor structure was corroborated by the recently published structure of the adenosine A_{2A}R, the closest homologue of the A_{2B}R [4]. To our knowledge, this is the first report that describes

the large influence of structural features at the extracellular region on receptor activation. It is likely that similar features are involved in the activation mechanism of other GPCRs, even though the specific three-dimensional structures will most likely differ between subfamilies or even subtypes.

MATERIALS AND METHODS

Random Mutagenesis

A KpnI restriction site was introduced in the adenosine A_{2B} receptor gene in the region encoding the second intracellular loop, making it possible to obtain a fragment with a suitable size for random mutagenesis [19]. Random mutations were induced in the fragment consisting of the first 372 base pairs of the A_{2B}R gene by using an error prone PCR method adapted from Fromant et al. [20]. The mutagenized fragments were subsequently reintroduced in an otherwise wild type A_{2B} receptor. The random mutagenized A_{2B}R library was obtained as described earlier by Beukers et al. [18].

Site-directed Mutagenesis

Site-directed mutants A_{2B}R_F71L and A_{2B}R_D74G were constructed by PCR mutagenesis using pDT-PGK_$A_{2B}R_{KpnI}$ as a template. The mutant A_{2B}R_F71L was created using primers containing an EcoR31I site for directional PCR product cloning purposes. The EcoR31I restriction enzyme was purchased from Fermentas (St. Leon-Rot, Germany). The primers used for the site-directed mutagenesis were:

5'-CATCATGGTCTCAGAAGTCAGTGCAGAGGCCCAGGC-3'

5'-CATCATGGTCTCACTTCTACGGCTGCCTCTTCC-3'

The mutant A_{2B}R_D74G was generated by Baseclear (Leiden, The Netherlands). For this purpose, the following primers were used:

5'-CAGCCTGGGCTTCTGCACTGGCTTCTACGGCTGCCTCTTCC-3'

5-'GGAAGAGGCAGCCGTAGAAGCCAGTGCAGAAGCCCAGGCTG-3'

Both mutant receptor genes were verified by double-stranded sequencing (LGTC, Leiden, The Netherlands).

Site-saturation Mutagenesis

Site-saturation mutagenesis on positions 71 and 74 in the first extracellular loop of the human adenosine A_{2B} receptor was performed based on the QuickChange Multi-Site Directed Mutagenesis system (Stratagene, Huizen, The Netherlands). The plasmid pDT-PGK_$A_{2B}R_{KpnI}$ was used as the template in this PCR-based mutagenesis method. The following primers containing a randomized codon at the sites of interest were used:

F71N: T211N_T212N_C213N 5'ATCACCATCAGCCTGGGCNNNTGCACTGACTTCTACGGC-3'

D74N: G220N_A221N_C222N 5'AGCCTGGGCTTCTGCACTNNNTTCTACGGCTGCCTCTTC-3'

Prior to transformation of the single stranded plasmids into XL10 Gold Chemical Competent *E.Coli* cells, the PCR product was treated with DpnI to remove methylated template. After selection on LB-Amp agar plates, 100 isolated plasmids from each mutagenesis project were chosen for identification by DNA sequencing to retrieve as many amino acid changes at the positions as possible.

Transformation in MMY24 S. cerevisiae strain

pDT-PGK_$A_{2B}R$ plasmids were transformed into an *S. cerevisiae* yeast strain according to the Lithium-Acetate procedure. The strain is derived from the MMY11 strain [21] and was further adapted to communicate with mammalian GPCRs through the introduction of a chimeric G protein [16]. The genotype of the MMY24 strain is: *MAT**a**his3 leu2 trp1 ura3can1 gpa1_::G_i3 far1_::ura3 sst2_::ura3 Fus1::FUS1-HIS3 LEU2::FUS1-lacZ ste2_::G418R.* To measure signaling of GPCRs, the pheromone signaling pathway of this strain was coupled via the FUS1 promotor to HIS3, a gene encoding the key enzyme in histidine production, imidazole glycerol-phosphate dehydrase. The degree of receptor activation was measured by the growth rate of the yeast on histidine-deficient medium.

Screening for increased activation in S. cerevisiae

The mutant $A_{2B}R$ library was screened in a yeast system for constitutively active receptors and/or receptors showing an increased potency of the full $A_{2B}R$ agonist 5'-N-ethylcarboxamidoadenosine (NECA) (Sigma-Alderich, Zwijndrecht, The Netherlands).The random mutagenesis screen was performed as described earlier by Beukers et al. [18]. The plasmid containing the $A_{2B}R$_F71L/D74G mutant identified from this screen was isolated and retransformed into the MMY24 yeast strain.

Solid growth assay

To characterize the mutant receptors further, concentration-growth curves were generated in a solid growth assay. In this assay, yeast cells from an overnight culture were diluted to around 400,000 cells/ml (OD_{600} ≈ 0.02), and droplets of 1.5 µl were spotted on selection agar plates, YNB-ULH, containing 7 mM 1,2,4-aminotriazole (3-AT) (Sigma-Alderich, Zwijndrecht, The Netherlands) and a NECA concentration ranging from 10^{-9} to 10^{-5} M. When monitoring responsiveness to an inverse agonist, ZM241385 (final concentration 10^{-5}M) was added to the selection plates [22]. A concentration range from 10^{-9} to 10^{-5} M was used in the concentration-growth curves with BAY 60-6583 (synthesized in house), a non-nucleoside agonist [23]. After incubation at 30°C for 50 h, the plates were scanned and receptor-mediated yeast growth was quantified with Quantity One imaging software from Bio-Rad (Hercules, CA). The amount of growth of yeast was calculated as the density of each spot with a correction for local background on the plate. Data were analyzed using nonlinear regression analysis software available in GraphPad Prism 5.0 (GraphPad Software, San Diego, CA).

Schild plot analysis

For the wild type A_{2B} receptor and for the mutant receptor D74W, concentration-growth curves of agonist NECA were recorded in the presence of increasing concentrations of the selective A_{2B}R antagonist PSB603. Schild analysis was performed using the appropriate equations available in GraphPad Prism 5.0.

Whole cell extracts and immunoblotting

Whole protein cell extracts were made from the transformed yeast cells using trichloroacetic acid (TCA). From an overnight culture, $1.2 \cdot 10^8$ yeast cells were harvested in mid-log phase. The cells were washed twice with 20% TCA after which they were broken by vigorous vortexing in the presence of glass beads. The yeast cell extracts were separated using SDS/PAGE and subsequently blotted on Hybond-ECL membranes. For this purpose, a sample of 4.0 µl containing 12 µg protein was loaded on a 12.5% SDS/PAGE gel. A semi-automated electrophoresis technique (PhastSystem™, Amersham Pharmacia Biotech) was used for SDS/PAGE as well as blotting. The antibody directed against the C-terminal region of the adenosine A_{2B} receptor was kindly provided by by Dr. I. Feoktistov (Vanderbilt University, Nashville).

Densitometric analysis of the protein bands was performed using the volume analysis tool present in the Quantity One imaging software from Bio-Rad (Hercules, CA). The aspecific band at approximately 45 kDa was used as loading control. The ratio between specific $A_{2B}R$ protein bands and aspecific bands was determined and the wild type receptor was set at 100%, the empty vector pDT-PGK at 0%. The experiment was performed in duplicate.

Whole cell radioligand binding experiments

Yeast cells expressing wild type or mutated $A_{2B}R$ were cultured overnight in rich YAPD medium. Cells were centrifuged for 5 minutes at 2000 x *g*, the pelleted cells were once washed with 0.9% NaCl. The cells were again centrifuged 5 minutes at 2000 x *g* and diluted in the assay buffer (50 mM Tris-HCl pH7.4 + 1 mM EDTA) to OD_{600}=40 (OD_{600} = 1 ≈ $2.5 \cdot 10^7$ cells/ml). Binding experiments were performed with 0.5-0.8 nM [^{3}H]PSB-603 and a final cell concentration of $25 \cdot 10^7$ cells/ml in a total volume of 100 µl [24]. Nonspecific binding was determined in the presence of 1 mM NECA. Samples were incubated for 1 hour at 25ºC while shaking vigorously to keep the yeast cells in suspension. Incubation was terminated by adding 1 ml ice-cold assay buffer. Bound from free radioligand was immediately separated by rapid filtration through Whatman GF/B filters pre-incubated with 0.1% polyethylenimine (PEI) using a Millipore manifold during which the filters were washed six times with ice-cold assay buffer. Filter-bound radioactivity was determined by scintillation spectrometry (Tri-Carb 2900TR; PerkinElmer Life and Analytical Sciences) after addition of 3.5 ml of PerkinElmer Emulsifier Safe.

Receptor homology modeling

The adenosine A_{2A} receptor is the closest homologue of the adenosine A_{2B} receptor, with 82.1 % amino acid similarity and 59.4 % identity. Recently, the high resolution crystal structure of the human adenosine A_{2A} receptor was published (PDB entry code: 3EML) [4]. A chimeric $A_{2B}R$-$A_{2A}R$ model was created in the Molecular Operating Environment (MOE) software package, version 2008.10 [25]. In this model, only the first extracellular loop of $A_{2A}R$ (T68–I80) was replaced by the residues making up the first extracellular loop of the $A_{2B}R$ (L69-L81) (**Figure 1B**). Since the remaining parts of the chimeric receptor were kept as they are in the $A_{2A}R$, this constitutes a partial homology model. Subsequently, a limited molecular mechanics

optimization was performed to reposition the residue side chains present in the EL1 and the neighboring EL2 in an optimal energetic state after substitution. The side chains were therefore able to form aromatic, charged and cysteine-cysteine interactions after the substitution, confirming the validity of the substitution. The optimization was performed using the AMBER99 force field, parameterized particularly for proteins and nucleic acids, as implemented in MOE [26]. The end result was a model of the A_{2A}R that carried the first extracellular loop of the A_{2B}R.

RESULTS

Random Mutagenesis

For the purpose of random mutagenesis, a limited sized fragment of 372 base pairs was used starting from the ATG until the KpnI site in the second intracellular loop. The KpnI restriction site was introduced by site-directed mutagenesis, resulting in a silent mutation. The fragment of interest encodes for the N-terminus, the first three transmembrane domains, the first extracellular loop, the first intracellular loop, and part of the second intracellular loop of the A_{2B}R. This fragment was subjected to a random mutagenesis PCR reaction and reintroduced in an otherwise wild type receptor, resulting in a library of approximately $4 \cdot 10^6$ plasmids containing mutant A_{2B}Rs. The library was screened for mutant receptors displaying constitutive activity and/or an increase in potency of the full A_{2B}R agonist NECA using a yeast system with growth as a simple read-out. This yeast strain has been genetically modified to enable mammalian GPCRs to couple to the yeast pheromone pathway that is subsequently able to stimulate transcription of the reporter gene HIS3. The ability of the yeast cell containing an active receptor to produce histidine can be used in a yeast growth assay on histidine-deficient medium, where growth of the yeast cells is positively correlated with activation of the adenosine A_{2B} receptors.

From the random mutagenesis screen only one receptor was identified containing mutations in the first extracellular loop. This receptor was found having two single point mutations simultaneously at positions corresponding to residues 71 (F71L) and 74 (D74G) in the protein structure (**Figure 1**). No combination of mutations at these positions with mutations in another area of the fragment was identified. Activation assays showed that the double mutant receptor showed a 2.6-fold increased level of

constitutive activity as well as a 2.7-fold increased potency for NECA compared to the wild type receptor (see also **Table 1**).

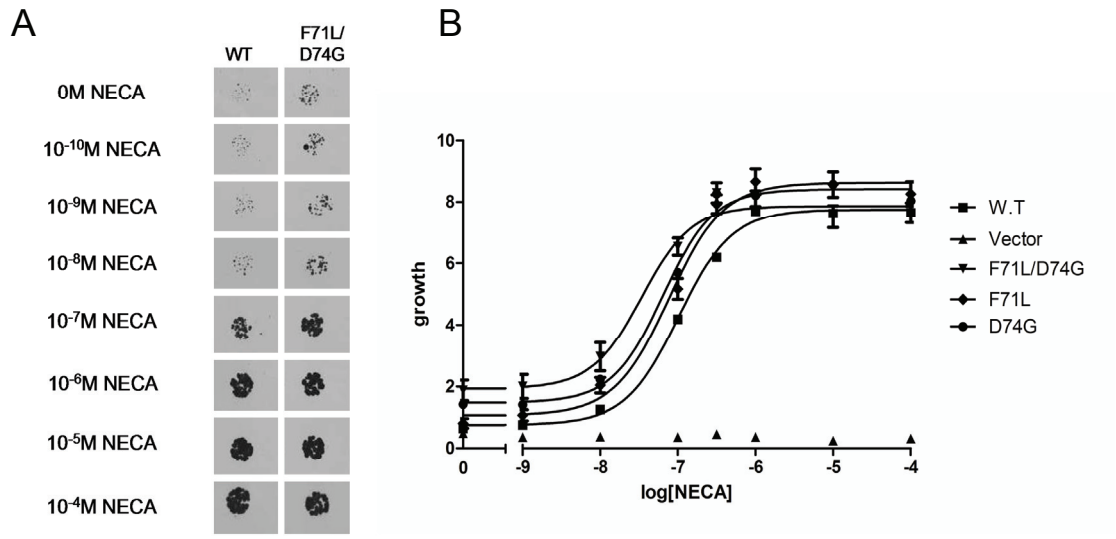

Figure 2. Receptor activation in a yeast growth assay. Yeast growth was measured with increasing NECA concentrations on selective agar plates lacking the markers uracil, leucine, and histidine. *(A)* Yeast growth density of a representative experiment, as seen on the solid selection plates. Growth of the MMY24 yeast strain expressing the wild-type (WT) human $A_{2B}R$ and of the strain expressing the double mutant receptor $A_{2B}R$_F71L/ D74G in the presence of varying concentrations of NECA. (*B*) Concentration-response curves of the WT (■) and mutant receptors F71L/D74G (▼),F71L (♦), and D74G (●).

Mutants in EL1 change potency of the agonist NECA

To decipher the role of the individual amino acids, we generated single point mutants F71L and D74G using site-directed mutagenesis. These mutants were also expressed in the MMY24 *S. cerevisiae* strain. The density of growth of the yeast cells that were transformed with the mutant receptors was monitored in response to the full agonist NECA on solid selection medium (**Figure 2**). Both single point mutants F71L and D74G show a concentration-response curve that is in between the double mutant and the wild type curves. The EC_{50} values of NECA were 67 and 47 nM on the F71L and D74G mutant receptor, respectively. Both receptors displayed constitutive activity as well, albeit less than the double mutant (see also **Tables 1 and 2**). Western blotting showed similar expression of all mutants compared to the wild type receptor (**Figure 3**).

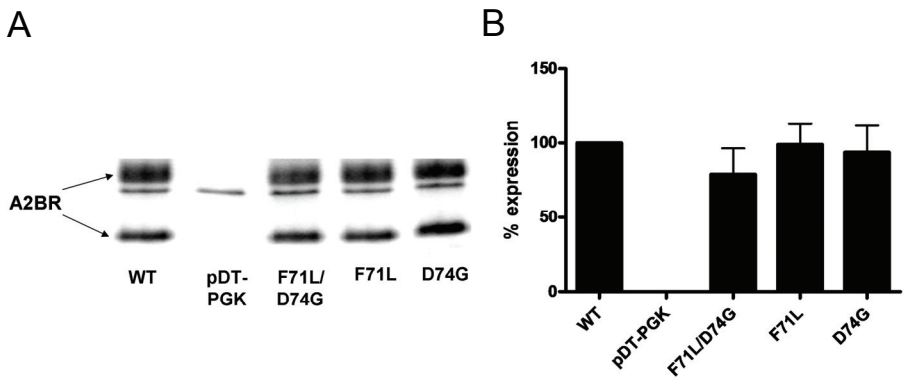

Figure 3. (*A*) Western blot showing expression levels of wild-type (WT) receptor, empty vector pDT-PGK, and mutants F71L/D74G, F71L, and D74G. Arrows indicate specific bands belonging to the adenosine A_{2B}R.
(B) Densitrometric analysis of the western blot showing relative expression levels compared to WT.

The inverse agonist ZM241385 inhibits constitutive activity of the mutant receptors

The activity of some mutant receptors was measured in response to an inverse agonist for the A_{2B}R, ZM241385. Only the mutants with more than twice the level of constitutive activity compared to the wild type, F71L/D74G and D74G, were studied. When adding 10 μM ZM241385 to the cultures, we observed that levels of constitutive activity of the mutant receptors F71L/D74G and D74G were suppressed to wild type levels (**Figure 4**). This suggests that the mutant receptors are still able to bind the inverse agonist ZM241385 and to reach an inactive state.

Figure 4. Effects of the inverse agonist ZM241385 on yeast growth. Growth was measured on selective agar plates, YNB-ULH, in the absence or presence of 10 μM of the inverse agonist ZM241385.
Vertical bars represent fold activity of the double-mutant F71L/D74G and the single-mutant D74G, compared to basal activity of the wild-type (WT) human A_{2B}R. Growth of yeast transformed with the empty vector pDT-PGK was measured as negative control.

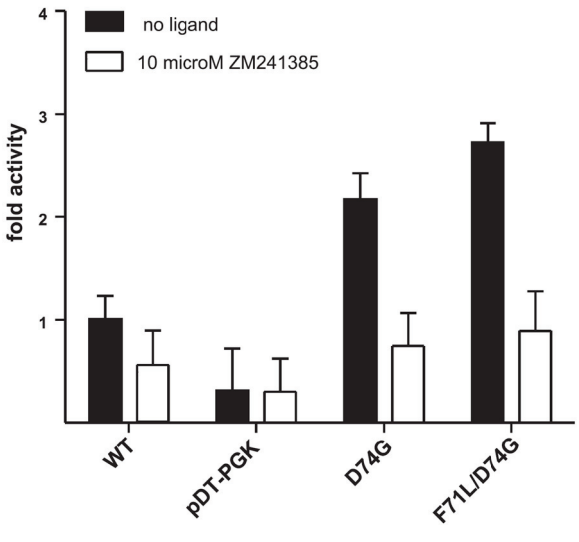

Site-saturation Mutagenesis

Next, site-saturation mutagenesis was performed on positions 71 and 74 of the $A_{2B}R$. From each of the two mutagenesis sites, 100 colonies were chosen for identification. Saturation mutagenesis at position 71 yielded 14 other amino acids. Only residues asparagine, glutamine, proline, threonine, and tryptophan, were not found. From saturation mutagenesis at site 74, 16 other naturally occurring amino acids were retrieved; residues histidine, methionine, and proline could not be identified in this case. The activity profiles of all retrieved mutants were tested in the yeast growth assay using solid selection medium as described previously.

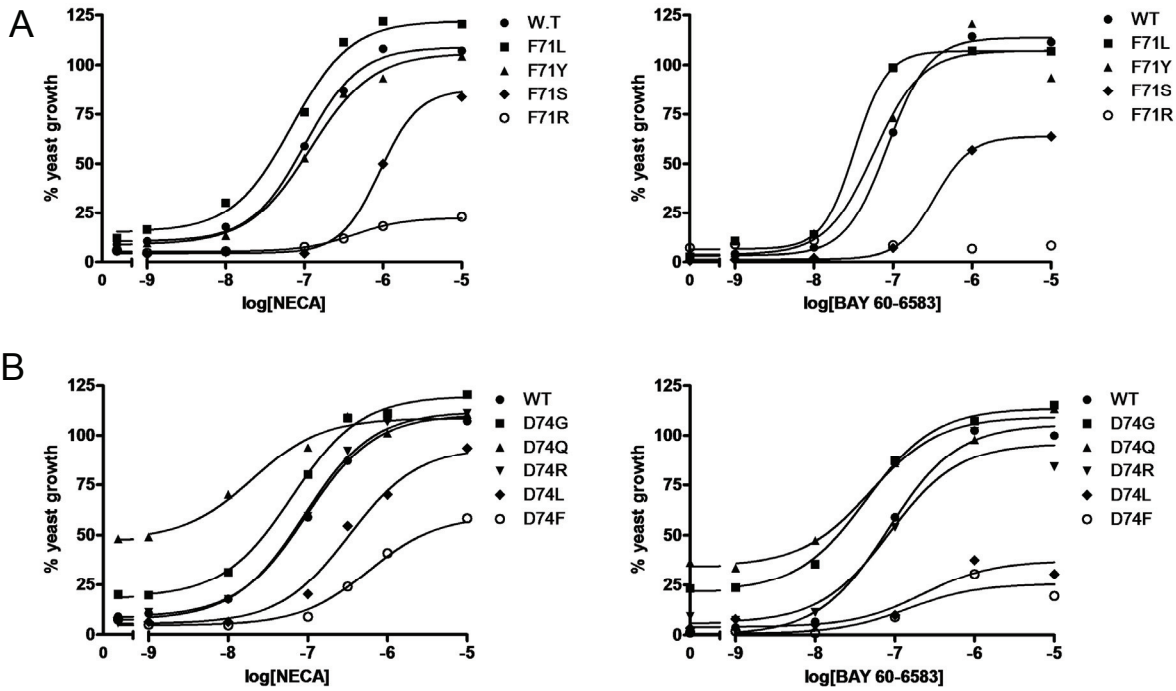

Figure 5. (A) Representative concentration-growth curves of F71X *(A)* and D74X mutant receptors *(B)*. Yeast growth was measured on selective agar plates YNB-ULH with increasing NECA or BAY 60-6583 concentrations. Mutant receptors F71L (■), F71Y (▲), F71S (♦), and F71R (○) show the variety in concentration-growth curves of the mutant receptors resulting from saturation mutagenesis. As a reference, the concentration-growth curve of the wild type human $A_{2B}R$ (●) is shown.

The mutant receptors at position 71 can be divided into two groups; mutant receptors with i) similar activation profiles compared to the wild type receptor and with ii) a decreased level of activity. In **Figure 5A**, a few representative concentration-growth curves are shown that demonstrate the range of different activation profiles. The first group comprising receptors in which the phenylalanine was mutated into an isoleucine, glutamic acid, tyrosine, lysine, and methionine, did not display a change in

activity levels (**Table 1**). Mutation into valine induced a small, but significant decrease in potency. The second group includes mutations that cause a large decrease in levels of activity or even a complete loss of activation. Residues belonging to this second group are histidine, aspartic acid, cysteine, serine, arginine, alanine, and glycine. All of these mutant receptors showed a decrease in NECA potency of at least 4-fold compared to the wild type receptor. The F71 mutant receptors that displayed the largest decrease in potency, with serine, arginine, alanine, or glycine, also showed a decrease in maximum intrinsic activity. Only the originally identified mutant F71L showed a small, but significant increase in potency. Besides the well characterized adenosine receptor agonist NECA, the activation profile of the mutant receptors was also investigated using the non-nucleoside agonist BAY 60-6583 [23]. This agonist represents a new class of adenosine receptor ligands, showing agonistic effect without having a ribose moiety. This chemically different agonist showed effects on the mutant receptor similar to the activation with NECA (**Figure 5A, Table 1**).

Activation profiles of mutations introduced at position 74 showed an even larger variation. In **Figure 5B**, several representative concentration-growth curves are depicted that demonstrate this variation in activation profiles in response to NECA as well as to BAY 60-6583. A number of mutations induced at position 74 caused an increase in potency and constitutive activity. These involve changing the aspartic acid into a glutamine, glutamic acid, asparagine or serine residue. Mutations into a lysine, tyrosine, alanine, arginine, or threonine, did not affect the response to NECA. However, when the aspartic acid was mutated into a tryptophan, cysteine, leucine, valine, phenylalanine or isoleucine, the activity was decreased or even lost. Most mutant receptors resembled the intrinsic activity of the wild type receptors or even showed a slight increase in maximal activation levels in response to NECA. However, residues cysteine, leucine, phenylalanine, and isoleucine, caused a decrease in intrinsic activity. The effects of the mutations at position 74 on receptor activity in response to the agonists NECA or BAY 60-6583 are summarized in **Table 2**. The effects of both agonists on the mutant receptors relative to the wild type receptor are similar.

Table 1. Characterization of the adenosine receptor A_{2B} receptor mutants at position 71 resulting from saturation mutagenesis. EC_{50} values (nM) are shown as means ± SEM of at least three independent experiments, each performed in duplicate. The mean values derived from the concentration-growth curves were used for calculation of the fold EC_{50} value, fold constitutive activity (CA), and percentage maximal activity (Emax), compared to the wild type receptor. The Emax represents the intrinsic activity of the receptor.

	NECA 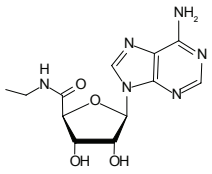			BAY 60-6583 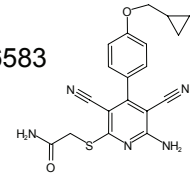		
Mutant	Fold CA	EC_{50} (nM)	Fold EC_{50}	% Emax	EC_{50} (nM)	Fold EC_{50}
WT	1.0	94±11	1.0	100	81±14	1.0
F71L/D74G	2.6	35±6	0.4	100	49±14	0.6
F71L	1.4	67±14	0.7	110	65±22	0.8
F71I	0.9	108±23	1.2	100	132±44	1.6
F71E	0.7	118±20	1.3	100	134±17	1.7
F71K	1.0	124±16	1.3	100	110±42	1.4
F71M	1.0	130±34	1.4	100	114±13	1.4
F71Y	0.9	147±36	1.6	100	101±12	1.3
F71V	0.7	167±21	1.8	100	171±29	2.1
F71H	0.3	437±58	4.6	100	226±9	2.8
F71D	0.5	442±105	4.7	95	387±123	4.8
F71C	0.2	589±74	6.2	100	312±24	3.9
F71S	0.4	933±157	9.9	82	319±19	3.9
F71R	0.5	N.D.	N.D.	21	N.D.	N.D.
F71A	0.5	N.D	N.D.	9	N.D.	N.D.
F71G	0.5	N.D	N.D.	5	N.D.	N.D.

Table 2. Characterization of the mutants at position 74 of the adenosine receptor A_{2B} receptor resulting from saturation mutagenesis. EC_{50} (nM) values are shown as means ± SEM of at least three independent experiments, each performed in duplicate. The mean values derived from the concentration-growth curves were used for calculation of the fold EC_{50} value, fold constitutive activity (CA), and percentage maximal activity (Emax), compared to the wild type receptor. The Emax represents the intrinsic activity of the receptor.

	NECA 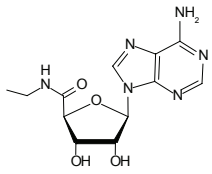			BAY 60-6583 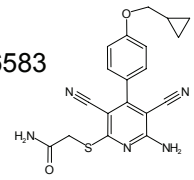		
Mutant	Fold CA	EC_{50} (nM)	Fold EC_{50}	% Emax	EC_{50} (nM)	Fold EC_{50}
WT	1.0	94±11	1.0	100	81±14	1.0
F71L/D74G	2.6	35±6	0.4	100	49±14	0.6
D74G	2.0	47±9	0.5	107	43±6	0.5
D74Q	4.8	30±6	0.3	100	35±7	0.4
D74E	2.2	49±5	0.5	109	66±11	0.8
D74N	3.5	61±14	0.7	103	45±16	0.5
D74S	4.3	68±23	0.7	104	48±7	0.6
D74K	2.2	84±11	0.9	107	85±17	1.0
D74Y	2.4	84±14	0.9	104	70±29	0.9
D74A	1.8	91±7	1.0	108	144±26	1.8
D74R	0.9	97±8	1.0	100	83±9	1.0
D74T	1.6	108±17	1.2	106	135±46	1.7
D74W	0.8	197±20	2.1	103	152±54	1.9
D74C	0.3	256±47	2.7	107	156±10	1.9
D74L	0.6	323±64	3.4	85	188±41	2.3
D74V	0.7	333±39	3.5	100	242±83	3.0

Radioligand binding to EL1 mutants

For further characterization of the EL1 mutant receptors retrieved by site-saturation mutagenesis, we performed radioligand binding experiments using the $A_{2B}R$ selective antagonist [^{3}H]PSB-603 [24]. Most mutant receptors showed specific binding of [^{3}H]PSB-603 similar to the wild type A_{2B} receptor. Only mutants F71K and D74N caused an increase in specific binding. Mutant receptor D74G showed a decreased specific binding of the radioligand compared to the wild type receptor, even though this receptor displayed an increase in potency in response to NECA and BAY 60-6583. Mutant receptors that led to a large decrease in agonist potency as observed in the solid growth assays, generally also showed decreased binding of the antagonist [^{3}H]PSB-603 (**Figure 6**).

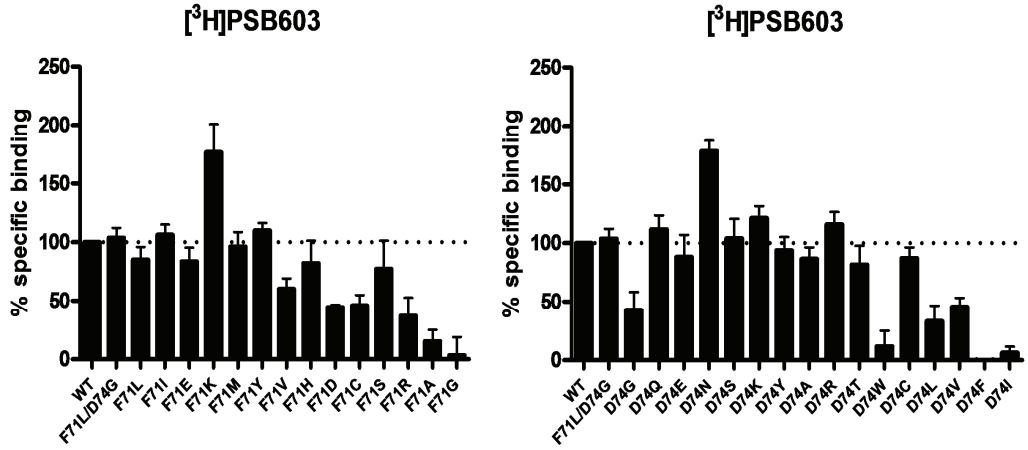

Figure 6. Single point competition binding assay with [^{3}H]PSB603. Binding experiments were performed at a radioligand concentration of 0.5-0.8 nM. Nonspecific binding was determined using 1 mM NECA. Specific [^{3}H]PSB603 binding to the wild type receptor was set to 100%. The mutant receptors are shown in descending order of activation as seen in the concentration-growth curves.

To examine whether this observation might be due to a decrease in antagonist affinity, we performed a Schild plot analysis. For this purpose, we chose one mutant receptor, D74W, which showed a decreased potency to the agonists but was still able to reach maximal activation levels in the concentration-growth curves, and compared its behavior to the wild-type receptor. Concentration-growth curves of the agonist NECA were recorded in the presence of increasing concentrations of the (unlabeled) antagonist PSB603, leading to rightward shifts. A Schild analysis of the curves yielded pA_2 values of 9.7 and 9.3 for the wild-type and mutant receptor, respectively (**Figure 7**).

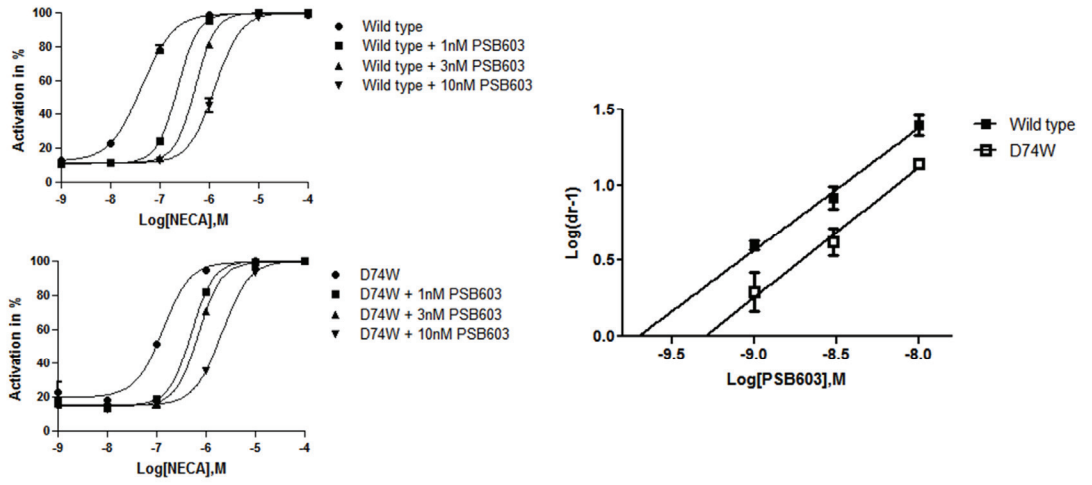

Figure 7. Schild plot analysis of PSB603 binding to WT and D74W receptors. Concentration-growth curves of NECA were recorded in the absence and presence of three concentrations of antagonist PSB603. The pA_2 value of PSB603 was determined from a Schild plot. Data are represented as mean ± SEM of three independent experiments, performed in duplicate.

DISCUSSION

A double mutant was found in a random mutagenesis study in which mutant adenosine A_{2B} receptors were selected based on their levels of increased constitutive and agonist-dependent activation. This mutant receptor contained two point mutations, both located in the first extracellular loop of the receptor. Until now, no reports have been published on this small loop as being involved in adenosine receptor activation. Both of the mutants' components, F71L and D74G, were generated through site-directed mutagenesis of the wild type A_{2B}R. Each of these two mutant receptors contributed to the effect on the receptor activity, inducing an increase in agonist potency as well constitutive activity compared to the wild type receptor. The level of constitutive activity could be inhibited to wild type levels by the inverse agonist ZM241385, showing that the mutant receptors are still functional and are not structurally locked in a certain receptor conformation.

Analysis of protein expression using Western Blotting indicated that the observed increase in receptor activation was not due to an increased expression level of the mutant receptors, which was further confirmed with radioligand binding studies (*vide infra*). Thus, the first extracellular loop appears to play an important role in the activation of the adenosine A_{2B} receptor with a special role for a phenylalanine located at position 71 and an aspartic acid at position 74.

Next, a site-saturation mutagenesis study was performed at the two positions to gain more insight in how and why this specific region is involved in the activation mechanism of the receptor. This study revealed that a single amino acid change at either of the two positions may result in a large alteration in activation profile. Quite a few of the residues at position 71 that enable the receptor to be fully activated by NECA share similar properties. They are like phenylalanine itself large, hydrophobic and bulky amino acids, such as (iso)leucine, tyrosine and methionine. However, glutamate and lysine are equally tolerated, which both are charged amino acids. Radioligand binding experiments revealed that almost all mutated receptors show similar binding of the antagonist [^{3}H]PSB603, indicating a similar expression profile. Only the mutant receptor with a lysine at the 71 position showed an increase in binding, which could be due to an increased affinity of the antagonist or a higher expression of the receptor. Several mutant receptors with a decreased potency to NECA, also showed a lower binding of [^{3}H]PSB603. This combined finding might be due to a decrease in receptor expression, but is most likely caused by a decrease in antagonist affinity, which we established to be the case for a mutation on position 74, discussed in the next paragraph. There is one other publication describing the influence of aromatic residues in EL1 on receptor activation. Härterich et al identified an aromatic π-stacking region in the neurotensin 1 receptor that might provide rigidity to the loop. Mutagenesis of these aromatic residues in EL1 interfered with receptor activation and strongly reduced ligand binding [27].

Mostly polar residues were found that maintain receptor activity at position 74. Charged residues seem to be equally favorable on this position. Both positively charged residues arginine and lysine show a potency to NECA similar to the wild type receptor, whilst glutamic acid with a negative charge like the wild-type aspartic acid, shows a two-fold increase in potency. The other residues that cause an increase in potency for NECA are glutamine and asparagine, the uncharged homologues of glutamic and aspartic acid, respectively. As was observed for the 71 position, binding of mutated receptors at the 74 position to the antagonist [^{3}H]PSB603 is mostly similar to the wild type receptor. It is therefore most likely that changes in receptor activation are not due to changes in receptor expression levels. Only mutant receptor D74N showed an increase in specific radioligand binding and might thus be expressed in higher amounts. When the aspartic acid was mutated into a glycine antagonist binding was decreased, even though its activation in response to an agonist was

increased. Its expression level in the immunoblot (**Figure 3**) was similar to that of the wild type receptor. Other mutant receptors with lower specific binding of the radioligand also showed a decreased activation profile with NECA. This could be due to a decrease in expression levels, but is more likely to be the result of a decrease in affinity to the antagonist. For this reason, a Schild plot analysis was performed using the mutant receptor D74W. This mutation caused a decrease in agonist potency, but was still able to induce maximal activation. The Schild plot indeed showed that the affinity for the antagonist PSB603 was decreased compared to the wild type receptor, which, as a consequence, may have yielded less specific binding of the radioligand at the concentration used.

Activation studies were also performed in the presence of a structurally different agonist, BAY 60-6583. This agonist lacks a ribose group that was previously thought to be important for agonist function and represents a new class of adenosine receptor agonists [23]. Concentration-growth curves of this agonist yielded similar results as seen with NECA, showing that the effects on activation are not specific for one chemical class of agonists.

Several studies on GPCRs have reported an important role for charged residues within the first extracellular loop in receptor activation, such as for the Ste2p receptor, the $VPAC_1$ receptor, and the V_{1a} vasopressin receptor. These reports confirm our finding that the polar nature of these residues promotes receptor activation [28,29,30,31].

EL1 in receptor activation

Contrary to the transmembrane domains, the extracellular loops of G protein-coupled receptors are highly divergent. Even within subfamilies, the amino acid sequence of the extracellular loops can vary greatly. This holds true for the subfamily of adenosine receptors as well. Compared to the high sequence similarity of the transmembrane domains among the adenosine receptor family (87% similarity and 71% identity between the four adenosine receptor subtypes), even the small first extracellular loop shows little resemblance. However, when investigating this sequence in the A_{2B} receptor among different species, we learned that this region is highly conserved (data not shown).

Table 3. Single point mutations reported in the first extracellular loop of other class A GPCRs. Mutations affecting receptor activation at the equivalent position of F71 and D74 in the $A_{2B}R$.

Position equivalent to F71			
Receptor	Mutation	Effect	Reference
CCKAR	F107A	Decrease in affinity as well as agonist potency	[32]
CCR5	W94A	Decreased receptor activity	[33]
CCKBR	F120A	Slightly reduced affinity for agonist	[34]
NK2R	W99C	Loss of affinity for agonist and antagonist	[35]
V2aR	F105V	Increase in agonist potency	[36]
Position equivalent to D74			
Receptor	Mutation	Effect	Reference
C5aR	G105D	Increase in affinity for agonist	[37]
RHO	G106W	Decreased levels of functional receptor in the plasma membrane	[38]

An investigation among all class A GPCRs shows that even though the amino acid sequence of the first extracellular loop can vary greatly, its length differs little. In fact, over 90% of class A GPCRs have between 50 and 53 amino acids in between the conserved 2.50 and 3.50 residues [39], which sequence stretch includes EL1. The adenosine A_{2B} receptor is among this majority. The conservation in length of the loop throughout the class A GPCR family could indicate a similar role for the first extracellular loop in receptor activation. Positions 71 and 74 in the $A_{2B}R$ are equivalent to the first and last residues of the WXFG motif described by Klco and co-workers [5]. The authors describe a role of this motif in activation, but not in ligand binding of the C5aR. However, disruption of the residues in the WXFG motif resulted in a loss of affinity for the ligand in other receptors, such as the tachykinin NK2 receptor and the AT_1 receptor [35,40]. The WXFG motif is widespread as it is present in most non-olfactory class A GPCRs. However, no such motif is present in adenosine receptors. Several mutations described in literature are listed in **Table 3**; these are located at positions equivalent to F71 and D74 in EL1. All of these mutations resulted in a change in receptor activation, showing some precedence for our findings. Further emphasis on the importance of the first extracellular loop in

GPCR activation stems from several somatic mutations, some of which have been implied to cause pathology. In patients with retinitis pigmentosa, two residues in the first extracellular loop of rhodopsin were found to be mutated [41,42]. A mutation in the vasopressin V2 receptor causes diabetes insipidus due to an increased potency for the agonist [36]. In the first extracellular loop of GPR54 a leucine was substituted by a proline, completely inhibiting signaling through the PLC pathway and causing isolated hypogonadotropic hypogonadism [43]. In the TSH receptor, two somatic mutations of a hydrophobic residue in EL1 causing constitutive activity of the receptor were found in hyperfunctioning thyroid adenomas [44].

Crystal structure of A_{2A}R as a model

Until now, the crystal structures of only a small number of class A GPCRs have been elucidated. All show a different conformation of the extracellular loops. The human adenosine A_{2A} receptor is the most recent structure published [4]. Of all G protein-coupled receptors, the A_{2B}R is most closely related to this receptor. Also, their first extracellular loops are similar. We have created a chimeric homology model of the A_{2B}R based on the A_{2A}R structure but carrying the EL1 of the A_{2B} receptor. As a result of the model building the numbering changed; F70 corresponds to F71 (A_{2B}R) and D73 to D74 (A_{2B}R) (**Figure 8**). The non-conserved disulfide bridge (C71-C159) between the centers of EL1 and EL2 that is unique in this crystal structure remains in place after a limited molecular mechanics optimization, indicating that the A_{2B}R is likely to have structural features in EL1 similar to the A_{2A}R. The most prominent motif in the extracellular region of the A_{2A}R structure is an anti-parallel β-sheet that is formed between EL1 and EL2, with the disulfide bridge in the centre connecting C71 in EL1 and C159 in EL2. The cysteines involved in this disulfide bond are only conserved in subtype 2 of the adenosine receptors (A_{2A}R and A_{2B}R). Together with the disulfide bridge between EL2 and the top of TM3 that is conserved among most class A GPCRs, this second cysteine bridge provides extra stability and causes EL2 to bend more closely to EL1. Even though the second extracellular loop differs greatly between the A_{2A}R and the A_{2B}R in length and in sequence, the cysteine involved in the nonconserved disulfide bond between EL1 and EL2 can be very well aligned in the two receptors. From this sequence alignment, it is plausible that in the A_{2B}R, this disulfide bond is present between C72 in EL1 and C167 in EL2. Many

GPCRs also contain additional, not conserved, extracellular cysteine residues that can form disulfide bonds that influence the tertiary receptor structure and receptor stability [45,46,47].

Several lipophilic residues are present within a radius of approximately 5 Å of the phenylalanine at position 71 in the crystal structure of the $A_{2A}R$ as well as in our chimeric $A_{2B}R$-$A_{2A}R$ model. All of these residues are pointing towards the protein. The phenylalanine is buried in between these lipohilic side chains and forms the onset of the anti-parallel β-sheet. At position 74, the aspartic acid is involved in receptor activity and is pointing outward in the aqueous environment. This spatial orientation, in which the phenylalanine is directed towards the protein and the aspartic acid is pointing outwards, is consistent with the presence of a β-sheet in which residues alternate above and below the sheet [48]. It is likely that the β-sheet's stability is altered (and hence the receptor activity), when (the properties of) positions 71 and 74 are changed.

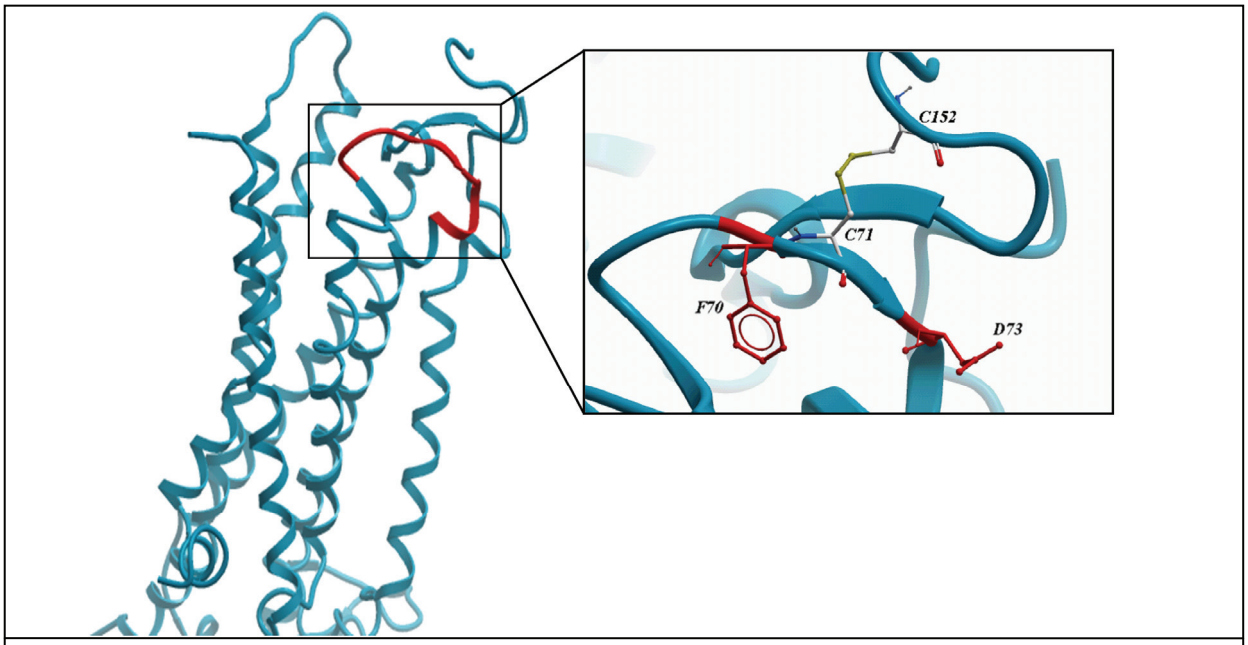

Figure 8. Ribbon representation of the chimeric receptor model based on the adenosine A_{2A} receptor structure (PDB: 3EML), carrying the EL1 of the $A_{2B}R$. The $A_{2A}R$ structure is shown in cyan, the $A_{2B}R$ EL1 in red. Inset: detailed view of the extracellular region, including the EL1. Here, the whole structure is colored cyan. The locations of the mutations are displayed in red; positions 70 and 73 correspond to the residues F71 and D74 in the $A_{2B}R$. The antiparallel β-sheet between EL1 and EL2 is shown by two arrows in the ribbon structure. The side chains of the cysteines forming the nonconserved disulfide bridge (C71-C159) are also shown with the sulfur atoms in yellow.

In conclusion, we have identified two residues located in the first extracellular loop, a phenylalanine and an aspartic acid, which are involved in the activation of the adenosine A_{2B} receptor. Site-saturation mutagenesis and activation growth studies in yeast have shown that a polar residue is necessary at position 74. At position 71, an amino acid appears to be required that can be buried in the vicinity of neighboring lipophilic residues pointing towards the transmembrane regions. Assuming that the first extracellular loop of the A_{2B}R adopts a similar tertiary structure as has been observed for the A_{2A}R, residues F71 and D74 are located at the verge of an anti-parallel β-sheet formed by EL1 together with EL2. Our results indicate that this unique structural feature is essential for normal receptor activation and mutations that alter the β-sheet's stability result in a large impact on the receptor's constitutive and agonist-induced activity. Given the conserved length of the first extracellular loop as well as other mutagenesis reports implicating this loop as being involved in activation, a similar function for the EL1 as described in this report might be the case in other class A GPCRs. However, since the presence of an anti-parallel β-sheet has so far only been established in the adenosine receptor structure, the activating influence of EL1 in other receptors may proceed through different structural features.

ACKNOWLEDGEMENTS

This research was performed under the auspices of the GPCR Forum, a program funded by the Dutch Top Institute Pharma (project D1-105).

REFERENCES

[1] Olah, M.E., Jacobson, K.A., Stiles, G.L., *J Biol Chem* (1994) 269:24692-24698.
[2] Klco, J., Wiegand, C., Narzinski, K., Baranski, T., *Nat Struct Mol Biol.* (2005) 12:320-326.
[3] Massotte, D., Kieffer, B.L., *Nat Struct Mol Biol* (2005) 12:287-288.
[4] Jaakola, V.P., Griffith, M.T., Hanson, M.A., Cherezov, V., Chien, E.Y., Lane, J.R., IJzerman, A.P., Stevens, R.C., *Science* (2008) 322:1211-1217.
[5] Klco, J., Nikiforovich, G., Baranski, T., *J Biol Chem.* (2006) 281:12010-12019.
[6] Vassart, G., Pardo, L., Costagliola, S., *Trends Biochem Sci* (2004) 29:119-126.
[7] Nurwakagari, P., Breit, A., Hess, C., Salman-Livny, H., Ben-Menahem, D., Gudermann, T., *J Mol Endocrinol* (2007) 38:259-275.
[8] Kleinau, G., Jaeschke, H., Mueller, S., Raaka, B.M., Neumann, S., Paschke, R., Krause, G., *Faseb J* (2008) 22:2798-2808.

[9] Sura-Trueba, S., Aumas, C., Carre, A., Durif, S., Leger, J., Polak, M., de Roux, N., *Endocrinology* (2009) 150:1043-1050.
[10] Mizutori, Y., Chen, C.R., McLachlan, S.M., Rapoport, B., *Mol Endocrinol* (2008) 22:1171-1182.
[11] Fredholm, B.B., Arslan, G., Halldner, L., Kull, B., Schulte, G., Wasserman, W., *Naunyn Schmiedebergs Arch Pharmacol* (2000) 362:364-374.
[12] Fredholm, B.B., IJzerman, A.P., Jacobson, K.A., Klotz, K.N., Linden, J., *Pharmacol Rev* (2001) 53:527-552.
[13] Wilson, C.N., *Br J Pharmacol* (2008) 155:475-486.
[14] Spicuzza, L., Di Maria, G., Polosa, R., *Eur J Pharmacol* (2006) 533:77-88.
[15] Hasko, G., Linden, J., Cronstein, B., Pacher, P., *Nat Rev Drug Discov* (2008) 7:759-770.
[16] Brown, A., et al., *Yeast* (2000) 16:11-22.
[17] Stewart, G.D., Valant, C., Dowell, S.J., Mijaljica, D., Devenish, R.J., Scammells, P.J., Sexton, P.M., Christopoulos, A., *J Pharmacol Exp Ther* (2009) 331:277-286.
[18] Beukers, M., van Oppenraaij, J., van der Hoorn, P., Blad, C., den Dulk, H., Brouwer, J., IJzerman, A., *Mol Pharmacol.* (2004) 65:702-710.
[19] Beukers, M., IJzerman, A., *Trends Pharmacol Sci.* (2005) 26:533-539.
[20] Fromant, M., Blanquet, S., Plateau, P., *Anal Biochem* (1995) 224:347-353.
[21] Olesnicky, N.S., Brown, A.J., Dowell, S.J., Casselton, L.A., *Embo J* (1999) 18:2756-2763.
[22] Li, Q., Ye, K., Blad, C.C., den Dulk, H., Brouwer, J., IJzerman, A.P., Beukers, M.W., *J Pharmacol Exp Ther* (2007) 320:637-645.
[23] Eckle, T., et al., *Circulation* (2007) 115:1581-1590.
[24] Borrmann, T., Hinz, S., Bertarelli, D.C., Li, W., Florin, N.C., Scheiff, A.B., Muller, C.E., *J Med Chem* (2009) 52:3994-4006.
[25] Chemical Computing Group, I., Molecular Operating Environment, Quebec, Canada, 2008.
[26] Wang, J., Cieplak, P., Kollman, P., *J Comput Chem* (2000) 21:1049-1074.
[27] Härterich, S., Koschatzky, S., Einsiedel, J., Gmeiner, P., *Bioorg Med Chem* (2008) 16:9359-9368.
[28] Bajaj, A., Connelly, S.M., Gehret, A.U., Naider, F., Dumont, M.E., *Biochim Biophys Acta* (2007) 1773:707-717.
[29] Langer, I., Vertongen, P., Perret, J., Waelbroeck, M., Robberecht, P., *Neuropharmacology* (2003) 44:125-131.
[30] Hauser, M., Kauffman, S., Lee, B.K., Naider, F., Becker, J.M., *J Biol Chem* (2007). 282(14):10387-97.
[31] Hawtin, S., Simms, J., Conner, M., Lawson, Z., Parslow, R., Trim, J., Sheppard, A., Wheatley, M., *J Biol Chem.* (2006) 281:38478-38488.
[32] Archer-Lahlou, E., Tikhonova, I., Escrieut, C., Dufresne, M., Seva, C., Pradayrol, L., Moroder, L., Maigret, B., Fourmy, D., *J Med Chem* (2005) 48:180-191.
[33] Genoud, S., Kajumo, F., Guo, Y., Thompson, D., Dragic, T., *J Virol* (1999) 73:1645-1648.
[34] Langer, I., Tikhonova, I.G., Travers, M.A., Archer-Lahlou, E., Escrieut, C., Maigret, B., Fourmy, D., *J Biol Chem* (2005) 280:22198-22204.
[35] Labrou, N.E., Bhogal, N., Hurrell, C.R., Findlay, J.B., *J Biol Chem* (2001) 276:37944-37949.
[36] Pasel, K., Schulz, A., Timmermann, K., Linnemann, K., Hoeltzenbein, M., Jaaskelainen, J., Gruters, A., Filler, G., Schoneberg, T., *J Clin Endocrinol Metab* (2000) 85:1703-1710.
[37] Cain, S.A., Woodruff, T.M., Taylor, S.M., Fairlie, D.P., Sanderson, S.D., Monk, P.N., *Biochem Pharmacol* (2001) 61:1571-1579.
[38] Sung, C.H., Schneider, B.G., Agarwal, N., Papermaster, D.S., Nathans, J., *Proc Natl Acad Sci U S A* (1991) 88:8840-8844.
[39] Ballesteros, J.A., Weinstein, H., *Methods Neurosci* (1995) 25:366–428.
[40] Hjorth, S.A., Schambye, H.T., Greenlee, W.J., Schwartz, T.W., *J Biol Chem* (1994) 269:30953-30959.
[41] Fishman, G.A., Stone, E.M., Gilbert, L.D., Sheffield, V.C., *Arch Ophthalmol* (1992) 110:646-653.
[42] Vaithinathan, R., Berson, E.L., Dryja, T.P., *Genomics* (1994) 21:461-463.
[43] Tenenbaum-Rakover, Y., Commenges-Ducos, M., Iovane, A., Aumas, C., Admoni, O., de Roux, N., *J Clin Endocrinol Metab* (2007) 92:1137-1144.
[44] Parma, J., Van Sande, J., Swillens, S., Tonacchera, M., Dumont, J., Vassart, G., *Mol Endocrinol* (1995) 9:725-733.
[45] Noda, K., Saad, Y., Graham, R.M., Karnik, S.S., *J Biol Chem* (1994) 269:6743-6752.
[46] Dohlman, H.G., Caron, M.G., DeBlasi, A., Frielle, T., Lefkowitz, R.J., *Biochemistry* (1990) 29:2335-2342.
[47] Moro, S., Hoffmann, C., Jacobson, K., *Biochemistry* (1999) 38:3498-3507.

[48] Branden, C., Tooze, J., Introduction to protein structure, Garland Publishing, New York and London, 1991.

CHAPTER 4

THREE "HOTSPOTS" IMPORTANT FOR ADENOSINE A_{2B} RECEPTOR ACTIVATION: A MUTATIONAL ANALYSIS OF TRANSMEMBRANE DOMAINS 4 AND 5 AND THE SECOND EXTRACELLULAR LOOP

This chapter was based upon:

M.C. Peeters, Q. Li, G.J.P. van Westen, A.P. IJzerman. Purinergic Signaling **2011** [In press]

ABSTRACT

G protein-coupled receptors (GPCRs) are a major drug target and can be activated by a range of stimuli, from photons to proteins. Despite the progress made in the last decade in molecular and structural biology, their exact activation mechanism is still unknown. Here we describe new insights in specific regions essential in adenosine A_{2B} receptor activation ($A_{2B}R$), a typical class A GPCR. We applied unbiased random mutagenesis on the middle part of the human adenosine A_{2B} receptor ($A_{2B}R$), consisting of transmembrane domains four and five (TM4 and TM5) linked by extracellular loop 2 (EL2), and subsequently screened in a medium-throughput manner for gain-of-function and constitutively active mutants (CAMs). For that purpose we used a genetically engineered yeast strain (*S. cerevisiae* MMY24) with growth as a read-out parameter. From the random mutagenesis screen, 12 different mutant receptors were identified that form three distinct clusters; at the top of TM4, in a cysteine-rich region in EL2, and at the intracellular side of TM5. All mutant receptors show a vast increase in agonist potency and most also displayed a significant increase in constitutive activity. None of these residues are supposedly involved in ligand binding directly. As a consequence, it appears that disrupting the relatively 'silent' configuration of the wild-type receptor in each of the three clusters readily causes spontaneous receptor activity.

INTRODUCTION

The adenosine receptors form a small subfamily of class A G protein-coupled receptors (GPCRs). Four subtypes of adenosine receptors are known (A_1R, $A_{2A}R$, $A_{2B}R$, and A_3R) that all bind the endogenous ligand adenosine. The A_1R and the A_3R subtypes are coupled to G_i proteins, hereby mediating the inhibition of adenylyl cyclase causing decreased levels of cAMP in the cell. The $A_{2A}R$ and $A_{2B}R$ signal mainly through G_s proteins resulting in the activation of adenylyl cyclase and an increase in intracellular cAMP levels. Of the adenosine subfamily, the $A_{2B}R$ subtype has been investigated least. Similar to all GPCRs, the $A_{2B}R$ is made up of seven transmembrane domains connected by three intracellular and three extracellular loops, an extracellular N-terminus, and an intracellular C-terminus. The adenosine A_{2B} receptor ($A_{2B}R$) has been implicated in several (auto)-immune diseases such as asthma and chronic obstructive pulmonary disease (COPD) and is therefore an interesting drug target [1].

In a previous study, random mutagenesis combined with a yeast screen for activating mutant receptors have been performed on two parts of the adenosine A_{2B} receptor in order to identify specific residues involved in the activation of the receptor [2,3]. Mutations were randomly introduced in two separate fragments of the receptor, one ranging from the ATG until a KpnI restriction site in the second intracellular loop and a second form the BglII restriction site in the third intracellular loop until the end of the receptor (**Figure 1**). These studies revealed many constitutively active mutations, both in the transmembrane domains as well as in the extracellular regions. The fragment that is in between the two restriction sites KpnI and BglII, encompassing transmembrane domain 4 (TM4), the second extracellular loop 2 (EL2), and transmembrane domain 5 (TM5), has so far not been examined. However, this region may be very important in the activation mechanism of the receptor. All three domains in this fragment have been implied to participate in the dynamic movements the receptor undergoes during activation [4]. Clear evidence for the importance of this region is also provided by the recently published crystal structures of both the antagonist-bound and agonist-bound adenosine $A_{2A}R$, the closest homologue of the $A_{2B}R$. In particular EL2 and TM5 appear to be involved directly in ligand binding and in conformational movements induced by agonist binding [5,6,7]. Also, EL2 has been

proposed to act as a negative regulator for the receptor, keeping it in its inactive state and is in many receptors part of the ligand binding site [8,9,10,11].

In the present study we examined the influence of EL2 and its two adjacent transmembrane domains, TM4 and TM5, of the adenosine A_{2B} receptor on receptor activation. We performed an unbiased random mutagenesis screen for gain-of-function mutations as well as constitutively active mutants (CAMs) , i.e. mutant receptors that show basal activity independent of an agonist. In these CAMs, the equilibrium between the inactive (R) and active conformation (R*) is shifted, so that the active state is energetically more favorable than in the wild type situation, similar to what occurs when the receptor binds an agonist [12]. Residues that are mutated to cause this shift in equilibrium are therefore likely to be involved in the on-and-off switch of the receptor and can provide us with information on the activation mechanism of the receptor.

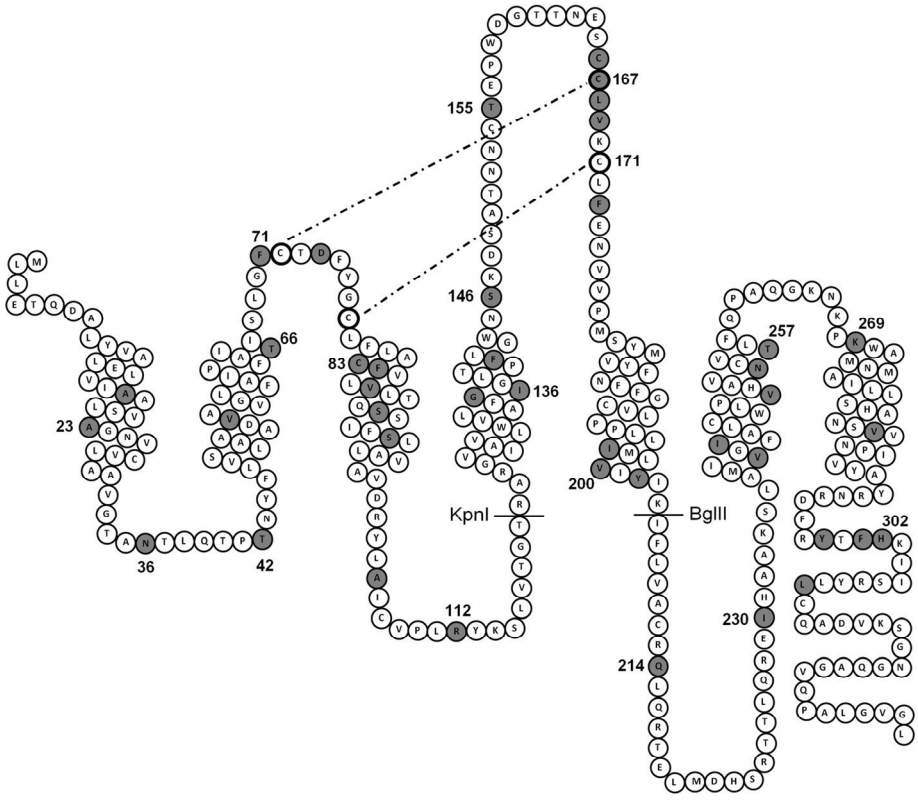

Figure 1. Snake-plot of the adenosine A_{2B} receptor. Mutated residues within the A_{2B}R identified to result in increased constitutive activity are indicated in grey. These mutations originate from two previously described screens. and the TM4-EL2-TM5 screen described in the current paper. The putative disulfide bridges are indicated with dotted lines. The disulfide bridge conserved in many class A GPCRs links $C78^{3.25}$ and $C171^{EL2}$. The non-conserved second disulfide bridge between EL1 and EL2 is based on an analogous bond in the crystal structures of the adenosine A_{2A}R (PDB: 3EML, 3QAK, 3YDO, 3YDV); it links $C72^{EL1}$ and $C167^{EL2}$. The restriction sites KpnI and BglII are indicated; they were used to obtain the fragment for random mutagenesis

We performed the screen for activating mutant receptors using a *S. cerevisiae* strain that has been genetically modified to serve as a reporter system with growth as an output parameter. This yeast system is an ideal background to monitor activation of a single GPCR, since the endogenous GPCR (Ste2) has been removed from the system while still maintaining the complete GPCR signaling machinery [13]. Several previous reports have proved this eukaryotic system to be predictive of the mammalian situation, as shown by functional and binding studies in CHO cells [2,14]. Several mutated residues were identified, causing the receptor to be highly increased in both agonist-induced and spontaneous activity. The results presented here can be of general interest in increasing our understanding of the activation mechanism of class A GPCRs, of adenosine receptors in particular as well as other members of this superfamily.

MATERIALS AND METHODS

DNA Constructs

The S*. cerevisiae* expression vector containing the adenosine A_{2B} receptor gene, the pDT-PGK_A_{2B}R plasmid, was kindly provided by Dr. Simon Dowell from GSK (Stevenage, UK). A KpnI restriction site was introduced in the A_{2B}R gene in the region encoding the second intracellular loop. Together with a restriction site in the third intracellular loop, BglII, it is possible to divide the receptor into three large fragments suitable for random mutagenesis. The fragment between these two restriction sites was used in the mutagenic PCR. This fragment encodes transmembrane domain four, the second extracellular loop, and transmembrane domain five (TM4-EL2-TM5).

Mutagenic PCR for the construction of the random mutagenesis library

The introduction of random mutations in the adenosine A_{2B} receptor was achieved by manipulating the polymerase chain reaction adapted from the method of Fromant et al. [15]. In this error-prone PCR method, the balance between Mg^{2+} ions and Mn^{2+} ions was shifted, compromising fidelity of the DNA polymerase enzyme. Furthermore, the introduction of mutations can be guided by adding excess of one of the nucleotides (the ‘forcing’ nucleotide). This technique makes it possible to

introduce mutations in fragments up to 400 bp in length. The DNA fragment encoding TM4-EL2-TM5 encompasses 262 bp. The mutagenic reaction contained 10 ng of template DNA, 0.1 µM concentrations of each primer, 0.2 mM concentrations of dNTPs as well as 3.4 mM concentrations of the nucleotide in excess dCTP, 0.5 mM $MnCl_2$, 4.7 mM $MgCl_2$, and 0.5 units of Super *Taq* polymerase without proofreading. The number of mutagenic PCR cycles was set to 10. Using these conditions, only a limited amount of mutations are introduced per fragment [16].

The following primers were used:

5'-GGTATAAAAGTTTGGTCACGGGTACCCGAGCAA-3'

5'-GAAGCTGCCTGCAGGCCACCAGGAAGATCTTAATG-3'

The mutagenic PCR products were submitted to agarose gel electrophoresis and the gel bands containing the mutated fragments were isolated from the gel and purified. Subsequently, the mutated fragments were amplified further with 10 cycles of a regular PCR with the same primer sets. After the error prone PCR, the normal fragment TM4-EL2-TM5 in the wild type receptor was replaced by the mutated fragments using the restriction sites KpnI and BglII and transformed into DH5α *E.Coli* competent cells (Invitrogen, San Diego, CA, USA). Plasmids were isolated from the culture resulting in a mutagenic adenosine A_{2B} receptor library.

Transformation in MMY24 S. cerevisiae strain

pDT-PGK_A_{2B}R plasmids were transformed into an *S. cerevisiae* yeast strain according to the Lithium-Acetate procedure [17]. The MMY24 strain is derived from the MMY11 strain and was further adapted to communicate with mammalian GPCRs through the introduction of a chimeric G protein [13]. The genotype of the MMY24 strain is: *MAT**a**his3 leu2 trp1 ura3can1 gpa1_::G_i3 far1 ::ura3 sst2_::ura3 Fus1::FUS1-HIS3 LEU2::FUS1-lacZ ste2_::G418R.* To measure signaling of GPCRs, the pheromone signaling pathway of this strain was coupled via the FUS1 promoter to HIS3, a gene encoding the key enzyme in histidine production, imidazole glycerol-phosphate dehydrase. The degree of receptor activation was measured by the growth rate of the yeast on histidine-deficient medium. A second reporter gene was placed under control of the FUS1 promoter; the LacZ gene. Transcription of this gene results in the production of the enzyme β-galactosidase. The presence of this enzyme is also a measure of receptor activation.

Random mutagenesis screen

The random mutagenesis screen was performed on selection agar medium in two steps. Firstly, yeast cells were selected for the presence of the plasmid pDT-PGK using selection medium lacking the markers uracil and leucine (YNB-UL). After 3 days of incubation at 30 ˚C, positive colonies were pooled. For the second selection step, 10^4 cells were spread onto selection medium lacking uracil, leucine, and histidine (YNB-ULH) to select for the pDT-PGK plasmid, the MMY24 yeast strain, and activity of the receptor, respectively. A concentration of 7 mM 3-aminotriazole (3-AT), a competitive inhibitor of imidazole glycerol-phosphate dehydrase, was added to the agar plates to suppress basal yeast growth that occurs in histidine-deficient medium. Also, a concentration of 1 nM of the full $A_{2B}R$ agonist 5'-*N*-ethylcarboxamido-adenosine (NECA) was added to the medium, a concentration at which yeast cells expressing the wild type human adenosine A_{2B} receptor still barely grow. After three days, colonies were selected and transferred to new selection plates. To further select for true active mutant receptors, we performed a qualitative β-galactosidase assay according to protocol #PT3024-1 from Clontech (Clontech laboratories, Mountain View, California). In brief, yeast colonies were transferred to a filter and lysed using repeated freeze-thawing with liquid nitrogen. The filter was then placed on top of several Whatman papers presoaked in Z-buffer (16.1 g/L Na_2HPO_4, 5.5 g/L NaH_2PO_4, 0.75 g/L KCl, 0.246 g/L $MgSO_4$, 0.3% β-mercaptoethanol) and 0.3 mg/ml X-gal (5-bromo-4-chloro-3-indolyl-β-D-galactosidase), a substrate of β-galacto-sidase. The filter was incubated at 30ºC until a blue color appeared. Colonies with a blue color were chosen for further characterization. Mutated receptors were sequenced and subsequently retransformed into the yeast strain to confirm their activated phenotype.

Liquid growth assay

To characterize the mutant receptors further, concentration-growth curves were generated in a liquid growth assay. This assay is on 96-wells scale and growth is easily determined by measuring absorption at a wavelength of 595 nm. In this assay, 150 µl liquid YNB-ULH medium with 7 mM 3-AT and a varying concentration of NECA (10^{-10}-10^{-5} M) was added to each well. A concentration range from 10^{-10} to 10^{-5} M was also used for the concentration-growth curves with BAY 60-6583 (2-[6-amino-3,5-dicyano-4-[4-(cyclopropylmethoxy)phenyl]pyridin-2-ylsulfanyl]acetamide;

synthesized in house), a non-nucleoside agonist [18]. Yeast cells from an overnight culture were diluted to around $4 \cdot 10^6$ cells/ml ($OD_{600} \approx 0.2$) and 50 µl was added per well. The 96-wells plate was then incubated for 35 hours in a Genios plate reader (Tecan, Durham, NC). at 30°C, keeping the cells in suspension by shaking every 10 minutes at 300rpm for 1 minute. Results originate from three independent experiments, performed in duplicate.

Solid growth assay

To monitor the response of the mutant receptors in the presence of the inverse agonist ZM241385 (4-{2-[7-amino-2-(2-furyl)[1,2,4]triazolo-[2,3-a][1,3,5]triazin-5-yl-amino]ethyl}phenol), a solid yeast growth assay was used. Yeast growth was determined based on growth density, rather than absorption at 595 nm; this enabled us to visualize the level of constitutive activity more clearly. In the solid growth assay, yeast cells from an overnight culture were diluted to around 400,000 cells/ml (OD600 ≈ 0.02), and droplets of 1.5 µl were spotted on selection agar plates, YNB-ULH, containing 7 mM 3-AT and a ZM241385 concentration ranging from 10^{-11} to 10^{-5} M. For the single point experiments, a final concentration of 10^{-5} M ZM241385 was used [19]. After incubation at 30°C for 50 h, the plates were scanned and receptor-mediated yeast growth was quantified with Quantity One imaging software from Bio-Rad (Hercules, CA). The growth rate of yeast was calculated as the density of each spot with a correction for local background on the plate. Results are obtained from four independent experiments, performed in quadruplicate.

Whole cell radioligand binding experiments

Yeast cells expressing wild type or mutated A_{2B}Rs were cultured overnight in rich YAPD (Yeast Extract Adenine Peptone Dextrose) medium. Cells were centrifuged for 5 minutes at 2000 xg, the pelleted cells were once washed with 0.9% NaCl. The cells were again centrifuged 5 minutes at 2000 xg and diluted in the assay buffer (50mM Tris-HCl pH7.4 + 1mM EDTA) to OD_{600}=40 ($OD_{600} = 1 \approx 2.5 \cdot 10^7$ cells/ml). Binding experiments were performed with 1.3 nM [^{3}H]PSB-603 (8-[4-[4-(4-Chlorophenyl) piperazine-1-sulfonyl)phenyl]]-1-propylxanthine; $K_{D,yeast}$ = 0.8 +/- 0.02 nM) and a final cell concentration of $25 \cdot 10^7$ cells/ml in a total volume of 100 µl [3,20]. Nonspecific binding was determined in the presence of 1mM NECA. For whole competition

curves a concentration range of 10^{-10}-10^{-3} M of the ribose agonist NECA, 10^{-10}-10^{-4} M of the non-ribose agonist BAY 60-6583, or 10^{-10}-10^{-4} M of the inverse agonist ZM241385 was used. Samples were incubated for 1 hour at 25ºC while shaking vigorously to keep the yeast cells in suspension. Incubation was terminated by adding 1ml ice-cold assay buffer. Bound from free radioligand was immediately separated by rapid filtration through Whatman GF/B filters pre-incubated with 0.1% polyethylenimine (PEI) using a Millipore manifold during which the filters were washed six times with ice-cold assay buffer. Filter-bound radioactivity was determined by scintillation spectrometry (Tri-Carb 2900TR; PerkinElmer Life and Analytical Sciences) after addition of 3.5 ml of PerkinElmer Emulsifier Safe. Results are obtained from three independent experiments, performed in duplicate.

Whole cell extracts and immunoblotting

Whole protein cell extracts were made from the transformed yeast cells using trichloroacetic acid (TCA). From an overnight culture, $1.2 \cdot 10^8$ yeast cells were harvested in mid-log phase. The cells were washed twice with 20% TCA after which they were broken by vigorous vortexing in the presence of glass beads. The yeast cell extracts were separated using SDS/PAGE and subsequently blotted on Hybond-ECL membranes. For this purpose, a sample of 4.0 µl containing 12 µg protein was loaded on a 12.5% SDS/PAGE gel. A semi-automated electrophoresis technique (PhastSystem™, Amersham Pharmacia Biotech) was used for SDS/PAGE as well as blotting. The antibody directed against the C-terminal region of the adenosine A_{2B} receptor was kindly provided by Dr. I. Feoktistov (Vanderbilt University, Nashville). Densitometric analysis of the protein bands was performed using the volume analysis tool as present in the Quantity One imaging software from Bio-Rad (Hercules, CA). The non-specific band at approximately 45 kDa was used as loading control. The ratio between specific $A_{2B}R$ protein bands (at 29 kDa and 48 kDa) and the non-specific band was determined and the wild type receptor was set at 100%, the empty vector pDT-PGK at 0%. The experiment was performed in duplicate. The relative expression levels represent expression of the whole receptor population, not distinguishing between cell surface and intracellularly expressed protein.

Bioinformatics - Mapping the mutated residues onto the adenosine A_{2A} receptor structure

The positions of the mutations identified in the random mutagenesis screen were mapped onto the corresponding positions in the crystal structure of the agonist-bound adenosine A_{2A} receptor (PDB: 2YDV) [7]. These corresponding positions were determined by a multiple sequence alignment created using ClustalW with default parameters. To make use of known crystallographic data, the sequences of the CXCR4 Chemokine (CXCR4R) receptor and the β_2-adrenergic (b2AR) receptor were included in this alignment. The EL2 was defined from the crystal structures of the A_{2A} receptor (residues 143 to 173), the CXCR4R (residues 175 to 192) and the b2AR (residues 171 to 196). The amino acids in the TM domains of the various receptors were related through their Ballesteros and Weinstein numbering [21].

Bioinformatics - cysteine occurrence analysis

To gain insight in the number of class A GPCRs that have multiple cysteines present in the second extracellular loop, we analyzed all human olfactory (415) and non-olfactory (221) class A GPCRs as present in the GPCRDB [22]. A cysteine count was performed on the second extracellular loop that for this analysis was defined as the fragment between residues 4.55 and 5.38 according to the Ballesteros and Weinstein numbering [21]. These two residues are located at the interface of the loop and the transmembrane domains, but are present within the membrane in all predictions.

RESULTS

Random mutagenesis screen in yeast

Mutations were randomly introduced in the fragment encoding for transmembrane domain 4 (TM4), the second extracellular loop (EL2), and transmembrane domain 5 (TM5) of the human adenosine A_{2B} receptor using an error-prone PCR reaction (**Figures 1 and 2**). The corresponding fragment in the wild type receptor was replaced after mutagenesis by the mutated fragments, which rendered a set of approximately 5000 different plasmids of which ca. 80% contained mutations. The mutations occurred in a low frequency; most of the mutant receptors contained single point mutations and the mutant receptor with the highest mutation frequency

contained 5 nucleotide changes. These results are comparable to a random mutagenic library of the first three transmembrane domains of the $A_{2B}R$ published by Beukers et al. [2]. After ligation, the plasmids were propagated in competent *E. coli* cells, resulting in the final mutant $A_{2B}R$ library (**Figure 2**). This mutant library was subsequently transformed in the *S. cerevisiae* MMY24 strain.

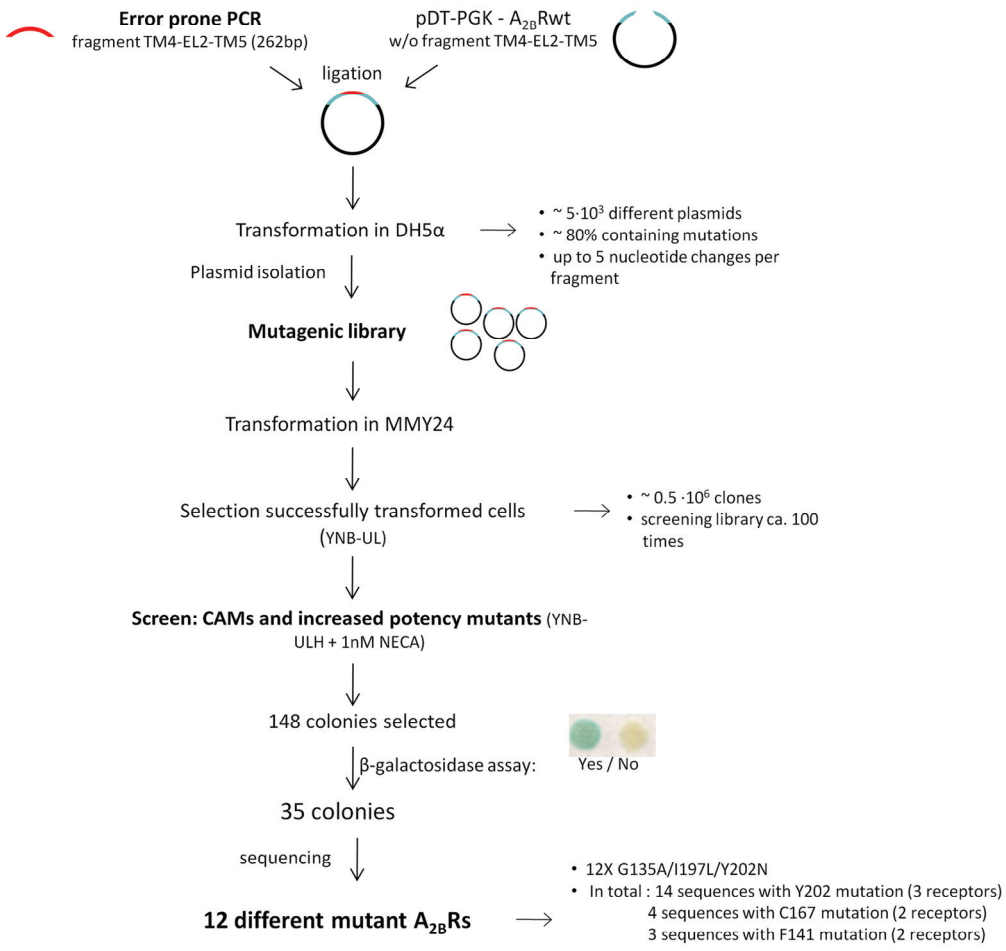

Figure 2. Schematic overview of the screen for activating mutations. The mutated fragments from the mutagenic PCR were reintroduced in an otherwise wild type $A_{2B}R$ in the pDT-PGK vector, resulting in the mutagenic $A_{2B}R$ library. The library was transformed in the MMY24 yeast strain and screened for mutant receptors with constitutive activity and/or an increased potency for NECA. As a second selection criteria, the presence of β-galactosidase was determined in a qualitative assay, resulting in a final selection of 35 yeast colonies. Sequencing revealed 12 different mutant receptors.

The MMY24 yeast strain has been genetically modified to enable mammalian GPCRs to couple to the yeast pheromone pathway with subsequent transcription of the reporter gene HIS3, increasing the histidine synthesis. We used this trait to specifically select yeast cells that express an active receptor by their ability to produce histidine and therefore grow on histidine-deficient medium. Before starting

the actual screen, we first selected yeast cells that were successfully transformed. We then screened the transformed MMY24 cells for an active phenotype on selection plates lacking uracil, leucine, and histidine (YNB-ULH) to select for the MMY24 yeast strain, the pDT-PGK plasmid, and activity of the receptor, respectively. By also adding a low concentration of 1 nM of the agonist NECA (EC_{50} value at wild type $A_{2B}R$: 137 +/- 10 nM, see also **Table 1**), we screened for both constitutively active mutants (CAMs) and mutant receptors with increased agonist potency. In total, ca. 0.5 million yeast clones were used for the final activation screen, so the library was screened approximately 100 times. From the screen, all well separated colonies that appeared on the selection plates were selected (a total of 148 yeast colonies). Besides the reporter gene HIS, a second reporter gene was incorporated into the MMY24 genome under the same promoter; the LacZ reporter gene, causing the yeast cell to also produce the enzyme β-galactosidase. To proceed with the most active mutant receptors, we performed a qualitative β-galactosidase assay. The colonies were lysed and the presence of the enzyme β-galactosidase was measured. The 35 colonies with the strongest response in this assay, out of the original 148, were selected, plasmids were isolated from the yeast cells and the mutations were identified by sequencing. Several of the nucleotide changes observed in the sequences resulted in the same amino acid changes in the $A_{2B}R$. Mutant receptor G135A$^{4.55}$/I197L$^{5.53}$/Y202N$^{5.58}$ was identified most, namely 12 times out of the 35 sequenced plasmids (shown in superscript are the positions according to the Ballesteros and Weinstein GPCR numbering system [21]) (**Figure 2, Table 1**). In total, 12 different mutant receptors were identified, containing altogether 13 mutated positions (**Figure 1**). Amongst the 12 mutant receptors, residues F141$^{4.61}$, C167^{EL2}, and Y202$^{5.58}$ were found mutated more than once. Amino acid changes of F141$^{4.61}$ were identified in two different receptors; in the single mutant F141L$^{4.61}$ and in the double mutant F141C$^{4.61}$/Y202C$^{5.58}$. The mutation C167S^{EL2} was found as a single mutant as well in combination with a residue outside of the cluster: T155^{EL2}. Mutations at position Y202$^{5.58}$ were present in three different mutant receptors: G135A$^{4.55}$/I197L$^{5.53}$/Y202N$^{5.58}$, F141C^{4,61}/Y202C$^{5.58}$, and Y202S$^{5.58}$ (**Table 1**). The mutated residues form three distinct clusters in the receptor; at the top of TM4, at a cysteine-rich area in EL2, and at the bottom of TM5. Four receptors contained mutations in TM4, forming a small cluster of three amino acids: G135$^{4.55}$, I36$^{4.56}$, and F141$^{4.61}$. In EL2 a total of seven residues were found mutated in five different mutant

receptors. Five of the seven residues form a tight cluster, namely $C166^{EL2}$, $C167^{EL2}$, $L168^{EL2}$, $V169^{EL2}$, and $F173^{EL2}$. The cluster seen in TM5 consists of three residues: $I197^{5.53}$, $V200^{5.56}$, and $Y202^{5.58}$ (**Figure 1, Table 1**).

Table 1. Characterization of the adenosine receptor A_{2B} receptor mutants identified from the random mutagenesis screen using the liquid yeast growth assay . Mutations are shown in the numbering of the $A_{2B}R$ protein as well as according to the Ballesteros and Weinstein GPCR numbering system (in superscript). EC_{50} values (nM) are shown as means ± SEM of at least three independent experiments, each performed in duplicate. Results with the ribose agonist NECA are shown for all mutant receptors. For wild type and mutant receptors $F141L^{4.61}$, $C167S^{EL2}$ and $Y202S^{5.58}$ also results with the non-ribose agonist BAY60-6583 are shown. % Emax represents the intrinsic activity of the receptor, where the maximal growth level of wild type receptor in response to the agonists was set as 100%. Fold CA represents the relative increase in growth compared to wild type when no agonist was present.

		NECA 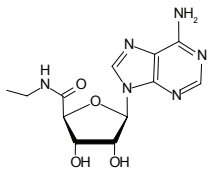		BAY 60-6583 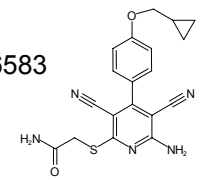	
Mutant	Fold CA	EC_{50} (nM)	% Emax	EC_{50} (nM)	% Emax
WT	1.0	137 +/- 10	100	48 +/- 3	100
$F141L^{4.61}$	1.5	5.4 +/- 0.8	99	9.0 +/- 0.6	102
$C167S^{EL2}$	6.3	8.8 +/- 1.4	100	23 +/- 3	98
$Y202S^{5.58}$	13	13 +/- 3	66	4.9 +/- 0.3	70
$G135A^{4.55}$/$I197L^{5.53}$/ $Y202N^{5.58}$	38	7.1 +/- 0.7	94		
$I136T^{4.56}$	1.5	10 +/- 2	100		
$F141C^{4.61}$/$Y202C^{5.58}$	9.7	15 +/- 2	68		
$S146R^{EL2}$/$V169A^{EL2}$	4.6	9.9 +/- 0.7	101		
$T155A^{EL2}$/$C167S^{EL2}$	3.3	9.3 +/- 1.9	100		
$C166L^{EL2}$	5.6	12 +/- 2	100		
$L168P^{EL2}$	5.5	11 +/- 3	101		
$F173L^{EL2}$	4.2	10 +/- 1	99		
$V200G^{5.56}$	5.0	13 +/- 2	90		

Constitutively active and gain-of-function mutants

To confirm the active phenotype, all 12 receptors were retransformed into the yeast strain and their pharmacology was investigated using yeast-growth assays. All mutant receptors showed an increase in constitutive activity, although less pronounced in mutant receptors F141L$^{4.61}$ and I136T$^{4.45}$ (1.5 times compared to wild type) (**Figure 3A, Table 1**). Mutant receptor G135A$^{4.55}$/I197L$^{5.53}$/Y202N$^{5.58}$ showed the largest increase in basal activity with yeast growth levels 38-fold over wild type, corresponding to 62% of the maximal activation level. The constitutive activity of this mutant receptor could be reduced by the inverse agonist ZM241385, however, a residual activity of 8% remained. The level of constitutive activity of the other 11 mutant receptors could be fully suppressed (**Figure 3A**). For mutant Y202S$^{5.58}$, a full concentration-growth inhibition curve with ZM241385 showed a potency of 31.3 +/- 4.4 nM for ZM241385. In comparison, in literature values between 13 and 50 nM have been reported for wild type A_{2B}R [23,24] (**Figure 3B**).

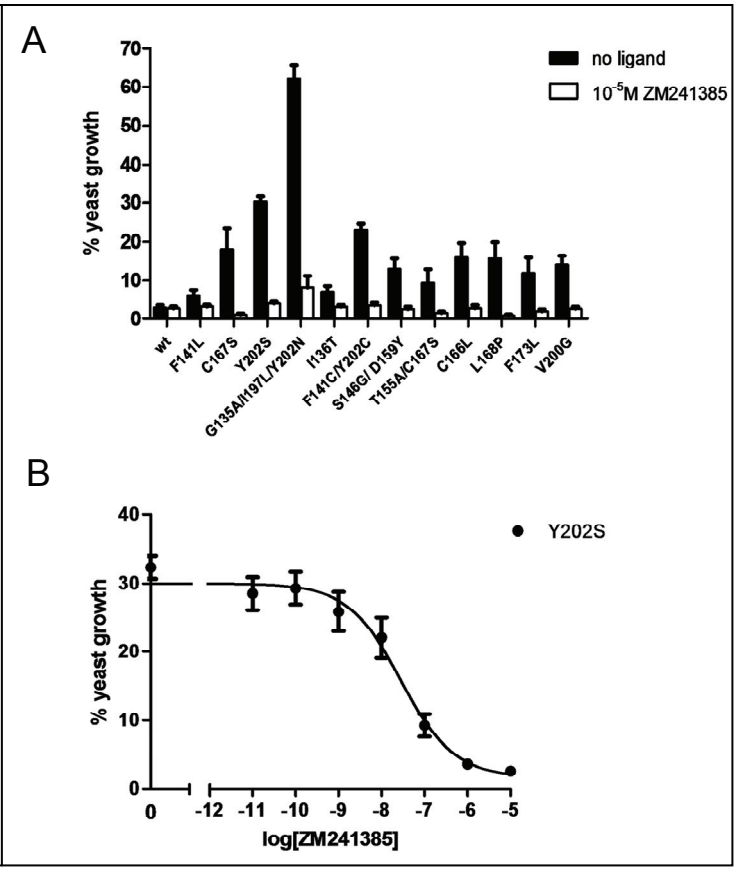

Figure 3. Constitutive activity of the mutant receptors determined in a solid yeast growth assay (*A*) Growth was measured on selective agar plates YNB-ULH in the absence of a ligand or in the presence of 10 µM of the inverse agonist ZM241385. The vertical bars in the graph represent the percentage spontaneous activity of wild type A_{2B}R and mutant receptors (black) and the response to ZM241385 (white). The maximal activation level of wild type receptor was set at 100%, the background of the selection plate was set at 0%. (*B*) Concentration-growth inhibition curve of mutant receptor Y202S$^{5.58}$. A concentration range of 10^{-11} to 10^{-5} M ZM241385 was added to the selection agar plates. The figure is representative of one experiment performed in quadruplicate. The IC_{50} value for ZM241385 was 31.3 +/- 4.4 nM, determined from four independent experiments

Concentration-growth curves revealed that all mutant receptors showed a large increase in potency of more than one log-unit for the full agonist NECA (**Table 1**). Curves of mutant receptors F141L$^{4.61}$, C167S^{EL2}, Y202S$^{5.58}$, G135A$^{4.55}$/I197L$^{5.53}$ /Y202N$^{5.58}$, and T155A^{EL2}/C167S^{EL2} are shown in **Figure 4**. Even though the level of constitutive activity in mutant G135A$^{4.55}$/I197L$^{5.53}$/Y202N$^{5.58}$ was very high, the maximal level of receptor activation could be reached in response to NECA in a dose-dependent manner, with an EC_{50} value of 7.1 +/- 0.7 nM compared to 137 +/- 10 nM seen for wild type $A_{2B}R$ (**Table 1**). Mutant receptor Y202S$^{5.58}$ also has a relatively high level of constitutive activity being 13-fold higher than wild type receptor. However, upon stimulation with NECA the maximum receptor activation (Emax) was lower than observed with wild type $A_{2B}R$. Similar results were observed for the receptor where Y202$^{5.58}$ was mutated in combination with residue F141: mutant receptor F141C$^{4.61}$/Y202C$^{5.58}$ (**Table 1**).

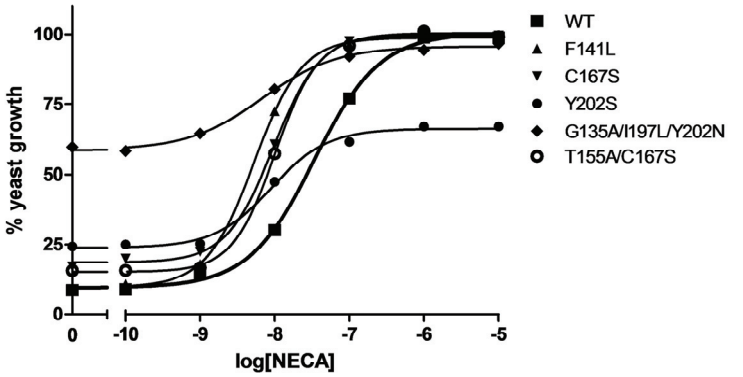

Figure 4.
Concentration- response curves from liquid yeast growth experiments. Curves are shown of wild type (WT ■) and mutant receptors F141L$^{4.61}$ (▲), C167S^{EL2} (▼), Y202S$^{5.58}$ (●), G135A$^{4.55}$/I197L$^{5.53}$/Y202N$^{5.58}$ (♦) and T155A^{EL2}/C167S^{EL2} (○). Curves are shown from a representative experiment. Data for all experiments are presented in Table 1.

Residues F141$^{4.61}$ (TM4), C167^{EL2} (EL2), and Y202$^{5.58}$ (TM5) were identified multiple times in the screen, suggesting a particular important function of these positions in receptor activation. For additional studies, we therefore focused on the single mutant receptors containing each of the residues; F141L$^{4.61}$, C167S^{EL2}, and Y202S$^{5.58}$. These single mutants were also studied with BAY60-6583, a structurally different $A_{2B}R$ agonist [18]. This full agonist lacks a ribose moiety that is present in the adenosine derivative NECA and previously thought to be essential for adenosine receptor activation. The chemical structures of both agonists NECA and BAY60-6583 are shown in **Tables 1 and 2**. BAY60-6583 was more than 5 times more potent at mutant receptor F141L$^{4.61}$; in comparison, NECA's potency was more than 25-fold increased. Both NECA and BAY60-6583 displayed a 10-fold increase in potency on

mutant Y202S$^{5.58}$. Mutant receptor C167S^{EL2} showed a small 2-fold increase in potency in response to BAY60-6583, with NECA this was over 15-fold. Western blot analysis of whole cell lysates showed a similar degree of expression of the mutant receptors compared to the wild type receptor, indicating that the increase in activation profile was not due to overall increases in receptor levels in the system, both intracellular and expressed at the cell surface. Results of mutant receptors F141L$^{4.61}$, C167S^{EL2}, and Y202S$^{5.58}$ are shown in **Figure 5**.

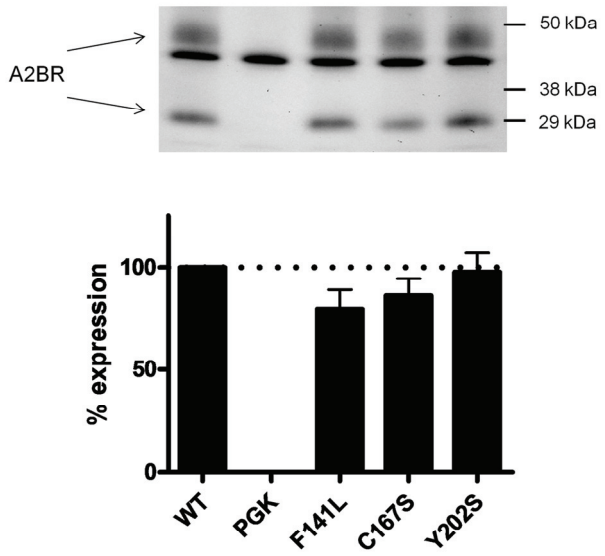

Figure 5. Western Blot Analysis. The relative expression of mutants F141L$^{4.61}$, C167S^{EL2}, Y202S$^{5.58}$ compared to the wild type receptor was determined using densitometric analysis of the Western blots. The ratio was determined between the density of the specific bands and the density of the non-specific band that is always present on the blot. Wild type receptor was set at 100%, the empty vector pDT-PGK was set at 0%. The experiment was performed in duplicate. One representative blot is shown in the upper panel. The arrows indicate the specific $A_{2B}R$ bands; these are located at ca. 29 kDa and 48 kDa.

Radioligand binding experiments on the activated mutant receptors

To investigate the influence of the mutated residues on binding next to activation, we performed radioligand binding experiments using the $A_{2B}R$ selective antagonist [^{3}H]PSB-603 [3,20]. Saturation binding experiments showed a K_D of the radioligand on whole yeast cells expressing the $hA_{2B}R$ of 0.81 +/- 0.02 nM (data not shown), in comparison, the K_D value determined on CHO cell membranes expressing the $hA_{2B}R$ was 0.40 +/- 0.19 nM [20]. Competition binding curves were made for wild type and mutant receptors with unlabeled NECA, BAY 60-6583, or ZM241385 as a displacer. For mutant receptor Y202S$^{5.58}$ we were not able to reach a high enough window to perform competition binding curves. This is likely due to a decrease in affinity for the radiolabeled antagonist [^{3}H]PSB-603 since no change in expression levels was observed (**Figure 5**).

Table 2. Competition binding experiments with the radiolabeled antagonist [^{3}H]PSB-603 ($K_{D,yeast}$ = 0.8 +/- 0.02 nM). Mutants F141L$^{4.61}$ and C167S^{EL2} were tested on their affinity for the full agonist NECA, the non-ribose agonist BAY 60-6583, and the inverse agonist ZM241385. IC_{50} values are shown as means ± SEM of at least three independent experiments, each performed in duplicate.

	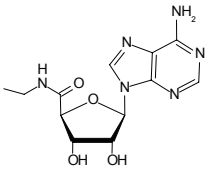	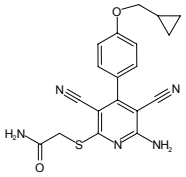	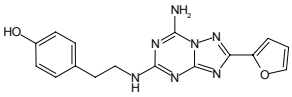
	IC_{50} (nM) NECA	IC_{50} (nM) BAY 60-6583	IC_{50} (nM) ZM241385
WT	1574 +/ 411	785 +/- 74	58 +/- 5
F141L$^{4.61}$	123 +/- 18	137 +/- 8	87 +/- 2
C167S^{EL2}	173 +/- 33	818 +/- 82	104 +/- 18

Mutant receptors F141L$^{4.61}$ and C167S^{EL2} showed a large increase in NECA affinity compared to the wild type receptor of 13-fold and 9-fold, respectively (**Table 2**). In the radioligand binding experiment with BAY 60-6583 as displacer, the affinity of mutant F141L$^{4.61}$ was again increased. In contrast, mutant C167S^{EL2} had an affinity for BAY 60-6583 similar to wild type A_{2B} receptor (**Figure 6, Table 2**). The affinity of the inverse agonist ZM241385 was also determined. Both mutant receptors did not show a large change in affinity for ZM241385 compared to wild type receptor, although the effect on F141L$^{4.61}$ was significant (**Table 2**).

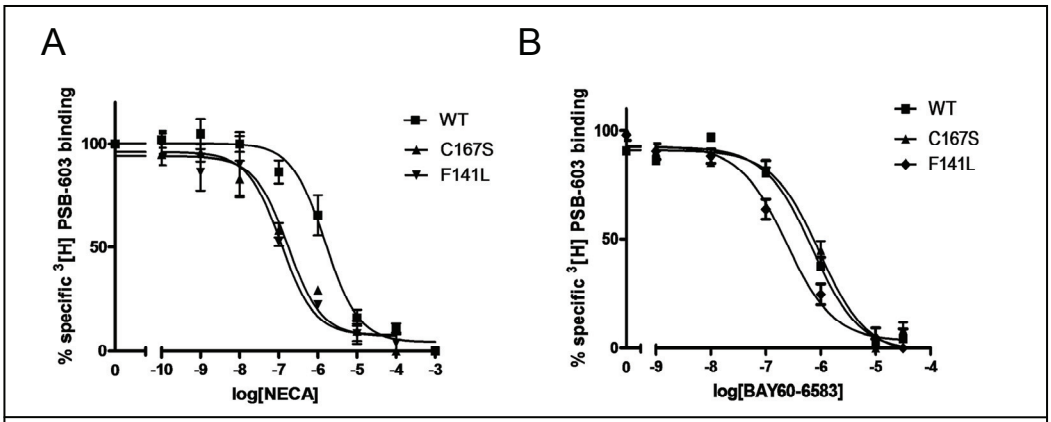

Figure 6. Competition binding curves using [^{3}H]PSB-603. (*A*) Displacement curves of wild type $A_{2B}R$ (■) and mutant receptor C167S^{EL2} (▲) with the ribose agonist NECA. (*B*) Displacement curves of wild type $A_{2B}R$ (■) and mutant receptor C167S^{EL2} (▲) with the non-ribose agonist BAY 60-6583. The graphs are the combined result of three independent experiments performed in duplicate.

Bioinformatic analyses

Recently, several crystal structures of the adenosine A_{2A} receptor have been elucidated (PDB entry codes: 3EML, 3QAK, 2YDO, 2YDV) [5,6,7]. The adenosine A_{2A} receptor is the closest homologue of the adenosine A_{2B} receptor, with 82.1 % amino acid similarity and 59.4 % identity. We mapped the mutated residues onto the crystal structure of the active A_{2A}R structure bound to NECA (PDB: 2YDV) in order to obtain a view on the 3D localization of the residues (**Figure 7**). The corresponding positions of the mutated A_{2B}R residues in the A_{2A}R sequence were determined by a multiple sequence alignment (**Figure 7A**). To improve the quality of the multiple sequence alignment and to determine the transition between loop and transmembrane domains, we also included sequences of two other crystallized GPCRs; the β_2-adrenergic (b2AR) receptor and the CXCR4 Chemokine (CXCR4R) receptor [25,26]**.** Also in the 3D view, clusters of mutations can be observed in the top of TM4 and the bottom of TM5 (**Figure 7B**). The corresponding positions of the cluster in EL2 appear to reside in a part of the loop that is involved in forming an anti-parallel β-sheet with EL1. It is very likely that this typical protein structure is also present in the A_{2B}R and constitutively active mutations in the putative β-strand in EL1 of this receptor have previously been described by our laboratory [3].

In the A_{2A} receptor structure, all three available cysteines in the second extracellular loop are involved in bridge formation. It has been proposed that formation of extracellular disulfide bridges may be an important general mechanism for regulating the activity of GPCRs [27]. The adenosine A_{2B}R has a high number of cysteines in EL2 that could all potentially form extracellular disulfide bridges. A previous sequence alignment analysis performed by De Graaf et al. already revealed that over 90% of class A GPCRs contain at least one cysteine in EL2 and that several receptors contain more. In most cases, the most downstream cysteine appeared involved in forming the conserved disulfide bridge with TM3 [28]. To investigate how common multiple cysteines are in class A GPCRs, we performed a cysteine occurrence analysis. We counted the number of cysteines present between residues 4.55 and 5.38 [21], a region that encompasses the second extracellular loop. The majority of non-olfactory receptors contains only one cysteine within EL2 (**Figure 8A**); this cysteine represents in most cases the conserved cysteine present in over 90% of class A GPCRs. From what is known from the currently available crystal structures this conserved cysteine forms a disulfide bridge with a cysteine present in the top of

TM3 that is essential for receptor structure and function. The adenosine $A_{2B}R$ is the only receptor with four cysteines in EL2, which is the highest cysteine count in this analysis. The adenosine A_{2A} receptor, the closest homologue of the $A_{2B}R$, contains one cysteine less with three cysteines in the loop. The other adenosine receptor subtypes, the A_1R and A_3R, only hold one cysteine in EL2. In EL2 of olfactory receptors, generally multiple cysteines are present; ca. 80% of the receptors contain three cysteines in the loop (**Figure 8B**). This special subfamily of class A GPCRs is responsible for our sense of smell by binding odorants. Metal ions, such as zinc, have been proposed to be essential in recognition and binding of odorants to their receptor, in which ligation of the metal ion to the thiol group of cysteine residues might play an important role [29].

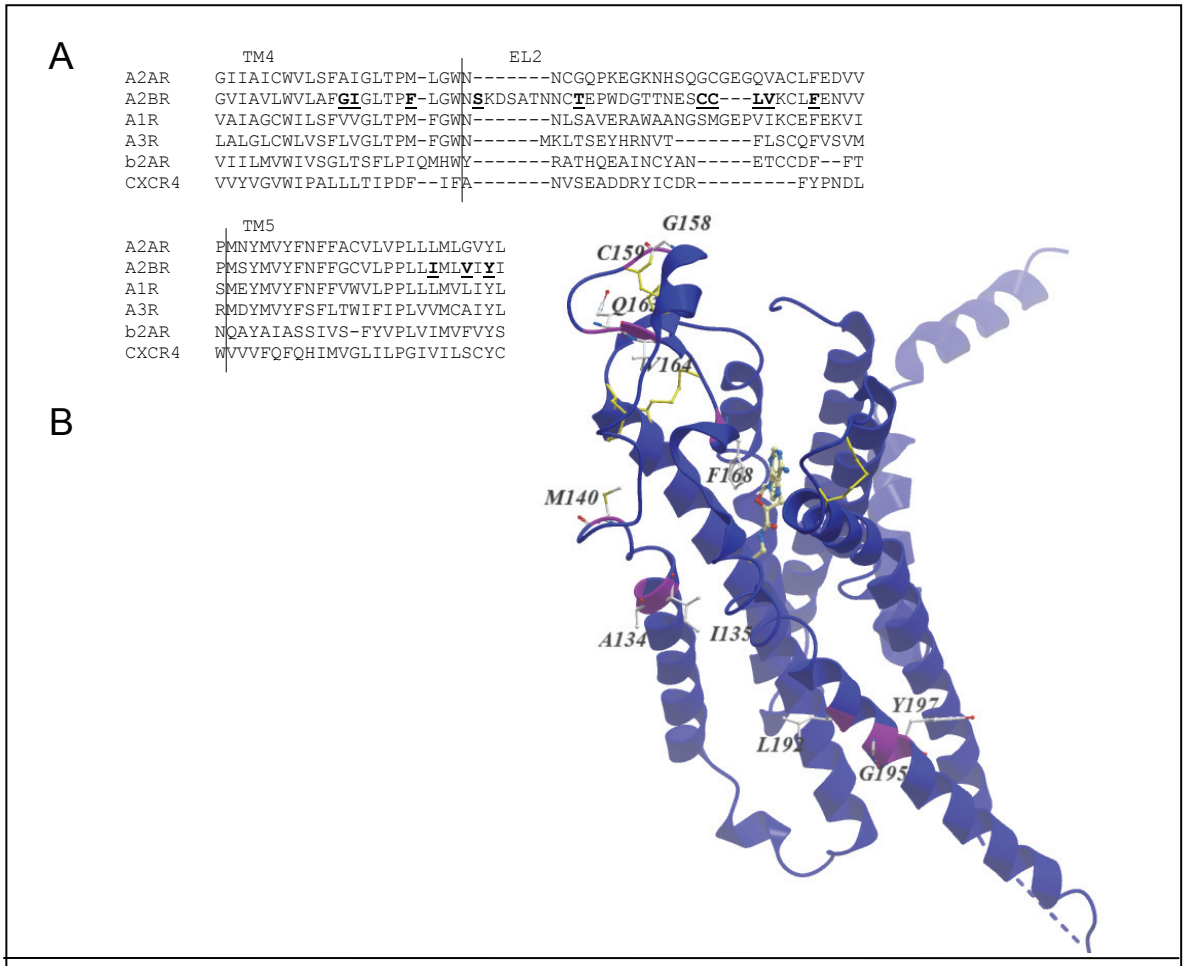

Figure 7. Mutated residues of the $A_{2B}R$ mapped on the crystal structure of the $A_{2A}R$.
(*A*) Multiple sequence alignment $A_{2B}R$ with all four adenosine receptor subtypes ($A_{2A}R$, $A_{2B}R$, A_1R, A_3R) as well as the sequences of two other crystal structures of CXCR4 and the β_2-adrenergic receptor (b2AR) to ensure the most plausible definition of EL2. The mutated residues are indicated in bold font and underlined. (*B*) Based on the multiple sequence alignment, the mutated residues identified in the random mutagenesis screen were mapped onto the crystal structure of the $A_{2A}R$ (PDB: 2YDV) (blue), the closest homologue of the $A_{2B}R$. The corresponding mutated residues and their side-chains are indicated in magenta. The ribbon representation also shows the co-crystallized ligand NECA as well as the three disulfide bridges that restrict EL2 in the A_{2A} receptor

DISCUSSION

A random mutagenesis screen for gain-of-function and constitutively active mutants (CAMs) was performed on fragment TM4-EL2-TM5 of the human adenosine A_{2B} receptor. These three regions of the receptor have been implied to participate in the dynamic movements the receptor undergoes during activation. Upon receptor activation, a coupling between movements of EL2 and TM5 has been observed as well as a rearrangement in the hydrogen-bonding networks connecting EL2 with the extracellular ends of TM4, TM5 and TM6 [4].

For the β_1-adrenergic receptor, the β_2-adrenergic receptor, (rhod)opsin, and the adenosine A_{2A} receptor, we now have access to crystal structures of both inactive and active conformations [5,6,7,30,31,32,33,34,35]. These structures reveal that in the transition between the inactive and the active conformation subtle changes at the extracellular surface and the ligand binding site lead to large movements at the intracellular surface. The lower regions of TM5 and TM6 show a particularly large displacement that is allowed by the presence of conserved prolines (5.50 and 6.50) that interrupt the hydrogen bond network within the helices.

From the screen, 12 different mutant receptors were identified. Most of these mutants show a significant increase in constitutive activity, with mutant G135A$^{4.55}$ /I197L$^{5.53}$/Y202N$^{5.58}$ even reaching a basal activity that is over 60% of the maximal activation level (**Figure 3**). All mutant receptors displayed a very large increase in potency for NECA compared to wild type, ranging from an improvement in activation of 11-fold (V200G$^{5.56}$) to even 25-fold (F141L$^{4.61}$) (**Table 1**). That we were able to identify mutant receptors with such large effects on activation further emphasizes the strength of using an unbiased random mutagenesis approach in combination with the *S. cerevisiae* system.

Three "hotspots" important for A_{2B}R activation

The residues found mutated in our screen are located in three distinct clusters: at the top of TM4, in a cysteine-rich region in EL2, and at the bottom half of TM5 (**Figures 1 and 7B**). Even though a number of mutant receptors contain multiple amino acid changes, no combinations between mutations in EL2 and the transmembrane domains were identified. This suggests that the influence of EL2 on receptor activation is at a different level than that of the transmembrane domains. There is

accumulating evidence that agonist binding and activation occur through a series of conformational intermediates, for which multiple switches are needed to be activated [36,37]. It is quite likely that the first switch is present at the site of ligand entry to the receptor, i.e. at the extracellular surface.

The cluster in TM4 consists of three amino acids; $G135^{4.55}$, $I136^{4.56}$, and $F141^{4.61}$. A saturated mutagenesis screen performed on the transmembrane domains of the complement factor 5a receptor (C5aR), also revealed important residues at the extracellular membrane interface of TM4, corresponding to positions 4.46, 4.53, 4.55, 4.57, 4.58, and 4.60 [38,39]. Very recently, Warne et al. published four structures of the β_1-adrenergic receptor bound to full and partial agonists. One difference between an antagonist and a full agonist bound β_1-adrenergic receptor is that a Van der Waals interaction is broken between positions 4.56 and 5.46. This results in a reduced interface between helix 4 and 5 that may be significant in the activation process [30]. In the inactive structure of the adenosine A_{2A} receptor (PDB:3EML), a similar Van der Waals interaction exists between $I135^{4.56}$ and $C185^{5.46}$. Also, a hydrogen bond is formed between $Q89^{3.37}$ and the backbone of $C185^{5.46}$ [5]. In the active structures of the $A_{2A}R$ (PDB: 3YDO/3YDV/ 3QAK), the cysteine side chain shifts and the hydrogen bond is broken [6,7]. Noteworthy is that in the 3YDO and 3YDV structures bound to adenosine and NECA respectively, position 3.37 was mutated (Q89A) [7].

The mutations found mutated in EL2 are located in a cysteine-rich region of the loop that may be involved in a β-strand structure in the loop as is seen in the structure of the $A_{2A}R$ (**Figure 7B**). The partnering strand in EL1 that is involved in forming the β-sheet with EL2, has previously been reported to be essential in $A_{2B}R$ activation [3]. EL2 has been suggested to act as a negative regulator that keeps the receptor in a silent state before agonist-induced activation [8,9,10]. The mutant receptors in EL2 that we identified all showed a large increase in receptor activation, both in response to the agonist NECA and independent of a ligand. This could suggest that the cysteine-rich cluster we identified in our screen has a similar regulating role in suppressing receptor activation in its basal state. The cysteine occurrence analysis on all human class A GPCRs revealed that the $A_{2B}R$ contains an exceptionally large number of four cysteines in EL2, whereas most non-olfactory class A GPCRs only contain one cysteine (**Figure 8**; see also an analysis by De Graaf et al., 2008) [28]. In

olfactory receptors the cysteine occurrence is much higher, which may be linked to metal ion binding [29].

In TM5, the mutated residues are found in a small cluster of three residues at the bottom of the helix: I197$^{5.53}$, V200$^{5.56}$, and Y202$^{5.58}$. From the crystal structure of the A_{2A}R, as well as additional mutagenesis data, several residues in TM5 have been indicated to play a role in agonist and/or antagonist binding: M177$^{5.38}$, F180$^{5.41}$, N181$^{5.42}$, and F182$^{5.43}$ [5,40]. The recently published active structures in which NECA and adenosine are co-crystallized, reveal that M177$^{5.38}$, N181$^{5.42}$ are directly involved in the ligand binding pocket of these ribose-containing agonists [7]. The residues identified in our screen are located much lower in the helix and are therefore unlikely to participate in the ligand binding pocket. However, the large increase in agonist potency and constitutive activity observed in our study implies that these residues are essential in receptor activation.

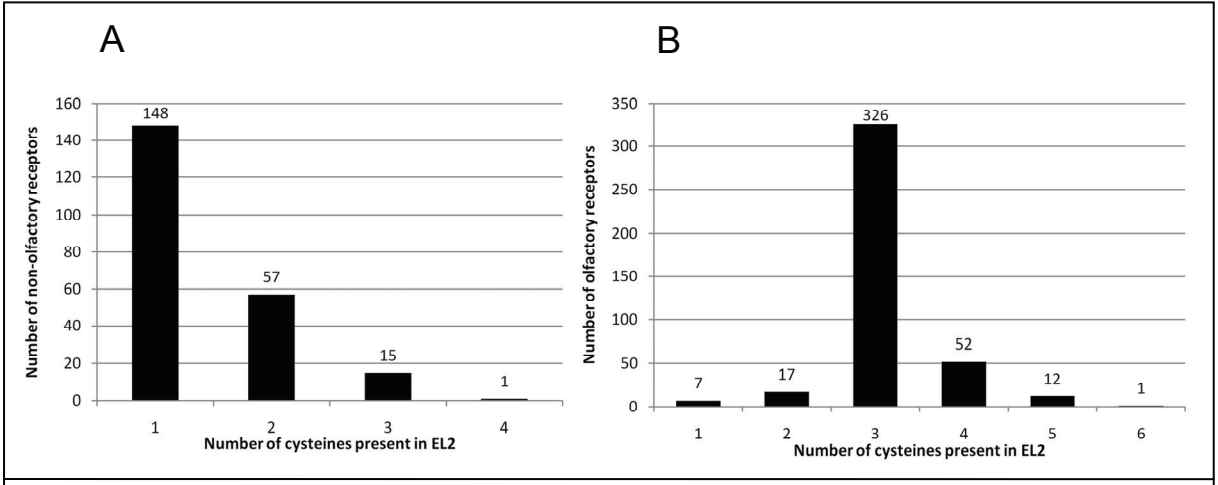

Figure 8. Cysteine occurrence analysis. The number of cysteines present in the second extracellular loop was counted in human class A GPCRS. For this analysis, the loop was defined between residues 4.55 (TM4) and 5.38 (TM5). The graphs represent all human class A GPCRs, either non-olfactory (*A*) or olfactory (*B*), as present in the GPCRDB (http://www.gpcr.org/7tm/), with on the x-axis the number of cysteines counted in EL2. The majority of non-olfactory receptors contains one cysteine in EL2, the adenosine A_{2B} receptor alone is responsible for the bar at 4 cysteines. Most olfactory receptors have three cysteines in the loop

CAMs in the adenosine A_{2B} receptor

The fragments upstream and downstream of the investigated fragment TM4-EL2-TM5 had been subjected to a random mutagenesis screen in a similar manner in our laboratory [2,3]. In **Figure 1**, the ensemble of CAM residues identified in the different studies is indicated in grey, from which we conclude that next to the described clusters in TM4, EL2, and TM5, similar series of residues exist in TM3 and TM6.

Even though the screening set up in all three screens (ATG-KpnI, TM4-EL2-TM5, and BglII-stop) was chosen such that both constitutively active mutants (CAMs) and gain-of-function mutants would be selected, all the identified mutant receptors displayed an increase in constitutive activity. The levels of constitutive activity ranged from a 1.5-fold change (F141L$^{4.61}$, N36D^{IL1}) compared to wild type receptor to an immense increase of 38-fold for mutant receptor G135A$^{4.55}$/I197L$^{5.53}$/Y202N$^{5.58}$. Interestingly, of all 41 residues identified in constitutively active mutants of the $A_{2B}R$, only 4 were actually involved in binding of either adenosine or NECA at the corresponding positions in the crystal structures of the $A_{2A}R$ published by Lebon et al.[7] These corresponding residues in the $A_{2B}R$ are: F173^{EL2}, V250$^{6.51}$, N254$^{6.55}$ and T257 $^{6.58}$. The last three, all residing in TM6, were identified in one particular multiple mutant receptor; Q214L/I230N/V240M/V250M/N254Y/T257S/K269stop (IL3/6.31 /6.41/6.51/6.55/6.58/EL3) [2]. The residue F173^{EL2} (F168 in $A_{2A}R$) directly interacts with all the ligands co-crystallized with the $A_{2A}R$ through a π-stacking contact. For the antagonist ZM241385 the triazolotriazine ring interacts with the phenylalanine, where in the agonists UK-432097, NECA, and adenosine, π-stacking occurs with the adenine moiety. In the study described here, the F173L^{EL2} mutant receptor displayed a large increase in potency for NECA. Mutating the corresponding F168^{EL2} in the $A_{2A}R$ into other aromatic residues resulted in a moderate decrease in activation of the receptor, mutation into an alanine virtually abolished activation [40]. Assuming that the F173^{EL2} in the $A_{2B}R$ has a similar role in binding, a large hydrophobic residue might be required at this position, however removing the aromatic side chain can even improve agonist access to the binding pocket.

Many of the CAMs in our studies only have one or two amino acid changes, indicating that quite subtle changes can lead to a large impact on the receptor activation mechanism and that these residues are not necessarily directly involved in either ligand binding or G protein-coupling.

Residues F141$^{4.61}$, C167^{EL2}, and Y202$^{5.58}$

The amino acids F141$^{4.61}$, C167^{EL2}, an Y202$^{5.58}$ were identified multiple times in the screen. This may indicate that these residues are of particular importance in the activation mechanism of the $A_{2B}R$. Position F141$^{4.61}$ has been reported previously as being involved in affinity and potency changes. The polymorphic variant M172I$^{4.61}$,

located at the corresponding position in the serotonin 1A receptor (5HT1A), displayed a 3-fold increase in agonist potency [41]. In another subtype of serotonin receptors, 5HT1B, substitution of the amino acid F185$^{4.61}$ by an alanine increased the affinities for several agonists [42]. In the study described here, mutating F141$^{4.61}$ to a leucine resulted in a 25-fold increase in potency for NECA and a 5-fold increase in potency in response to the non-ribose agonist BAY60-6583 (**Figure 2, Table 1**). Radioligand binding studies revealed that affinity for both agonists was also largely increased (**Table 2**). The residue is located at the onset of EL2, pointing outwards (**Figure 7B**). Although the residue is at great distance from the putative binding pocket of both NECA and BAY60-6583, it is firmly involved in both agonist activation and binding [43]. The location of the residue does suggest a main role in positioning EL2, and could therefore be indirectly involved in shaping the entry of the agonist binding pocket.

Mutant receptor C167S^{EL2} showed an increase of ca. 16-fold in potency for the adenosine derivative NECA as well as a constitutive activity that was 6-fold higher compared to wild type (**Table 1**). Radioligand binding experiments also revealed an increase in binding affinity for the adenosine derivative NECA (**Figure 5**). Interestingly, when we activated the C167S^{EL2} mutant with BAY 60-6583, a structurally different agonist that lacks a ribose moiety, only a 2-fold change in potency was observed and affinity remained unchanged compared to wild type (**Figure 5, Table 1**). Residue C167^{EL2} is likely able to form a non-conserved disulfide bridge with a cysteine in EL1 in the A_{2B}R as seen in the crystal structure of the closest family member, the A_{2A}R [3] (**Figure 1**). Our results indicate that the putative disulfide bridge between C167^{EL2} and C72^{EL1} is important for ribose agonist binding and activation, but less so for non-ribose agonists. Schiedel et al. recently performed a site-directed mutagenesis study on the cysteine residues present in EL2 of the A_{2B}R. Mutating C167^{EL2} to a serine resulted in a 2.5-fold increase in potency for BAY60-6583, similar to our observations, although the response to NECA of this mutant receptor was less pronounced in their study [44]. The tyrosine at position 202$^{5.58}$ is highly conserved among class A GPCRs (88%) and there are several studies reporting this position as being important in receptor activation and G protein signaling. A somatic mutation in the thyroid stimulating hormone receptor (TSHR) involved in toxic adenoma, Y601N$^{5.58}$, showed increased levels of constitutive activity, but was unable to couple to Gq/11 [45]. Very recently, Sansuk et al.

proposed that movement at the extracellular side of TM5 is transduced as a set of structural rearrangements toward the intracellular side, so enabling interactions of Y5.58 with R3.50 in the cytoplasmic side of the receptor [46]. When comparing the inactive and active structures of the adenosine A_{2A} receptor, we learned that Y5.58 (Y197 in the $A_{2A}R$) displays a large rotameric shift upon activation. While in the inactive structure bound to ZM241385 the conserved $Y197^{5.58}$ is located in between TM3 and TM6, in the agonist-bound forms this residue moves outward allowing TM5 to shift toward TM6. As a result, the intracellular ends of TM5 and TM6 move closer together in the active structures compared to the inactive structure, enabling access of the G protein [5,6,7]. In our screen, mutant $Y202S^{5.58}$ showed a 13-fold increase in constitutive activity that could be reduced to wild type levels in response to the inverse agonist ZM241385 with an IC_{50} comparable to the wild type receptor, indicating that the mutation does not lock the receptor in an active conformation [23,24] **(Figure 3**). NECA potency was 11-fold increased, but maximal activation levels could not be reached, suggesting a decrease in coupling to and signaling through the G protein (**Figure 2, Table 1**).

Concluding remarks

By applying an unbiased random mutagenesis approach with subsequent phenotype screening in a robust yeast system, we identified three hotspots in the $A_{2B}R$ that show a vast increase in both spontaneous and agonist-induced activity. None of the identified residues within these three clusters are part of the ligand binding pocket, yet, they are involved in agonist potency and affinity. Some of the identified residues, like $C167^{EL2}$, most likely contribute to an $A_{2B}R$-specific response to agonists. Others, such as $F141^{4.61}$ and $Y202^{5.58}$, might be part of a general activation mechanism for class A GPCRs. An overview of all the CAMs in the $A_{2B}R$ identified so far, indicates that there are several clusters of amino acids responsible for maintaining the subtle equilibrium that exist between the active conformation R^* and the inactive conformation R of the receptor and that these residues are not necessarily directly involved in either ligand binding or G protein coupling. In more general terms the results presented here could be of great use in unraveling the molecular details of GPCR activation.

ACKNOWLEDGEMENTS

This research was performed under the auspices of the GPCR Forum, a program funded by the Dutch Top Institute Pharma (project D1-105). The authors thank Bas Vroling and the GPCRDB (http://www.gpcr.org/7tm/) for help with the cysteine occurrence analysis. They also are greatly indebted to Prof C.E. Müller of Bonn University for the gift of [^{3}H]PSB-603.

REFERENCES

[1] Fredholm, B.B., IJzerman, A.P., Jacobson, K.A., Linden, J., Muller, C.E., *Pharmacol Rev* (2011) 63:1-34.
[2] Beukers, M., van Oppenraaij, J., van der Hoorn, P., Blad, C., den Dulk, H., Brouwer, J., IJzerman, A., *Mol Pharmacol.* (2004) 65:702-710.
[3] Peeters, M.C., van Westen, G.J., Guo, D., Wisse, L.E., Muller, C.E., Beukers, M.W., IJzerman, A.P., *FASEB J* (2011) 25:632-643.
[4] Ahuja, S., et al., *Nat Struct Mol Biol* (2009) 16:168-175.
[5] Jaakola, V.P., Griffith, M.T., Hanson, M.A., Cherezov, V., Chien, E.Y., Lane, J.R., IJzerman, A.P., Stevens, R.C., *Science* (2008) 322:1211-1217.
[6] Xu, F., Wu, H., Katritch, V., Han, G.W., Jacobson, K.A., Gao, Z.G., Cherezov, V., Stevens, R.C., *Science* (2011).
[7] Lebon, G., Warne, T., Edwards, P.C., Bennett, K., Langmead, C.J., Leslie, A.G., Tate, C.G., *Nature* (2011) 474:521-525.
[8] Klco, J., Wiegand, C., Narzinski, K., Baranski, T., *Nat Struct Mol Biol.* (2005) 12:320-326.
[9] Massotte, D., Kieffer, B.L., *Nat Struct Mol Biol* (2005) 12:287-288.
[10] Peeters, M.C., van Westen, G.J., Li, Q., IJzerman, A.P., *Trends Pharmacol Sci* (2011) 32:35-42.
[11] Jaakola, V.P., IJzerman, A.P., *Curr Opin Struct Biol* (2010) 20:1-14.
[12] Smit, M., Vischer, H., Bakker, R., Jongejan, A., Timmerman, H., Pardo, L., Leurs, R., *Annu Rev Pharmacol Toxicol.* (2007) 47:53-87.
[13] Brown, A., et al., *Yeast* (2000) 16:11-22.
[14] Stewart, G.D., Valant, C., Dowell, S.J., Mijaljica, D., Devenish, R.J., Scammells, P.J., Sexton, P.M., Christopoulos, A., *J Pharmacol Exp Ther* (2009) 331:277-286.
[15] Fromant, M., Blanquet, S., Plateau, P., *Anal Biochem* (1995) 224:347-353.
[16] Beukers, M., IJzerman, A., *Trends Pharmacol Sci.* (2005) 26:533-539.
[17] Gietz, D., St Jean, A., Woods, R.A., Schiestl, R.H., *Nucleic Acids Res* (1992) 20:1425.
[18] Eckle, T., et al., *Circulation* (2007) 115:1581-1590.
[19] Li, Q., Ye, K., Blad, C.C., den Dulk, H., Brouwer, J., IJzerman, A.P., Beukers, M.W., *J Pharmacol Exp Ther* (2007) 320:637-645.
[20] Borrmann, T., Hinz, S., Bertarelli, D.C., Li, W., Florin, N.C., Scheiff, A.B., Muller, C.E., *J Med Chem* (2009) 52:3994-4006.
[21] Ballesteros, J.A., Weinstein, H., *Methods Neurosci* (1995) 25:366–428.
[22] Vroling, B., Sanders, M., Baakman, C., Borrmann, A., Verhoeven, S., Klomp, J., Oliveira, L., de Vlieg, J., Vriend, G., *Nucleic Acids Res* (2011) 39:D309-319.
[23] de Zwart, M., Vollinga, R.C., Beukers, M.W., Sleegers, D.F., Kunzel, J.K.V.D., de Groote, M., IJzerman, A.P., *Drug Development Research* (1999) 48:95-103.
[24] Ongini, E., Dionisotti, S., Gessi, S., Irenius, E., Fredholm, B.B., *Naunyn Schmiedebergs Arch Pharmacol* (1999) 359:7-10.
[25] Wu, B., et al., *Science* (2010) 330:1066-1071.
[26] Rosenbaum, D.M., et al., *Science* (2007) 318:1266-1273.
[27] Storjohann, L., Holst, B., Schwartz, T.W., *Biochemistry* (2008) 47:9198-9207.
[28] de Graaf, C., Foata, N., Engkvist, O., Rognan, D., *Proteins* (2008) 71:599-620.
[29] Wang, J., Luthey-Schulten, Z.A., Suslick, K.S., *Proc Natl Acad Sci U S A* (2003) 100:3035-3039.

[30] Warne, T., Moukhametzianov, R., Baker, J.G., Nehme, R., Edwards, P.C., Leslie, A.G., Schertler, G.F., Tate, C.G., *Nature* (2011) 469:241-244.
[31] Park, J.H., Scheerer, P., Hofmann, K.P., Choe, H.W., Ernst, O.P., *Nature* (2008) 454:183-187.
[32] Rasmussen, S.G., et al., *Nature* (2011) 469:175-180.
[33] Rasmussen, S.G., et al., *Nature* (2007) 450:383-387.
[34] Palczewski, K., et al., *Science* (2000) 289:739-745.
[35] Warne, T., Serrano-Vega, M.J., Baker, J.G., Moukhametzianov, R., Edwards, P.C., Henderson, R., Leslie, A.G., Tate, C.G., Schertler, G.F., *Nature* (2008) 454:486-491.
[36] Kobilka, B.K., Deupi, X., *Trends Pharmacol Sci* (2007) 28:397-406.
[37] Ahuja, S., Smith, S.O., *Trends Pharmacol Sci* (2009) 30:494-502.
[38] Baranski, T., Herzmark, P., Lichtarge, O., Gerber, B., Trueheart, J., Meng, E., Iiri, T., Sheikh, S., Bourne, H., *J Biol Chem.* (1999) 274:15757-15765.
[39] Geva, A., Lassere, T.B., Lichtarge, O., Pollitt, S.K., Baranski, T.J., *J Biol Chem* (2000) 275:35393-35401.
[40] Jaakola, V.P., Lane, J.R., Lin, J.Y., Katritch, V., IJzerman, A.P., Stevens, R.C., *J Biol Chem* (2010) 285:13032-13044.
[41] Del Tredici, A.L., Schiffer, H.H., Burstein, E.S., Lameh, J., Mohell, N., Hacksell, U., Brann, M.R., Weiner, D.M., *Biochem Pharmacol* (2004) 67:479-490.
[42] Granas, C., Nordvall, G., Larhammar, D., *Eur J Pharmacol* (1998) 349:367-375.
[43] Sherbiny, F.F., Schiedel, A.C., Maass, A., Muller, C.E., *J Comput Aided Mol Des* (2009) 23:807-828.
[44] Schiedel, A.C., Hinz, S., Thimm, D., Sherbiny, F., Borrmann, T., Maass, A., Muller, C.E., *Biochem Pharmacol* (2011) 82(4):389-99.
[45] Arseven, O.K., Wilkes, W.P., Jameson, J.L., Kopp, P., *Thyroid* (2000) 10:3-10.
[46] Sansuk, K., Deupi, X., Torrecillas, I., Jongejan, A., Nijmeijer, S., Bakker, R., Pardo, L., Leurs, R., *Mol Pharmacol* (2011) 79:262-269.

CHAPTER 5

SCREENING FOR CONSTITUTIVELY INACTIVE MUTANTS OF THE ADENOSINE A_{2B} RECEPTOR IN *S. CEREVISIAE*

This chapter was based upon:

M.C. Peeters, Q. Li, G.J.P. van Westen, C.E. Müller, A.P. IJzerman. **2011** (manuscript in preparation)

ABSTRACT

Despite decades of extensive research on G protein-coupled receptors (GPCRs) and the recent elucidation of several high resolution crystal structures, the activation mechanism of these membrane-bound proteins is still largely unknown. Here we describe a new screening method that can greatly aid in the search for specific residues and domains involved in the activation process of GPCRs. By altering the parameters of a random mutagenesis screen using the MMY24 *S. cerevisiae* strain, we successfully screened a region of the human adenosine A_{2B} receptor that includes transmembrane domain 4 (TM4), the second extracellular loop (EL2), and transmembrane domain 5 (TM5), for constitutively inactive mutant receptors (CIMs). The screen resulted in the identification of 22 single and double mutant receptors, all showing a decrease in constitutive activity as well as in agonist potency. A particular important region located at the extracellular half of TM5 was discovered with $C190^{5.46}$ as a key player. This new screening strategy could be applied to all GPCRs that can be functionally expressed in yeast.

INTRODUCTION

G protein-coupled receptors (GPCRs) form one of the largest protein families known and are involved in a wide variety of physiological processes. They constitute the major drug targets of today's medicines, representing approximately 40% of drugs used in the clinic [1] . Therefore, much research is and has been devoted to the elucidation of the function of this large family of membrane proteins, the general structure of which includes seven conserved transmembrane domains connected by intra- and extracellular loops. We now have access to a handful of high resolution crystal structures that allow a hitherto unprecedented three-dimensional view of the receptor [2,3]. However, the currently available structures are only beginning to inform us about the more dynamic process of receptor activation, and, hence, other experimental approaches, such as mutation studies, are still very much needed. GPCRs are supposed to exist in multiple conformations. In a simple scheme an equilibrium exists between an inactive (R) and active conformation (R*) [4]. This assumes a basal activation state of the receptor corresponding to the fraction of R* in the total receptor population. This activation state is essential in maintaining physiological function and many pathogenic mutations have been reported that disturb the equilibrium causing an increase in activation (Constitutively Active Mutants or CAMs) or a decrease in basal activity (Constitutively Inactive Mutants or CIMs) [5,6,7]. These mutations have not only increased our knowledge on the pathophysiology in which GPCRs play a role, but also advanced our insight in the structure-function relationship of GPCRs. Furthermore, CIMs have been found beneficial to stabilize receptors for crystallization purposes, e.g. the β_1-adrenergic receptor [8].

Next to more classical site-directed mutational studies, random mutagenesis approaches have proven to be a very useful tool in identifying residues important for receptor function in an unbiased way [9,10,11]. *S. cerevisiae* is an attractive expression system for subsequent screening since it offers the genetic engineering tools typical of a microorganism while possessing a eukaryotic type of signaling pathway and post-translational modification. During the last decade various GPCRs have been successfully expressed in *S. cerevisiae* [12,13]. Several previous reports

have shown that GPCR function in this eukaryotic system resembles their action in mammalian cell lines [14,15].

The adenosine A_{2B} receptor ($A_{2B}R$) is part of a small subfamily of class A GPCRs, the adenosine receptors. The family consists of four subtypes, the A_1R, $A_{2A}R$, $A_{2B}R$, and A_3R, of which the $A_{2B}R$ has been studied least. Although all adenosine receptors are activated by adenosine, the $A_{2B}R$ has a markedly lower affinity for the endogenous ligand compared with the other three subtypes [16]. Upon metabolic stress, extracellular adenosine is accumulated in the body, activating first the A_1R, $A_{2A}R$ and A_3R subtypes. Only when the adenosine levels rise to high micromolar concentrations, the low affinity $A_{2B}R$ is activated [17]. Activation of the $A_{2B}R$ is essential at this time point in regulating the body's immune response. It is therefore an interesting drug target for several (auto)-immune diseases such as COPD and asthma [18,19,20]. Identifying residues important for activating (or inactivating) the receptor could be of great use in designing drugs for this target.

Here, we describe a new method to screen for constitutively inactive mutants (CIMs) of the adenosine A_{2B} receptor. We created an undirected random mutagenesis library of the $A_{2B}R$ containing mutations in the region encoding transmembrane domain 4 (TM4), the second extracellular loop (EL2), and transmembrane domain 5 (TM5). This library was subsequently screened in a *S. cerevisiae* expression system for a loss-of-function phenotype. This *S. cerevisiae* strain has been genetically modified to serve as a reporter system with growth as an output parameter, and has been used previously as a tool to screen for mutant receptors with *increased* activity compared to wild type receptor [15,21,22]. By adjusting two screening parameters, i.e. the concentration of an inhibitor of histidine synthesis and the selection time, we were able to use the same yeast system to screen for mutant receptors with *decreased* activity. The CIM screening method could be applied to all other GPCRs that can be functionally expressed in yeast. The results obtained for the $A_{2B}R$ proved greatly beneficial in experimentally supporting the structural changes observed between the inactive and active conformations of the closest family member, the $A_{2A}R$, and could provide new insights in the activation mechanism of other class A GPCR family members.

MATERIALS AND METHODS

DNA Constructs

The S*. cerevisiae* expression vector containing the adenosine A_{2B} receptor gene, the pDT-PGK_A_{2B}R plasmid, was kindly provided by Dr. Simon Dowell from GSK (Stevenage, UK). A KpnI restriction site was introduced in the A_{2B}R gene in the region encoding the second intracellular loop, making it possible to divide the receptor into three large fragments suitable for random mutagenesis.

Mutagenic PCR for construction of the random mutagenesis library

Introducing random mutations in the adenosine A_{2B} receptor was achieved by manipulating the polymerase chain reaction adapted from the method of Fromant et al. [23]. The mutagenic PCR reaction was performed in the presence of 10 mM Tris-HCL (pH 9.0), 50 mM KCl, 0.1% Triton X-100, 10 ng of template DNA, 0.1 µM concentrations of each primer, 0.2 mM dATP, 0.2 mM dTTP, 0.2 mM dGTP, 3.4 mM of the nucleotide in excess dCTP, 0.5 mM $MnCl_2$, 4.7 mM $MgCl_2$, and 0.5 units of Super *Taq* polymerase without proofreading (HT Biotechnology LTD, Cambridge, England). The number of mutagenic PCR cycles was set to 10 (PCR cycling conditions: 95ºC for 30 s, 59 ºC for 30 s, 72 ºC for 30s). Using these conditions, only a limited amount of mutations are introduced per fragment [9].

The following primers were used:

5’-GGTATAAAAGTTTGGTCACGGGTACCCGAGCAA-3’

5’-GAAGCTGCCTGCAGGCCACCAGGAAGATCTTAATG-3’

The resulting fragment comprises the region of the adenosine A_{2B} receptor gene that encodes transmembrane domain four (TM4), the second extracellular loop (EL2), and transmembrane domain five (TM5). The mutagenic PCR products were submitted to agarose gel electrophoresis and the gel bands containing the mutated fragments were isolated from the gel and purified. Subsequently, the mutated fragments were amplified further with 10 cycles of a regular PCR with the same primer sets and a polymerase with proofreading, AccuPrime *Pfx* DNA polymerase (Invitrogen, La Jolla, CA, USA) according to the guidelines provided by the manufacturer.

The wild-type fragment TM4-EL2-TM5 in the receptor was subsequently replaced by the mutated fragments using the restriction sites KpnI and BglII, resulting in a mutagenic pDT-PGK- A_{2B}R receptor library.

Transformation in MMY24 S. cerevisiae strain

pDT-PGK_A_{2B}R plasmids were transformed into an *S. cerevisiae* yeast strain according to the Lithium-Acetate procedure [24]. The strain is derived from the MMY11 strain [25] and was further adapted to communicate with mammalian GPCRs through the introduction of a chimeric G protein [13]. The genotype of the MMY24 strain is: *MAT**a**his3 leu2 trp1 ura3can1 gpa1_::G_i3 far1 ::ura3 sst2_::ura3 Fus1::FUS1-HIS3 LEU2::FUS1-lacZ ste2_::G418R.* To measure signaling of GPCRs, the pheromone signaling pathway of this strain was coupled via the FUS1 promotor to HIS3, a gene encoding the key enzyme in histidine production, imidazole glycerol-phosphate dehydrase. The degree of receptor activation was measured by the growth rate of the yeast on histidine-deficient medium.

Screen for inactive mutant receptors

Initially, we plated the transformed MMY24 yeast cells onto Yeast Nitrogen Based (YNB) agar-medium lacking leucine and uracil to select for plasmid-containing transformants. After incubation of 24 hrs, the plates were washed with liquid YNB medium and the transformants were pooled. We then started the actual screen for constitutively inactive mutant receptors by plating the cells onto YNB agar-medium lacking leucine, uracil and histidine (YNB-ULH) but with 1 mM 1,2,4-aminotriazole (3AT, Sigma-Aldrich, Zwijndrecht, The Netherlands) (plating density: ~ 10,000 cells per 100 mm plate). From our previous experience we had learned that a single yeast transformant containing WT receptor needs about 3 days to reach a full colony, while yeast with a constitutively active mutant receptor reached this stage even faster. With this knowledge, we marked the colonies that had already appeared within three days, and ignored them. One day later, after 4 days of screening, the first set of 100 colonies that then appeared was randomly selected. After 6 days of screening, a second set of colonies were selected. Plasmids were isolated from the yeast colonies using the ZymoPrep II Yeast Plasmid Miniprep kit (Zymo Research, Orange, CA, USA) and mutations were identified using double-stranded sequencing (LGTC,

Leiden, The Netherlands). Mutant receptors containing single or double mutations were retransformed into the yeast strain to confirm their inactivated phenotype.

Solid growth assay

To characterize the mutant receptors further, concentration-growth curves were generated in a solid growth assay. In this assay, yeast cells from an overnight culture were diluted to around 400,000 cells/ml (OD_{600} ≈ 0.02), and droplets of 1.5 µl were spotted on selection agar plates, YNB-ULH, containing 7 mM 3AT and a concentration of 5'-N-ethylcarboxamidoadenosine (NECA), a full agonist on the A_{2B} receptor, ranging from 10^{-9} to 10^{-5} M. After incubation at 30°C for 50 h, the plates were scanned and receptor-mediated yeast growth was quantified with Quantity One imaging software from Bio-Rad (Hercules, CA). The amount of yeast growth was calculated as the density of each spot with a correction for local background on the plate. Data were analyzed using nonlinear regression analysis software available in GraphPad Prism 5.0 (GraphPad Software, San Diego, CA).

Liquid growth assay and Schild plot analysis

Similar concentration-growth curves can be produced using liquid selection medium. This assay is in a higher-throughput 96-well format and growth is easily determined by measuring absorption at a wavelength of 595 nm. In this assay, 150 µl liquid YNB-ULH medium with 7 mM 3AT and a varying concentration of ligand was added to each well. Yeast cells from an overnight culture were diluted to around $4 \cdot 10^6$ cells/ml (OD_{600} ≈ 0.2) and 50 µl was added per well. The 96-wells plate was then incubated for 35 hours in a Genios plate reader (Tecan, Durham, NC) at 30°C, keeping the cells in suspension by shaking every 10 minutes at 300 rpm for 1 min. The final absorption values at 595 nm after 35 hours were used as input for the concentration-response curves. Data were analyzed using nonlinear regression analysis software available in GraphPad Prism 5.0 (GraphPad Software, San Diego, CA).

For the wild type A_{2B} receptor and for the mutant receptors $I136L^{4.56}$ and $T162S^{EL2}/S180C^{5.36}$, concentration-growth curves of agonist NECA were recorded in the presence of increasing concentrations of the selective A_{2B}R antagonist PSB603 [22, 26]. Schild analysis was performed using the appropriate equations available in GraphPad Prism 5.0.

Whole cell radioligand binding

Yeast cells expressing wild type or mutated $A_{2B}R$ were cultured overnight in rich YAPD (Yeast-extract Adenine Peptone Dextrose) medium. Cells were centrifuged for 5 minutes at 2000 x *g*, and the cell pellet was once washed with 0.9% NaCl. The cells were again centrifuged for 5 min at 2000 x *g* and diluted in the assay buffer (50 mM Tris-HCl pH7.4 + 1 mM EDTA) to OD_{600}=40 (an OD_{600} value of 1 corresponds to approx. $2 \cdot 10^7$ cells/ml). Binding experiments were performed with 1.2 nM [^{3}H]PSB-603 and a final concentration of $25 \cdot 10^7$ cells/ml in a total volume of 100 µl [26]. Nonspecific binding was determined in the presence of 1 mM NECA. Samples were incubated for 1 hour at 25 ºC while shaking vigorously to keep the yeast cells in suspension. Incubation was terminated by adding 1 ml ice-cold assay buffer. Bound from free radioligand was immediately separated by rapid filtration through Whatman GF/B filters pre-incubated with 0.1% polyethylenimine (PEI) using a Millipore manifold during which the filters were washed six times with ice-cold assay buffer. Filter-bound radioactivity was determined by scintillation spectrometry (Tri-Carb 2900TR; PerkinElmer Life and Analytical Sciences) after addition of 3.5 ml of PerkinElmer Emulsifier Safe.

Whole cell extracts and immunoblotting

Whole protein cell extracts were made from the transformed yeast cells using trichloroacetic acid (TCA). From an overnight culture, $1.2 \cdot 10^8$ yeast cells were harvested in mid-log phase. The cells were washed twice with 20% TCA after which they were broken by vigorous vortexing in the presence of glass beads. The yeast cell extracts were separated using SDS/PAGE and subsequently blotted on Hybond-ECL membranes. For this purpose, a sample of 1.0 µl containing 3 µg protein was loaded on a 12.5% SDS/PAGE gel. A semi-automated electrophoresis technique (PhastSystem™, Amersham Pharmacia Biotech) was used for SDS/PAGE as well as blotting. The antibody directed against the C-terminal region of the adenosine A_{2B} receptor was kindly provided by Dr. I. Feoktistov (Vanderbilt University, Nashville). A low range molecular weight standard was used to assess the MW of the bands (Bio-Rad, Hercules, CA). Selective $A_{2B}R$ bands are found at 29 kDa and 48 kDa.

Densitometric analysis of the protein bands was performed using the volume analysis tool as present in the Quantity One imaging software from Bio-Rad (Hercules, CA).

The aspecific band at approximately 45 kDa was used as loading control. The ratio between specific $A_{2B}R$ protein bands and the aspecific band was determined and the wild type receptor was set at 100%, the empty vector pDT-PGK at 0%.

Mapping mutated residues onto the $A_{2A}R$ structure

The positions of the mutations identified in the random mutagenesis screen were mapped onto the corresponding positions in the crystal structure of the adenosine A_{2A} receptor co-crystallized with agonist NECA [27]. These corresponding positions were determined by a multiple sequence alignment created using ClustalW with default parameters. To make use of known crystallographic data, the sequences of the CXCR4 Chemokine (CXCR4) receptor and the β2-adrenergic (b2AR) receptor were also included in this alignment [28,29]. The EL2 was defined from the crystal structures of the A_{2A} receptor (residues 143 to 173), the CXCR4 (residues 175 to 192) and the b2AR (residues 171 to 196).

RESULTS

*General strategy used*We expressed a mutagenized library of the human adenosine A_{2B} receptor in the *Saccharomyces cerevisiae* strain MMY24 [13]. The pheromone signaling pathway of the wild-type MATa mating type yeast uses the Ste2p receptor, a G protein-coupled receptor. Upon activation of this receptor, a mitogen-activated protein kinase cascade is activated through the endogenous Gpa1p G protein, resulting in the transcription of mating genes such as FUS1. The engineered yeast strain MMY24 that we used lacks the endogenous Ste2p receptor, while still maintaining the G protein signaling machinery. To enable G protein coupling to human receptors expressed in this platform, a chimeric Gαi3 protein was introduced of which the last four amino acids of the otherwise yeast G protein were exchanged with the human sequence. Moreover, the HIS3 gene encoding the enzyme imidazole glycerol-phosphate dehydrase (IGPD) that is crucial for the production of the yeast essential amino acid histidine was placed behind the FUS1 promoter [13]. As a result, in the absence of histidine, the only yeast cells able to grow are those in which the expressed GPCR is active (**Figure 1A**).

Even though expression of IGPD is under control of the FUS1 promoter, the yeast strain produces a basal level of histidine without an active receptor present. To suppress the resulting basal growth of the yeast cells, a competitive inhibitor of the enzyme IGPD, 1,2,4-aminotriazole (3AT) is routinely added in order to measure growth that is only caused by an activated receptor. When recording a concentration-growth curve with increasing concentrations of 3AT, we noticed a difference in response between yeast cells that express the human $A_{2B}R$ and those that are only transformed with the empty vector pDT-PGK (**Figure 1B**). At a concentration of 1 mM 3AT, the window between the two curves was most pronounced. At this concentration, yeast cells with an empty vector hardly grew in contrast to yeast cells expressing the $A_{2B}R$. Mutant $A_{2B}Rs$ that display increased activation showed a larger than wild-type response at this 3AT concentration (data not shown). We hypothesized that mutant receptors with decreased activity would 'reside' in between the curves of the wild-type receptor and that of the empty vector. We set out to design a screening method that would select these less active, but still vital mutant receptors.

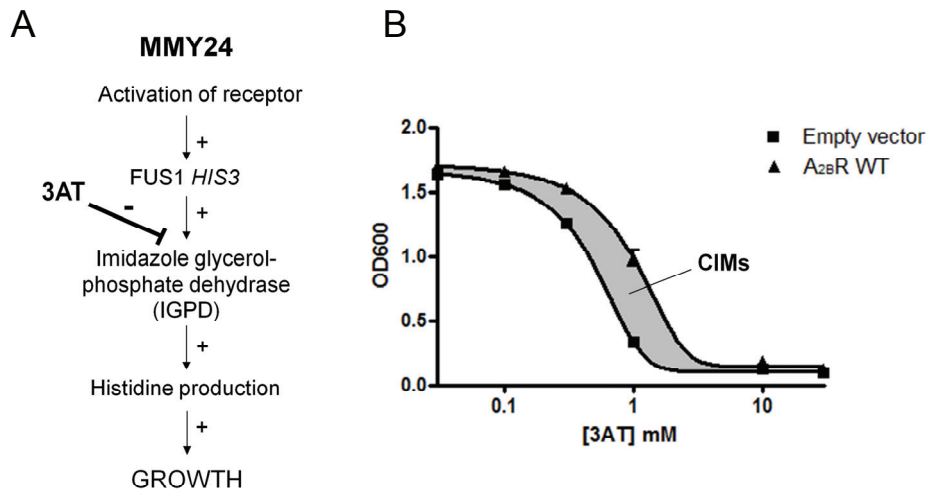

Figure 1. General principle of the yeast genetic screen. *(A)* Schematic representation of the effect of receptor activation in the MMY24 yeast strain. Upon activation, signaling through the G protein pathway leads to transcription of the HIS3 gene. This results in the production of histidine by the cell enabling the yeast cells to grow on histidine-deficient medium. 1,2,4-aminotriazole (3AT) is a competitive inhibitor of the enzyme IGPD, and suppresses growth levels in a dose-response manner. *(B)* Concentration- growth curves with increasing concentrations of 3AT in yeast cells transformed with wild type $A_{2B}R$ or empty vector. The area between the two curves is where receptors with decreased activation profiles can be found.

Random mutagenesis and yeast genetic screen

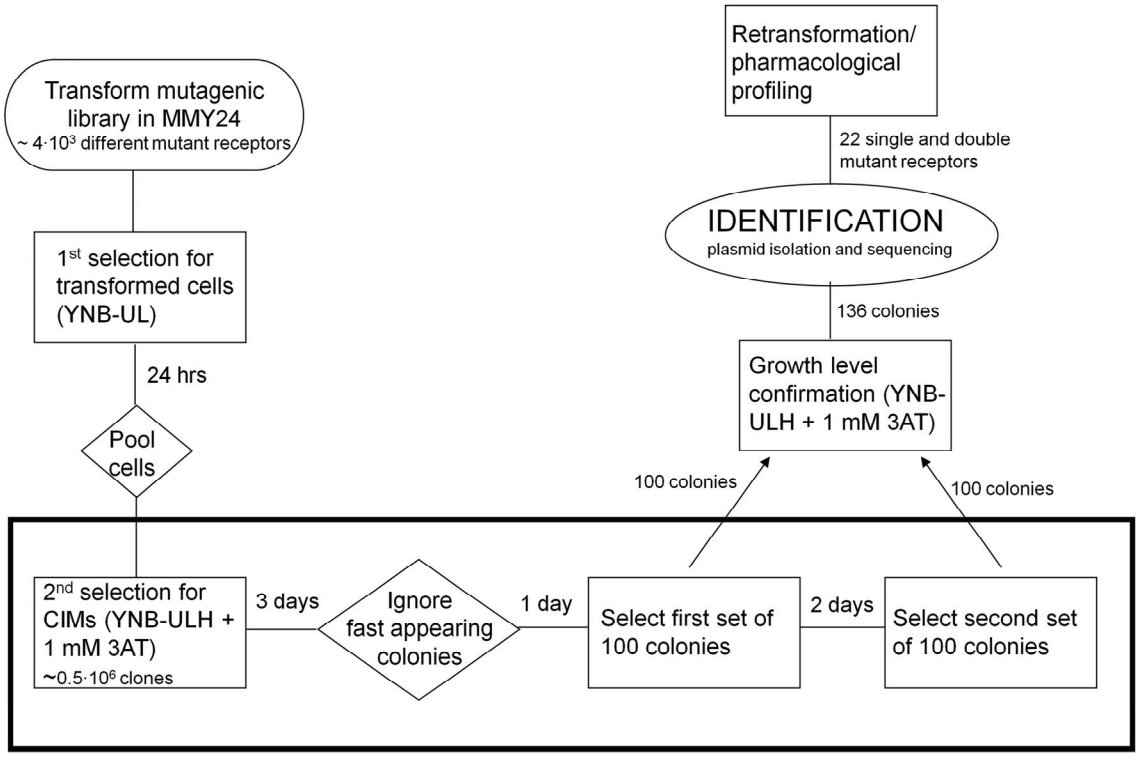

Figure 2. Flow scheme of the screen set-up. After transformation of the library, a first selection is performed for successfully transformed cells. After 24 hrs, cells are pooled and spread onto selection plates without the marker histidine (H) and with a concentration of 1mM 3AT to start the actual screen (indicated in the box). After 3 days, colonies are marked but ignored. The first selection round is one day later, after 4 days. A second selection takes places 2 days after the first, in total after 6 days. All colonies were checked independently in comparison with wild type receptor on new selection plates. From the positive clones, plasmid was isolated, sequenced, and retransformed to characterize the identified mutant receptors.

The protocol we followed is depicted as a flow scheme in **Figure 2**. A silent mutation was introduced in the second intracellular loop of the $A_{2B}R$ gene in order to insert a KpnI restriction site. Using this and the BglII restriction site, the receptor gene was divided into three parts that each has a suitable length for random mutagenesis purposes. For the random mutagenesis experiments in the present study a fragment of 262 base pairs encoding transmembrane domain 4 (TM4), the second extracellular loop (EL2) and transmembrane domain 5 (TM5) was used. Mutations were randomly introduced using a mutagenic PCR where an excess of the nucleotide dCTP was added. The PCR conditions were optimized to generate a large number of mutated receptors with a relatively low mutation frequency. After mutagenesis, the normal fragment TM4-EL2-TM5 in the wild type receptor was replaced by the mutated

fragments using the restriction sites KpnI and BglII, resulting in a mutagenic adenosine A_{2B} receptor library containing approximately 4000 different mutant receptors, ranging from a one-nucleotide change to a maximum of five mutations per fragment. The mutagenized A_{2B}R library was expressed in the MMY24 yeast strain and screened for an inactivating phenotype using selection plates lacking histidine and with 1 mM 3AT as discussed before (**Figure 2**). At this concentration yeast expressing the wild type A_{2B}R was still able to grow, but cells containing the empty vector did so only marginally, if at all. To eliminate yeast cells from the screening library that did not contain a plasmid, we first pre-screened for successfully transformed yeast cells. In total, ca. 0.5 million yeast clones were used for the final inactivation screen, so the library was screened approximately 100 times. To avoid selecting mutant receptors with increased levels of activity, we also introduced a time restraint. The more active a receptor, the more histidine the yeast cell produces. This results in more, but also faster growth of the cells. In our hands a yeast cell expressing wild type A_{2B}R typically needs 72 hrs to form a reasonably sized colony, while yeast with more active receptors reach this stage sooner. By applying this time frame as a threshold, we ignored receptors with increased activation and only focused on the less active mutants. We used two time points at which we selected colonies, after 4 days and again after 6 days of screening. At each of these two time points we randomly picked 100 colonies. All 200 colonies were subjected to a second selection procedure to confirm their growth levels. True hits were considered colonies that were able to grow on selection plates containing 1 mM 3AT, but less than the wild type receptor (the green bars in **Figure 3**). Other colonies not meeting our criteria, were not sequenced (the red bars in **Figure 3**). Approximately 70% of the selected colonies met these criteria, yielding 136 colonies of interest. The high hit rate indicates that the parameters used in the previous screen were successful.

Plasmids were isolated from ‘hit’ colonies and mutations were identified by sequence analysis. Among the plasmids isolated from the first selection at day 4, only a few wild type receptors were still present. Most mutant receptors contained one or two amino acid changes. Plasmids isolated from the second selection at day 6 contained no wild type receptors anymore. The identified mutant receptors at this stage showed larger defects with more multiple amino acid changes, and also deletion mutants were found. This selection also contained expected “receptor killers”, like a mutation

of the cysteine at position 171^{EL2}. This cysteine is part of the conserved disulfide bridge formed with a cysteine in TM3 that is present in over 90% of all class A GPCRs and is considered essential in receptor structure and function. Mutant receptors containing only one or two amino acid changes, in total 22 mutants, were chosen for further characterization and were retransformed into the yeast strain to confirm their inactive phenotype.

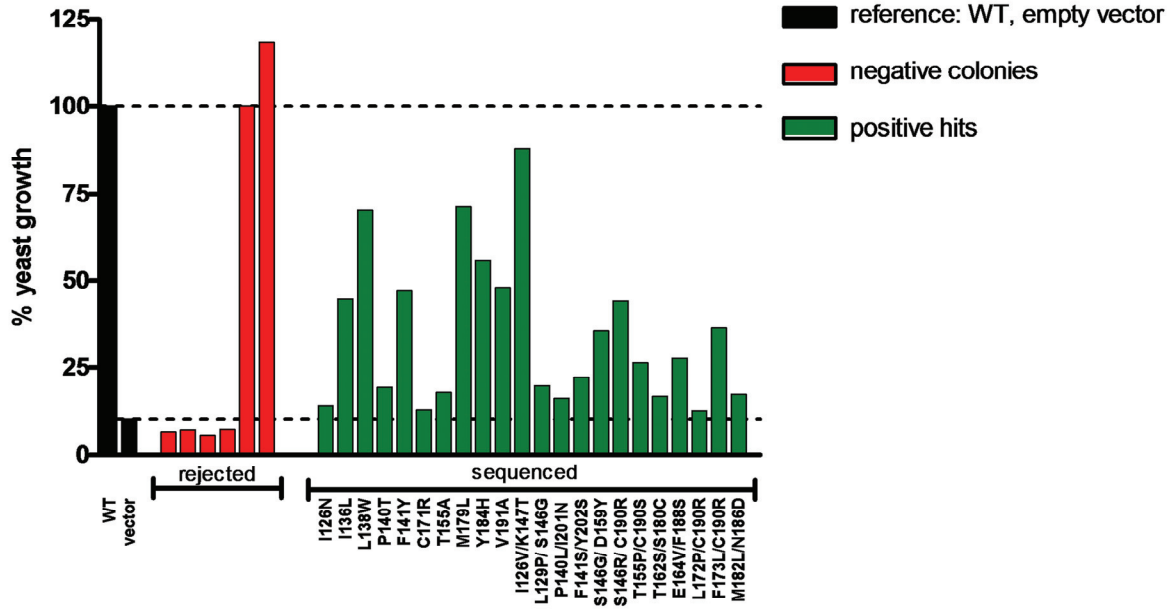

Figure 3. Results from reconfirmation screen. A total of 200 colonies selected from the CIM screen were subjected again to selection plates containing 1 mM 3AT. Positive hits were clones that showed growth levels lower than wild type, but higher than the empty vector (green). Receptor mutations from these colonies were identified by sequencing. Colonies that grew less than the empty vector or more than wild type were rejected (red). A selection of mutant receptors is shown in the graph, where growth of wild type (WT) is set to 100%, 0% was set to the background of the selection plate.

Characterization of mutant adenosine A_{2B} receptors

We mapped the mutated residues found in the single and double mutants onto the snake-plot of the A_{2B}R sequence in red (**Figure 4**). The residues are present all over the mutated fragment (indicated in the figure as between the restriction sites KpnI and BglII), with a large number of mutated residues located at the top half of TM5. The isolated plasmids containing one or two amino acid changes were retransformed into the MMY24 yeast strain and full concentration-growth curves were recorded to investigate their pharmacologic profile.

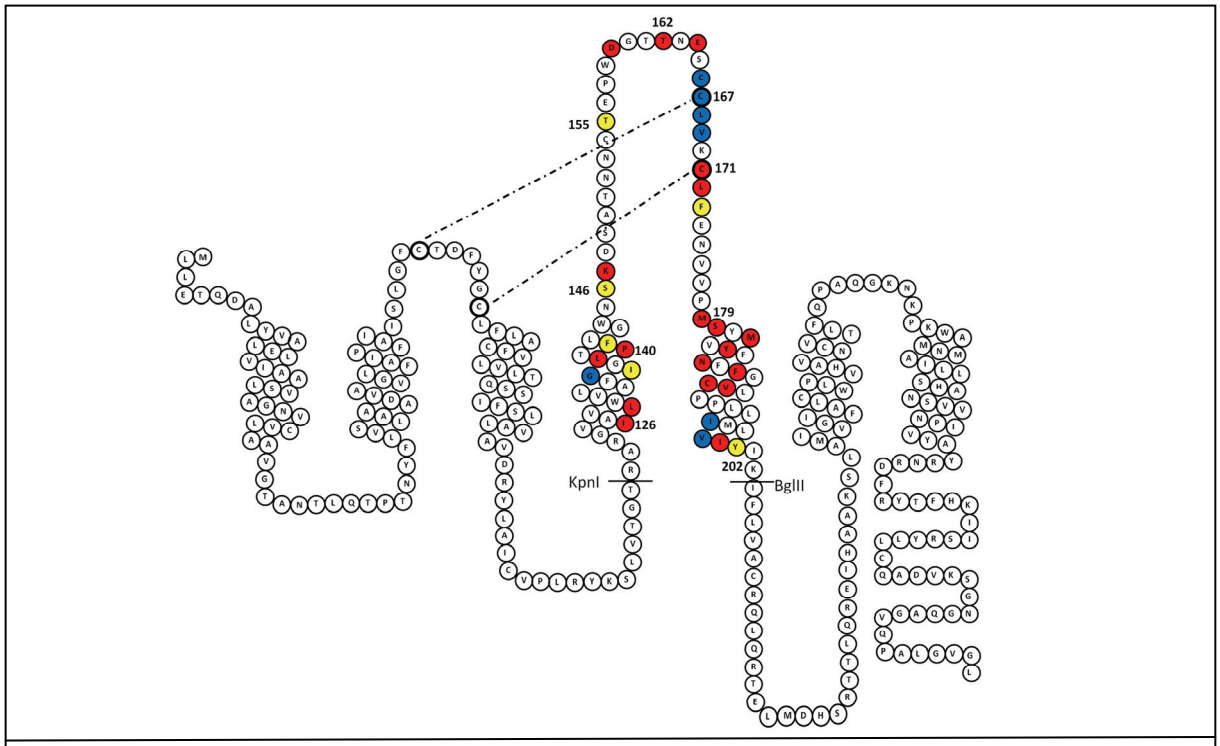

Figure 4. Snake-like representation of the adenosine A_{2B} receptor sequence showing both CIM and CAM residues identified in our screens. Residues found mutated as single and double mutant receptors in the CIM screen are shown in red. The CAM residues identified in a previous screen are shown in blue. Overlapping residues are shown in yellow. The putative disulfide bridges are indicated with dotted lines. The disulfide bridge conserved in many class A GPCRs links C78 and C171. The non-conserved second disulfide bridge between EL1 and EL2 based on the crystal structures of the adenosine $A_{2A}R$, links C72 and C167. The restriction sites KpnI and BglII are indicated that were used to obtain the fragment for random mutagenesis.

All of the 22 mutant receptors tested showed a decrease in potency vs wild-type in response to the full agonist NECA (see **Figure 5** for five representative mutants), ranging from a slight decrease in potency ($T162S^{EL2}/S180C^{5.36}$) to a full loss of activation ($C171R^{EL2}$). Only three mutant receptors ($I136L^{4.56}$, $T155A^{EL2}$, $T162S^{EL2}/S180C^{5.36}$) were still able to reach near-maximal activation levels. A full list of all the tested mutant receptors and their response to NECA is in **Table 1**.

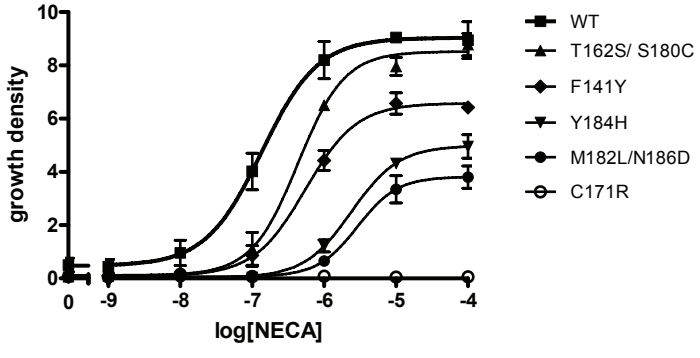

Figure 5.
Representative concentration-growth curves of mutant receptors. Yeast growth was measured on selective agar plates YNB-ULH with increasing NECA concentrations. Mutant receptors T162S/S180C (▲), F141Y (♦), Y184H (▼), M182L/N186D (●), and C171R (○), show a representative variety of concentration-growth curves of the mutant receptors identified from the screen. As a reference, the concentration-growth curve of the wild type human $A_{2B}R$ (■) is shown.

Table 1. Characterization of the adenosine receptor A_{2B} receptor mutants with one or two amino acid changes identified from the random mutagenesis screen. EC_{50} values (μM) in response to NECA are shown as means ± SEM of at least three independent experiments, each performed in duplicate. The mean values derived from the concentration-growth curves were used for calculation of the percentage maximal activity (Emax) and the level of constitutive activity (Fold CA), compared to the wild type receptor

Mutant	Fold CA	EC_{50} (μM) NECA	% Emax
WT	1.0	0.14 +/- 0.03	100
$I126N^{4.46}$	0.1	-	-
$I136L^{4.56}$	0.03	1.6 +/- 0.4	101
$L138W^{4.58}$	0.1	-	-
$P140T^{4.60}$	0.1	6.1 +/- 1.0	63
$F141Y^{4.61}$	0.2	0.55 +/- 0.1	73
$T155A^{EL2}$	0.4	1.1 +/- 0.1	102
$C171R^{EL2}$	0.04	-	-
$M179L^{5.35}$	0.1	4.2 +/- 1.1	70
$Y184H^{5.40}$	0.1	2.8 +/- 0.5	55
$V191A^{5.47}$	0.3	14.0 +/- 1.3	53
$I126V^{4.46}/K147T^{EL2}$	0.001	1.1 +/- 0.3	60
$L129P^{4.49}/S146G^{EL2}$	0.2	-	-
$P140L^{4.60}/I201N^{5.57}$	0.2	-	-
$F141S^{4.61}/Y202S^{5.58}$	0.1	-	-
$S146G^{EL2}/D159Y^{EL2}$	0.1	0.4 +/- 0.05	71
$S146R^{EL2}/C190R^{5.46}$	0.1	-	-
$T155P^{EL2}/C190S^{5.46}$	0.1	0.7 +/- 0.1	70
$T162S^{EL2}/S180C^{5.36}$	0.3	0.4 +/- 0.1	96
$E164V^{EL2}/F188S^{5.44}$	0.3	-	-
$L172P^{EL2}/C190R^{5.46}$	0.01	-	-
$F173L^{EL2}/C190R^{5.46}$	0.1	-	-
$M182L^{5.38}/N186D^{5.42}$	0.1	3.5 +/- 0.4	42

Western blot analysis showed that all mutant receptors are being expressed in the yeast cells, most of which in comparable amounts to wild type. Expression levels range from ca. 60% (S146G^{EL2}/D159Y^{EL2}) to ca. 135% (L138W$^{4.58}$). Two representative western blots are shown in **Figure 6**.

Figure 6. Western Blot of several mutant A_{2B} receptors with different activation profiles. Cell lysates of yeast cells transformed with wild type receptor, empty vector pDT-PGK, and mutant receptors were separated by SDS/PAGE and blotted on Hybond-ECL membranes. The arrows indicate the specific bands belonging to the adenosine A_{2B}R; these are located at ca. 29 kDa and 48 kDa.

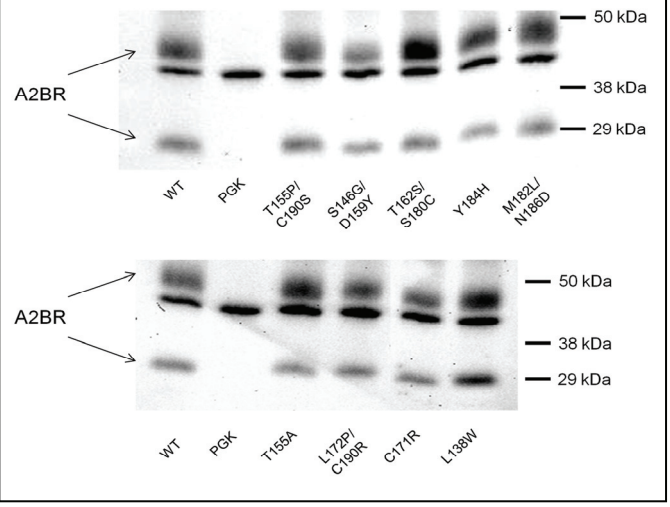

Next, we performed single point radioligand binding experiments using the A_{2B}R selective radiolabeled antagonist [^{3}H]PSB-603 [22,26] and the full agonist NECA (1 mM) as the displacing unlabeled ligand to define non-specific binding. Only three mutant receptors were able to reach levels of binding similar to the wild type receptor (**Figure 7**). All other mutant receptors had decreased levels of binding or were not able to bind the radiolabeled antagonist at all. To investigate whether this loss of radioligand binding was due to a decrease in antagonist affinity next to agonist potency, we performed a Schild plot analysis. Mutant receptors I136L$^{4.56}$ and T162S^{EL2}/S180C$^{5.36}$ were subjected to an increasing concentration of the antagonist PSB-603 in the presence of a concentration range of the agonist NECA and concentration-growth curves were measured (**Figure 8**). Both mutants showed an increase in NECA's EC_{50} value, but were still able to reach maximal growth levels compared to wild type receptor. In the single point radioligand binding assay, mutant I136L$^{4.56}$ bound the radiolabeled antagonist as avidly as wild type receptor, however, mutant T162S^{EL2}/S180C$^{5.36}$ showed a large decrease in radiolabeled antagonist binding. The pA_2 values measured from the Schild plot were 9.2 for wild type, 9.0 for mutant I136L$^{4.56}$, and 8.4 for mutant T162S^{EL2}/S180C$^{5.36}$, indicating that antagonist

affinity for the latter mutant was indeed compromised by the mutation, explaining the lack of radioligand binding (**Figure 8)**.

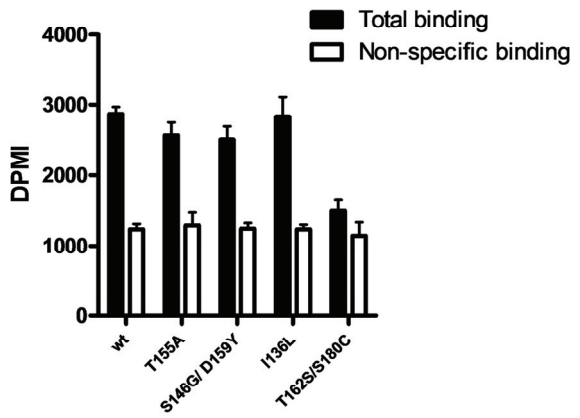

Figure 7. Single point competition binding assay with [^{3}H]PSB603. Binding experiments were performed at a radioligand concentration of 1.2 nM. Non-specific binding was determined using 1 mM NECA, shown in white bars. Total binding is shown in black bars. The mutant receptors shown were able to bind [^{3}H]PSB603 similar to wild type receptor at this concentration. Mutant T162S/S180C is one mutant receptor representative of many mutants with a large decrease in total binding.

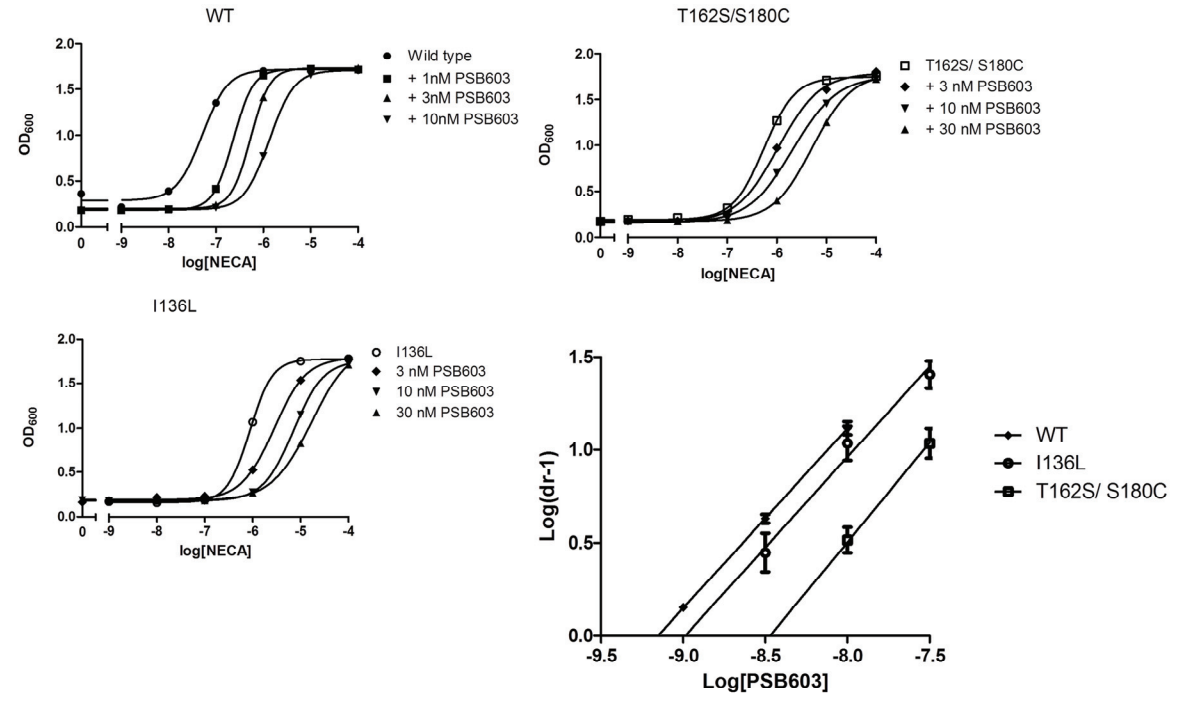

Figure 8. Schild plot analysis of PSB603 binding to WT and mutant receptors T162S/S180C and I136L. *(A)* Concentration-growth curves of NECA were recorded in the absence and presence of three concentrations of antagonist PSB603. *(B)* The pA_2 values of PSB603 were determined from a Schild plot (WT: 9.2, I136L: 9.0, T162S/S180C: 8.4).

Mapping mutated residues onto the $A_{2A}R$ structure

The adenosine A_{2A} receptor, the structure of which was recently elucidated [30], is the closest homologue to the adenosine A_{2B} receptor, with 82 % amino acid similarity and 59 % identity [22]. Therefore, the structure of the A_{2A} receptor could be predictive

of the spatial orientation of the $A_{2B}R$ amino acid residues. To determine which positions in the $A_{2A}R$ correspond to the $A_{2B}R$ CIMs, we created a multiple sequence alignment using all four subtypes of adenosine receptors as well as two other crystallized GPCRs, the β_2-adrenergic receptor [29] and the CXCR4 chemokine receptor [28] (**Figure 9A)**. Since the EL2 of the $A_{2B}R$ is longer than that of the $A_{2A}R$, two residues important for receptor inactivation could not be mapped onto the structure, namely adjacent $S146^{EL2}$ and $K147^{EL2}$. When aligning EL2 of the $A_{2A}R$ with the $A_{2B}R$, the equivalent positions of these two $A_{2B}R$ residues are located in a gap in the alignment (**Figure 9A**). The 3D representation in **Figure 9B**, like **Figure 4**, shows that most mutated residues are found near or in the extracellular region of the receptor; in the top half of TM4, in EL2, and in the top half of TM5. The mutated cluster in EL2 is located in a flexible part of the loop, upstream of the β-strand and in the helical structure as present in the NECA-bound $A_{2A}R$ structure (**Figure 9B**).

DISCUSSION

We set out to develop a new screening method for fast identification of inactivating mutations in the adenosine A_{2B} receptor. In the past, CAMs have provided great insight in how GPCRs can adapt an active conformation, similar to what occurs when an agonist is present [5,21,31]. CIMs represent an inactive state of the receptor, mimicking more the presence of an inverse agonist. By increasing our knowledge on this lesser explored spectrum of the activation mechanism, we aim to provide an enhanced insight of what occurs during receptor activation.

Li and coworkers reported on a different yeast system in which it is possible to screen for inactivating mutations [32]. Their system is highly engineered to only enable yeast cells containing inactive mutant receptors to survive by the introduction of the CAN1 reporter gene. When the receptor is activated, it promotes the expression of a transporter protein for the cytotoxic agent canavanine that leads to cell death. The use of this elegant system proved very successful in screening for residues that are functionally important in the M_3 muscarinic acetylcholine receptor (M_3R) [32,33]. The screening method described here is different in that it does not need a separately constructed system to screen for inactivating or activating mutant receptors. By

simply changing the concentration of the histidine synthesis inhibitor 3AT and the introduction of a specific time frame, we used one and the same system to also screen for inactivating mutant receptors. Also, our screen set-up does not require the presence of an agonist when selecting inactivating mutant receptors. This is beneficial, since then not only mutations that affect the binding and activation mode of that specific agonist are favoured. After identification of the mutant receptors, it is possible to verify their phenotype and investigate their pharmacologic profile again in the same system, without the need of more time-consuming procedures like expressing the mutant receptors in a mammalian cell system. This makes the initial selection of residues of interest faster and more convenient.

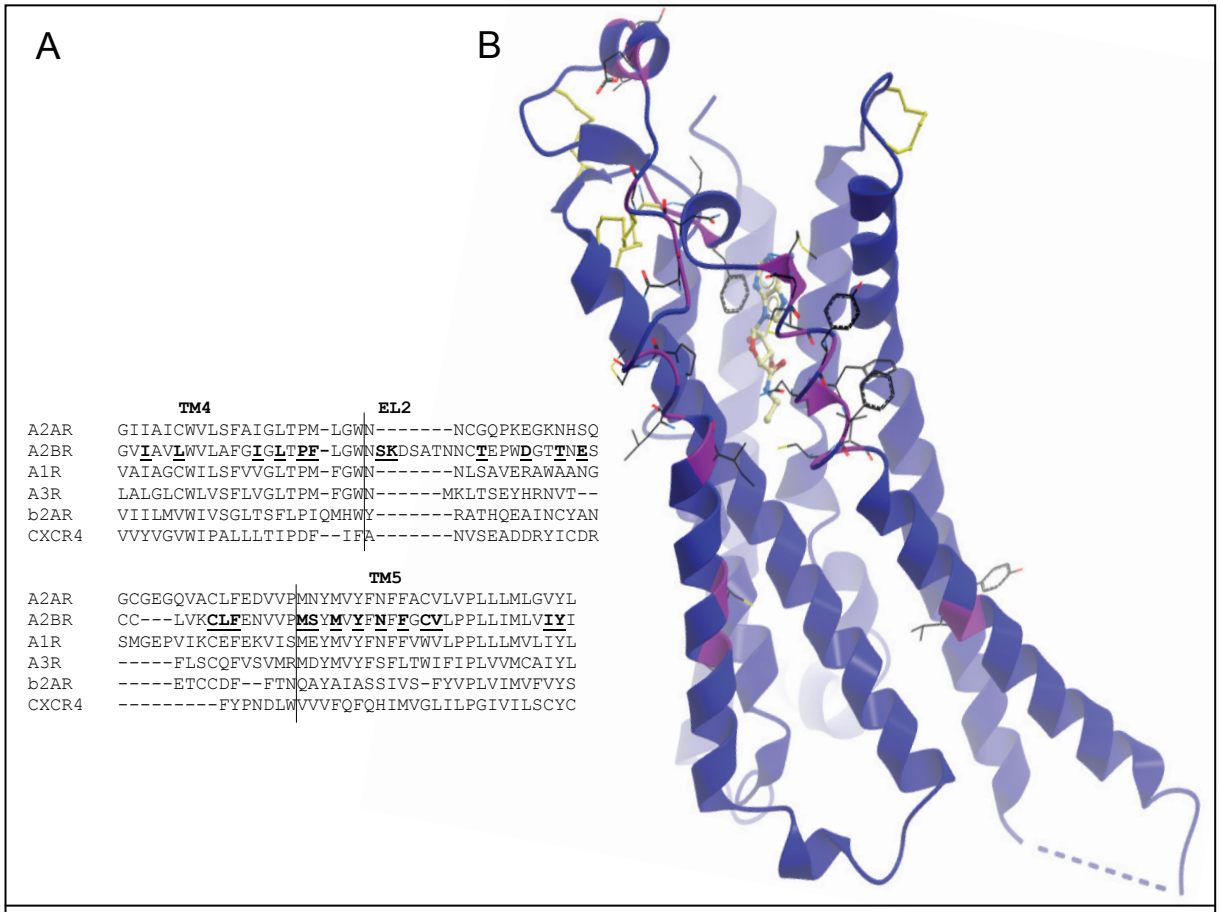

Figure 9. Mutated residues of the $A_{2B}R$ mapped on the crystal structure of the $A_{2A}R$ co-crystallized with NECA. *(A)* The multiple sequence alignment of the $A_{2A}R$ and $A_{2B}R$. The whole alignment was constructed using all four adenosine receptor subtypes as well as the sequence of two other crystal structures (of CXCR4 and β_2-adrenergic receptor) to ensure correct determination of EL2. The transitions between TM domains and EL2 are indicated with vertical lines, the mutated residues are indicated in bold font and underlined. *(B)* Based on the multiple sequence alignment described in Materials and Methods, the mutated residues identified from the screen were mapped onto the crystal structure of the $A_{2A}R$ (PDB: 3YDV) (blue), the closest homologue of the $A_{2B}R$. The mutated residues with their side chains are indicated in magenta. The ribbon representation also shows the co-crystallized ligand NECA (atoms colored) as well the disulfide bridges (yellow) that restrict EL2.

The CIM screen

We started with a random mutagenesis library in which in low frequency mutations were introduced in the fragment TM4-EL2-TM5 of the $A_{2B}R$. We subsequently transformed this library in the MMY24 yeast strain and started to screen at a concentration of 1 mM 3AT, a concentration at which, as a negative control, yeast containing only the expression vector was not able to produce enough histidine to allow substantial growth. However, yeast expressing the wild type $A_{2B}R$ was able to grow at this concentration of 3AT, reaching 50% of the maximal growth level at even lower concentrations of 3AT (**Figure 1**). We selected yeast colonies at two time points in the screen, after 4 days and after 6 days of screening. All selected colonies were first subjected to a reconfirmation procedure, where we looked at relative growth compared to wild type $A_{2B}R$ and a negative control in which only the expression vector was transformed (**Figures 2 and 3**). Out of the 200 colonies tested in this second round 136 colonies showed the correct phenotype (61 originating from day 4 and 75 from day 6 of the selection), indicating that the screen with the chosen parameters was successful (**Figure 3**). Among the colonies that failed this reconfirmation round, only a few showed a higher growth level than wild type (all present in first selection round at day 4). Most colonies that were discarded showed even less growth than the negative control and therefore most likely did not contain a functional receptor. Sequencing of the hits showed that after 4 days of screening the most relevant results were obtained. Mutant receptors showed many single and double amino acid changes, and only a low amount of wild type receptors was found in this selection. After 6 days however, more defects were found, including frame-shifts, deletions and expected “receptor killers”, such as mutation of the conserved cysteine at position 171^{EL2} in EL2.

Characterizing the mutant A_{2B} receptors

All receptors with one or two amino acid changes, in total 22 different mutant receptors, were used for further characterization. All of these single and double mutants showed a decrease in activation profile compared to the wild type receptor. Some were still able to reach full activation levels, others could not be activated by the agonist at all (**Figure 5, Table 1**). Even though several mutant receptors showed no activation whatsoever, they could all be expressed in the yeast system at levels

quite comparable to the wild-type receptor. A representative selection of these is shown in the Western Blot experiment in **Figure 6**. We were also able to measure specific radioligand binding to the A_{2B} wild-type receptor in yeast – in fact one of the few observations of radioligand binding to GPCRs expressed in yeast cells. For that, we used the recently described high-affinity antagonist [^{3}H]PSB-603 [26]. We also demonstrated specific binding to some mutant receptors, while most receptors did not display any binding (**Figure 7**). The Schild plot analysis for double mutant $162S^{EL2}$/$S180C^{5.36}$ in **Figure 8** suggests that this lack of radioliogand binding may be correlated with a decrease in antagonist affinity as determined in the functional growth assay.

In **Figure 9B**, we mapped the mutated residues onto the NECA-bound crystal structure of the adenosine A_{2A} receptor (PDB entry code: 3YDV), showing the putative 3D positions of the three mutated clusters [27]. Random mutagenesis studies of another GPCR expressed in yeast, the complement factor 5a receptor (C5aR), also revealed amino acid clusters important for receptor activation at the extracellular membrane interface that included TM4 and TM5 [34,35]. However, only two residues in the C5aR are located at positions corresponding to mutations found in the screen described here, namely at position 4.58 and 5.42 (L138 and N186 in the A_{2B}R).

The mutations present in TM4 are all pointing to the helical bundle. Presumably, disturbance of these inter-helix interactions may indeed interfere with the activation mechanism of the receptor. TM4 has not been found to play a role in coordinating receptor ligands through direct interactions in any of the available crystal structures. However, it is involved in Van der Waals interactions with TM5, as seen in the inactive crystal structures of the β_1-adreneric receptor and the adenosine A_{2A} receptor. These interactions are disturbed or changed in the activated structure [27,30,36].

In EL2, most residues that upon mutation cause the receptor to lose its ability to be fully activated are located in the more flexible, less restricted regions of the loop. It seems that despite the restrictions imposed by disulfide bridges, the second extracellular loop needs a certain amount of conformational flexibility for efficient receptor activation as has been suggested previously [33,37,38]. The conserved cysteine (C171) in EL2 was found affected too. The disulfide bridge in which it

participates has been reported as essential for maintaining GPCR structure and function [39]. Also F173^{EL2} was found mutated in one of the receptors in our mutant library. A phenylalanine at the corresponding position in the A_{2A}R interacts directly with the bound ligand in all four available crystal structures (**Figure 9B** shows the NECA-bound structure PDB:3YDV) [27,30,40].

In TM5, the mutations are mainly located at the centre of the α-helix. In the active crystal structures of the adenosine A_{2A}R, only two residues in TM5 directly contribute to the ligand binding site of NECA and adenosine, namely M177$^{5.38}$ and N181$^{5.43}$ [27]. In our CIM screen, we identified a double mutant in which the two corresponding residues in the A_{2B} receptor were mutated; M182L$^{5.38}$/N186D$^{5.42}$. This mutant receptor had a 25-fold decrease in potency for NECA and was only able to reach 42% of the maximal activation level. Also, no antagonist binding could be observed in the radioligand binding experiments. The other identified residues are not in close proximity (within 5 Å) of the A_{2A}R ligand binding pocket, although they have a strong impact on receptor activation and so form a good starting point in unravelling the activation mechanism and conformational changes of the adenosine A_{2B} receptor.

A number of amino acid positions are found several times in different mutant receptors, like I126$^{4.46}$, P140$^{4.60}$ and F141$^{4.61}$ in TM4, S146^{EL2} and T155^{EL2} in EL2, and C190$^{5.46}$ in TM5. These positions are found mutated into different residues, but also in different combinations with other mutated residues, indicating an especially important role in receptor activation. Residue C190$^{5.46}$ was identified in four different mutant receptors, either mutated to a serine or arginine (S146R^{EL2}/C190R$^{5.46}$, T155P^{EL2}/C190S$^{5.46}$, L172P^{EL2}/C190R$^{5.46}$, F173L^{EL2}/C190R$^{5.46}$), all in combination with a mutation located in EL2. Only mutant receptor T155P^{EL2}/C190S$^{5.46}$ was still able to show an agonistic response to NECA, although potency was reduced 5-fold and the maximal activation level could not be reached (**Table 1**). The corresponding position C185$^{5.46}$ in the A_{2A}R appears to be responsible for a bulge in TM5 that occurs after activation. When comparing the inactive structure (PDB:3EML) bound to ZM241385 with the active structures (PDB: 3QAK/3YDO/3YDV) bound to UK-432097, NECA and adenosine, respectively, TM5 moves slightly inwards, towards TM6. A movement of C185$^{5.46}$ initiates a sequence of changes via V186$^{5.47}$ and H250$^{6.52}$, hereby tightening the ligand binding pocket [27,40]. In the inactive A_{2A}R structure, a Van der Waals interaction exists between C185$^{5.46}$ and I135$^{4.56}$, similar to

the interaction observed in the β_1-adrenergic receptor [8,30]. The corresponding residue in TM4 in the $A_{2B}R$, $I136^{4.56}$, was also identified as a single mutant in our CIM screen. This $I136L^{4.56}$ mutant showed a large decrease in constitutive activity as well as an 11-fold decrease in NECA potency. In the inactive conformation of the $A_{2A}R$, the backbone of $C185^{5.46}$ is also connected by a hydrogen bond to residue $Q89^{3.37}$in TM3. In the active structures, this hydrogen bond cannot be formed anymore. It needs to be noted though that in the NECA and adenosine bound structures, residue $Q89^{3.37}$ has been mutated to an alanine to increase the thermostability of the receptor for crystallization purposes.

Residue $C190^{5.46}$ identified in our screen, is located at the bottom of the cluster in TM5. The other residues present in the cluster might be essential in facilitating the movement of the intracellular half of TM5 and participate in the ligand binding pocket (such as residues $M182^{5.38}$ and $N186^{5.42}$).

Constitutively active mutants (CAMs) versus constitutively inactive mutants (CIMs)

The same mutagenic library as employed in the study described here was previously used by us to screen for constitutively active mutant (CAM) receptors [21]. We used the same MMY24 yeast screen and the same technical approach, with the exception that the screen was performed in the presence of 7 mM 3AT and that colonies were selected after three days instead of the delayed approach described for the CIM screen. From the CAM screen, 12 different mutant receptors were identified that besides increased constitutive activity also displayed an increase in potency for the agonist NECA. The CAMs appeared to form three small clusters; at the top of TM4, in a cysteine-rich region in EL2, and at the bottom of TM5. In **Figure 4**, the identified residues are indicated from both the CIM (in red) and the CAM (in blue) screens. The yellow residues indicate positions that were found mutated in both screens. The previously described CAM clusters in TM4 and TM5 are now also sites for constitutively inactivating mutations. The CAM cluster in EL2, however, remains intact and is therefore likely important in silencing the receptor in its basal state. At the extracellular half of TM5, only CIMs were identified, indicating that this region has an opposite function.

Concluding remarks

By applying our new screening method, we were able to identify residues that are involved in maintaining the equilibrium between the inactive (R) and active (R*) receptor conformation in the absence of a ligand. This yeast screening strategy allowed for a rapid identification of functionally important residues in a typical class A GPCR, the adenosine A_{2B} receptor. This approach may be well applicable to other GPCRs that can be functionally expressed in yeast. Also, the CIMs identified from the newly developed screen, provide detailed insights in the activation mechanism of the A_{2B}R and revealed a particular important role for the upper half of TM5 in facilitating the conformational changes in the process of receptor activation. When these residues are mutated, receptor activity is compromised, either by directly changing the ligand binding site or by influencing conformational changes at a more distant location. The results obtained from this study can help clarify the changes observed between different structural conformations of the crystal structures available and provide mechanistic insight in the activation mechanism of class A GPCRs.

ACKNOWLEDGEMENTS

This research was performed under the auspices of the GPCR Forum, a program funded by the Dutch Top Institute Pharma (project D1-105).

REFERENCES

[1] Kristiansen, K., *Pharmacol Ther* (2004) 103:21-80.
[2] Deupi, X., Standfuss, J., *Curr Opin Struct Biol* (2011) doi 10.1016/j.sbi.2011.06.002.
[3] Peeters, M.C., van Westen, G.J., Li, Q., IJzerman, A.P., *Trends Pharmacol Sci* (2011) 32:35-42.
[4] Leff, P., *Trends Pharmacol Sci* (1995) 16:89-97.
[5] Cotecchia, S., Fanelli, F., Costa, T., *Assay Drug Dev Technol.* (2003) 1:311-316.
[6] Tao, Y.X., *Pharmacol Ther* (2006) 111:949-973.
[7] Kleinau, G., Jaeschke, H., Mueller, S., Worth, C.L., Paschke, R., Krause, G., *Cell Mol Life Sci* (2008) 65:3664-3676.
[8] Warne, T., Serrano-Vega, M.J., Baker, J.G., Moukhametzianov, R., Edwards, P.C., Henderson, R., Leslie, A.G., Tate, C.G., Schertler, G.F., *Nature* (2008) 454:486-491.
[9] Beukers, M., IJzerman, A., *Trends Pharmacol Sci.* (2005) 26:533-539.
[10] Decaillot, F., Befort, K., Filliol, D., Yue, S., Walker, P., Kieffer, B., *Nat Struct Biol.* (2003) 10:629-636.
[11] Hagemann, I., Narzinski, K., Floyd, D., Baranski, T., *J Biol Chem.* (2006) 281:36783-36792.
[12] Minic, J., Sautel, M., Salesse, R., Pajot-Augy, E., *Curr Med Chem* (2005) 12:961-969.

[13] Brown, A., et al., *Yeast* (2000) 16:11-22.
[14] Stewart, G.D., Valant, C., Dowell, S.J., Mijaljica, D., Devenish, R.J., Scammells, P.J., Sexton, P.M., Christopoulos, A., *J Pharmacol Exp Ther* (2009) 331:277-286.
[15] Beukers, M., van Oppenraaij, J., van der Hoorn, P., Blad, C., den Dulk, H., Brouwer, J., IJzerman, A., *Mol Pharmacol.* (2004) 65:702-710.
[16] Fredholm, B.B., IJzerman, A.P., Jacobson, K.A., Linden, J., Muller, C.E., *Pharmacol Rev* (2011) 63:1-34.
[17] Fredholm, B.B., *Cell Death Differ* (2007) 14:1315-1323.
[18] Wilson, C.N., *Br J Pharmacol* (2008) 155:475-486.
[19] Spicuzza, L., Di Maria, G., Polosa, R., *Eur J Pharmacol* (2006) 533:77-88.
[20] Hasko, G., Linden, J., Cronstein, B., Pacher, P., *Nat Rev Drug Discov* (2008) 7:759-770.
[21] Peeters, M.C., Li, Q., Van Westen, G.J., IJzerman, A.P., *Purinergic Signal* (2011) In press.
[22] Peeters, M.C., van Westen, G.J., Guo, D., Wisse, L.E., Muller, C.E., Beukers, M.W., IJzerman, A.P., *FASEB J* (2011) 25:632-643.
[23] Fromant, M., Blanquet, S., Plateau, P., *Anal Biochem* (1995) 224:347-353.
[24] Gietz, D., St Jean, A., Woods, R.A., Schiestl, R.H., *Nucleic Acids Res* (1992) 20:1425.
[25] Olesnicky, N.S., Brown, A.J., Dowell, S.J., Casselton, L.A., *Embo J* (1999) 18:2756-2763.
[26] Borrmann, T., Hinz, S., Bertarelli, D.C., Li, W., Florin, N.C., Scheiff, A.B., Muller, C.E., *J Med Chem* (2009) 52:3994-4006.
[27] Lebon, G., Warne, T., Edwards, P.C., Bennett, K., Langmead, C.J., Leslie, A.G., Tate, C.G., *Nature* (2011) 474:521-525.
[28] Wu, B., et al., *Science* (2010) 330:1066-1071.
[29] Rosenbaum, D.M., et al., *Science* (2007) 318:1266-1273.
[30] Jaakola, V.P., Griffith, M.T., Hanson, M.A., Cherezov, V., Chien, E.Y., Lane, J.R., IJzerman, A.P., Stevens, R.C., *Science* (2008) 322:1211-1217.
[31] Kobilka, B.K., Deupi, X., *Trends Pharmacol Sci* (2007) 28:397-406.
[32] Li, B., Scarselli, M., Knudsen, C., Kim, S., Jacobson, K., McMillin, S., Wess, J., *Nat Methods.* (2007) 4:169-174.
[33] Scarselli, M., Li, B., Kim, S., Wess, J., *J Biol Chem.* (2007) 282:7385-7396.
[34] Baranski, T., Herzmark, P., Lichtarge, O., Gerber, B., Trueheart, J., Meng, E., Iiri, T., Sheikh, S., Bourne, H., *J Biol Chem.* (1999) 274:15757-15765.
[35] Geva, A., Lassere, T.B., Lichtarge, O., Pollitt, S.K., Baranski, T.J., *J Biol Chem* (2000) 275:35393-35401.
[36] Warne, T., Moukhametzianov, R., Baker, J.G., Nehme, R., Edwards, P.C., Leslie, A.G., Schertler, G.F., Tate, C.G., *Nature* (2011) 469:241-244.
[37] Avlani, V.A., Gregory, K.J., Morton, C.J., Parker, M.W., Sexton, P.M., Christopoulos, A., *J Biol Chem* (2007) 282:25677-25686.
[38] Massotte, D., Kieffer, B.L., *Nat Struct Mol Biol* (2005) 12:287-288.
[39] Palczewski, K., et al., *Science* (2000) 289:739-745.
[40] Xu, F., Wu, H., Katritch, V., Han, G.W., Jacobson, K.A., Gao, Z.G., Cherezov, V., Stevens, R.C., *Science* (2011).

CHAPTER 6

THE SECOND EXTRACELLULAR LOOP OF THE ADENOSINE A_1 RECEPTOR PLAYS A ROLE IN BOTH RECEPTOR ACTIVATION AND ALLOSTERIC MODULATION

This chapter was based upon:

M.C. Peeters, L.E. Wisse, A. Dinaj, B. Vroling, G. Vriend, A.P. IJzerman.

(Manuscript in preparation)

ABSTRACT

The adenosine A_1 receptor is a member of the large membrane protein family that signals through G proteins, the G protein-coupled receptors (GPCRs). GPCRs consist of seven transmembrane domains connected by thee intracellular and three extracellular loops. Their N-terminus is extracellular, the C-terminal tail is in the cytoplasm. The transmembrane domains in subfamilies that bind the same endogenous ligand, such as dopamine or adenosine, tend to be highly similar. In contrast, the loop regions can vary greatly, both in sequence and in length, and the role these loops have in the activation mechanism of the receptors remains unclear. Here, we investigated the activating role of the second and third extracellular loop of the human adenosine A_1 receptor. By means of an $(Ala)_3$ mutagenic scan in which consecutive sets of three amino acids were mutated into alanines and a classical alanine scan, we revealed a strong regulatory role for the second extracellular loop (EL2) of the human adenosine A_1 receptor. Besides many residues in the second and the third extracellular loops important for adenosine A_1 receptor activation, we also identified two residues in EL2, a tryptophan and a glutamate, that affect the influence of the allosteric modulator PD81,723. These results, combined with a comparison of the different receptor loop regions, provide insight in the activation mechanism of this typical class A GPCR and further emphasize the unique pharmacological profile the loops can provide to individual receptors, even within subfamilies of GPCRs.

INTRODUCTION

G protein-coupled receptors (GPCRs) constitute the largest family of membrane signaling proteins, able to bind and transmit signals of a wide variety of endogenous ligands ranging from proteins such as chemokines and gonadotropic hormones to small molecules such as adenosine [1]. The involvement in many physiological process as well as the ability to be targeted by synthetic ligands, make this family an attractive drug target. Over the last decade much progress has been made in understanding the activation mechanism of this large superfamily, greatly aided by the elucidation of several high resolution crystal structures [2,3,4]. These new insights combined with mutagenesis data have resulted in a paradigm shift in GPCR research. The limited view that ligand binding and G protein coupling only are important for signal transduction and receptor activation is broadening to include the distinct role of the extracellular domains of GPCRs [5]. The extracellular domains are the least conserved elements of GPCR structure, varying both in sequence and in length even within subfamilies. Also the structural divergence observed between the different crystal structures published so far, suggests that the role of the extracellular loops may be unique for each individual receptor. In that context mutagenesis studies may be informative in two aspects: they shed light on how the loops contribute to receptor activation and pinpoint to differences between family members.

In the current study, we examined the second and third extracellular loop (EL2 and EL3) of the adenosine A_1 receptor (A_1R), a typical class A GPCR. The A_1R is part of a small subfamily that recognizes the endogenous nucleoside adenosine. Four members of this family have been identified, the A_1R, $A_{2A}R$, $A_{2B}R$ and A_3R. The four subtypes have different affinities for the endogenous ligand; the A_1R is a high affinity receptor (Ki ≈ 100 nM) where the $A_{2B}R$ displays a very low affinity for adenosine (Ki ≈ 15,000 nM). Also their intracellular signaling pathways differ, with the A_1R and A_3R coupling to G_i proteins and subsequently decreasing cAMP levels, and the $A_{2A}R$ and $A_{2B}R$ coupling mainly to G_s proteins thereby increasing intracellular cAMP concentrations [6]. Already in the early nineties Olah and coworkers provided evidence that extracellular loops are involved in differences in ligand recognition between adenosine receptor subtypes [7]. The authors created chimeric receptors, substituting EL2 or a region encompassing transmembrane domains 6 and 7 (including EL3) of the A_1R into the A_3R resulting in enhanced affinities of both A_1R

selective agonists and antagonists compared to wild-type A_3R. A particularly important region responsible for the observed effects was shown to be the C-terminal part of EL2. The second extracellular loop of the adenosine A_1R might also contain a binding site for allosteric ligands as has recently been speculated by Narlawar et al. They studied the behavior of bivalent ligands that connect an orthosteric ligand with an allosteric modulator to probe the location of the allosteric site relative to the orthosteric site [8]. EL2 has also been suggested as the binding site for allosteric modulators at other GPCRs, such as the M_2 muscarinic acetylcholine receptor (M_2R) and the M_4 muscarinic acetylcholine receptor (M_4R) [9,10].

In contrast to EL2, the third extracellular loop (EL3) is very small in all adenosine receptor subtypes. Nonetheless, EL3 has been proposed to be important in signaling in various GPCR family members [11,12,13]. Furthermore, this loop is involved in shaping the ligand binding pocket of both the antagonist ZM241385 and the agonists UK-432097, NECA, and adenosine in the published crystal structures of the adenosine A_{2A} receptor [3,14,15]. In the UK-432097 bound active structure, EL3 appeared forced outwards to accommodate the large biphenylic substituent on the N^6 position of the adenine moiety [3]. This might indicate a role for EL3 too in activation of the receptor.

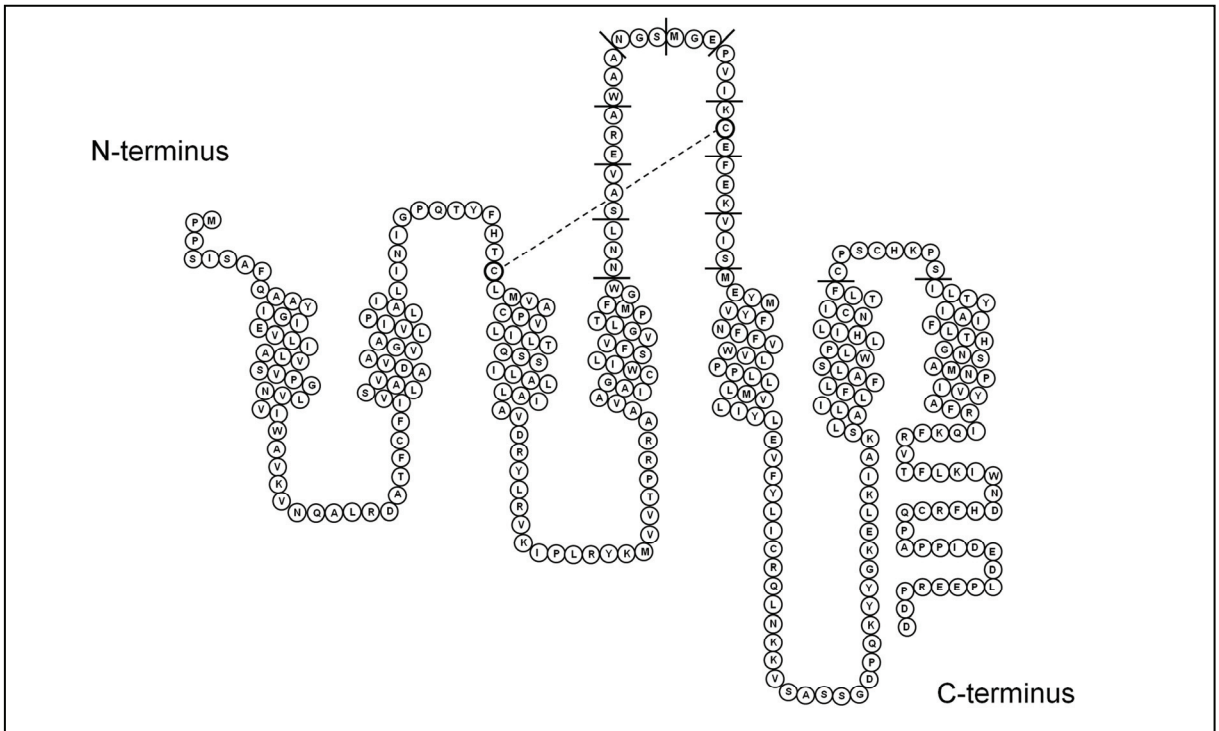

Figure 1. Snake-plot representation of the human adenosine A_1 receptor. The disulfide bridge conserved in many class A GPCRs links C80 and C169 (bold circles) and is indicated with the dotted line. The $(Ala)_3$ triplets in EL2 are shown with straight lines, also the section used for mutagenesis in EL3 is marked.

We performed a mutational analysis on both the second and third extracellular loop by using a classical alanine scan and investigated the effects on activation and ligand binding. Since EL2 is relatively large, we first scanned the loop by performing an $(Ala)_3$-scan in which triplets of amino acids were replaced by alanines. Interesting regions were then further characterized by single residue site-directed mutagenesis. To evaluate the mutant receptors, we made use of a robust yeast system, the MMY24 *S. cerevisiae* strain. This yeast system is an ideal background to monitor activation of a single GPCR, since its only endogenous GPCR has been removed from the system while still maintaining the complete GPCR-signaling machinery [16]. Several previous reports have proved this eukaryotic system to be predictive of the mammalian situation [17,18]. Besides investigating the effect of the alanine mutations on receptor activation and ligand binding, we also explored the ability of the allosteric modulator PD81,723 ((2-amino-4,5-dimethyl-3-thienyl)-[3-(triflurомethyl)-phenyl] methanone) to enhance the agonist-induced effect in the various mutant receptors. The results presented here, show a strong involvement of the second extracellular loop in receptor function by positively regulating A_1R activation. This is contradictory to the previously proposed role of EL2 as a negative regulator of the receptor [19,20]. Furthermore, we report a possible interaction of the allosteric modulator PD81,723 with a specific residue in EL2. Also EL3 is important in receptor activation; in particular two proline residues in this loop appear to be important in providing rigidity to this protein region.

MATERIALS AND METHODS

Mutagenesis

The *S. cerevisiae* expression vector containing the human adenosine A_1 receptor gene, pDT-PGK_hA_1R, that was used for all the mutagenesis procedures described in this paper was kindly provided by Dr. Simon Dowell from GSK (Stevenage, UK).

$(Ala)_3$-scan

For the initial screening of the second extracellular loop of the hA_1R, we replaced consecutive sets of three amino acids by an alanine; the $(Ala)_3$-scan. Where an alanine already existed, the residue was not mutated. Also the cysteine at position 169 was kept unchanged. The mutations were introduced using the QuikChange

Multi-Site Directed Mutagenesis system (Stratagene, Huizen, The Netherlands). The $(Ala)_3$-scan yielded ten mutant receptors.

Site-directed mutagenesis

The single alanine mutations introduced in the second extracellular loop as well as the single alanine scan of the third extracellular loop of the hA_1R were performed using the QuikChange II Site Directed Mutagenesis system (Stratagene, Huizen, The Netherlands). Twelve additional mutant receptors of EL2 and eight alanine mutant receptors of EL3 were created. All mutant receptor genes were verified by double-stranded sequencing (LGTC, Leiden, The Netherlands).

Transformation in MMY24 S. cerevisiae strain

pDT-PGK_hA_1R plasmids were transformed into an *S. cerevisiae* yeast strain according to the Lithium-Acetate procedure [21]. The strain is derived from the MMY11 strain [22] and was further adapted to communicate with mammalian GPCRs through the introduction of a chimeric G protein [16]. The genotype of the MMY24 strain is: *MAT**a**his3 leu2 trp1 ura3can1 gpa1_::G_i3 far1_::ura3 sst2_::ura3 Fus1::FUS1-HIS3LEU2::FUS1-lacZ ste2_::G418R.* To measure signaling of GPCRs, the pheromone signaling pathway of this strain was coupled via the FUS1 promotor to HIS3, a gene encoding the key enzyme in histidine production, imidazole glycerol-phosphate dehydrase. The degree of receptor activation was measured by the growth rate of the yeast on histidine-deficient medium.

Liquid yeast growth assay

To characterize the mutant receptors further, concentration-growth curves were generated in a liquid growth assay. Yeast colonies expressing wild type or mutant hA_1 receptor were inoculated in 2.5ml YNB-UL (Yeast Nitrogen Based medium lacking the markers uracil and leucine) and incubated overnight at 30°C. The cultures were diluted to an OD_{600} of 0.002 (≈ $4 \cdot 10^4$ cells/ml) in medium without histidine (YNB-ULH medium), resulting in a final concentration of $1 \cdot 10^4$ cells/ml in the assay. Concentration-growth curves were performed in YNB-ULH medium with 7 mM 3AT, 0.8 IU/ml adenosine deaminase (ADA) (Roche Diagnostics, Almere, The Netherlands) and varying concentrations of CPA (N^6-cyclopentyladenosine) (Tocris Cookson Ltd, Avonmouth, United Kingdom) (10^{-7} – 10^{-11}M) in the presence or absence of 1 μM PD81,723 ((2-amino-4,5-dimethyl-3-thienyl)-[3-(trifluromethyl)-phenyl]methanone)

(synthesized in house). Growth represented by the absorbance at 595nm was measured over a period of 35 hrs in a Genios plate reader (Tecan, Durham, NC). Data was analyzed using nonlinear regression analysis software available in GraphPad Prism 5.0 (GraphPad Software, San Diego, CA).

Whole yeast cell radioligand binding experiments

Yeast cells expressing wild type or mutated A_1Rs were cultured overnight in rich YAPD (Yeast-extract Adenine Peptone Dextrose) medium. Cells were centrifuged for 5 minutes at 2000 xg, the pelleted cells were once washed with 0.9% NaCl. The cells were again centrifuged 5 minutes at 2000 xg and diluted in the assay buffer (50mM Tris-HCl pH7.4 + 1mM EDTA) to OD_{600}=40 (OD_{600} = 1 ≈ $2.5 \cdot 10^7$ cells/ml). Also, 1 U/ml ADA was added to the cells. Binding experiments were performed with 5 nM [^{3}H]DPCPX and a final cell concentration of $25 \cdot 10^7$ cells/ml in a total volume of 100 µl. Nonspecific binding was determined in the presence of 10 µM CPA. For whole competition binding curves a concentration range of 10^{-10}-10^{-5} M of the agonist CPA was used in the presence or absence of the allosteric modulator 10 µM PD81,723.
Samples were incubated for 1 hour at 25ºC while shaking vigorously to keep the yeast cells in suspension. Incubation was terminated by adding 1 ml ice-cold assay buffer. Bound from free radioligand was immediately separated by rapid filtration through Whatman GF/B filters pre-incubated with 0.1% polyethylenimine (PEI) using a Millipore manifold during which the filters were washed six times with ice-cold assay buffer. Filter-bound radioactivity was determined by scintillation spectrometry (Tri-Carb 2900TR; PerkinElmer Life and Analytical Sciences) after addition of 3.5 ml of PerkinElmer Emulsifier Safe.

Whole yeast cell extracts and immunoblotting

Whole protein cell extracts were made from the transformed yeast cells using trichloroacetic acid (TCA). From an overnight culture, $1.2 \cdot 10^8$ yeast cells were harvested in mid-log phase. The cells were washed twice with 20% TCA after which they were broken by vigorous vortexing in the presence of glass beads. The yeast cell extracts were separated on 12.5% SDS page gels and transferred to a PVDF transfer membrane (GE healthcare, Diegem, Belgium) using a semi-dry Western blotting set (Sigma–Aldrich, Zwijndrecht, The Netherlands). The antibody directed

against the C-terminal region of the adenosine A_1 receptor was used for immunodetection (Sigma-Aldrich, Zwijndrecht, The Netherlands). Densitometric analysis of the protein bands was performed using the volume analysis tool as present in the Quantity One imaging software from Bio-Rad (Hercules, CA). The aspecific band that is seen in all yeast extracts, including empty yeast cell extracts, was used as loading control. The ratio between specific A_1R protein bands and aspecific bands was determined and the wild-type receptor was set at 100%, the empty vector pDT-PGK at 0%.

Bioinformatic analysis

A multiple sequence alignment of the A_1R, $A_{2A}R$, $A_{2B}R$, and A_3R receptors was created with T-Coffee using the default settings, followed by small manual corrections based on structural considerations, sequence conservation and correlation patterns in EL2 and IL3 [23]. Start and end positions of the loops were selected based on manual inspection of the crystal structure of the human $A_{2A}R$ receptor (PDB: 3EML). The Phylip package was used to calculate distances between the individual receptors (both the complete receptor sequences as well as the loop segments), and to generate the distance trees [24]. The scoring tables are shown in Chapter 7, Figure 5).

RESULTS

$(Ala)_3$-scan of the second extracellular loop (EL2)

To gain insight in the role of the second extracellular loop of the human adenosine A_1 receptor (hA_1R) in receptor activation, we first set out to identify specific regions in the loop that influence activity. For this purpose, we designed an $(Ala)_3$-scan, where consecutive sets of three amino acids were mutated into alanine residues **(Figure 1)**. Where an alanine residue already existed, the corresponding codon was kept unchanged. Also, the cysteine at position 169 was not mutated, since this residue has been proven in the past to be essential for receptor function, as it is part of the highly conserved disulfide bridge with C80 in TM3 [25].

The $(Ala)_3$-scan rendered 10 different mutant receptors that were tested for their activation profile in a liquid yeast growth assay. This assay is based on a gene

reporter system incorporated in the *S. cerevisiae* MMY24 strain. When the expressed human receptor is activated by an agonist, the yeast pheromone signaling pathway is activated through a chimeric yeast-mammalian G protein leading to subsequent transcription of the HIS3 reporter gene. As a result, the yeast cells produce the essential amino acid histidine that allows the cells to grow on histidine-deficient medium in a dose dependent manner. Concentration-growth curves of all 10 $(Ala)_3$ mutant receptors are shown in **Figure 2.**

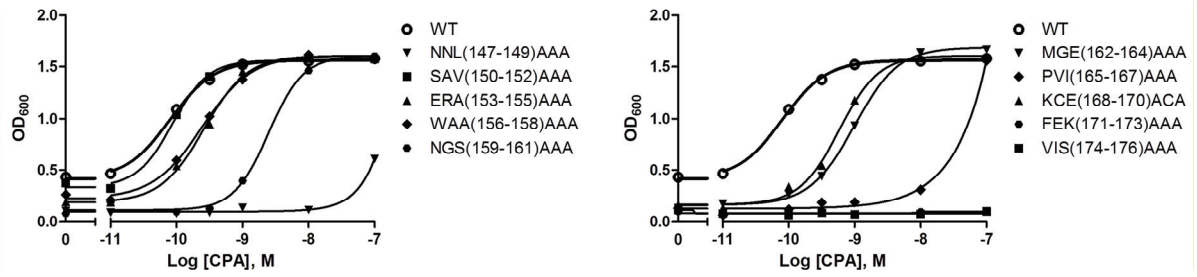

Figure 2. Representative concentration-growth curves of the triple $(Ala)_3$-mutant receptors using increasing concentrations of the agonist CPA. The liquid yeast growth assay was used to characterize the mutant receptors, where OD_{600} represents the level of yeast growth and thus receptor activation. Representative curves of wild type receptor (WT) are shown in open circles, the triple mutant receptors are indicated with closed symbols.

The level of constitutive activity the wild-type A_1R displays is relatively high, approx. 25% of the maximal response under the assay conditions used. Except for mutant SAV(150-152)AAA, all triple mutant receptors show a decrease in potency for the selective A_1R agonist N^6-cyclopentyladenosine (CPA). SAV(150-152)AAA is also the only mutant receptor that did not display a significant decrease in constitutive activity (see also **Table 1**). Especially the start and end of the loop sequence, represented by triplets NLL(147-149), FEK(171-173), and VIS(174-176) are highly sensitive to the alanine mutations, showing no or barely any response to the agonist. Three other triple mutant receptors that show a more than one log unit decrease in potency were NGS (159-161)AAA, MGE(162-164)AAA, and PVI(165-167)AAA (**Figure 2, Table 1**). A Western blot analysis showed that all receptors were expressed in the yeast cells, even the mutant receptors that were greatly affected by the alanine mutations. A number of receptors appeared to be present in larger quantities compared to the wild type A_1R, most notably for the SAV(150-152)AAA construct **(Figure 3)**.

Table 1. Characterization of the adenosine A_1R mutant receptors of the second extracellular loop, both triple $(Ala)_3$-mutants and single alanine mutants, using the liquid yeast growth assay. The level of constitutive activity (CA) of wild type receptor (WT) and mutants is represented by the OD_{600} +/ SEM measured in the absence of CPA. EC_{50} values of the agonist CPA (nM) and percentage maximal activity (Emax) are shown as means ± SEM of three independent experiments, each performed in duplicate. Mean values derived from the concentration-growth curves were used for calculation of the fold EC_{50} value, the shift of EC_{50} in the presence of the allosteric modulator PD81,723 (PD81).

Mutant	CA (OD_{600})	EC_{50} (nM) CPA	% Emax	EC_{50} (nM) + PD81	Shift EC_{50} + PD81
WT	0.43 +/- 0.04	0.10 +/- 0.01	100 +/- 1	0.06 +/- 0.01	1.6
NNL(147-149)AAA	0.10 +/- 0.03	> 100	39 +/- 3		
SAV(150-152)AAA	0.38 +/- 0.03	0.10 +/- 0.04	100 +/- 1	0.06 +/- 0.03	1.6
ERA(153-155)AAA	0.19 +/- 0.03	0.28 +/- 0.01	100 +/- 1	0.19 +/- 0.05	1.5
E153A	0.10 +/- 0.01	0.43 +/- 0.02	101 +/- 1		
R154A	0.50 +/- 0.03	0.12 +/- 0.02	103 +/- 1		
WAA(156-158)AAA	0.26 +/- 0.04	0.25 +/- 0.08	100 +/- 1	0.22 +/- 0.09	1.1
NGS (159-161)AAA	0.08 +/- 0.01	2.4 +/- 0.2	102 +/- 2	1.7 +/- 0.3	1.4
N159A	0.25 +/- 0.03	0.35 +/- 0.01	100 +/- 1		
G160A	0.09 +/- 0.03	0.71 +/- 0.01	101 +/- 2		
S161A	0.12 +/- 0.02	0.41 +/- 0.07	94 +/- 1		
MGE(162-164)AAA	0.13 +/- 0.03	1.0 +/- 0.06	106 +/- 1	0.44 +/- 0.05	2.2
M162A	0.47 +/- 0.16	0.12 +/- 0.02	102 +/- 1		
G163S	0.03 +/- 0.01	2.1 +/- 0.09	96 +/- 1		
E164A	0.46 +/- 0.15	0.15 +/- 0.002	102 +/- 1		
PVI(165-167)AAA	0.13 +/- 0.05	> 100	99 +/- 1		
P165A	0.15 +/- 0.05	0.61 +/- 0.05	102 +/- 1		
V166A	0.08 +/- 0.01	0.64 +/- 0.04	101 +/- 1		
I167A	0.06 +/- 0.003	4.5 +/- 0.2	103 +/- 1		
KCE(168-170)ACA	0.17 +/- 0.03	0.56 +/- 0.02	101 +/- 1	0.33 +/- 0.06	1.7
E170A	0.10 +/- 0.01	0.40 +/- 0.06	102 +/- 1		
FEK(171-173)AAA	0.10 +/- 0.01	No response			
VIS(174-176)AAA	0.11 +/- 0.002	No response			

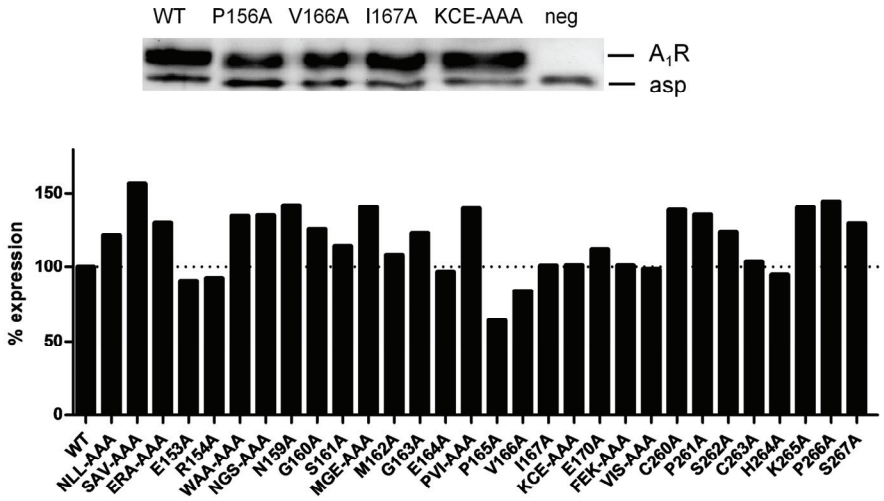

Figure 3. Western blot analysis of all EL2 and EL3 mutant receptors. In the upper panel, a representative blot is shown with four mutant receptors, the empty plasmid pDT-PGK as negative control, and the wild type receptor (WT). The upper lane represents the specific A_1R band and the lower band represents the aspecific band (asp). The lower panel shows the bar graph resulting from the densitometric analysis. The ratio was determined between the density of the specific band and the density of the non-specific band. Wild type receptor was set at 100%, the empty vector pDT-PGK was set at 0%.

Single alanine mutations EL2

To further investigate specific residues that influence adenosine A_1 receptor activation, we created single alanine mutations of several positions where we mainly focused on the central part of the loop. The $(Ala)_3$ mutant receptor WAA(156-158)AAA only contained a mutation of the tryptophan at position 156 and already represented a single mutant receptor. The 12 new single mutant receptors were analyzed in the functional liquid yeast growth assay (**Table 1**). A selection of the resulting concentration-growth curves is shown in **Figure 4**.

Similar to the $(Ala)_3$ mutant selection, most single alanine mutations compromised receptor activation both in response to the agonist CPA and independently of a ligand (constitutive activity). Even though several mutant receptors displayed a large potency decrease, they were all able to reach (near) maximal activation levels compared to wild-type receptor in response to CPA. Looking at the three most affected $(Ala)_3$ mutants, we observed an additive effect of the individual alanine mutant receptors within the NGS(159-161) triplet with position G160 having the largest, 7-fold potency decrease as well as a 4.8-fold decrease in constitutive activity. The 10-fold decrease in CPA potency of the $(Ala)_3$ mutant MGE(162-164)AAA appeared solely due to the single mutant G163A that even shows a potency

decrease of 21-fold compared to wild type receptor as well as a 14-fold decrease in basal activity. Mutating the other 2 residues in this triplet, M162 and E164 resulted in a negligible effect on activation when investigated separately. These two residues appeared to rescue activation to some extent when combined with G163A. In the triplet PVI(165-167), again an additive effect was seen of which the main effect is caused with isoleucine 167 mutated to an alanine, resulting in a 45-fold decrease of agonist potency. This mutant receptor also showed the largest impact on constitutive activity of the three single alanine mutants, showing a 7.2-fold decrease compared to wild-type receptor. Both mutant receptors P165A and V166A showed a 7-fold decrease in CPA's potency. These receptors were the only mutants that showed a somewhat decreased expression level compared to the wild-type receptor (**Figure 3**).

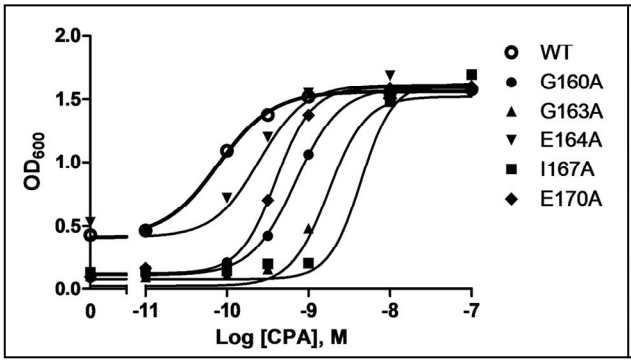

Figure 4. Representative concentration-growth curves of a selection of single alanine mutant receptors of EL2 using increasing concentrations of the agonist CPA. The liquid yeast growth assay was used to characterize the mutant receptors, where OD_{600} represents the level of yeast growth and thus receptor activation. Representative curves are shown of wild type receptor (WT)(○), G160A (●), G163A (▲), E164A (▼), I167A (■), E170A (♦)

Next, we performed radioligand binding experiments using the single mutant collection, including the W156A mutant receptor. We firstly determined whether a large enough window could be obtained to perform whole competition binding curves. For the binding experiments a concentration of 5 nM of the antagonist [^{3}H]DPCPX was used, a concentration that is more than 3 times the Kd value of the wild type receptor (Kd_{wt} on yeast: ≈ 1.5 nM, data not shown). Even with this increased amount of radioligand and an excess of unlabeled CPA, for a number of the mutant receptors, only a low level of specific binding was observed **(Figure 5A, Table 2).** The mutant receptors for which we observed specific binding greater than 60% compared to wild type receptor were used to perform full competition binding curves (**Figure 5B, Table 2**). From the competition binding curves, no decrease in affinity for CPA was observed, even though some of the mutants, like S161A and N159A, did show a decrease in potency for CPA in the yeast growth assays.

Table 2. Radioligand binding experiments of the single alanine mutations in the second extracellular loop, using the selective antagonist [^{3}H]DPCPX. Single point measurements and competition binding curves were performed using the unlabeled agonist CPA. Percent specific binding and IC_{50} values are shown as means ± SEM of three independent experiments, each performed in duplicate. Mean values derived from the competition binding curves were used for calculation of the shift in IC_{50} in the presence of the allosteric modulator PD81,723 (PD81)

Mutant	% specific binding	IC_{50} (nM)	IC_{50} (nM) + PD81	Shift IC_{50} + PD81
WT	100	167 +/- 25	69 +/- 8	2.4
E153A	41 +/- 5			
R154A	103 +/- 8	166 +/- 38	72 +/- 17	2.3
W156A	74 +/- 11	161 +/- 6	141 +/- 10	1.1
N159A	71 +/- 6	170 +/- 10	64 +/ 3	2.6
G160A	34 +/- 5			
S161A	77 +/- 4	169 +/- 11	75 +/- 18	2.3
M162A	89 +/- 4	130 +/- 5	55 +/- 5	2.4
G163A	12 +/- 1			
E164A	60 +/- 2	192 +/- 7	58 +/- 4	3.3
P165A	18 +/- 3			
V166A	14 +/- 3			
I167A	8 +/- 2			
E170A	43 +/- 5			

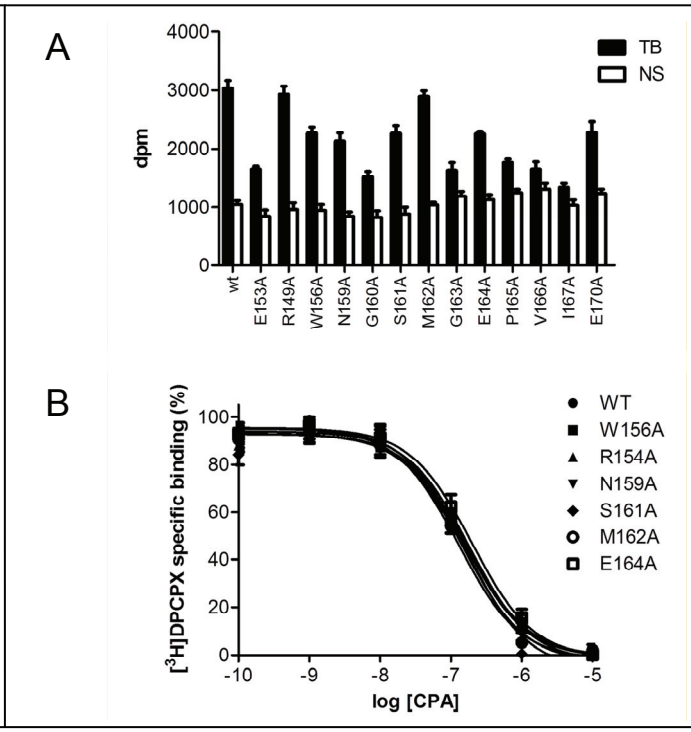

Figure 5.
Radioligand binding experiments of single alanine mutant receptors of EL2. (*A*) Single point competition binding assay with [^{3}H]DPCPX.
Binding experiments were performed at a radioligand concentration of 5 nM. Non-specific binding was determined using 10 µM CPA.
(B) Competition binding curves with [^{3}H]DPCPX using increasing concentrations of unlabeled CPA as displacer of wild type receptor (●) and the single mutants W156A (■), R154A (▲), N159A (▼), S161A (♦), M162A (○), and E164A (□). Total binding was set at 100%, non-specific binding at 0%.

Allosteric modulation

To investigate whether our mutants were sensitive to allosteric modulation, we performed concentration-growth curves with CPA on the $(Ala)_3$ mutants in the presence of 1 µM PD81,723, a selective allosteric modulator of the A_1R. Where we normally use 10 µM of the allosteric modulator in binding studies, we were not able to exceed a concentration of 1 µM in the functional experiments due to the intrinsic agonistic effect of PD81,723 that concealed the modulating effect on CPA activation. The increase in agonist potency in the presence of PD81,723 observed for the wild type receptor was 1.6 fold under these conditions. A significant decrease was noticed for mutant receptor W156A and an increase in response to PD81,723 was observed for mutant receptor MGE(162-164)AAA **(Figure 6A, Table 1)**.

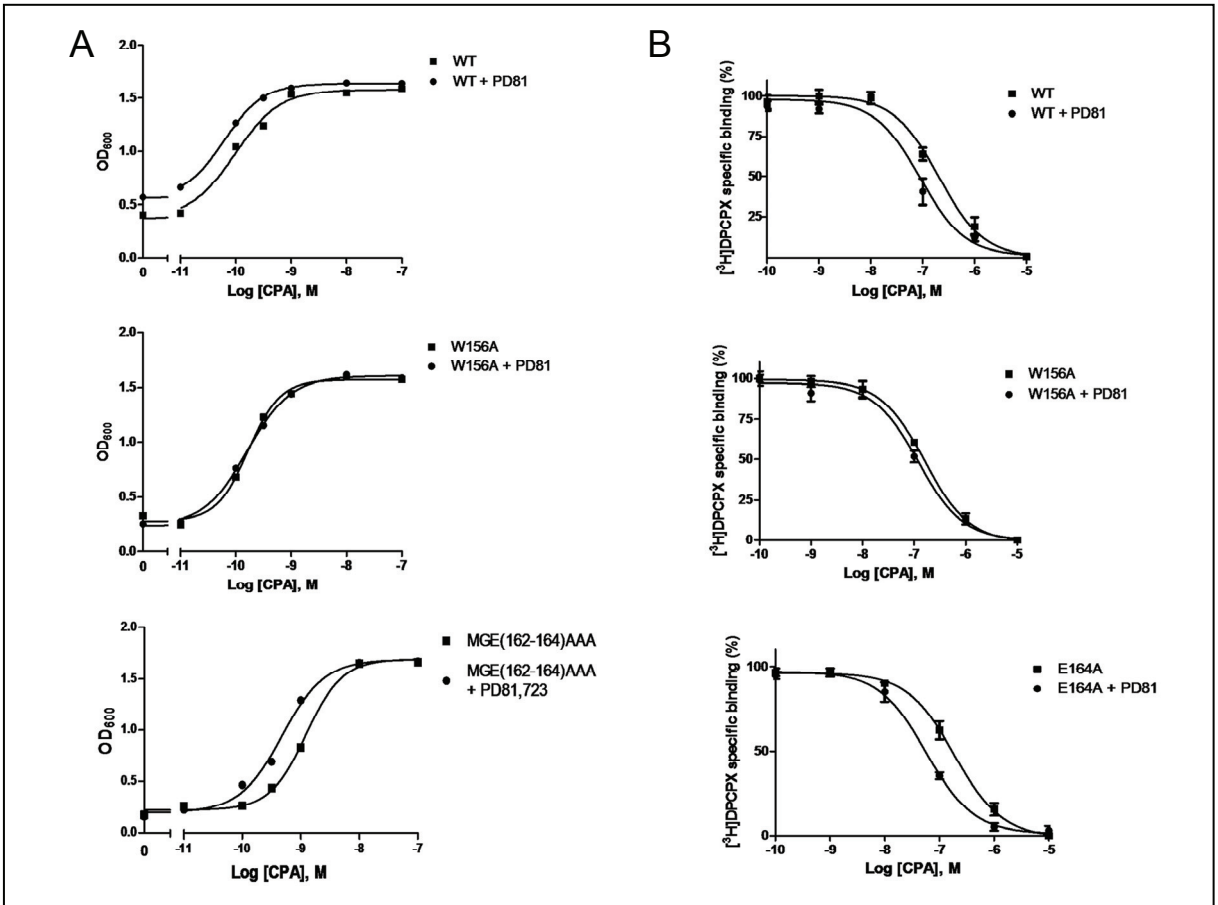

Figure 6. (*A*) Concentration-growth curves using increasing concentrations of the agonist CPA of wild type receptor, and mutant receptors W156A and MGE(162-164)AAA in the absence (■) and presence of the allosteric modulator PD81,723 (●). (*B*) Competition binding curves with [^{3}H]DPCPX using increasing concentrations of unlabeled CPA as displacer of wild type receptor, and mutant receptors W156A and E164A in the absence (■) and presence of the allosteric modulator PD81,723 (●)

When subjecting the single mutant receptors W156A and E164A (part of the MGE triplet) to radioligand competition binding experiments in the presence of 10 μM PD81,723, we noticed similar effects **(Figure 6B)**. The affinity of CPA for the wild type receptor was increased 2.4 fold when competition curves were performed in the presence of the allosteric enhancer PD81,723. In contrast, mutant receptor W156A showed no significant change in CPA affinity in the presence of PD81,723 and mutant receptor E164A showed an increase in affinity that was even greater than observed for wild type, namely 3.3 fold **(Table 2)**.

Alanine scan of the third extracellular loop

The third extracellular loop was also subjected to an alanine scan. The loop is relatively small, therefore, we performed a single alanine scan in which all eight residues were mutated **(Figure 1)**. The results of the functional liquid yeast growth assays are listed in **Table 3**.

Table 3. Characterization of the adenosine A_1R mutant receptors of the third extracellular loop, using the liquid yeast growth assay. The level of constitutive activity (CA) of wild type receptor (WT) and mutants is represented by the OD_{600} +/ SEM measured in the absence of CPA. EC_{50} values of the agonist CPA (nM) and percentage maximal activity (Emax) are shown as means ± SEM of three independent experiments, each performed in duplicate.

Mutant	CA (OD_{600})	EC_{50} (nM)	Fold EC_{50}	% Emax
WT	0.43 +/- 0.03	0.10 +/- 0.01	1.0	100 +/- 1
C260A	0.26 +/- 0.02	0.14 +/- 0.01	1.5	100 +/- 1
P261A	0.27 +/- 0.09	0.25 +/- 0.07	2.5	96 +/- 3
S262A	0.27 +/- 0.06	0.19 +/- 0.02	1.9	103 +/- 1
C263A	0.31 +/- 0.6	0.10 +/- 0.02	1.0	102 +/- 1
H264A	0.38 +/- 0.13	0.16 +/- 0.05	1.6	102 +/- 1
K265A	0.16 +/- 0.08	0.18 +/- 0.03	1.8	102 +/- 1
P266A	0.21 +/- 0.09	0.36 +/- 0.06	3.6	101 +/- 0.5
S267A	0.16 +/- 0.07	0.22 +/- 0.01	2.2	101 +/- 1

Compared to the mutagenesis results observed for EL2, the effects on activation by the mutations in EL3 were relatively small. The largest effect was seen when the two

prolines were mutated, P261A and P264A, where CPA's potency was decreased by respectively 2.5 and 3.6 fold, respectively. Of the eight EL3 mutant receptors, only H264A showed similar levels of constitutive activity. Basal activity was decreased in all other mutants, with K265A and S267A displaying the largest decrease of 2.7-fold. All mutant receptors were again able to reach maximal activation levels in response to CPA. A Western blot analysis showed that the mutant receptors were expressed at similar levels compared to WT or even somewhat higher **(Figure 3).**

Bioinformatics analysis - loop similarity

The adenosine A_1 receptor is a member of a small subfamily together with three other adenosine receptors, $A_{2A}R$, $A_{2B}R$, and A_3R. In transmembrane sequence, the A_1R is most related to the A_3R, and these two receptors also share the same signaling pathway, coupling both to G_i proteins. The question remains though, whether the loops and their function are just as comparable. Also, we were wondering to what extent we can compare the structural information of the extracellular loops that is available from the crystal structure of one subtype, the $A_{2A}R$, to other adenosine receptor subtypes. To investigate this, we performed a sequence similarity analysis in which we compared all loop sequences of the receptors with each other. Multiple sequence alignments were created with the T-Coffee alignment method using the complete sequence of all four adenosine receptors as well as the three intracellular loops (ILs) and the three extracellular loops (EL2) separately [23]. Based on these multiple sequence alignments we calculated the distance of the loop and receptor sequences using the Phylip package and created distance trees that represent the relative similarity of the fragments [24]. The results of the analysis are shown in **Figure 7.** The distance tree placed left of the snake plot represents the similarity of the full receptor sequences. This tree shows that within the adenosine subfamily, the $A_{2A}R$ and $A_{2B}R$ are most similar to each other and that also the A_1R and A_3R are grouped together. A similar tree is observed for IL3, the loop that is thought to be the most influential in G protein coupling [26]. In contrast, the other intra- and extracellular loops show different results. The EL2 is most similar in the $A_{2A}R$ and $A_{2B}R$, however, the A_1R shows the largest distance from the A_3R and is also quite different from the $A_{2A}R$. In EL3, the A_1R resembles the $A_{2A}R$ most, closely followed by the $A_{2B}R$. Also here, the loop of the A_3R resembles the A_1R least.

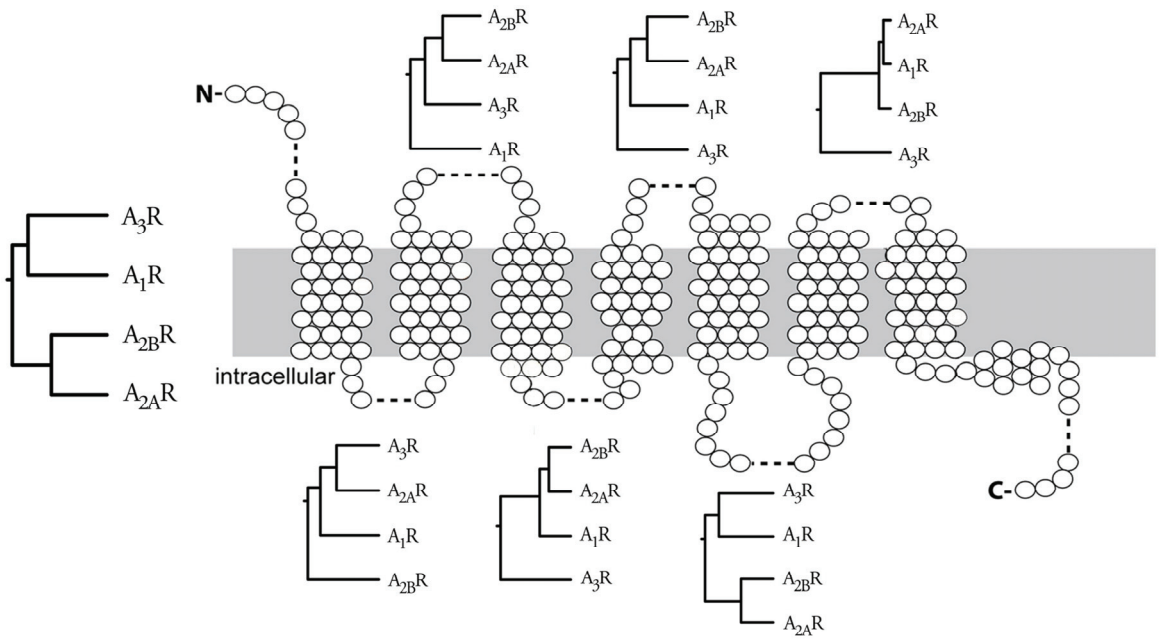

Figure 7. Loop similarity analysis. Multiple sequence alignments were used to create distance trees, representing sequence similarity of the whole protein and the separate loops of the four adenosine receptor subtypes. The distance tree created for the whole protein sequences is shown left of the schematic snake-plot. The trees corresponding to the similarity of each of the three intracellular and the three extracellular loops are positioned next to the loops, indicated in the snake-plot.

DISCUSSION

Over the last decade, the extracellular domains of GPCRs have gained significant interest [5]. Both experimental data and the published crystal structures clearly demonstrate that the extracellular loops are not just involved in cell surface expression and anchoring in the cell membrane, but are active participants in the activation mechanism. Of the adenosine receptors subfamily, we now have access to both inactive and active structures of the $A_{2A}R$ subtype that have provided us with new insights in how the receptor transitions between the two conformational states [3,14,15]. They show that the second and third extracellular loops interact with the bound ligands and are shaping the ligand binding site, indicating a role in binding and recognition of the ligand, but also in initiating receptor activation. However, the extracellular region is highly divergent even within the adenosine receptor subfamily and it is so far unclear to what extent we can extrapolate information obtained from

one receptor to another. We therefore decided to explore both the second and third extracellular loop in another adenosine receptor subtype, the adenosine A_1 receptor.

A positive regulating role of EL2 in adenosine A_1 receptor activation

To investigate the role of the second extracellular loop of the human adenosine A_1 receptor, we made use of an $(Ala)_3$-scan as well as a classical single alanine point mutation method. Many residues were identified to be important for adenosine A_1 receptor activation. Except for a low number of residues that could be mutated without consequences for receptor activation (SAV(150-152), R154, and M162), all alanine mutations caused the receptor to display a decreased activation profile (**Table 1)**. The mutation E170K is the only naturally occurring variant in EL2 that has been described in the Natural Variant (NaVa) database [27], and has been associated with colorectal cancer [28]. Mutating the glutamic acid into the much smaller alanine in our investigation resulted in a 4-fold decrease in agonist potency. The low level of specific binding obtained in the radioligand binding experiments indicates that also antagonist binding was compromised (**Figures 4 and 5**). The mutant receptors that displayed the largest decrease in receptor activity had mutated glycines and a mutated isoleucine, G160A, G163A, and I167A , that showed a 7-fold, 21-fold, and 45-fold decrease in CPA potency, respectively, as well as a large decrease in constitutive activity (**Table 1, Figure 4**). All three mutant receptors also showed low specific binding of [^{3}H]DPCPX in radioligand binding experiments (**Table 2**). Of all amino acids, glycine residues provide the largest flexibility to a protein structure, while alanine provides more constraints to the protein backbone. It therefore appears that EL2 of the A_1R is greatly dependent on the level of flexibility induced by the glycine residues. Also, since none of the mutated residues showed any increased constitutive activity or agonist potency, we conclude from these results that EL2 in the wild-type A_1R acts as a positive regulator of the receptor activation mechanism. It is not only involved in activation of the receptor in response to a ligand, but also in maintaining the level of basal activity that is relatively high for the human A_1R (**Figure 4**). Interestingly, the decrease in constitutive activity and potency did not involve a vast decrease in maximal activation levels (Emax). The mutant receptors are thus still fully functional, but appear to require a higher energy level to change conformational states.

One unique EL2 for each individual receptor?

There has been much speculation of how the second extracellular loop influences GPCR activation. Several reports have described an important role of EL2 in both positive and negative regulation of the activation mechanism [5]. A saturation mutagenesis study on the complement factor 5a receptor (C5aR) revealed many constitutively active receptors. These results led to the conclusion that EL2 might play an unexpected role as a negative regulator of receptor activation [19,20]. Other mutagenesis studies corroborated this suggested role of EL2, like mutagenesis studies of the of the M_1 and M_2 muscarinic acetylcholine receptor (M_1R and M_2R) and a site-directed mutagenesis study on the thrombin receptor that also resulted in several EL2 mutants with increased constitutive activity [9,29,30]. Contrary to these findings, several other EL2 mutagenesis studies did not yield constitutively active mutants, suggesting another role for EL2 [31,32]. Also, a random mutagenesis screen on another subtype of muscarinic acetylcholine receptors, the M_3R, led to the identification of about twenty mutant receptors containing single amino acid changes in EL2 that were inactive in yeast and proved to be important for efficient agonist-induced M_3R activation but not for agonist binding [33]. The apparent contradictory results observed in the muscarinic acetylcholine receptors, suggest that even within closely related subfamilies, the role of EL2 can differ.

Recently, our laboratory conducted a low frequency random mutagenesis screen on the adenosine A_{2B} receptor, a family member of the A_1R. This study revealed a particular “hotspot” of residues in a cysteine-rich region of EL2 that resulted in constitutive activity of the receptor [34]. This implies that also within the small adenosine receptor subfamily, EL2 can adopt a different role in activating the receptor. Where EL2 of the $A_{2B}R$ seems to contain a motif that negatively regulates activation, EL2 of the A_1R appears to act as a positive regulator. This raises questions on how to interpret the recently published crystal structures of the adenosine $A_{2A}R$ in view of the other members of the subfamily and how reliable homology models can be concerning the extracellular loops. EL2 varies greatly in both amino acid sequence and length among the adenosine receptors and also the number of extracellular cysteines is different. The $A_{2A}R$ contains three extracellular cysteines in the loop that are all able to form disulfide bridges that determine the extracellular structure [3,14,15]. The A_1R contains only a single cysteine residue in EL2 that is part of the conserved cysteine bridge with TM3. A loop similarity analysis

we conducted further underlines the individual character of the extracellular loops. Phylogenetic analysis classically groups the $A_{2A}R$ and $A_{2B}R$ subtypes and the A_1R and A_3R subtypes together [35], this is also shown in the distance tree we created for the full receptor sequences in **Figure 7**. A similar similarity tree is observed when comparing the third intracellular loop (IL3) of all four subtypes. This loop is thought to be the key determinant in G protein coupling [26]. The other intra- and extracellular loops however, show a different classification. In EL2 the $A_{2A}R$ and $A_{2B}R$ are still most similar, however, the A_1R is most distant from the A_3R. Of all adenosine receptor subtypes, the A_1R is most similar to the $A_{2B}R$. However, this distance seems to be large enough for the loop to act differently in receptor activation and suggests that structurally the loops are hard to compare.

Involvement of residues W156 and E164 in allosteric modulation

Besides investigating the role of EL2 in activation alone, we also studied its involvement in the enhancing effect of the A_1R allosteric modulator PD81,723. Many GPCRs, including the adenosine A_1 receptor, have been shown to be allosterically modulated by both small molecule ligands and ions [36,37]. In the family of muscarinic acetylcholine receptors (MRs) several residues have been identified that participate in the binding of allosteric ligands [38]. In the M_2R an EDGE motif centrally located in EL2 was shown to be involved in the binding of prototypical MR modulators [9,39]. Also, a phenylalanine in EL2 of the M_4R has been demonstrated to interact with the allosteric agonist LY2033298, whereas it did not influence binding of orthosteric agonists [10].

Of all four adenosine receptor subtypes, the A_1R receptor is the most studied receptor on this subject and several allosteric modulators have been described for this receptor [6,40]. Recently, Narlawar et al. suggested that the allosteric modulator binding site in the A_1R might reside close to or within the second extracellular loop by an approach linking the orthosteric and allosteric site with bivalent ligands and docking studies [8]. Allosteric binding sites can originate by chance during evolution and are therefore likely to be found in a less conserved region. EL2 might indeed be a probable site of allosterism considering its high sequence variability even within subfamilies.

To investigate if one of our EL2 alanine mutant receptors changed the effect on allosteric modulation, we tested the effect of PD81,723, a selective allosteric enhancer of agonist binding and function on the A_1R, on the receptor's potency for CPA. A first functional test on the $(Ala)_3$ mutant receptors revealed that PD81,723 lost its ability to increase CPA potency with mutant WAA(156-158)AAA (W156A), but seemed to increase this effect on mutant receptor MGE(162-164)AAA (**Table 1, Figure 6A**). Subsequent radioligand binding experiments showed that also the increase in CPA affinity by PD81,723 on mutant W156A was lost. In contrast, the single mutant E164A, part of the triple mutant MGE(162-164)AAA, showed an increased effect of PD81,723 on CPA affinity compared to wild type receptor (**Table 2, Figure 6B**). The corresponding position in the A_{2A}R, E161, showed an increase in affinity for the nonxanthine adenosine antagonist CGS 15943 (9-chloro-2-(furyl)[1, 2 , 4]triazolo[1, 5-c]quinazolin-5-amine) (6 fold) when mutated to an alanine but not for other ligands [41]. Mutant E164A in the A_1R showed a decreased specific binding with [^{3}H]DPCPX (60%) and no significant change in CPA affinity (**Table 2**).

The other mutant receptors tested showed responses to PD81,723 comparable to wild-type A_1 receptor. These results imply a role of EL2 in binding and modulation of the allosteric enhancer PD81,723 and confirm the hypothesis that an allosteric binding site might be present in EL2 of the A_1R.

EL3 in A_1R activation

Similar to the mutagenesis study on the EL2 of the A_1R, an alanine scan performed on all 8 amino acids of the third extracellular loop did not yield any mutants that increased the activation profile. All mutant receptors, except H264A, showed a decrease in constitutive activity. Two prolines in EL3, P261 and P266, were found to be most sensitive to the alanine conversion showing a decrease in CPA potency of 2.5- and 3.6-fold compared to wild type respectively (**Table 3)**. Mutant receptor P261Q of the hA_1R has been described in the GPCR Natural Variant (NaVa) database as a naturally occurring polymorphism and arose from the NIH full-length cDNA project [27,42]. No functional data is available for the P261Q mutant receptor and the mutation has so far not been linked to any disease state. However, our results indicate that this proline residue is important for normal function of the A_1R. Proline residues in general are quite rigid amino acids, often introducing a kink in the

backbone. The effect of the proline mutations in our study implies that this rigidity in EL3 is an important feature in receptor activation. Similar to the EL2 mutant receptors, all EL3 alanine mutations were still able to reach the maximal level of activation in response to CPA. Even though the proline mutations affect basal activation levels and agonist potency, they are fully functional in transmitting the activation signal.

High resolution structures of the adenosine A_{2A} receptor subtype were published both in an inactive state with the antagonist ZM241385 and in an active conformation with the agonists UK- 432097, NECA, and adenosine bound to the receptor [3,14,15]. This receptor subtype contains many extracellular cysteine residues that are all capable of forming disulfide linkages. Also in EL3, a disulfide bridge is seen in the structures. The A_1R is the only other adenosine receptor subtype that would be able to form such a disulfide bridge. It is mainly due to this resemblance that in our loop similarity study, the A_1R is closest related to the $A_{2A}R$ (**Figure 7**). The EL3 of the A_3R is far distant in similarity to the other subtypes and most distant from the A_1R, which can be explained by the low number of amino acids present in the A_3R. Scholl et al. performed a study on all nine native cysteines present in the human adenosine A_1 receptor, two of which are located in the third extracellular loop. Neither cysteine residues were shown to influence agonist and antagonist binding. Our study shows that also for A_1R activation, C260 and C263 are not essential and that mutation to an alanine also does not decrease expression levels (**Table 3 and Figure 3**). This suggests that if the A_1R is also able to connect the two cysteines in a disulfide bridge, this is not an essential structural feature for normal function of this receptor. Further research will show whether the possible disulfide bridge is involved in other processes, such as ligand selectivity or ligand directed signaling.

In conclusion, by applying site-directed scanning mutagenesis on the second and third loop of the adenosine A_1 receptor, we identified a number of residues important for receptor activation. Contrary to a putative role for the second extracellular role, as previously described, to act as a dimmer switch for activation, the loop appears to be an activator of the adenosine A_1 receptor. Also, we provided evidence that EL2 accommodates at least part of the allosteric binding site.

The results presented here, provide new insights in the role extracellular loops play in the activation mechanism of class A GPCRs and further emphasize that this role can very well vary between individual receptors, even within subfamilies.

ACKNOWLEDGEMENTS

This research was performed under the auspices of the GPCR Forum, a program funded by the Dutch Top Institute Pharma (project D1-105).

REFERENCES

[1] Fredriksson, R., Lagerstrom, M.C., Lundin, L.G., Schioth, H.B., *Mol Pharmacol* (2003) 63:1256-1272.
[2] Peeters, M.C., van Westen, G.J., Guo, D., Wisse, L.E., Muller, C.E., Beukers, M.W., IJzerman, A.P., *FASEB J* (2011) 25:632-643.
[3] Xu, F., Wu, H., Katritch, V., Han, G.W., Jacobson, K.A., Gao, Z.G., Cherezov, V., Stevens, R.C., *Science* (2011) 332:332-337.
[4] Lane, J.R., Jaakola, V.P., Ijzerman, A.P., *Adv Pharmacol* (2011) 61:1-40.
[5] Peeters, M.C., van Westen, G.J., Li, Q., IJzerman, A.P., *Trends Pharmacol Sci* (2011) 32:35-42.
[6] Fredholm, B.B., IJzerman, A.P., Jacobson, K.A., Linden, J., Muller, C.E., *Pharmacol Rev* (2011) 63:1-34.
[7] Olah, M.E., Jacobson, K.A., Stiles, G.L., *J Biol Chem* (1994) 269:24692-24698.
[8] Narlawar, R., Lane, J.R., Doddareddy, M., Lin, J., Brussee, J., IJzerman, A.P., *J Med Chem* (2010) 53:3028-3037.
[9] Avlani, V.A., Gregory, K.J., Morton, C.J., Parker, M.W., Sexton, P.M., Christopoulos, A., *J Biol Chem* (2007) 282:25677-25686.
[10] Nawaratne, V., Leach, K., Felder, C.C., Sexton, P.M., Christopoulos, A., *J Biol Chem* (2010) 285:19012-19021.
[11] Klco, J., Nikiforovich, G., Baranski, T., *J Biol Chem.* (2006) 281:12010-12019.
[12] Kleinau, G., Jaeschke, H., Mueller, S., Raaka, B.M., Neumann, S., Paschke, R., Krause, G., *Faseb J* (2008) 22:2798-2808.
[13] Lawson, Z., Wheatley, M., *Biochem Soc Trans* (2004) 32:1048-1050.
[14] Lebon, G., Warne, T., Edwards, P.C., Bennett, K., Langmead, C.J., Leslie, A.G., Tate, C.G., *Nature* (2011) 474:521-525.
[15] Jaakola, V.P., Griffith, M.T., Hanson, M.A., Cherezov, V., Chien, E.Y., Lane, J.R., IJzerman, A.P., Stevens, R.C., *Science* (2008) 322:1211-1217.
[16] Brown, A., et al., *Yeast* (2000) 16:11-22.
[17] Beukers, M., van Oppenraaij, J., van der Hoorn, P., Blad, C., den Dulk, H., Brouwer, J., IJzerman, A., *Mol Pharmacol.* (2004) 65:702-710.
[18] Stewart, G.D., Valant, C., Dowell, S.J., Mijaljica, D., Devenish, R.J., Scammells, P.J., Sexton, P.M., Christopoulos, A., *J Pharmacol Exp Ther* (2009) 331:277-286.
[19] Klco, J., Wiegand, C., Narzinski, K., Baranski, T., *Nat Struct Mol Biol.* (2005) 12:320-326.
[20] Massotte, D., Kieffer, B.L., *Nat Struct Mol Biol* (2005) 12:287-288.
[21] Gietz, D., St Jean, A., Woods, R.A., Schiestl, R.H., *Nucleic Acids Res* (1992) 20:1425.
[22] Olesnicky, N.S., Brown, A.J., Dowell, S.J., Casselton, L.A., *Embo J* (1999) 18:2756-2763.
[23] Notredame, C., Higgins, D.G., Heringa, J., *J Mol Biol* (2000) 302:205-217.
[24] Felsenstein, J., PHYLIP (Phylogeny Inference Package) version 3.6, Department of Genome Sciences, University of Washington, Seattle, 2005.

[25] Scholl, D.J., Wells, J.N., *Biochem Pharmacol* (2000) 60:1647-1654.
[26] Olah, M.E., *J Biol Chem* (1997) 272:337-344.
[27] Kazius, J., Wurdinger, K., van Iterson, M., Kok, J., Back, T., IJzerman, A.P., *Hum Mutat* (2008) 29:39-44.
[28] Sjoblom, T., et al., *Science* (2006) 314:268-274.
[29] Goodwin, J.A., Hulme, E.C., Langmead, C.J., Tehan, B.G., *Mol Pharmacol* (2007) 72:1484-1496.
[30] Nanevicz, T., Wang, L., Chen, M., Ishii, M., Coughlin, S.R., *J Biol Chem* (1996) 271:702-706.
[31] Decaillot, F., Befort, K., Filliol, D., Yue, S., Walker, P., Kieffer, B., *Nat Struct Biol.* (2003) 10:629-636.
[32] Parnot, C., Bardin, S., Miserey-Lenkei, S., Guedin, D., Corvol, P., Clauser, E., *Proc Natl Acad Sci USA* (2000) 97:7615-7620.
[33] Scarselli, M., Li, B., Kim, S., Wess, J., *J Biol Chem.* (2007) 282:7385-7396.
[34] Peeters, M.C., Li, Q., Van Westen, G.J., IJzerman, A.P., *Purinergic Signal* (2011) In press.
[35] Fredholm, B.B., IJzerman, A.P., Jacobson, K.A., Klotz, K.N., Linden, J., *Pharmacol Rev* (2001) 53:527-552.
[36] Keov, P., Sexton, P.M., Christopoulos, A., *Neuropharmacology* (2010) 60:24-35.
[37] Bridges, T.M., Lindsley, C.W., *ACS Chem Biol* (2008) 3:530-541.
[38] Digby, G.J., Shirey, J.K., Conn, P.J., *Mol Biosyst* (2010) 6:1345-1354.
[39] Jager, D., et al., *J Biol Chem* (2007) 282:34968-34976.
[40] Baraldi, P.G., Iaconinoto, M.A., Moorman, A.R., Carrion, M.D., Cara, C.L., Preti, D., Lopez, O.C., Fruttarolo, F., Tabrizi, M.A., Romagnoli, R., *Mini Rev Med Chem* (2007) 7:559-569.
[41] Kim, J., Jiang, Q., Glashofer, M., Yehle, S., Wess, J., Jacobson, K., *Mol Pharmacol.* (1995) 49:683-691.
[42] Gerhard, D.S., et al., *Genome Res* (2004) 14:2121-2127.

CHAPTER 7

GENERAL DISCUSSION, FUTURE PERSPECTIVES AND CONCLUSION

The research described in this thesis has provided new insights in the activation mechanism of class A GPCRs and in particular of adenosine receptors. By a variety of mutagenesis approaches and the use of a robust yeast reporter gene system, we identified several regions and amino acid positions that contribute to both agonist responses and constitutive activity of the human adenosine A_1 receptor and the human adenosine A_{2B} receptor. These results reveal new and surprising roles of the extracellular loops in the activation mechanism, greatly contributing to our notion of receptor activation.

In this chapter, I will compare and discuss the knowledge gathered in the separate chapters, providing a view of the results in a broader context.

CONSTITUTIVELY ACTIVE MUTANTS (CAMS) IN THE A_{2B}R

The level of constitutive or basal activity a receptor displays depends on the equilibrium between the inactive (R) and the active state (R*) and the energy required to transition between the two as was originally postulated in the two-state-receptor model [2]. Where it is essential for some signaling pathways to remain largely inactive until a specific time point, e.g. after hormone secretion (for the thyroid stimulating hormone receptor (TSHR)), other GPCRs need to exhibit a high level of activation to constantly keep the signaling pathway 'on', as is the case for the viral chemokine receptors but also for some neurotransmitter GPCRs like the opioid and cannabinoid receptors [3,4,5]. It is believed that all GPCRs, including orphan receptors, show some level of constitutive activity and that this basal activity is essential in normal receptor function [6]. Since constitutive activity is in fact the first step in the receptor activation mechanism, studying mutations that result in an increase or decrease in spontaneous activity can reveal much on how the receptor is activated and which residues are involved in this mechanism.

In Chapter 4, the results of a random mutagenesis study were described where we screened for constitutively active and gain-of-function mutations of the adenosine A_{2B} receptor. The mutated fragment used in this study encompassed transmembrane domains 4 and 5 (TM4, TM5) and the second extracellular loop (EL2), obtained by the two DNA restriction sites KpnI and BglII (**Figure 1**). Previously in our laboratory, the fragment upstream of the KpnI restriction site and the fragment downstream of the BglII restriction site were also submitted to a random mutagenesis screen. Many

of the mutations identified from these screens were published by Beukers et al. in 2004 [7]. The two mutated residues in the first extracellular loop (EL1) that were discussed in Chapter 3 were originally identified from the screen performed on the first part of the receptor, involving the N-terminus, transmembrane domains 1, 2, and 3 (TM1, TM2, TM3), the first and second intracellular loops (IL1, IL2) and the first extracellular loop (EL1) (**Figure 1**).

Now that we have finally screened the full receptor, we can assemble the various findings into a more general picture of which residues are involved in constitutive activity and which positions have a main function in silencing the $A_{2B}R$ in its basal state.

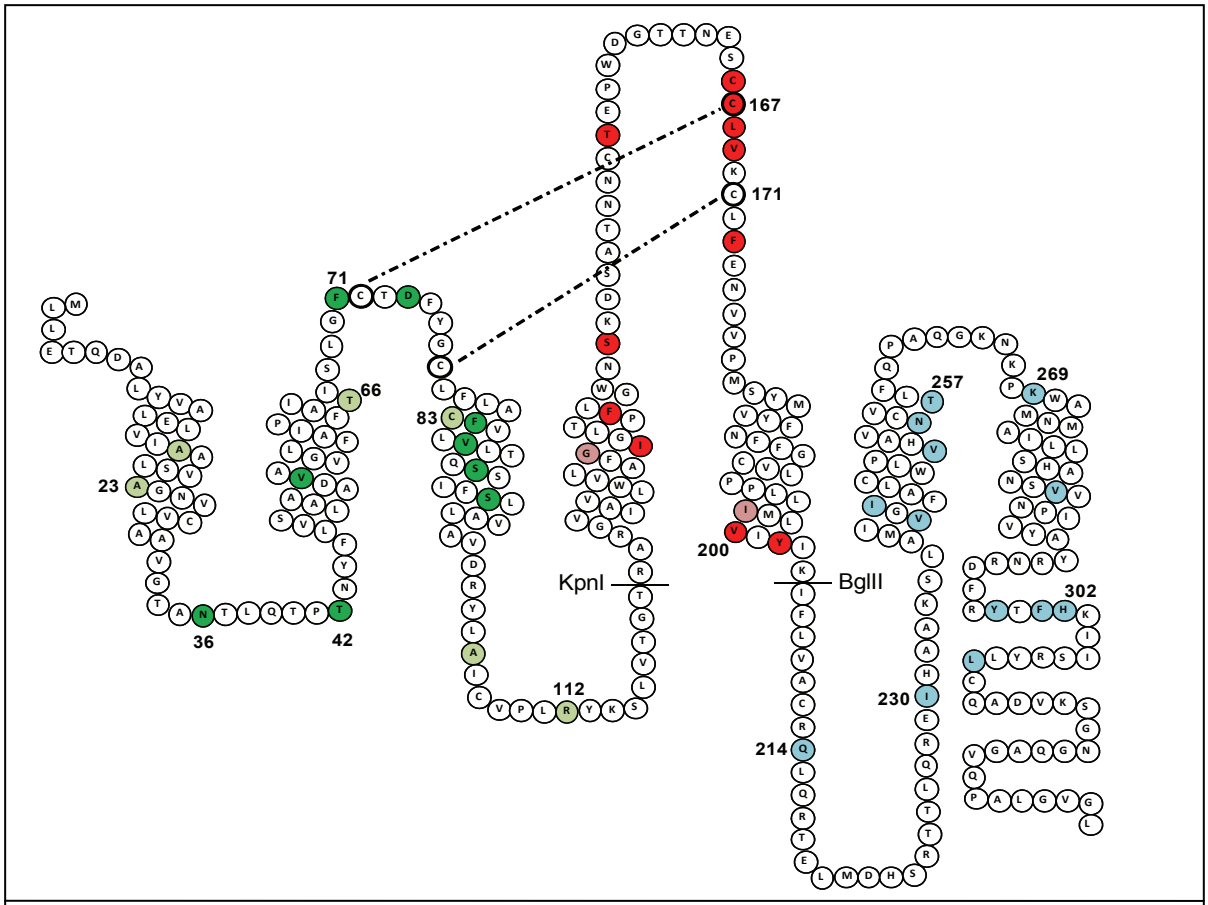

Figure 1. Snake plot of the adenosine $A_{2B}R$. Dotted lines indicate disulfide bridges. The disulfide bridge conserved in many class A GPCRs links C78 and C171. The non-conserved second disulfide bridge between EL1 and EL2, as present in the crystal structure of the adenosine $A_{2A}R$ (PDB: 3EML) and proposed to exist in the $A_{2B}R$ as well, links C72 and C167. The restriction sites *Kpn*I and *Bgl*II that were used to obtain the three fragments for random mutagenesis are in the second and third intracellular loop. Residues that were found mutated in the three separate CAM screens performed on the $A_{2B}R$ are shown in color. Bright red and green residues were found mutated in single and double mutant receptors; light green, red, and blue residues were identified in mutant receptors that contained more than 2 amino acid changes.

From the random mutagenesis screen performed on the first part of the receptor, 12 interesting mutant receptors were identified, 10 of which contained only one or two amino acid changes in the protein. As was discussed in Chapter 4, the screen of the middle fragment of the $A_{2B}R$ rendered 12 different mutant receptors. Of this selection, only one receptor contained three amino acid changes (G135A$^{4.55}$/I197L$^{5.53}$ /Y202N$^{5.58}$), the remaining mutant receptors were single or double mutants. The results of the screen performed on the last part of the receptor showed a different view. Firstly, only three mutant receptors could by identified that displayed constitutive activity. Secondly, all three mutant receptors contained multiple amino acid changes, one receptor even consisted of 7 mutations: Q214L^{IL3}/I230N$^{6.31}$ /V240M$^{6.41}$/V250M$^{6.51}$/N254Y$^{6.55}$/T257S$^{6.58}$/K269stop$^{7.32}$. In **Figure 1**, all the residues identified in the three separate screens are indicated in color; a brighter shade represents residues identified in single or double mutants and the lighter shade represents the residues identified in mutant receptors with more than three amino acid changes. Besides the clusters in TM4 , EL2, and TM5 described in Chapter 4, we now also observe similar series of residues exist in TM3 and TM6.

The relatively low amount of CAMs identified in the $A_{2B}R$ is consistent with the apparent necessity of the receptor to remain silent until high levels of adenosine are reached in stress events [8]. Activation of the receptor has been implicated in autoimmune diseases and inflammatory disorders, such as asthma [9].

Even though the technical set-up in all three screens was chosen such that both constitutively active mutants (CAMs) and gain-of-function mutants would be selected, all the identified mutant receptors displayed an increase in constitutive activity. The levels of constitutive activity of the mutant receptors ranged from a 1.5-fold change (F141L$^{4.61}$, N36D^{IL1}) compared to wild type receptor to an immense increase of 38-fold for mutant receptor G135A$^{4.55}$/I197L$^{5.53}$/Y202N$^{5.58}$.

A comparison between the inactive and active crystal structures of the $A_{2A}R$ suggest that the domains TM6 and TM7 undergo the largest conformational movement upon receptor activation [10,11,12] (**Figure 2**). These domains are clearly important in the activation mechanism and contain several switches needed for G protein activation in many class A GPCRs, such as W6.48 and Y7.53 [13,14]. In our CAM screen, we did identify a number of residues in TM6 that can result in an increase in both constitutive activity and potency when mutated.

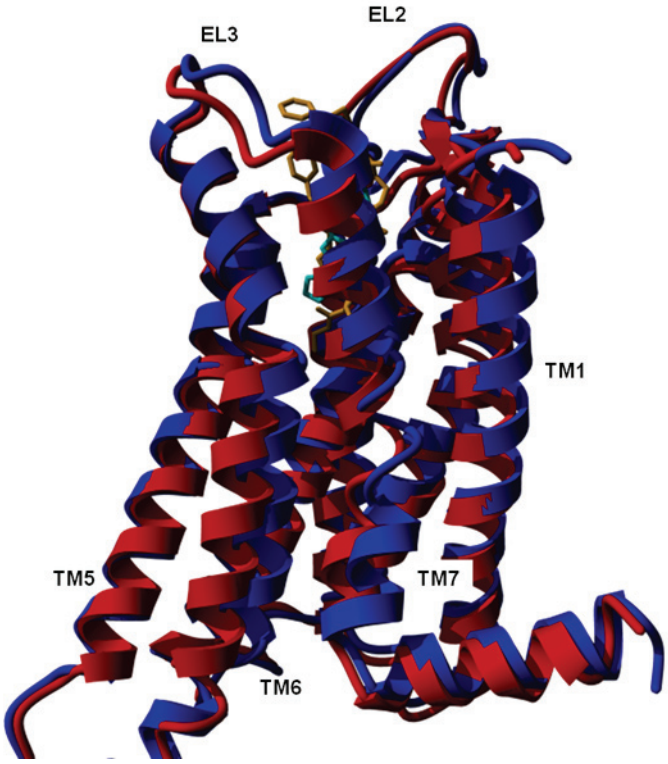

Figure 2. Overlay of the inactive (shown in blue, with the bound antagonist in cyan (PDB:3EML)) and the active structure (shown in red, with the bound agonist in orange (PDB:3QAK)) of the adenosine A_{2A} receptor. The largest movements are observed in TM6 that rotates outwards, and TM7 that shows an inwards movement. The figure was created by the software program YASARA [1].

Also, we identified another prominent switch in receptor activation: Y5.58 (Y197 in the A_{2A}R) at the bottom of TM5. The aromatic side chain displays a large rotameric shift upon activation. While in the inactive structure bound to ZM241385 the conserved $Y197^{5.58}$ is located in between TM3 and TM6, in the agonist-bound forms this residue moves outward allowing TM5 to shift toward TM6. As a result, the intracellular ends of TM5 and TM6 move closer together in the active structures compared to the inactive structure, enabling access of the G protein [10,11,12]. Besides Y5.58, that has been suggested to be involved in disturbing the ionic lock between TM3 and TM6, we did not identify any mutations at the proposed "general" GPCR activation switches such as the DRY-motif at the bottom of TM3 and the toggle-switch residue W6.48 [14].

Another important residue in our mutational analysis was F173 in EL2; mutation to a leucine yielded a large increase in both constitutive activity and potency for the agonist NECA. The corresponding position in the adenosine A_{2A} receptor (F168) is involved in both the binding of the A_{2A}R antagonist ZM241385 and the agonists UK-432097, NECA, and adenosine that were co-crystallized in the published X-ray structures [10,11,12]. Mutant receptor $Q214L^{IL3}$/$I230N^{6.31}$/$V240M^{6.41}$/$V250M^{6.51}$ /$N254Y^{6.55}$/$T257S^{6.58}$/$K269stop^{7.32}$ that was identified in the BglII-stop screen also contained three residues involved in agonist binding: $V250^{6.51}$, $N254^{6.55}$, $T257^{6.58}$ [7,12]. Besides these four residues, all positions identified from the CAM screens are located at distance from the adenosine binding site. This proves that (constitutive) activity of the receptor is not just determined by the ligand binding site or the

intracellular region where the G protein binds to the protein, but that many other regions of the receptor contribute to the activation mechanism. When a mutation disturbs these regions, e.g. by inducing more flexibility, the energy levels necessary for the transition between activation states are lowered, leading to an increased active receptor population reflected by a higher potency for the agonist and increased basal activation.

So far, only a limited number of natural variants have been identified in the $A_{2B}R$ that result in an amino acid change. In the GPCR Natural Variants database, mutations $A35V^{1.60}$, $L96F^{3.43}$, $G137R^{4.57}$, and $K316R^{C\text{-term}}$ are described [15]. None of these residues were identified in the random mutagenesis screens of the $A_{2B}R$.

CAMs IN THE EXTRACELLULAR LOOPS

In both the random mutagenesis screen of the first fragment (ATG-KpnI) and the screen of the second fragment (TM4-EL2-TM5) of the $A_{2B}R$, CAMs were identified in the extracellular region (**Figure 1**). These mutations were not found in combination with mutations in the transmembrane domains, suggesting that the influence of EL2 on receptor activation is at a different level than that of the transmembrane domains.

No CAMs were identified in EL3, even though in the $A_{2A}R$ crystal structure this loop also seems to influence the shape of the ligand binding pocket of both ZM241385 and UK-432097 [10,11]. The structures of the $A_{2A}R$ bound to the much smaller NECA and adenosine do not show this involvement of EL3, indicating that its role is unique for larger ligands such as ZM241385 and UK-432097 [12].

The mutated residues identified in EL2 that cause constitutive activity, are located in a small cluster in a cysteine-rich region of the loop (see also Chapter 4). One of these cysteines (C167 in the $A_{2B}R$) is potentially involved in a non-conserved disulfide bridge with C72 in EL1 (indicated with a dotted line in **Figure 1**). The equivalent positions in the adenosine $A_{2A}R$ are able to form such an additional disulfide bridge as seen from the crystal structures of this receptor [10,11,12]. In these structures another structural feature connects EL1 and EL2; that is an anti-parallel β-sheet (shown with opposite arrows in **Figure 3**). When comparing the inactive structure of the $A_{2A}R$ bound to ZM241385 with the active structures bound to NECA and adenosine, we observe a movement of this region of ca. 2.5 Å parallel to the ligand

binding pocket, implicating the anti-parallel β-sheet in receptor activation. The two mutated residues identified in EL1 of the $A_{2B}R$, F71 and D74, are on either side of C72 and are located within the β-strand in EL1 (Chapter 3). In **Figure 3**, we have mapped our $A_{2B}R$ mutations onto the corresponding positions in the crystal structure of the $A_{2A}R$ according to the sequence alignment. This 3D perspective shows that residues F71 and D74 in EL1 further extend the CAM cluster identified in EL2.

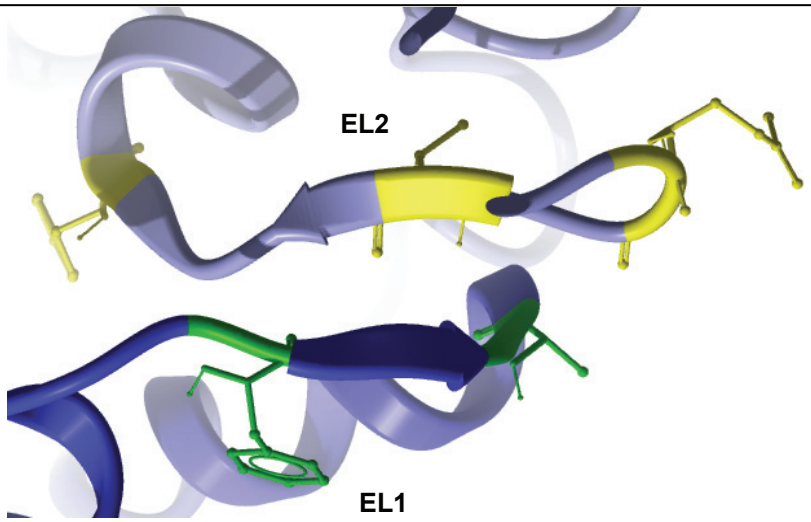


```
EL1:
A2AR    66 ISTGFCAAC 74
A2BR    67 ISLGFCTDF 75

EL2:
A2AR   143 WN-------NCGQPKEGKNHSQGCGEGQVACLFEDVV 172
A2BR   144 WNSKDSATNNCTEPWDGTTNESCC---LVKCLFENVV 177
```

Figure 3. Top view of the adenosine $A_{2A}R$ structure showing the corresponding positions of the CAMs of the $A_{2B}R$ in EL1 (green) and EL2 (yellow) according to the multiple sequence alignment. The figure was created with Molsoft ICM version 3.6-1 h.
In the alignments of EL1 and EL2 of the $A_{2A}R$ and the $A_{2B}R$, the mutated positions of the $A_{2B}R$ are shown in red.

Also, the constitutively active mutants are centered around the anti-parallel β-sheet. Not only does this further confirm our hypothesis that a structural feature linking EL1 to EL2 exists in the $A_{2B}R$ as seen in the $A_{2A}R$ structure, but it also indicates an essential role for the anti-parallel β-sheet and the non-conserved disulfide bridge in $A_{2B}R$ activation. When these residues are mutated, they influence the interaction between the loops, hereby allowing the receptor to display an increase in constitutive activity. However, when the structural conformation is compromised too much, for instance by mutating the hydrophobic and large phenylalanine at position 71 to the small and hydrophilic glycine, activation is completely lost (Chapter 3).

CAMs vs CIMs

In Chapter 4, a random mutagenesis screen of the $A_{2B}R$ was described containing mutations in the fragment TM4-EL2-TM5, where mutant receptors were selected that displayed constitutive activity (CAMs) or increased potency to the agonist NECA. In Chapter 5, we made use of the same mutagenic library, but selected for a different phenotype, namely constitutively **in**active mutant receptors (CIMs). To our knowledge, we are the first to examine a GPCR for both activating and inactivating mutations using an unbiased random mutagenesis approach. We used the same random mutagenesis library and the same host yeast strain (MMY24) without any additional modifications, which allows for a direct comparison of CAMs and CIMs. This was unique too, as we were able to design a screening method using only slight changes in the selection procedure to discriminate between different activation phenotypes.

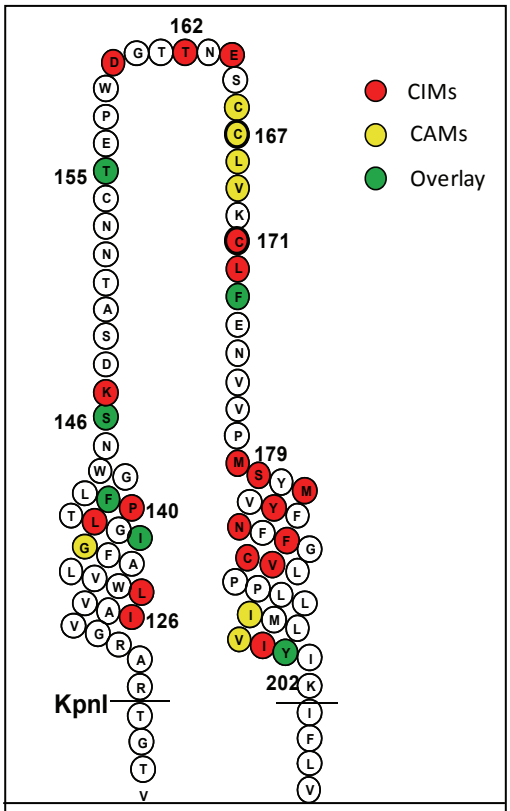

Figure 4. Snake plot view of the $A_{2B}R$ fragment (TM4-EL2-TM5) used in both the CIM screen and the CAM screen. In red all the residues identified from the CIM screen are indicated, in yellow the CAM residues are shown and the green residues were found in both screens.

The first observed difference between the CAM and the CIM screen are the number of mutated receptors identified. In the CAM screen we identified 11 different single and double mutant receptors and one triple mutant that fulfilled the requirements of the selection procedure. The CIM screen rendered a larger amount of mutant receptors, of which we chose the 22 single and double mutants to investigate further. Also, where in the CAM screen we did not identify any combinations of mutated residues in EL2 and either of the two transmembrane domains, several of those were found in the CIM screen. Especially mutations in TM5 were often combined with a mutation in EL2 within one mutant receptor. This was the case in six different mutant receptors, four of which contained a mutation of C190$^{5.46}$, indicating an important role for this residue in receptor activation. In the inactive structure of the adenosine $A_{2A}R$, the corresponding position C185$^{5.46}$ is involved in a

Van der Waals interaction with residue I135$^{4.56}$. This latter residue was also identified in our CIM screen: I136L$^{4.56}$. Also, a hydrogen bond exists between the side chain of Q89$^{3.37}$ with the backbone of C185$^{5.46}$ [10]. In the active structures, a rotameric shift of the side chain of C185$^{5.46}$ occurs which in turn causes the movement of V186$^{5.47}$ and ultimately a shift of H250$^{6.52}$ by 2 Å into the ligand binding pocket. As a result, the hydrogen bond between Q89$^{3.37}$ and C185$^{5.46}$ is broken [11,12]. The observed shift of C185$^{5.46}$ is more pronounced in the structures where NECA and adenosine are bound compared to the UK-432097 bound structure. It needs to be noted though that in the structures with NECA and adenosine, the stabilizing mutation Q89A$^{3.37}$ was introduced [12].

In **Figure 4**, all the positions identified in both screens are indicated, with CAMs in red and CIMs in yellow. In Chapter 4, we noted 3 distinct clusters of the CAMs identified from the screen. The clusters at the top of TM4 and the bottom of TM5 seem also susceptible for inactivating mutations and three of the residues in these regions were found in both screens (I136$^{4.56}$, F141$^{4.61}$, and Y202$^{5.58}$). It has to be noted though, that the mutation of Y202 in the CAM (Y202S$^{5.58}$) is the same as in the CIM screen (F141S$^{4.61}$/ Y202S$^{5.58}$). However, in the CIM mutant the mutated residue is found in combination with a mutation of the phenylalanine at position 141$^{4.61}$ that is therefore presumably the responsible mutation for the observed phenotype, i.e. a 10-fold decrease in constitutive activity and a complete loss of the ability to be activated by the agonist NECA (Chapter 5). In the crystal structures of the A_{2A}R, a shift of the side chain of this amino acid (a methionine in A_{2A}R) is observed upon activation, which might facilitate the movement of EL2 (*vide infra*).

The third CAM cluster in EL2 remains a full CAM cluster and no mutations were identified in this region that resulted in a decrease in agonist potency. Besides a specific CAM region, we also identified a typical CIM region at the top of TM5, in which only residues were shown as mutated to cause a decrease in receptor activation. Of all CIM receptors identified, only mutant M182L$^{5.38}$/N186D$^{5.42}$ is likely involved in agonist binding, as the corresponding positions in the A_{2A}R directly interact with adenosine in the crystal structure [12]. The cytoplasmic half of TM5 undergoes a inward movement towards TM6 upon activation resulting from a 4 Å shift of C185$^{5.46}$ that is accompanied by a rotameric switch of the tyrosine at position 5.58 (Y202 in the A_{2B}R). The upper part of TM5 remains overall in position when the

receptor is in the active or inactive state [11,12]. Maintaining the position of the top half of TM5 might be essential to facilitate the movements of the bottom half of TM5 and TM6 and TM7. This could be the main reason that mutations in this region result in decreased receptor activation or even complete loss of the signaling ability. The vasopressin V2 receptor is perhaps the best known receptor in which inactivating mutations are responsible to cause disease. Over 100 missense mutations have been identified that are involved in diabetes insipidus and also here, many mutated residues are located at the top of TM5, indicating that this region might be an important area in other class A GPCRs as well [16].

As mentioned above, several of the residues identified from the activation screen were found again in the inactivating screen (indicated in green in **Figure 4**). Position F141$^{4.61}$ for instance, was found mutated to a tyrosine and a serine in the CIM screen, but caused a large increase in NECA potency when mutated into a leucine. An isoleucine at position 136$^{4.56}$ was found to decrease NECA potency when mutated to a leucine, however, when mutated to a threonine it resulted in an increased potency for NECA. This emphasizes that even subtle changes can lead to large effects in receptor function that are not necessarily caused by a direct intervention with the ligand binding site or G protein coupling.

EXTRACELLULAR LOOPS…HOW DIFFERENT CAN THEY BE?

In Chapter 2, an overview was given of the extracellular loops as seen in the crystal structures of the five class A GPCRs that were available in 2010: rhodopsin, β_1-adrenergic receptor, β_2-adrenergic receptor, adenosine A_{2A} receptor, and the chemokine receptor CXCR4 [10,17,18,19,20]. A striking outcome of this comparison was that the extracellular loops show large differences in structure. Especially EL2 was completely different in each known receptor structure. Since the publication of this review, the crystal structures of two new receptors were elucidated: the dopamine D3 receptor and the histamine H1 receptor [21,22]. These structures showed yet again a different structural organization of the extracellular loops. The dopamine D3 receptor structure is perhaps most similar to the adenosine A_{2A} receptor structure, with EL2 bending towards EL1 and an additional disulfide bridge being present within EL3. However, no other non-conserved disulfide bridges are observed and EL3 seems to be more distant from the other two extracellular loops,

bending strongly outwards and not participating in the ligand binding pocket. Also, no specific structural features in EL2 such as the anti-parallel β-sheet in the $A_{2A}R$ or a helical structure in the β_1-adrenergic and β_2-adrenergic receptor are present in the dopamine D3 receptor structure. Interestingly, the newest crystal structures of the $A_{2A}R$ with NECA and adenosine co-crystallized now also appear to contain a helical structure in EL2, where in both the ZM241385 and the UK-432097 bound crystals, no structure could be determined [10,11,12].

With now seven known class A GPCR structures and seven different extracellular conformations, we can only expect to see many more differences in structural arrangements in crystal structures that will be elucidated in the future. So, how different can the extracellular loops be? Will they also differ within subfamilies that show high sequence similarity and are able to be activated by the same endogenous ligands? The mutational analysis of the extracellular loops discussed in this thesis and especially the results shown in Chapter 6 would indicate that this might actually be the case. An indication for this is readily provided in the sequence analysis shown in Figure 8 of Chapter 6. In this analysis, the sequences of the loops of all four adenosine receptors were aligned and distance trees were formed based on the alignment score. When we create such a tree for the alignments of the whole protein sequences, the distance tree is as previously reported in literature, with the $A_{2A}R$ and $A_{2B}R$ subtypes and the A_1R and A_3R subtypes grouped together [23]. **Figure 5** shows the trees of the whole protein alignment and of the alignments of the three extracellular loops.

All three extracellular loops show a different distance tree compared to the tree formed based on the whole protein sequence. Both in EL1 and EL2, the $A_{2A}R$ and $A_{2B}R$ are still closest related, however, the A_1R is not grouped together with the A_3R anymore. In Chapters 3, 4, and 5, we have discussed the mutation data of the $A_{2B}R$ in view of the only available crystal structure of the adenosine subfamily, the $A_{2A}R$. The $A_{2A}R$ and the $A_{2B}R$ are the closest related family members within the subfamily, and also their extracellular loops are closely related (**Figure 5**). However, it is most likely that these two receptors also differ in structure at the extracellular surface. For instance, not all the disulfide bridges formed in the $A_{2A}R$ are possible in the $A_{2B}R$ and the length of both EL2 and EL3 differs as well. Using the $A_{2A}R$ crystal structure to explain mutations in EL2 in other adenosine subtypes may be problematic, as is demonstrated by the results of the alanine scan on EL2 of the A_1R described in

Chapter 6. Where we identified a “hot spot” for CAMs in EL2 of the adenosine $A_{2B}R$ that is likely to act as a negative regulator for receptor activation, EL2 in the A_1R appears to have a more activating role. Almost all alanine conversions induced in the loop resulted in a decreased receptor activation profile. A similar difference in function of the second extracellular loop appears to be present within the muscarinic acetylcholine receptors (MR). Mutagenesis studies on the M_1R and M_2R resulted in several EL2 mutations that showed increased activity, while a random mutagenesis screen on the M_3R yielded many inactivating mutations [24,25,26].

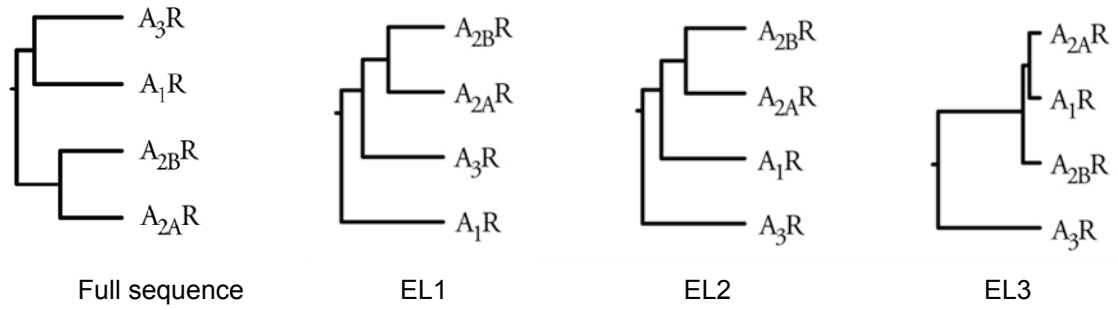

	Full sequence				EL1				EL2				EL3			
	A_1R	$A_{2A}R$	$A_{2B}R$	A_3R	A_1R	$A_{2A}R$	$A_{2B}R$	A_3R	A_1R	$A_{2A}R$	$A_{2B}R$	A_3R	A_1R	$A_{2A}R$	$A_{2B}R$	A_3R
A_1R	0.0	0.9	1.0	0.8	0.0	2.5	1.2	1.5	0.0	2.0	1.7	2.3	0.0	0.8	1.1	36
$A_{2A}R$	0.9	0.0	0.6	1.2	2.5	0.0	0.8	2.4	2.0	0.0	1.3	3.2	0.8	0.0	3.0	5.9
$A_{2B}R$	1.0	0.6	0.0	1.2	1.6	0.8	0.0	0.9	1.7	1.3	0.0	1.9	1.1	3.0	0.0	12
A_3R	0.8	1.1	1.2	0.0	1.5	2.4	0.9	0.0	2.3	3.2	1.9	0.0	36	5.9	12	0.0

Figure 5. Loop similarity analysis. Multiple sequence alignments were used to create distance trees, representing sequence similarity of the whole protein and the separate loops of the four adenosine receptor subtypes. The distance tree created for the whole protein sequences and the trees corresponding to the similarity of each of the three extracellular loops are shown. Below the distance trees the alignment score tables are shown on which the distance trees were based. The alignment scores were calculated using the Phylip package.

FUTURE PERSPECTIVES

Thermostability and CIMs

Since the release of the first crystal structure of a human class A GPCR in 2007, that of the β_2 adrenergic receptor, many more structures have followed [10,11,12,17,18,19,20,21,22,27,28,29,30]. However, this does not mean that we have solved all the challenges involved in crystallizing membrane proteins. All the receptors crystallized so far (except for opsin) have been greatly modified to obtain the high quality crystals needed to elucidate their structures. The two main successful approaches so far include: i) insertion of a T4 lysozyme at the intracellular part of the receptor and ii) introducing mutations that increase the stability of the receptor outside of the cell membrane [31]. These “bio-stable” mutations are numerous and often involve mutations of residues known to be important in receptor activation and structure. Also, the search for such stabilizing mutations is laborious and involves manually scanning the entire receptor sequence.

Applying an unbiased screening method, like the yeast growth screens discussed in this thesis, can contribute greatly to this particular challenge. Since receptors with a decreased activation profile tend to be more stable than wild type or constitutively active receptors [32,33], the newly developed CIM screen would be particularly useful (Chapter 5). By using a random mutagenesis approach where mutations are introduced in low frequency in combination with the described screening method, interesting mutations can be identified in an unbiased fashion that would otherwise not have been found easily in more biased approaches such as a typical alanine scan. In short: let nature do the work instead of the scientist. As shown in Chapter 5, the mutant receptors that are identified using this method contain limited receptor changes that are mostly outside of the ligand binding and G protein coupling regions and are often still able to be activated by an agonist, indicating that the receptors are still very much functional.

We could take this even one step further and also employ yeast screening to directly identify mutant receptors that are more stable when isolated from their membrane environment. Increasing the thermal stability of a receptor has proved to be beneficial in keeping the isolated receptor stable enough for crystallization purposes [34,35]. Again, it is very laborious to identify mutations that improve thermal stability. So far, the receptor has to be (partially) isolated to confirm that the designed mutant receptor

indeed increases stability. A screening method that quickly identifies mutations to possessing this phenotype would dramatically reduce the efforts needed to reach the actual crystallization stage. One method would be to submit the yeast cells after transformation with a mutagenic library to a heat shock that will destroy the wild type GPCR of interest. Only yeast cells containing mutant receptors that can resist this heat shock are able to grow on the selection plates. The major challenge in this procedure is to develop a heat shock protocol in which the wild type GPCR is greatly compromised, but that the host is able to endure. Efforts to develop and optimize such a screen are currently undertaken in our laboratory and the preliminary results are promising.

"Full-family" Crystallization

Earlier in this chapter, I raised the following question: How different in structure can the extracellular loops be? To get an answer to at least part of this question more class A GPCR structures would need to be elucidated, ideally of all members belonging to one subfamily. The adenosine receptor subfamily would be an exceptionally good candidate. Even though the subfamily consists of only four subtypes, they all respond differently to the endogenous ligand adenosine and even signal differently upon activation by this agonist. Also, all four receptors now have their own designed set of ligands, both orthosteric and allosteric (for A_1R and A_3R), that are highly selective for that subtype [36]. Furthermore, their extracellular domains are highly divergent in sequence and also in length in the case of the second and third extracellular loops. Especially the A_3R seems to be quite distant from the other three subtypes, even when compared to the A_1R that appears closely related at first sight (**Figure 5**). Crystallizing this particular adenosine receptor would be of great interest, not in the least since a number of allosteric ligands have been identified for this receptor [36,37]. So far, no GPCR structures have been elucidated yet with an allosteric modulator bound. And while mutagenesis studies and the use of bivalent ligands have given us clues to where allosteric binding sites might be located, an exact binding pocket has yet to be determined [26,38] (also Chapter 6).

Besides the adenosine subtypes, the class A GPCR superfamily contains more small receptor subfamilies that despite high sequence similarity displays different activation profiles. The muscarinic acetylcholine receptors (MRs), for instance, exist in five different subtypes of which the M_1R, the M_3R and the M_5R couple to G_q proteins

while the subtypes M_2R and M_4R transmit their signal through G_i proteins [39]. Much mutagenesis data is available for this receptor subfamily, including information that suggests specific residues that could be involved in the allosteric binding site [26,40,41,42].

Also the family of histamine receptors would be an attractive candidate for full-family crystallization. This subfamily consists of four family members, coupling either to G_q, G_s, or G_i proteins resulting in a wide variety of responses. Their involvement in immune regulation has made them interesting drug targets [43]. One of the family members, the histamine H_1 receptor, has recently been crystallized by Shimamura et al. [22]. Gaining thorough structural insights would help to explain the mechanisms through which drugs initiate their desirable effects and adverse reactions.

Ligand directed signaling and activation states

In recent years, it has become clear that receptors do not follow a linear sequential process of activation. Different ligands are able to stabilize different conformational states of the receptor, potentially resulting in different intracellular signaling that does not necessarily include coupling to a G protein [44,45]. Several “biased ligands” that show a preference for one particular signaling pathway have been identified for various GPCRs, including 5-HT_2 serotonin receptors, adrenergic receptors, dopamine receptors and opioid receptors [46]. Biased signaling has also been observed for the adenosine receptor subfamily [47]. It is more than likely that in the activation of these different signaling pathways, different activation mechanisms and different receptor residues are involved. Furthermore, ligands that cause activation of the same pathway as the endogenous ligand could stabilize the active conformations differently. An indication of this has been presented in Chapters 3 and 4, in which we subjected a selection of mutant receptors to the non-ribose agonist BAY60-6583. This structurally distinct ligand showed no changes in activation response compared to NECA on mutations present in EL1, whereas BAY60-6583’s potency was affected by mutations in EL2. Therefore, it would be of great interest to investigate the effect of the mutations described in this thesis on a wide variety of ligands, including the endogenous agonist adenosine. In the studies on the $A_{2B}R$ described in this thesis, we made use of the more potent adenosine derivative NECA as it is more convenient in functional in vitro studies considering the low affinity and the metabolic instability of adenosine. The only difference between NECA and adenosine is an altered 5’

position on the ribose moiety, however, this addition leads to a substantial increase in potency for the A_{2B} receptor [48]. It would be highly informative to investigate which residues might be involved in this improvement in potency. This might also provide insights in the origin of the low affinity the A_{2B}R has for adenosine compared to the other subtypes.

Post-translational modifications

In this thesis, we did not go into detail concerning a particular topic in protein research; the post-translational modifications a protein can undergo. Nonetheless, these modifications can also contribute to receptor activation. EL2 is often the site for glycosylation; over 32% of class A GPCRs possess at least one consensus N-glycosylation site in the second extracellular loop [49]. Glycosylation may play a role in cell surface expression rather than ligand binding or activation as shown for the vasopressin 1a receptor [50]. The adenosine receptors all contain at least one possible glycosylation site. In the adenosine A_{2B} receptor these are $N153^{EL2}$ and $N163^{EL2}$; neither positions have been identified in the screens described in this thesis (Chapters 4 and 5). In the adenosine A_1 receptor a possible site for glycosylation is located at residue $N159^{EL2}$ (http://www.gpcr.org/7tm/). Mutating this residue to an alanine resulted in a 4-fold decrease in potency for the agonist NECA but this mutant receptor could still reach maximal activation levels (Chapter 6).

OVERALL CONCLUSION

The research described in this thesis demonstrates intricate details of GPCR activation. Through evolution, GPCRs have evolved in many different fine-tuned subtypes, all with their own sets of ligands, levels of constitutive activity and transmitted signals. Even though all 800 subtypes of GPCRs in humans look alike, not two receptors behave the same. Originally, it was thought that mainly two domains determine the activation profile of each receptor, i.e. the ligand binding site and the domain responsible for G protein coupling. That this view is over-simplified is clearly demonstrated in this thesis, especially regarding the extracellular loops. With each receptor structure that has been elucidated so far, a different extracellular structural arrangement is seen. Together with the experimental data that has become

available over the last decade, including the results presented here, we conclude that the extracellular domains are certainly not just anchors to maintain the receptor in the membrane but active participants in the activation mechanism defining each unique receptor.

REFERENCES

[1] Krieger, E., Koraimann, G., Vriend, G., *Proteins* (2002) 47:393-402.
[2] Leff, P., *Trends Pharmacol Sci* (1995) 16:89-97.
[3] Kobilka, B.K., Deupi, X., *Trends Pharmacol Sci* (2007) 28:397-406.
[4] Seifert, R., Wenzel-Seifert, K., *Naunyn Schmiedebergs Arch Pharmacol* (2002) 366:381-416.
[5] Vischer, H.F., Hulshof, J.W., de Esch, I.J., Smit, M.J., Leurs, R., *Ernst Schering Found Symp Proc* (2006) 187-209.
[6] Bond, R.A., IJzerman, A.P., *Trends Pharmacol Sci* (2006) 27:92-96.
[7] Beukers, M., van Oppenraaij, J., van der Hoorn, P., Blad, C., den Dulk, H., Brouwer, J., IJzerman, A., *Mol Pharmacol.* (2004) 65:702-710.
[8] Fredholm, B.B., *Cell Death Differ* (2007) 14:1315-1323.
[9] Wilson, C.N., *Br J Pharmacol* (2008) 155:475-486.
[10] Jaakola, V.P., Griffith, M.T., Hanson, M.A., Cherezov, V., Chien, E.Y., Lane, J.R., IJzerman, A.P., Stevens, R.C., *Science* (2008) 322:1211-1217.
[11] Xu, F., Wu, H., Katritch, V., Han, G.W., Jacobson, K.A., Gao, Z.G., Cherezov, V., Stevens, R.C., *Science* (2011) 332(6027):322-7.
[12] Lebon, G., Warne, T., Edwards, P.C., Bennett, K., Langmead, C.J., Leslie, A.G., Tate, C.G., *Nature* (2011) 474:521-525.
[13] Nygaard, R., Frimurer, T.M., Holst, B., Rosenkilde, M.M., Schwartz, T.W., *Trends Pharmacol Sci* (2009) 30:249-259.
[14] Ahuja, S., Smith, S.O., *Trends Pharmacol Sci* (2009) 30:494-502.
[15] Kazius, J., Wurdinger, K., van Iterson, M., Kok, J., Back, T., IJzerman, A.P., *Hum Mutat* (2008) 29:39-44.
[16] Schoneberg, T., Schulz, A., Biebermann, H., Hermsdorf, T., Rompler, H., Sangkuhl, K., *Pharmacol Ther* (2004) 104:173-206.
[17] Wu, B., et al., *Science* (2010) 330:1066-1071.
[18] Palczewski, K., et al., *Science* (2000) 289:739-745.
[19] Warne, T., Serrano-Vega, M.J., Baker, J.G., Moukhametzianov, R., Edwards, P.C., Henderson, R., Leslie, A.G., Tate, C.G., Schertler, G.F., *Nature* (2008) 454:486-491.
[20] Rosenbaum, D.M., et al., *Science* (2007) 318:1266-1273.
[21] Chien, E.Y., et al., *Science* (2010) 330:1091-1095.
[22] Shimamura, T., et al., *Nature* (2011) 475:65-70.
[23] Fredholm, B.B., IJzerman, A.P., Jacobson, K.A., Klotz, K.N., Linden, J., *Pharmacol Rev* (2001) 53:527-552.
[24] Goodwin, J.A., Hulme, E.C., Langmead, C.J., Tehan, B.G., *Mol Pharmacol* (2007) 72:1484-1496.
[25] Scarselli, M., Li, B., Kim, S., Wess, J., *J Biol Chem.* (2007) 282:7385-7396.
[26] Avlani, V.A., Gregory, K.J., Morton, C.J., Parker, M.W., Sexton, P.M., Christopoulos, A., *J Biol Chem* (2007) 282:25677-25686.
[27] Murakami, M., Kouyama, T., *Nature* (2008) 453:363-367.
[28] Cherezov, V., et al., *Science* (2007) 318(5854):1258-65.
[29] Rasmussen, S.G., et al., *Nature* (2011) 469:175-180.
[30] Rasmussen, S.G., et al., *Nature* (2007) 450:383-387.
[31] Jaakola, V.P., IJzerman, A.P., *Curr Opin Struct Biol* (2010) 20:1-14.
[32] Kobilka, B., Schertler, G.F., *Trends Pharmacol Sci* (2008) 29:79-83.
[33] Gether, U., Ballesteros, J.A., Seifert, R., Sanders-Bush, E., Weinstein, H., Kobilka, B.K., *J Biol Chem* (1997) 272:2587-2590.
[34] Serrano-Vega, M.J., Magnani, F., Shibata, Y., Tate, C.G., *Proc Natl Acad Sci U S A* (2008) 105:877-882.

[35] Standfuss, J., Xie, G., Edwards, P.C., Burghammer, M., Oprian, D.D., Schertler, G.F., *J Mol Biol* (2007) 372:1179-1188.
[36] Fredholm, B.B., IJzerman, A.P., Jacobson, K.A., Linden, J., Muller, C.E., *Pharmacol Rev* (2011) 63:1-34.
[37] Muller, C.E., *Curr Top Med Chem* (2003) 3:445-462.
[38] Narlawar, R., Lane, J.R., Doddareddy, M., Lin, J., Brussee, J., IJzerman, A.P., *J Med Chem* (2010) 53:3028-3037.
[39] Brown, D.A., *J Mol Neurosci* (2010) 41:340-346.
[40] Gregory, K.J., Hall, N.E., Tobin, A.B., Sexton, P.M., Christopoulos, A., *J Biol Chem* (2010) 285:7459-7474.
[41] Jager, D., et al., *J Biol Chem* (2007) 282:34968-34976.
[42] Nawaratne, V., Leach, K., Felder, C.C., Sexton, P.M., Christopoulos, A., *J Biol Chem* (2010) 285:19012-19021.
[43] Hill, S.J., et al., Histamine receptors, IUPHAR database (IUPHAR-DB), 2008.
[44] Kenakin, T., *Trends Pharmacol Sci* (2007) 28:407-415.
[45] Zheng, H., Loh, H.H., Law, P.Y., *IUBMB Life* (2010) 62:112-119.
[46] Urban, J.D., et al., *J Pharmacol Exp Ther* (2007) 320:1-13.
[47] Verzijl, D., Ijzerman, A.P., *Purinergic Signal* (2011).
[48] de Zwart, M., Link, R., von Frijtag Drabbe Kunzel, J.K., Cristalli, G., Jacobson, K.A., Townsend-Nicholson, A., AP, I.J., *Nucleosides Nucleotides* (1998) 17:969-985.
[49] Conner, M., Hawtin, S.R., Simms, J., Wootten, D.L., Lawson, Z., Conner, A.C., Parslow, R.A., Wheatley, M., *J Biol Chem* (2007) 282:17405-17412.
[50] Hawtin, S.R., Davies, A.R., Matthews, G., Wheatley, M., *Biochem J* (2001) 357:73-81.

SUMMARY

The quest for the exact activation mechanism of GPCRs is still very much ongoing. With each new discovery in the GPCR research field, it becomes more evident how very complex these proteins work. Even though the number of elucidated structures are increasing fast and many questions about what a receptor looks like and how it functions can be answered more confidently, even more new questions have arisen. The research in this thesis has aimed to contribute an important part of the puzzle and answer a few of these new questions.

In **Chapter 1**, subjects that are being discussed in this thesis were introduced. Main themes, like mutagenesis, constitutive activity and the S. cerevisae system received most attention in this chapter. The research described in this thesis has focused most on the extracellular loops of GPCRs and their role in the activation mechanism. We therefore devoted **Chapter 2** to an elaborate description of what we have learned so far about the role of the extracellular loops using recent literature as well as the crystal structures that were available at that time.

In **Chapter 3**, the first extracellular loop (EL1) of the adenosine A_{2B} receptor ($A_{2B}R$) was investigated. From a random mutagenesis screen in a S. cerevisiae yeast expression model using the first part of the receptor, we discovered a mutant receptor with two amino acid changes in EL1: F71L and D74G. Thorough mutational and pharmacological analysis of these two positions taught us that this part of the receptor was essential in activation of the $A_{2B}R$. At position 71 the property of hydrophobicity played an important role, while at position 74 hydrophilicity was key. The elucidation of the crystal structure of the adenosine A_{2A} receptor greatly helped us in explaining these results. The two positions appear to reside at the edges of a β-strand in EL1 that can form a sheet with the second extracellular loop (EL2). The properties of residues 71 and 74 are essential in maintaining this very important three-dimensional protein structure.

In **Chapter 4**, we applied a similar random mutagenesis screen for an increased activation profile as was described in Chapter 3, now using the second part of the $A_{2B}R$ encompassing transmembrane domain 4 (TM4), the second extracellular loop (EL2), and transmembrane domain 5 (TM5). The results revealed three “hotspots” important for constitutive activity as well as agonist potency. The clusters of amino

acids appear responsible for maintaining the subtle equilibrium that exist between the active conformation R^* and the inactive conformation R of the receptor. These residues are not necessarily directly involved in either ligand binding or G protein coupling.

After screening for increased active mutant receptors, we also wanted to investigate mutations that result in deactivation of the receptor in **Chapter 5**. For this purpose, we developed a new screening method using the same S. cerevisiae system, the MMY24 strain, that allowed us to specifically select for this inactive phenotype. In order to expand on the knowledge obtained in Chapter 4, we again used the mutated library of the $A_{2B}R$ in which random mutations were introduced in the fragment encompassing TM4, EL2, and TM5. The mutated receptors that were identified from the screen all showed a decrease in both constitutive activity as well as agonist potency. A particular important region located at the extracellular half of TM5 was discovered with $C190^{5.46}$ as a key player that is important in facilitating the conformational changes in the process of receptor activation. A comparison with the data obtained in Chapter 4 showed that a cysteine-rich cluster in EL2 acts as a negative regulator of activation, keeping the receptor silent, whereas the cluster at the top of TM5, only several residues downstream in the receptor, acts in an opposite way.

In **Chapter 6**, we investigated another subtype of the adenosine receptor subfamily; the adenosine A_1 receptor (A_1R). The role in activation of the second and third extracellular loop (EL2 and EL3) was examined by means of a triple alanine scan (Ala_3-scan) and a singular alanine scan (Ala-scan). Many residues in both loops proved important for A_1R function, all influencing receptor activation negatively when mutated. Especially EL2 appears to act as a positive regulator in receptor activation. This is contradictory to the role of the motif identified in EL2 of the $A_{2B}R$ that appears to have an opposite role. Furthermore, we identified two residues in EL2, a tryptophan and a glutamate, that affect the influence of the allosteric modulator PD81,723.

The research described in the previous chapters was brought together in a general discussion in **Chapter 7**. By combining all the results and conclusions of the individual chapters, we obtained a more complete view of how adenosine receptors can be activated. Also, this chapter provides future perspectives based on these final conclusions.

SAMENVATTING

De zoektocht naar het exacte activatiemechanisme van GPCRs is nog altijd in volle gang. Met elke nieuwe ontdekking in het GPCR onderzoeksveld wordt het steeds duidelijker hoe enorm complex deze eiwitten functioneren. Het aantal kristalstructuren van GPCRs neemt snel toe en deze hebben al veel vragen kunnen beantwoorden over hoe receptoren eruit zien en hoe ze werken, maar hebben minstens zoveel nieuwe vragen opgeroepen. Het doel van het onderzoek dat wordt beschreven in dit proefschrift was om bij te dragen aan het oplossen van de activatie-puzzel en een deel van deze nieuwe vragen te beantwoorden .

In **Hoofdstuk 1** introduceren we onderwerpen die aan de orde komen in dit proefschrift. De nadruk in dit hoofdstuk ligt vooral op hoofdthema's als mutagenese, constitutieve activiteit en het S. cerevisiae systeem. Aangezien het onderzoek in dit proefschrift zich vooral richtte op de extracellulaire loops van GPCRs en hun rol in receptoractivatie, is **Hoofdstuk 2** volledig gewijd aan dit onderwerp. Met behulp van recente literatuur en de beschikbare kristalstructuren, geven we een uitgebreid overzicht van wat we tot nu geleerd hebben over de functie van extracellulaire loops.

In **Hoofdstuk 3** beschrijven we het onderzoek naar de eerste extracellulaire loop (EL1) van de adenosine A_{2B} receptor ($A_{2B}R$). Een random-mutagenesescreen in een S. cerevisiae expressiesysteem waarvoor we het eerste deel van de receptor muteerden, leverde een interessante mutant op met twee aminozuurveranderingen in EL1: F71L en D74G. Uitgebreide mutationele en farmacologische analyses van deze twee posities wezen uit dat dit gedeelte van de receptor essentieel is in het activatieproces van de $A_{2B}R$. Op positie 71 bleek dat de eigenschap hydrofobiciteit zeer belangrijk is, terwijl op positie 74 juist hydrofiliciteit nodig is. De opheldering van de adenosine A_{2A} receptorstructuur hielp ons om deze resultaten te verklaren. Posities 71 en 74 zijn gelokaliseerd aan de uiteinden van een β-strand in EL1 die een sheet kan vormen met de tweede extracellulaire loop (EL2). De eigenschappen van aminozuren op de twee posities zijn essentieel in het handhaven van deze zeer belangrijke driedimensionale eiwitstructuur.

In **Hoofdstuk 4** pasten we een vergelijkbare random-mutagenesescreen toe voor gemuteerde receptoren met een hoger activatieprofiel zoals beschreven in Hoofdstuk 3. Voor deze screen introduceerden we random mutaties in het tweede deel van de

$A_{2B}R$, namelijk transmembraan domein 4 (TM4), de tweede extracellulaire loop (EL2), en transmembraan domein 5 (TM5). Deze screen leverde mutaties op in drie "hotspots" in de receptor belangrijk voor constitutieve activiteit en agonist potentie. De drie clusters van aminozuren lijken verantwoordelijk te zijn voor het handhaven van het evenwicht dat bestaat tussen de actieve conformatie R* en de inactieve conformatie R van de receptor. Deze residuen zijn niet noodzakelijk direct betrokken bij ligand binding of G eiwit koppeling. Na het screenen voor gemuteerde receptoren met een hogere activiteit wilden we in **Hoofdstuk 5** ook mutaties onderzoeken die zorgen voor een verminderde activatie. Hiervoor hebben we een nieuwe screening methode ontwikkeld met ons S. cerevisae system, de MMY24 stam, waardoor we nu ook specifiek kunnen selecteren voor dit inactieve fenotype. Om ook de kennis te kunnen gebruiken uit Hoofdstuk 4 hebben we bij de inactieve screen weer gebruik gemaakt van de mutatie-bank van de $A_{2B}R$ waar random mutaties geïntroduceerd waren in het fragment TM4-EL2-TM5. De gemuteerde receptoren die we identificeerden uit deze screen lieten allemaal een verminderde constitutieve activiteit zien, maar ook een verminderde activatie door de agonist. We ontdekten een bijzonder belangrijke regio in TM5, met een sleutelrol voor $C190^{5.46}$. Deze regio blijkt belangrijk voor het faciliteren van de conformationele veranderen die de receptor ondergaat tijdens activatie, met name aan het intracellulaire gedeelte van TM5. Een vergelijking met de data verkregen in Hoofdstuk 4 liet zien dat een cysteine-rijk gedeelte in EL2 een negatieve regulerende rol heeft in activatie, ervoor zorgend dat de receptor inactief blijft. Het cluster bovenin TM5 waar alleen inactiverende mutaties gevonden werden, heeft een tegenovergestelde rol en reguleert activatie eerder positief.

In **Hoofstuk 6** beschrijven we het onderzoek naar een ander subtype van de adenosine receptor: de adenosine A_1 receptor (A_1R). De rol van de tweede en derde extracellulaire loop (EL2 en EL3) werd onderzocht door middel van een drievoudige alanine scan (Ala_3-scan) en een enkele alanine scan (Ala-scan). Veel residuen in beide loops bleken belangrijk voor A_1R functie en mutaties hadden een negatieve invloed op receptoractivatie. Met name EL2 lijkt een positieve regulerende rol te hebben in receptoractivatie. Dit staat in tegenstelling tot de rol van het cysteine-rijk gedeelte in EL2 van de $A_{2B}R$ dat juist als negatieve regulator lijkt te fungeren. Verder hebben we twee residuen geïdentificeerd in EL2, een tryptofaan en een glutamaat, die een rol spelen in de allostere modulatie van PD81,723.

Het onderzoek beschreven in de voorafgaande hoofdstukken wordt samengebracht in een discussie in **Hoofdstuk 7**. Door alle resultaten en conclusies van de individuele hoofdstukken te combineren zijn we in staat om een vollediger beeld te krijgen van het activatiemechanisme van adenosine receptoren. Ook worden in dit hoofdstuk verschillende toekomstperspectieven beschreven die voortkomen uit het onderzoek.

SAMENVATTING VOOR EEN LEEK

Ons lichaam is volledig opgebouwd uit individuele cellen. Iedere cel is omgeven door een celmembraan waarin detectoren, de receptoren, aanwezig zijn. Deze receptoren tasten constant de omgeving af naar moleculen die ze herkennen. Er zijn erg veel verschillende receptoren, die allemaal een andere lichaamseigen stof herkennen (het ligand), en in reactie daarop een specifiek signaal doorgeven dat leidt tot een biologisch effect. De grootste groep receptoren die wij hebben zijn G eiwit gekoppelde receptoren (in het Engels: G protein-coupled receptors of GPCRs). Deze heten zo, omdat ze binnen de cel het signaal doorgeven via speciale eiwitten: de zogenoemde G eiwitten.

Er zijn meer dan 800 verschillende GPCRs in het menselijk lichaam bekend die allemaal net iets anders zijn en een ander biologisch effect teweegbrengen als ze geactiveerd worden. Ze hebben allemaal wel een zelfde globale opbouw met een begin buiten de cel, waarna ze zich 7 keer door de membraan slingeren en eindigen met een staart aan de binnenkant van de cel (**Figuur 1**). De delen van de receptor die zich in het membraan bevinden noemen we trans-membraan domeinen. Deze zijn aan de binnenkant van de cel verbonden met drie intracellulaire loops en aan de buitenkant van de cel met drie extracellulaire loops. Het ligand bindt meestal binnen de trans-membraan domeinen ter hoogte van het membraan en het G eiwit bindt aan het gedeelte van de receptor dat zich binnen in de cel bevindt.

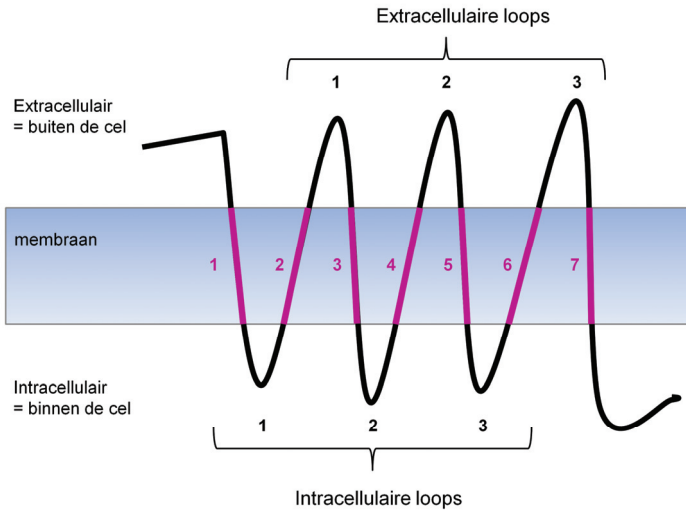

Figuur 1. Schematische voorstelling van een G eiwit gekoppelde receptor. De receptor heeft zijn begin buiten de cel, extracellulair, slingert dan 7 keer door de membraan heen en eindigt binnen in de cel, intracellulair. De delen van de receptor die in het membraan zitten (in het paars) worden de 7 transmembraan domeinen genoemd. Deze domeinen worden aan de buitenkant van de cel verbonden met 3 extracellulaire loops en aan de binnenkant van de cel met 3 intracellulaire loops.

Omdat GPCRs betrokken zijn bij vrijwel elk biologisch effect in het lichaam, van pijn tot emoties tot voortplanting, zijn het interessante doelwitten voor medicijnen. Met een synthetisch middel dat net als het natuurlijke ligand in de receptor past, kun je namelijk de activiteit en dus het biologische effect van zo'n receptor beïnvloeden. Er zijn inmiddels synthetische stoffen bekend die de receptor kunnen activeren, kunnen blokkeren of zelfs de receptor helemaal kunnen uitzetten. Om een idee te geven: ongeveer 40% van alle medicijnen die je kunt krijgen bij de apotheek zijn gericht tegen GPCRs. Je kunt dan denken aan bètablokkers, antidepressiva en anti-allergie middelen etc. We weten dat deze medicijnen werken doordat ze een receptor kunnen binden en zo het gewenste biologische effect geven. We weten echter nog niet wat er nu precies gebeurt met de receptor zodra die het medicijn heeft herkend en hoe die het signaal hierna doorgeeft. Dit is een van de redenen dat we voor veel medicijnen bijwerkingen nog altijd niet kunnen voorkomen. Een andere hele goede reden om deze familie van receptoren te onderzoeken is dat foutjes (mutaties) die soms optreden in het DNA ervoor kunnen zorgen dat een receptor zich net iets anders gaat gedragen en een ziekte veroorzaakt, zoals kanker, diabetes en astma.

De adenosine receptoren die besproken worden in dit proefschrift zijn leden van de enorme familie van G eiwit gekoppelde receptoren. Het lichaamseigen ligand dat adenosine receptoren activeert is het molecuul adenosine. Als de receptoren dit ligand detecteren zal het lichaam onder andere het hartritme gaan aanpassen en het slaapritme reguleren. Maar adenosine heeft ook een effect op het immuunsysteem als er door stress veel meer van dit molecuul aangemaakt wordt in het lichaam. Een zeer bekend voorbeeld van een niet-lichaamseigen ligand voor adenosine receptoren is cafeïne, dat in grote hoeveelheden aanwezig is in koffie, thee, en ook in verschillende energiedrankjes. Cafeïne kan de receptor binden, maar niet activeren. Cafeïne blokkeert juist adenosine receptoren, zodat adenosine zelf niet kan binden. Dit maakt dat mensen na overmatig gebruik van cafeïne moeite hebben om in slaap te komen of zelfs hartkloppingen ervaren (**Figuur 2**).

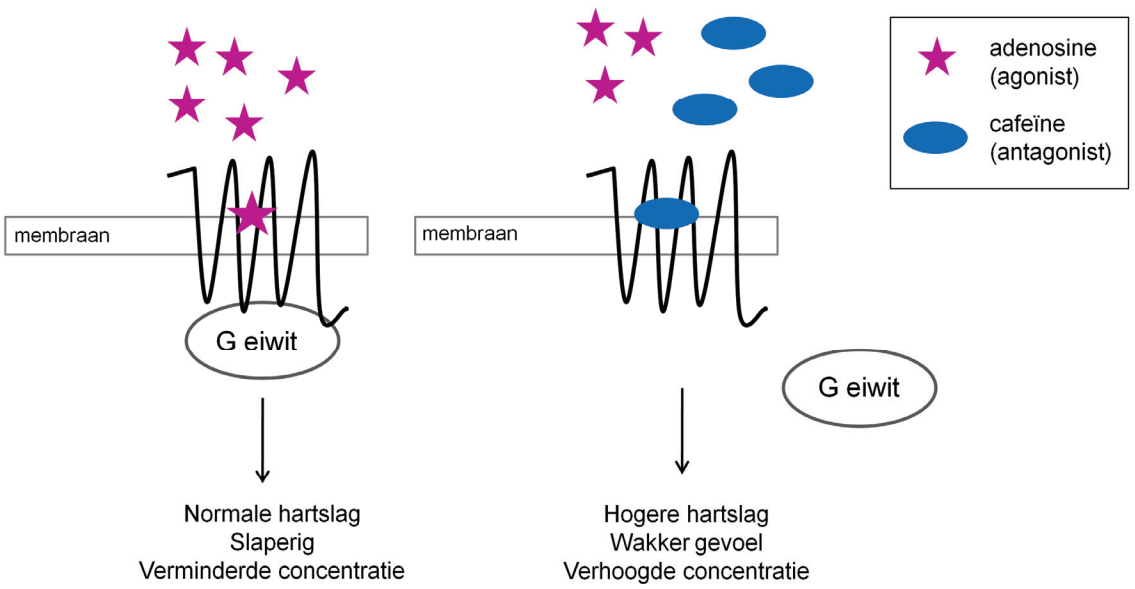

Figure 2. De adenosine receptor heeft dezelfde opbouw als alle andere GPCRs met zeven transmembraan domeinen. Wanneer adenosine aanwezig is (links) dan kan het molecuul de receptor binden en via het G eiwit een signaal doorgeven. Dit leidt tot een stabiele hartslag en vooral vroeg in de morgen en later op de dag tot een slaperig gevoel en een verminderde concentratie. Als je dan wat koffie drinkt, blokkeert de cafeïne de receptor waardoor adenosine niet meer kan binden en de receptor dus niet meer kan activeren (rechts). Het resultaat is dat je je meer alert voelt, je hartslag omhoog gaat en je concentratie verhoogt.

Het doel van mijn onderzoek was om meer te weten te komen over hoe GPCRs en meer specifiek hoe adenosine receptoren geactiveerd kunnen worden. Met andere woorden: welke delen van deze receptoren belangrijk zijn bij het doorgeven van het signaal vanaf het moment dat het ligand in de buurt is. Een speciale interesse had ik in de extracellulaire loops, dat zijn de verbindingen buiten de celmembraan tussen de transmembraan domeinen (**Figuur 1**). Deze extracellulaire loops werden tot voor kort alleen beschouwd als een soort ankers om de receptor in de membraan te houden. Het is pas zeer recent dat men begint in te zien dat ze wel degelijk belangrijk zijn voor activatie van de receptor.

Om te onderzoeken hoe de receptor zich gedraagt heb ik bewust foutjes (mutaties) aangebracht in menselijke receptoren en gekeken in hoeverre ze nog geactiveerd konden worden. Het is niet mogelijk om dit direct in mensen of zelfs proefdieren te testen en dus heb ik gebruik gemaakt van een ander organisme: gist. Dit is dezelfde gist die we gebruiken bij het bakken van brood, maar met een paar genetische aanpassingen. Deze aanpassingen hebben ervoor gezorgd dat alleen die gistcellen die een actieve receptor hebben kunnen groeien op een speciale voedingsbodem.

Door deze eigenschap kunnen we de gist nu zelf laten “kiezen” welke mutaties zorgen voor een bepaalde verandering van de receptor, dit noemen we screenen. Met deze aanpak hebben we gescreend voor mutaties die zorgen dat de receptoren meer actief worden, maar ook voor mutaties die leiden tot minder actieve receptoren. Zeker het screenen voor verminderde activiteit is erg lastig en ik ben één van de eersten die hiervoor een methode heeft ontwikkeld. Ook was ik de eerste die een receptor heeft onderzocht op zowel activerende als inactiverende mutaties. Deze aanpak heeft veel verassende inzichten opgeleverd over hoe de adenosine receptoren geactiveerd kunnen worden. Zo heb ik een specifieke regio ontdekt die een belangrijke taak heeft bij het inactief houden van de receptor. Als je hier een foutje maakt, wordt de receptor meer actief en kan zelfs een signaal doorgeven zonder een ligand. Ik heb ook een gebied gevonden dat juist belangrijk is om de receptor actief te laten worden. Als je hier een mutatie in aanbrengt kan de receptor moeilijk of zelfs helemaal niet meer geactiveerd worden.

Een andere opmerkelijke ontdekking was dat zelfs receptoren die heel erg veel op elkaar lijken zich net iets anders gedragen na het herkennen van een ligand. Dit verschil zit vooral in de extracellulaire loops, dus de gebieden die zich buiten de cel bevinden.

Wat ik met het onderzoek in dit proefschrift heb bewezen is dat de extracellulaire loops een grote rol spelen bij de activatie van receptoren en dat dit voor iedere receptor net iets anders kan zijn waardoor ze het unieke karakter van de receptor bepalen. Dit betekent daardoor ook dat bij het ontwerpen van medicijnen, of het vaststellen van een ziekte-veroorzakende mutatie er niet zomaar vanuit kan worden gegaan dat iedere receptor ongeveer hetzelfde is. Iedere receptor is uniek en moet ook zo bekeken worden.

LIST OF PUBLICATIONS

M.C. Peeters, G.J.P. van Westen, Q. Li, A.P. IJzerman. Importance of the extracellular loops in G protein-coupled receptors for ligand recognition and receptor activation.Trends in Pharmacological Sciences **2011**, 32(1):35-42.

M.C. Peeters, G.J.P. van Westen, D. Guo, L.E., Wisse, C.E. Müller, M.W. Beukers, A.P.IJzerman. GPCR structure and activation: an essential role for the first extracellular loop in activating the adenosine A2B receptor. FASEB J. **2011**, 25(2):632-43.

M.C. Peeters, Q. Li, G.J.P. van Westen, A.P. IJzerman. Three "hotspots" important for adenosine A_{2B} receptor activation: a mutational analysis of transmembrane domains 4 and 5 and the second extracellular loop. Purinergic Signalling **2011** [Epub ahead of print]

M.C. Peeters, Q. Li, G.J.P. van Westen, C.E. Müller, A.P. IJzerman. Screening for Constitutively Inactive Mutants of the Adenosine A_{2B} Receptor in *S. cerevisiae***.** (manuscript in preparation)

M.C. Peeters, L.E. Wisse, A. Dinaj, B. Vroling, G. Vriend, A.P. IJzerman. The second extracellular loop of the adenosine A_1 receptor plays a role in both receptor activation and allosteric modulation. (manuscript in preparation)

CURRICULUM VITAE

Miriam Peeters werd geboren op 30 april 1982 te Hoevelaken, en groeide op in Dongen, Noord-Brabant. Haar middelbare schoolopleiding volgde zij aan het Sint Oelbert Gymnasium te Oosterhout (NB), waar zij in 2001 haar eindexamen behaalde. Vervolgens studeerde zij Moleculaire Levenswetenschappen aan de Radboud Universiteit te Nijmegen. In augustus 2002 behaalde zij het propedeutisch examen, gevolgd door het doctoraal examen in augustus 2006. Tijdens de doctoraalfase van haar studie doorliep ze twee researchstages, beide met een duur van negen maanden. De eerste stage deed zij bij de afdeling Humane Genetica aan het Universitair Medisch Centrum St. Radboud te Nijmegen onder begeleiding van Dr. Ilse Gosens en Dr. Ronald Roepman. Hier deed zij onderzoek naar intracellulaire interactoren van het eiwit MPP5 dat mogelijk betrokken is bij de oogziekte Retinitis Pigmentosa. Haar afstudeerstage deed zij bij de afdeling Assay Development van Solvay Pharmaceuticals te Weesp onder begeleiding van Drs. Elina Hessels en Dr. Jurjen Frankena. Tijdens deze stage ontwikkelde zij een nieuwe assay om signaaltransductie te onderzoeken van een klasse C G Protein-Coupled Receptor (GPCR).

In 2007 begon Miriam aan het in dit proefschrift beschreven promotieonderzoek bij de afdeling Farmacochemie aan de Universiteit Leiden onder begeleiding van Prof. Ad IJzerman. Dit onderzoek maakte deel uit van het TI-Pharma initiatief “GPCR forum for established targets” (D1-105). Tijdens haar promotieperiode presenteerde zij haar onderzoek op meerdere nationale en internationale congressen en heeft zij op uitnodiging van Prof. Ueda een lezing aan de universiteit van Nagasaki in Japan gegeven. Tevens ontving zij tijdens de FIGON Dutch Medicines Days 2009 de eerste prijs in de nationale AIO-competitie met haar presentatie getiteld: “An essential role for the first extracellular loop”. Eerder dat jaar won ze met deze presentatie ook de AIO-competitie op het LACDR Spring Symposium, waar zij ook de posterprijs in ontvangst nam. In 2010 won ze een internationale presentatieprijs op de Purinergic Signaling Conference in Tarragona (Spanje) .

CURRICULUM VITAE (ENGLISH)

Miriam Peeters was born on April 30th 1982 in Hoevelaken, and grew up in Dongen, Noord Brabant, The Netherlands. After graduating from secondary school at the Sint Oelbert Gymnasium te Oosterhout (NB) in 2001, she started her study Molecular Life Sciences at the Radboud University in Nijmegen. In June 2002, she passed the propaedeutic exam, followed by the Master's degree in August 2006. During her Master studies, she did two internships, both with a duration of nine months. Her first internship was at the department of Human Genetics at the University Medical Centre St. Radboud in Nijmegen under the supervision of Dr. Ilse Gosens and Dr. Ronald Roepman. Here, she investigated intracellular interactors of the protein MPP5 that might be involved in the eye disorder Retinitis Pigmentosa. Her second internship was done at the department Assay Development of Solvay Pharmaceuticals in Weesp under the supervision of Drs. Elina Hessels and Dr. Jurjen Frankena. During this training period, she developed a new functional assay to investigate signal transduction of a class C G Protein-Coupled Receptor.

In 2007, Miriam started the PhD research as described in this thesis at the department of Medicinal Chemistry at Leiden University under the supervision of Prof. Ad IJzerman. This research was part of the TI-Pharma initiative "The GPCR forum for established targets" (D1-105). During her PhD, she presented her research at several national and international congresses and gave a lecture at the University of Nagasaki in Japan upon invitation of Prof. Ueda. At the FIGON Dutch Medicines Days 2009, she received the first prize at the national PhD-student competition with her presentation entitled: "An essential role for the first extracellular loop in activating the adenosine A_{2B} receptor". Earlier that year, this presentation was awarded with the first prize in the PhD-student competition at the LACDR Spring Symposium, where she also received the poster prize. In 2010 she also received the presentation award in an international competition at the Purinergic Signaling Conference in Tarragona (Spain).

NAWOORD

Vier jaar werken als AIO levert niet alleen een mooi proefschrift op (al zeg ik het zelf), maar vooral heel veel waardevolle herinneringen en dierbare vrienden en collega's. Zonder de geweldige sfeer en collegialiteit van de afdeling Farmacochemie zouden deze vier jaar heel wat minder plezierig zijn geweest. Iedereen leefde altijd ontzettend mee bij tegenslag, maar juichte nog harder mee bij goed nieuws. Ik had ook geen beter kantoor kunnen treffen met Henk, Elisabeth, Qilan (Ann), Annelien, Joanke, en Clara. Jullie hebben me door de jaren heen vele discussies met mijn computer horen voeren, maar hadden daar veel begrip voor. Met zo'n clubje bio's in een kleine ruimte was er ook altijd tijd voor het aanhoren van en meedenken bij mijn theorieën en dat heeft ook zeker bijgedragen aan het ontstaan van dit proefschrift. Ann, I am grateful for your help with many of the chapters in this thesis, I really enjoyed working together. Thea, door jou heb ik me minder eenzaam gevoeld als moleculair bioloog op de afdeling. Al sta je nergens als mede-auteur op mijn publicaties, jouw bijdrage was onmisbaar bij allemaal. Gerard, jouw "plaatjes" hebben dit proefschrift helemaal af gemaakt. Wat waren we een goed team! Samen hebben we zelfs gezorgd dat het review werd gepubliceerd als "feature article" met bijbehorende cover in TiPS. Ik ben ook erg blij dat jij mij vandaag bijstaat als paranimf samen met Clara. I also want to mention all the bachelor and master students I had the privilege of supervising: Lisanne, Dong, Admira, Jorine, Rachel, Jan, and Sarah. I hope you learned as much from me as I did from you. En Ad, niet alleen was dit proefschrift niet geworden zoals het is zonder jouw aanmoediging en inzet, ik had waarschijnlijk ook niet het lef gehad om op de grote podia te spreken zoals ik nu gedaan heb. De prijzen die ik heb gewonnen zijn zeker deels ook van jou.

Bas, ook jij verdient hier een speciaal plaatsje; mijn helpdesk in Nijmegen. Jij en jouw GPCRDB waren van onschatbare waarde. En Hanka: wie had ooit gedacht dat wij weer samen achter een computer terecht zouden komen! Ik vond het erg leuk en leerzaam om samen een dagje in "the cave" door te brengen. Veel van de discussie in hoofdstuk 7 heb ik aan die dag te danken.
Ik heb ook veel te danken aan de afdeling Moleculaire Genetica in Leiden, en dan vooral Patrick, Tieneke, Hans, en Riekje. Van jullie heb ik zoveel geleerd over hoe ik

met mijn gisten om moest gaan. Jullie stonden altijd klaar voor advies of gewoon een praatje. Ik heb mijn schitterende blots in hoofdstuk 6 volledig te danken aan jou, Patrick! Zet ‘m op voor jouw laatste loodjes! Het zal ongetwijfeld een schitterend boekje worden. Wat betreft hulp en advies op gist-gebied mogen ook zeker Marco Siderius en Jan Paul Bebelman van de Vrije Universiteit Amsterdam en Simon Dowell van GSK hier niet ontbreken.

Natuurlijk had ik dit werk nooit zo goed kunnen doen zonder de support van mijn familie. Mama, ontzettend bedankt voor al je steun en luisterend oor. Bij een probleem kon ik je altijd bellen, en al zei je niets, aan het einde van het gesprek was het opgelost. De jaarlijkse spa-uitjes hebben ook zeker bijgedragen om steeds weer gemotiveerd verder te gaan. Papa en Els, jullie hebben me altijd laten weten hoe trots jullie waren en toonden altijd erg veel interesse in mijn werk. Artikelen werden direct uitgeprint en gelezen, ook al begrepen jullie het misschien niet altijd helemaal. Mijn broer Jos en mijn zusjes Noortje en Lotte wil ik ook graag bedanken, we vormen samen een bijzondere familie! Ik hoop dat het mijn enthousiasme was dat nu ook Lotte heeft geïnspireerd een wetenschapper te worden. Farmacochemie, pas op, misschien komt er over een aantal jaren nog een Peeters het lab onveilig maken. En last but not least, Pim bedankt voor alles. Je hebt me altijd gesteund en klaagde nooit als ik door zenuwen voor een spannende dag jouw nachtrust ernstig beperkte. Onze reis naar Japan zal ik nooit vergeten en heeft mij geïnspireerd tot de lay-out van dit proefschrift.

Groetjes Miriam

ABBREVIATIONS

[^{3}H]DPCPX	[^{3}H] 1,3-dipropyl-8-cyclopentylxanthine
[^{3}H]PSB-603	[^{3}H] 8-[4-[4-(4-Chlorophenyl) piperazine-1-sulfonyl)phenyl]]-1-propylxanthine
3AT	1,2,4-aminotriazole
A_1R	Adenosine A_1 receptor
A_{2A}R	Adenosine A_{2A} receptor
A_{2B}R	Adenosine A_{2B} receptor
A_3R	Adenosine A_3 receptor
ADA	Adenosine deaminase
ATP	Adenosine triphosphate
BAY60-6583	2-[6-amino-3,5-dicyano-4-[4-(cyclopropylmethoxy) phenyl]pyridin-2-ylsulfanyl]acetamide
BSA	Bovine serum albumin
cAMP	Cyclic adenosine-5'-monophosphate
CGS21680	2-[4-(2-carboxyethyl)phenethylamino]-5'-*N*-ethylcarboxamidoadenosine
CHAPS	3-[(3-Cholamidopropyl)dimethylammonio]-1-propanesulfonate
CHO cells	Chinese hamster ovary cells
CPA	N^6-cyclopenthyladenosine
DMEM	Dulbecco's modified Eagle's medium
DMSO	Dimethylsulfoxide
DPCPX	1,3-dipropyl-8-cyclopenthylxantine
EDTA	Ethylene diamine tetraacetic acid
EC_{50}	Half-maximal effective concentration (potency)
EL1	First extracellular loop
EL2	Second extracellular loop
EL3	Third extracellular loop
E_{max}	Maximal effect (efficacy)
GPCR	G protein-coupled receptor
IC_{50}	Half maximal inhibitory concentration (affinity)
IGPD	Imidazole glycerol-phosphate dehydrase
K_D	Equilibrium dissociation constant
K_i	Equilibrium inhibition constant (absolute affinity)
NECA	5'-*N*-ethylcarboxamidoadenosine
PBS	Phosphate-buffered saline
PCR	Polymerase Chain Reaction
PD81,723	(2-amino-4,5-dimethyl-3-thienyl)-[3 (trifluoromethyl)phenyl]methanone
PSB-603	8-[4-[4-(4-Chlorophenyl) piperazine-1-sulfonyl)phenyl]]-1-propylxanthine
S. cerevisiae	Saccharomyces cerevisiae
YNB medium	Yeast nitrogen based
YAPD medium	Yeast extract-peptone-dextrose supplemented with adenine
ZM241385	(4-(2-[7-amino-2(furyl {1,2,4}-triazolo {2,3-a {1,3,5}triazin 5-yl-aminoethyl)phenol